UNIVERSITY
of
GLASGOW

DEPARTMENT OF CIVIL ENGINEERING

BANKFULL AND OVERBANK FLOW IN A STRAIGHT COMPOUND CHANNEL WITH A GRADED SEDIMENT BED : DEGRADATIONAL BEHAVIOUR

thesis

submitted to the faculty of engineering

in candidacy for the degree of doctor of philosophy

by

CHRIS M. FULLER

GLASGOW

THE UNITED KINGDOM

FEBRUARY, 1998

Declaration

I declare that this thesis is a record of the original work carried out, solely by myself, in the Department of Civil Engineering at the University of Glasgow, during the period of October 1994 to October 1997.

This thesis has not been presented elsewhere in consideration for a higher degree.

Chris M. Fuller, B.Eng

February 1998

Acknowledgements

I would like to express my sincere gratitude to several people without whom this research would not have been possible, nor would this thesis ever have been completed.

Dr. G. Pender I thank for his unfailing support, advice, criticism and encouragement. Dr. T.B. Hoey I thank for his advice and his generosity with time for the discussion of ideas. My thanks also go to Prof. D.A. Ervine for his support and guidance.

My thanks go to the department and the successive heads, Dr. J.G. Herbertson and Prof. N. Bicanic, for the provision of considerable facilities.

The Aberdeen collaborators are also acknowledged for their equal part in the running of the overall project. I especially wish to thank my friend and colleague Dr. Anthony Brown, without whom the data presented could not have been collected.

From the time spent at HR Wallingford I would like to thank Dr. R. Bettess and Mary Johnstone for all their help and discussions.

I thank Ken McColl, the department computing manager, for his excellent and continual technical support over the three years. I would also like to extend my gratitude to my fellow research colleagues for their friendship; Ruth Clarke, Alan Cuthbertson, Graeme Forbes, Andy MacAuley, Vincent Peloutier and Sharon Sloan.

Last but by no means least, I would like to thank my friends and family for their unconditional support throughout my work. Particular thanks must go to Nigel Royle and the lovely Lilian Wanless who were there for me when I needed support most.

Abstract

An extensive experimental programme is reported upon. Laboratory flume experiments were used to examine the behaviour of graded sediment transport, in a straight compound channel. The experiments covered a range of initial bed slopes, relative depths and upstream sediment feed conditions. The results presented relate specifically to six degradation experiments.

Degradation is an important process in fluvial systems. It describes the reactions of a bed to excessive tractive forces, forces sufficient to cause erosion of a non-cohesive bed surface. Understanding the small scale processes involved in degradation is essential if accurate sediment transport models are to be developed to facilitate estimates of natural channel behaviour. To date, detailed examinations of degradational transport behaviour have been scarce. The studies of degradational transport that have been reported on have all involved inbank open channel flows. The importance of examining sediment transport behaviour during overbank, compound channel flow is clearly apparent, particularly so when one considers that, multi-stage channels are heralded as an environmentally acceptable method for flood alleviation.

Within this thesis a substantial literature review is presented. The review covers the broad topics of sediment transport and compound channels. The two sub-topics of graded sediment behaviour and straight compound channels are given greater attention due their relevance to the author's research.

The transport rates observed during the degradational experiments are presented, and their common pattern of decline analysed and discussed. The general pattern of decline is found to match transport declines reported by other researchers. Regressions are fitted to each transport rate data set. The recorded transport rate data is also used to estimate the weight of material transported from the bed. The resulting values are compared between experiments, with reference to experimental conditions

of initial bed slope and relative depth ratio. The results from both (the regression transport rates and the estimates of material transported). show an increase in transport for an increase in relative depth or initial bed slope.

Methods of estimating main channel boundary shear stress from non-intrusive measurements of hydraulic conditions are examined. Results for the reported experiments show a lower value of shear stress for the shallow overbank relative depth than for the bankfull condition. Although the result agrees with reported results in terms of boundary shear stress, the result is in conflict with the increase in sediment transport observed between the above flow conditions. Consequently, it is suggested that boundary shear stress alone, as estimated here, may not be a suitable parameter on which to base sediment transport predictions for overbank flow conditions. In addition, the relationship between unit stream power and sediment transport is examined and found to demonstrate a continuous trend. Both parameters increase between bankfull and shallow overbank conditions, and increase again between shallow overbank and deep overbank conditions. Unit stream power, as estimated here, may therefore form a better basis for overbank flow, sediment transport, prediction techniques.

The evolution of bed surface and bedload compositions are also presented for the same degradational experiments. The effects of the two experimental variables, initial bed slope and relative depth, are considered with reference to a proposed ranking order of transporting potential between the experiments. The results suggest complex fractional transport behaviour, controlled by the relationship between an experiment's transport potential and the graded bed material composition.

All the work presented in this volume was made possible by the Engineering and Physical Science Research Council grant no. GR/J67567.

Measured data relating to the experiments conducted is available from the Universities of Aberdeen and Glasgow, and from the web site http://www.civil.gla.ac.uk/research/GSRP.

Table of Contents

List of Figures

List of Tables

Notation

A	cross-sectional area
B	side slope factor [Wark (1993)]
C	Chezy coefficient
C_D	coefficient of drag
D	local flow depth
D_i, d_i	particle diameter, fraction I
D_{50}, d_{50}	particle diameter for which 50% of composition finer
e	base of natural logarithms
f	Darcy - Weisbach friction factor
f_i	size fraction composition percentage in bed surface
g	gravitational acceleration
h	flow depth
h	main channel depth, bed to bankfull level
H	main channel flow depth, bed to water surface level
n	Manning's roughness coefficient
P	wetted perimeter
p_i	size fraction composition percentage in bedload
q	unit flow
q_b	unit transport rate
$Q_{approx.}$	approximate discharge
$Q_{ave.}$	yearly average discharge
R	hydraulic radius
R^2, r^2	correlation coefficient
S_{xf}	longitudinal friction slope, energy line gradient
u	local velocity
U, $\bar{u}$	depth averaged velocity
u_*	shear velocity
V	area averaged velocity

x	streamwise coordinate
y	vertical coordinate
z	height above bed
z_0	bed roughness height corresponding to $u = 0$
κ	von Karman constant
ν	kinematic viscosity
ν_t	depth averaged lateral turbulent viscosity [Wark (1993)]
ρ	density of water
ρ_f	density of fluid
ρ_s	density of sediment
σ_g	standard geometric deviation
τ	shear stress
τ_c, $\tau_{cr,j}$	critical shear stress
τ_{0l}	local boundary shear stress
ω	unit stream power

Chapter 1

Introduction

1.1 Background

The ability to predict sediment transport is important when assessing a rivers response to engineering projects. Poor prediction can result in significant sums of money having to be spent on remedial works. In the UK, problems relating to sediment cost in excess of £10 million per annum. As UK rivers are not particularly active, the global cost of sediment related problems must be significantly greater than this.

Even within a relatively small area like the UK, the range and diversity of river engineering projects can vary significantly. Two recent examples are the River Spey abstraction scheme (Mackie-Dawson et al 1988), and the Maidenhead flood alleviation scheme on the River Thames (Clear Hill 1994). Both of these projects require the engineer to predict the river channel response to a reduction in flow. In the case of the Spey, this is because water is being removed from the channel. In the case of the Thames, it is because the water is being diverted from the main channel through a secondary flood relief channel. In terms of channel hydraulics both problems are therefore similar. However, the Spey is a fast flowing, gravel bed river in the north east of Scotland, with an average discharge of $Q_{ave} = 64.4m^3/s$ (at the Boat O'Brig gauging station). The Thames at Maidenhead in the south of England, on the other hand, has experienced major flood discharges of $Q_{approx.} = 500m^3/s$, is generally slower flowing and has a finer bed material composition.

Solving the hydraulic problems associated with these schemes is relatively straight forward and within the competence of most practising engineers. However, the

sediment transport predictions pose a much more complex problem. The solution requires detailed knowledge of the prediction methods used, the assumptions made in their development and the range of their applicability. There is therefore a strong technical and economic case for improving methods of graded sediment transport prediction.

Commitment to maintaining natural ecosystems is viewed with such importance within the UK that, engineering projects, requiring to alter natural channels, must take steps to minimise the damage to the environment. As the channel bed not only controls stability (a traditional concern to engineers) but also influences the ecology and fish habitat (Carling 1984, Crisp and Carling 1989), sediment transport prediction is an important component of such schemes. To this effect, the Scottish Office recently spent £3 million on habitat conservation during the realignment of the Evan Water as part of the upgrade of the A74 to motorway. Indeed, the environmental benefit obtained from natural rivers is such that in some cases rehabilitation is economically justified. On the River Poole in Sydenham, London, £2.5 million was spent during a rehabilitation project. Understanding and the ability to predict gravel bed behaviour is therefore an important component in the continued provision and maintenance of the economic and environmental benefit provided by rivers.

Many formula already exist for the prediction of graded sediment transport. Most of these were originally designed using uniform grain size material and are applicable to graded material through the inclusion of hiding functions (White and Day 1982, Parker and Sutherland 1990, Pender and Li 1995). Some formula do exist that have been specifically designed for graded sediment transport prediction (Einstein 1950, Parker 1990). However, all the existing methods are limited in their application, often due to the range of data from which they were derived (Pender and Li 1996). Indeed, when applied to the same data the results from the different prediction techniques can be wide ranging.

Recent research has shown that graded sediment transport is regulated by the complex interaction of sediment and water through the influences of small scale processes (Parker et al 1982a, Wilcock 1992, Sutherland 1991, Tait and Willetts 1991, Tait 1993). It is thought that the most important interaction is that between bed roughness, bed surface layer composition and hydraulic shear stress. Traditionally prediction methods have been derived from regression analysis of laboratory transport experiments. The parameters measured during such experiments have often been limited, resulting in only a few of the published data sets possessing the necessary information (USWES 1935, Day 1980, Gibbs and Neill 1972, 1973).

It is only through understanding and conceptualisation of the physical processes involved in graded sediment transport, that reliable and widely applicable prediction methods will be developed (Tait and Willetts 1991, Sutherland 1991). Further detailed experimental programmes are therefore required to improve the understanding of the physical processes and to support the development of numerical prediction models (Willetts et al 1987, Holly and Rahuel 1990, Armanini 1995, Pender and Li 1995).

The following three sub-sections are by way of introduction to two areas of research, and one series of work central to the research presented in this thesis. All three topics are covered in more detail in Chapter 2, which includes a review of the literature published on each topic.

1.1.1 Concepts of Graded Sediment Transport

Any attempt to predict graded sediment transport must account for the interaction between different size fractions present in the material. Larger particles are inherently less mobile than smaller material. However, in a mixture larger particles are relatively more mobile than they would be in a uniform mix of material, while finer particles are relatively less mobile. This is due to the larger particles protruding further from a mixed material, bed while smaller particles remain sheltered behind the larger particles.

Selective transport takes place when the magnitude of the applied tractive force is between the critical force for movement of the finest material, and that for the largest material. If the applied tractive force is greater than the critical tractive force for the largest material then all size fractions will be readily entrained and the bedload will approximate the substrate composition (Parker 1982b, 1990).

Traditionally the variation in particle mobility with size has been modelled using hiding functions or reduced hiding functions. Application of such functions adjust the critical conditions for each size fraction based solely on grain size distribution of the material examined (Li 1995).

For a graded sediment transport model to be successful it must take account of selective transport through adjustments in the bed surface composition and the transport rate itself. As material is removed from the bed surface certain size fractions will become less abundant, which means those sizes are less available for transport. The continual adjustment of the bed surface is described by the behaviour of the active layer (Parker 1982a).

In most natural conditions the supply rate of sediment to a reach is either greater or less than the transport rate out of the reach, but the two are very rarely equal. In this way graded sediment transport is a non-equilibrium process. The continual adjustment of the selective transport and transport rate in time and space are reflected by the vertical changes in the active layer composition. The active layer is defined as the layer from which material is either entrained into the flow or deposited into the substrate. The composition of the active layer adjusts in such a way as to try to stabilise sediment transport, this is know as armouring (Parker and Sutherland 1990).

Research has shown that quantitatively the hiding effects in graded sediment are affected by several factors. The grain size distribution in the active layer, the channel geometry, the turbulent pressure fluctuations in the bed region and other hydraulic parameters have all been cited as influencing hiding (Li 1995).

It is clear then that the modelling of graded sediment behaviour is a very complex problem. Due to the number of interacting parameters computational modelling has therefore been used by many researchers in order to run transport simulations. Traditional numerical models have been based on four empirical sediment relationships (Li 1995).

(a) One important sediment characteristic is its resistance factor, and indeed, most transport formula are linked to hydraulic roughness directly or indirectly. Roughness can be defined using coefficients such as Chezy's or Manning's. However, inaccuracy affects both the hydraulic component of the model and the evaluation of transport. There are a number of factors which influence flow resistance. For gravel beds, grain roughness is dominant, while for sand beds, form roughness is also important. Other factors affecting flow resistance include vegetation, river bends and overbank flow (Li 1995).

(b) The interaction of different size fractions, as previously mentioned, is also important. The hiding affect is traditionally accounted for using a hiding function or reduced hiding function.

(c) The choice of which sediment transport formula to use is particularly difficult. A number of formula exist in the literature but in order to choose the most appropriate method one requires a good background knowledge of sediment transport and existing formulae. Different formulae will provide different degrees of accuracy in different conditions. However, even the best choice may not prove very accurate as most of the transport formula available were developed based on uniform size material movement.

(d) The last of the four important factors, traditionally deemed to affect the bed transporting process, is the active layer thickness. A number of suggestions have been made on how to define this, mostly relating it to representative particle

diameter, e.g. a constant scaling with D_{90} by Parker and Sutherland (1990) and $2D_{84}$ by Hoey and Ferguson (1994).

1.1.2 Concepts of Compound Channel Flow

A considerable amount of research work has been undertaken recently examining the characteristics of flow in compound channels with fixed boundaries. Within this thesis sediment transport will be examined during overbank flow conditions and so it is desirable to introduce some compound channel concepts.

A compound channel can be defined as consisting of a simple main channel with a flood plain or berm, on one or both sides. During normal or low flow events the discharge is contained within the main channel. However, during a high flow or flood event the flood plains become inundated. Thus, the flood plains are usually dry but convey discharge during flood events.

During periods when the flood plains are an active part of the channel the flow characteristics are different from those of a single channel. Within a single channel the velocity distribution is continuous with the maximum velocities in the centre of the channel and the minimum values at the channel edge. The flow mechanics in a compound channel are more complicated. Generally the depth of flow is significantly shallower over the flood plains than over the main channel. This often creates a discontinuity in the velocity distribution between the flow at the edge of the main channel and the flow at the edge of the flood plain. Because the flood plains spend much of the time dry, they tend to be overgrown and so their hydraulic roughness is significantly greater than that of the main channel. This leads to greater differences between the flow characteristics of the main channel and flood plain sections (Wormleaton and Hadjipanos 1985).

In compound channels both wetted perimeter and hydraulic radius show a discontinuity at the bankfull stage. For a small rise in stage level above bankfull, a large increase in wetted perimeter occurs. The area of flow only increases marginally

and consequently there is a decrease in the hydraulic radius. If these variations are applied in a back calculation of uniform flow theory to predict bed roughness a reduction is computed between the bankfull stage and the low overbank stage. This prediction is not representative of bed roughness characteristics, it is actually a result of the non-linear interaction of the geometric cross-sectional parameters.

The difference in flow characteristics between a single channel cross-section and a compound channel cross-section are therefore significant. The result of the characteristics of a compound channel is that the velocity of the flow on the flood plains is much less than the flow in the main channel. From other areas of hydraulics it is known that, if co-flowing streams of significantly different velocities exist, then there is an exchange of fluid and momentum between them (Chadwick and Morfett 1986). The existence of such a shear layer between the main channel and flood plain is why compound channels behave differently from simple channels. The shear layer effects both the overall channel capacity and the local flood plain and main channel boundary shear stress values, reducing them in the main channel and increasing them on the flood plain.

1.1.3 Introduction to Series C

The Flood Channel Facility (FCF) was built at HR Wallingford in 1986, funded by the then Science and Engineering Research Council. It was conceived because government departments, researchers and professional bodies all identified a need to improve estimation of discharge capacity in channels with flood plains (Knight and Sellin 1987). Such a large scale facility was required as there is uncertainty about whether the complex hydraulics observed during small scale investigations are significant at a realistic scale. Technology didn't allow sufficient detail to be recorded during field investigations and so large scale laboratory research was undertaken.

The FCF is 50m long and 10m wide and can accommodate a flow depth of up to 0.5m. The total discharge available from the pumps is 1.1 cumecs. Between 1986 and

1989 the facility was used for Series A work, examining the hydraulics of flow in straight compound channels. Series B then ran from 1989 to 1990 and investigated meandering compound channel flow.

Series C work began at HR Wallingford in 1994. The work was funded by the Engineering and Physical Science Research Council (EPSRC) with additional support from HR Wallingford, the UK National Rivers Authority (NRA) and the Ministry of Agriculture, Fisheries and Foods (MAFF). The purpose of the programme was to gain a greater understanding of various aspects of sediment transport.

Because of the difficulty and expense involved in changing the slope of the moulded FCF the Tilting Flume Facility (TFF) was made available by HR Wallingford for Series C. During the first set of grants two groups were involved in work at the Oxfordshire site, both examining straight compound channels. One group examined the behaviour of a uniform material bed and utilised the FCF, while the other examined that of a graded sediment bed and took advantage of the TFF. The work presented in this thesis is the result of the research carried out in the TFF between the joint grant holders at the Universities of Aberdeen and Glasgow.

1.2 Research Aims

Ackers (1992a) produced a method for predicting flow in compound channels as a result of the work done in Series A and B. If the predicted flow resulting from this method is used to predict sediment transport in the channel it is found that the transport decreases during the transition between bankfull and shallow overbank flow.

Work has also been completed examining the difference in transport predicted using section averaged velocity and depth and that using pointwise predictions summed across the channel (Seed 1996). The two have been found to differ by up to 40%.

Bettess (1997) therefore concluded that there are still characteristics of sediment transport in river channels that require further investigation to provide greater understanding. Three years previously Bettess (1994) published the results of a scoping review of sediment transport research in the FCF. The scoping review was carried out in 1993, by HR Wallingford on behalf of the NRA and MAFF, to consider their research needs along with those of the Department of the Environment and the EPSRC. The result was a number of outlined objectives for the Series C programme.

1.2.1 Overall Series C Programme Aims

The research carried out was aimed at helping to provide prediction methods for:

- the conveyance of channels carrying sediment transport during overbank flow. This was linked to the impact of sediment movement and bed forms on the conveyance of a channel.
- the impact on the mechanisms and characteristics of flow caused by bed features.
- the quantity of sediment transferred onto the flood plain from the main channel, assuming this is a function of flow characteristics, geometry and sediment size.
- the rate of bank erosion in relation to the current width, the regime width, the flow characteristics, the bank height and the bank material.

From the end-users point of view the aims of the Series C research were more specific.

1. Provide methods for the prediction of graded and uniform sediment transport behaviour, in both straight and meandering channels, during both inbank and overbank flow.
2. Define the alluvial resistance parameters for both straight and meandering channels, again during both inbank and overbank flow.

3. Predict the transfer of sediment from the main channel to the flood plain during overbank flow conditions.

1.2.2 Separate Grant and Thesis Research Objectives

The overall aims of the Series C programme are long term goals. They will only be fully achieved through on going research into sediment transport behaviour and with the accumulation of detailed data sets. The aims of the grant (EPSRC grant No. GR/J67567), through which the author was employed, were stepping stones towards the overall objectives.

The experimental programme, described in detail within Chapter 3, was designed around the following grant aims and objectives.

(A) Examine the development of bed topography and texture with time, for different imposed flow conditions.

(B) Determine changes in flow resistance during graded sediment transport in two-stage channels.

(C) Investigate the relationship between bed texture, grain packing and hydraulic roughness.

(D) Produce data to aid design of future graded sediment transport experiments, possibly to be conducted in the Flood Channel Facility.

The specific aims of the author's research had to run in parallel with those of the grant. The objectives are outlined below and were tackled by the author during the period of experimental research and analysis.

(i) To investigate the influence of initial bed slope and stage level on graded sediment transport rates, during degradation, in a two-stage channel.

(ii) To investigate the relationship between graded sediment transport, during degradation, and the associated conditions, at bankfull and shallow overbank flow depths in a two-stage channel.

(iii) To investigate the fractional composition of sampled bedload during the evolution of degradational graded sediment transport experiments in a two-stage channel.

1.3 Layout of Thesis

This thesis contains seven chapters, the contents of which are previewed below.

Chapter 1 - This chapter is intended to provide a brief introduction to a significant problem in river engineering. Also included are introductions to the two basic river engineering subjects of graded sediment transport and compound channels, an introduction to the larger programme of work (Series C) and to the aims of this research project.

Chapter 2 - In the second chapter a substantial literature review is carried out of work involving sediment transport and compound channels. A more detailed introduction is given to both than is provided in Chapter 1. The idea of a threshold of incipient motion is introduced, along with the general mechanics of bedload transport. The difference in graded sediment transport behaviour compared to that of uniform sediment transport is examined and a selection of prediction methods for both are briefly introduced. A section on hiding functions is included, the traditional method used to account for graded sediment behaviour when applying formulae derived from uniform sediment data, and this is complimented by a section discussing the need for a new approach. Finally, within the chapter published work on compound or two-stage channels is reviewed and the relevance of the current work identified.

Chapter 3 - The full programme of experiments carried out is presented in conjunction with a description of both the apparatus and procedures used. The groupings available for the examination of specific variables are presented and each piece of instrumentation described. The procedure used for each experiment is then described to illustrate the quality of the data collected.

Chapter 4 - This brief chapter describes the basic processing undertaken to produce data for use in the research analysis, from the raw collected data.

Chapter 5 - The fifth chapter of this thesis analyses and discusses the sediment transport rates of the five bankfull and overbank degradational experiments examined. The common trend in transport rate decline is discussed. Two methods of estimating boundary shear stress in the main channel, from the non-intrusive measurements, are introduced. The results are compared to transport rates from least squares regression curves fitted to the recorded transport rate data. The weight of material transported by each experiment is also examined and compared to the predicted boundary shear stress values. Finally, the relationship between unit stream power and sediment transport behaviour is examined for each of the experiments.

Chapter 6 - The evolution of the bed surface and the bedload compositions are examined for the five degradational experiments analysed in Chapter 5, plus one additional bankfull experiment. The effects of two variables, initial bed slope and relative depth ratio, are examined. Several characteristics of the experiments, introduced in Chapter 5, are used to establish a suggested order of transporting potential between the experiments. Initial bed conditions are shown to be similar through the use of a statistical technique and the evolutions of bed compositions, bedload compositions and fraction mobility examined.

Chapter 7 - The last chapter contains a summary of the conclusions and suggested further work related to each of the previous chapters. A brief review of the work undertaken is given followed by section devoted to each chapter.

Appendix A - The daily records of the experiments examined within this thesis are presented in this appendix to allow any reader to assess the validity of the results produced.

Chapter 2

Sediment Transport and Compound Channel Flow

2.1 An Introduction to Sediment Transport

Prediction of sediment transport is essential to engineers if they are to assess river response to engineering projects, such as dam construction, water abstraction, channel re-sectioning and flood protection. These can all change the hydraulics and sediment supply conditions within a river reach and result in significant changes in a river's behaviour. Even without the intervention of engineering projects the dynamic nature of rivers can be problematic. Deposition in harbours and estuaries can restrict the navigable waterways and deposition in rivers can increase flood risk. While erosion can destroy valuable agricultural land and near river structures, e.g. bridges, weirs or flood protection measures.

The accuracy problem with sediment transport prediction is well known. Since the classical work of Shields (1936) many other researchers have revisited the problem (e.g. Einstein 1942, 1950; Bagnold 1966; Ackers and White 1973, 1990; Yang 1984; Armanini and Di Silvio 1988; Parker 1990). These investigations have led to many transport prediction formulae which can produce wide ranging results when applied to the same problem. When used in engineering design this uncertainty results in two potential problems;

(i) increased construction costs due to over-conservatism in design, arising from the uncertainty, and

(ii) unanticipated sediment related problems with the finished works.

The situation is further complicated when the sediment under consideration is graded rather than uniform, in composition. The failure of the existing sediment transport prediction techniques, when applied to graded sediment, can be partly explained by the data used in their derivation. Almost all of the methods used in

practise have been developed by adjusting prediction methods originally developed for uniform sediments. The most common approach is to introduce the concept of hiding, where the graded sediment is split into a number of size fractions and the critical shear stress of each fraction is adjusted to account for the presence of the others. Research has shown that the transport rate of sediment in channels is regulated by complex interaction mechanisms, that the hiding function approach fails to account for (Parker et al 1982a; Wilcock 1992; Sutherland 1991; Tait and Willetts 1992). These processes include; turbulence coherent flow structures, size fraction interaction and surface layer re-arrangement among others. It is unlikely that these processes can be fully accounted for by adjusting traditional tractive force or probabilistic sediment transport equations. There is therefore a strong case for research in the area of graded sediment transport. Research in this area may identify and quantify the influences of the processes that are taking place, and develop revised graded sediment prediction methods from first principles.

As previously discussed, the current approach to the problem is to adapt existing formulae to take account of the interactions now seen to be clearly important in transport prediction (White and Day 1982; Parker and Sutherland 1990; Pender and Li 1996). This relies on statistical regression of available data to produce a model applicable over a wide range of conditions. So far reasonable correlations have been achieved between simulations and laboratory data (Proffitt and Sutherland 1983; Willetts et al 1987; Pender and Li 1995), but the current formulae are still limited in application.

One limiting factor is the lack of available data with which to calibrate and test proposed prediction advances. Although a significant amount of work has been carried out examining sediment transport, most of the resulting data sets are insufficiently detailed. They mostly include macro scale measurements of transport rates and hydraulic conditions. These are sufficient for statistical regression but lack the detail to improve the simulations of the small scale physical processes now thought to be important.

It is through the understanding and conceptualisation of these physical processes, controlling the interaction between water and sediment, that the reliability and range of application will be improved (Tait and Willetts 1991; Sutherland 1991).

2.1.1 Incipient Motion

The science of sediment transport is concerned with the relationship between flowing water and sediment particles. It is therefore necessary to understand the importance of the physical properties of water, the individual sediment particles and the bulk sediment involved. For water the significant properties are specific weight, mass density, dynamic viscosity and kinematic viscosity. All of these are sensitive to changes in temperature. For the individual particle; size, shape, density, specific weight and fall velocity properties are all important. For the bulk sediment; size distribution, specific weight and the porosity properties of the bed material are all important (Yang 1996).

Sediment transport occurs at the interface between a moving fluid and an erodible boundary. Transport can occur in two ways. Particles can move either by rolling, sliding or skipping along the boundary or can be fully entrained into the flow itself and transported along within the flow. The first of these two transport types is called bedload and the second suspended load. In rivers there is often another transport process occurring along with the bedload and suspended load. This is called wash load and consists of material which is significantly finer than the erodible boundary of the river. This very fine material is brought into the river system by the run off from the catchment area. It usually remains in suspension until the flow reaches quiescent conditions such as a reservoir, storage pond or the coast. It is therefore important that when field measurements of transport rates are taken the wash load is assessed and it must not be included when comparing measured transport rates with predicted values obtained by calculation.

Bedload transport is the first to occur with increasing power of flow. If the size of material allows, suspended load transport may occur with increasing power of flow. Often bedload occurs on its own or with some suspended load but it is very rare for suspended load to occur in isolation.

2.1.1.1 Threshold of Movement

The threshold of movement of a particle can be visualised by considering a spherical object such as a marble on a flat horizontal surface (figure 2.1). To cause the marble to move only a very small horizontal force is required. This is because the resistance to movement of the spherical marble resting on the smooth horizontal surface is very small. The force just large enough to cause the marble to move defines the threshold of movement. If the marble is then place on top of a tightly packed horizontal surface of equally sized marbles it will rest in a stable position between 3 of the marbles (figure 2.1). The force required to move the marble in any horizontal direction is considerably greater than that which was required to move the marble previously. Thus the threshold of movement is higher for the marble in the second case than it was for the first. Such idealisation has been the basis of work examining the effects of bed conditions on the threshold of motion (James 1990, 1993).

For sediment particles at an erodible boundary the surface on which they rest is not smooth as it consists of more sediment particles. The particles are also very rarely spherical. As a collective bed the particles are much more stable than if they had been exposed to the same condition as single grains. A proportionate amount of the shear force applied to the boundary is applied to the exposed surface of each prominent particle.

Many authors have carried out detailed experiments examining the critical threshold of movement for mobile beds. However due to the stochastic nature of sediment transport it has proved difficult to define the precise conditions of initial movement. Indeed, different investigators have labelled essentially the same conditions in

different ways, e.g. initial motion, the point when several grains are moving, weak movement and critical movement. Most of the resulting incipient motion criteria are derived from either shear stress, velocity or probability conditions.

2.1.1.2 Critical Shear Stress Approach

Shields (1936) and White (1940) both used the shear stress approach to incipient motion. White assumed that the lift force and the force due to gravity acting down the slope of the bed were both insignificant in their influence on initial movement. White further derived that the critical shear stress of a particle was proportional to its diameter. He also suggested it to be a function of the particle density and shape, the fluid properties and the arrangement of the bed over which it had to move.

Shields' work on incipient motion is perhaps the most well known (Shields 1936). He believed that the forces acting on a particle at incipient motion were difficult to express analytically. Dimensional analysis was therefore used to determine dimensionless parameters and establish a framework for determining their relationship. He believed that the important factors in the determination of incipient motion were: the shear stress τ, the density difference between the sediment and fluid (ρ_s - ρ_f), the particle diameter d, the kinematic viscosity ν and gravitational acceleration g. He then grouped these into two dimensionless quantities:

$$\frac{d\sqrt{\tau_c/\rho}}{\nu} = \frac{du_*}{\nu} \qquad \text{Equation 1.1}$$

$$\frac{\tau_c}{d(\rho_s - \rho)g} = \frac{\tau_c}{d\rho g[(\rho_s/\rho) - 1]} \qquad \text{Equation 1.2}$$

where u_* is the shear velocity. The relationship between the two parameters was then determined experimentally. The right hand side of equation 1.1 is the Reynolds

number relating to the grain. The left hand side of equation 1.2 is the ratio of shear force to gravity force and is known as the entrainment function. Shields plotted the entrainment function against the Reynolds grain number and demonstrated that the nature and effect of the transport process was a function of the position on the diagram. The threshold of movement line was later added by Rouse (1939). The Shields diagram has been extensively used by engineers since, as a criterion for incipient motion.

2.1.1.3 Critical Velocity Approach

Several authors have investigated the possibility of defining the threshold of mobility using a critical velocity (e.g. Fortier and Scobey 1926; Hjulstrom 1935; ASCE Sedimentation Task Committee, Vanoni 1977; Yang 1973, 1996. Of these most have produced results through observation rather than analytical approaches. Some of the work has related to average flow velocities due to the difficulty in directly measuring the channel bottom velocity without disturbing the transport process. Yang (1973, 1996) presented an incipient motion criterion describing the relationship between a dimensionless critical average flow velocity and the grain Reynolds number. Yang's approach is based on theories of fluid mechanics but also relies on some experimental derivations.

Although the two approaches of critical velocity and critical shear stress are presented here in separate sections, the two parameters can be related to each other by equation 2.3 below (Pender and Li 1995).

$$u_{cr,j} = C\sqrt{\frac{\tau_{cr,j}}{\rho g}} \qquad \text{Equation 2.3.}$$

Where $u_{cr,j}$ is the critical velocity for size fraction j, C is the Chezy coefficient, $\tau_{cr,j}$ is the critical shear stress for size fraction j, ρ is the density of water and g is gravitational acceleration. Essentially the two approaches are therefore very similar.

2.1.1.4 Probabilistic Approach

The incipient motion of a single sediment particle is dependent on the location of the particle, the instantaneous strength of turbulence and the orientation of both. These conditions can be described by probability functions and for this reason some investigators have taken a probabilistic approach to the determination of incipient motion. Gessler (1965) measured the probability that grains of a specific size will remain in the bed and not be entrained. He found that the probability depends mainly on the Shields parameter and slightly on the grain Reynolds number. He further found that the ratio of the critical shear stress τ_c, from the Shields diagram, and the boundary shear stress τ, related directly to the probability that the sediment particle would stay in the bed.

Other incipient motion criteria have also been investigated by research. All follow similar principles to those outlined in the sections above. Meyer-Peter and Muller (1948) proposed that the size of sediment particle at incipient motion was related to the channel slope, mean flow depth and bed roughness. Mavis and Laushey (1948) used the competent bottom velocity to calculate the size of particle at incipient motion, where competent bottom velocity was defined as 70% of the mean flow velocity. The US Bureau of Reclamation (1987) produced a diagram relating the critical tractive force to the mean diameter, and Ferguson (1994) examined the use of critical discharge for predicting entrainment of particles from a poorly sorted gravel bed. He concluded that a critical discharge approach may not be theoretically superior to other approaches, such as the use of a critical shear stress, but that it may prove to be of practical value.

2.1.2 General Mechanics of Bedload Transport

Most natural flows are turbulent (Chadwick and Morfett 1986), which means that the eddy transport processes are a major part of the general body of flow. At the granular boundary of the bed there exists a sub-layer of flow. This comprises of

'pools' of stationary or slow moving fluid. The structure of the sub-layer is not stable however, and high momentum eddies continually disrupt this region of flow. These eddies originate from the turbulent zone above and cause the low momentum fluid from the sub-layer to be ejected. The momentum difference between the two fluid zones generates a shearing action which in turn generates more turbulent eddies. In this way the eddy transport process is self perpetuating.

The fluid flow subjects the granular bed material beneath the sub-layer flow to fluctuating impulsive forces. If at any point the force is great enough a prominent grain will be dislodged and will roll over its neighbouring grains until it regains stability. If the imposed forces are sufficient to cause more wide spread movement then the collisions and interactions between mobile material produces a more complex flow structure. With an increase in the strength of the flow conditions grain instability penetrates further into the bed. This means that bedload can be most simply represented by a series of layers of sediment sliding over each other. An analogy with laminar flow suggests that the velocity distribution of these layers is linear. The largest velocity being at the surface of the bed and the velocity decreasing into the bed, away from the fluid forces. This model has been used as the basis of various sediment transport equations based on tractive force, such as Du Boys (1879) and Shields (1936).

2.1.3 Uniform Sediment Transport Prediction Methods

As for the investigation of incipient motion, different authors have used different approaches to produce prediction methods for uniform sediment transport. The most commonly applied techniques are based on; boundary shear stress, flow velocity, energy slope, stream power or probabilistic approaches.

The following sections introduce the reader to the different approaches taken to sediment transport prediction methods. The limited examples given have been chosen as they are some of the most well known or commonly used. More complete

and comprehensive reviews are available in literature (White et al 1973a,b; White et al 1975; Yang 1996).

2.1.3.1 Boundary Shear Stress Approach

Initial investigations into sediment transport behaviour focused on the less complex case of uniform sediment transport. Work started at the end of the 19th century with a study by Du Boys (1879). He assumed that the tractive force (shear stress) acting on a movable, non-cohesive, uniform sediment boundary, caused the sediment particles to move in layers along the bed. He proposed that each layer would be of equal thickness. Under equilibrium conditions the tractive force of the fluid flow in the channel would be balanced by the total resistance generated by the moving layers.

Shields' approach to uniform sediment transport prediction is semi-empirical (Shields 1936). He studied incipient motion by examining conditions of non-zero sediment transport rates and carefully measuring the flow conditions. He then obtained a condition for threshold of movement by backwards extrapolation of the relationship between the applied conditions and sediment transport. From his predicted flow conditions at the point of initial motion and using his measurements during conditions of non-zero transport, he was able to derive a semi-empirical transport equation. In his work he reasoned that particle entrainment was a function of the Reynolds number relating to the grain conditions rather than the general fluid flow conditions.

Kalinske (1947) based his idea for the prediction of bedload discharge on the local velocity and shear stress in the bed region. He included terms for the fluctuations of these quantities due to turbulence. This resulted in a relationship that predicts sediment transport at values of average shear stress lower than the critical shear stress for the material. This is an important characteristic in terms of simulating observed transport behaviour.

2.1.3.2 Flow Velocity Approach

The velocity approach is often interchangeable with the shear stress approach due to the link between boundary shear stress and flow velocity. Van Rijn (1984a,b) developed bedload and suspended load formulae based on the difference between the sediment's critical velocity at the threshold of movement and the applied fluid velocity. For the computation of bedload he proposed that bedload transport rate was a product of saltation height, particle velocity and bedload concentration within the near-bed, flow region. He developed his formula by numerically solving the equations of motion for solitary particles to produce saltation heights and particle velocities. Experiments with gravel bedload transport were then used to calibrate his resulting mathematical model. The result was a simple expression defining bedload concentration as a function of the flow and sediment characteristics. From the reference concentration of bedload transport and from measured concentration profiles, Van Rijn's suspended load formula was developed and calibrated. The result is a method for computing suspended load as the depth-integration of the product of local sediment concentration and flow velocity.

2.1.3.3 Energy Slope Approach

Meyer-Peter et al (1934) published work from an extensive series of laboratory experiments examining sediment transport behaviour. From this they produced a bedload prediction formula relating sediment transport to the discharge and energy slope of the channel. The work was then further developed to produce the commonly employed Meyer-Peter and Muller equation (Meyer-Peter and Muller 1948). The updated relation takes account of the specific weights of the fluid and sediment, the geometry of the channel and the size of the material, as well as the energy slope of the flow.

2.1.3.4 Stream Power Approach

Bagnold (1966) produced an equation for sediment transport which many believe is limited in being applicable only to the transport of a specific range of sands in water. However, the equation is interesting in that it is based on the immersed weight of sediment per unit bed area in motion. Movement occurs when the entrainment force of the fluid is greater than the resistive force of the grain. This can be seen from a basic examination of the forces acting on a particle in a fluid flow, the resistance being a function of the immersed weight of the particle. Bagnold proposed that the power to maintain the sediment transport is provided by the fluid flow. He then developed his equation to derive sediment transport predictions from the flow conditions or stream power.

Another popular transport prediction equation based on the power concept is that of Engelund and Hansen (1967). The authors applied Bagnold's stream power concept and the similarity principle to obtain their sediment transport function. The application of the similarity principle, strictly speaking, limits the application of the equation to flow with dune beds. They found through measured data however, that their prediction method was applicable to both dune beds and the upper flow regimes associated with uniform sediment.

An extensively used development in the field of sediment transport prediction is the series of equations presented by Ackers and White (1973). Again the basic approach is based on the stream power concept of Bagnold. This time physical considerations and dimensional analysis are used to produce functions based on three dimensionless quantities. The first of the three quantities is a sediment transport parameter based on the stream power concept. For the bedload this means that the effective stream power is based on the flow velocity near the bed and the net shear force acting on the grains. The theory suggests that only part of the shear stress acting on the channel bed is effective in causing movement of bedload, while it is all effective in causing suspended load. The second quantity is the particle mobility number. This is taken as a function of the applied shear stress and the immersed weight of the grain. The final

quantity is the dimensionless particle size number which expresses the relationship between the immersed weight of the grain and the viscous forces acting. The functions resulting from the work were calibrated over a wide range of experimental and field measurements and are reported to have a good correlation. By this definition, more than 50% of the predicted transport rates were between half and twice the measured transport rates. In 1990 Ackers and White reported a revision of the theory (Ackers and White 1990). This followed uncertainty over the confidence that could be placed in predictions of transport concerning fine and coarse sediments. The revision included the re-derivation of the empirical parameters using the now increased, volume of sediment transport data available. The result was small changes to the equations, producing lower predictions of sediment transport for fine and coarse sediments.

2.1.3.5 Probabilistic Approach

Einstein (1942) introduced two important concepts that differed from those employed previously to predict sediment transport. Firstly, he decided to avoid the critical criteria for incipient motion, as he believed these to be difficult to define. Secondly, he decided to relate sediment transport to the turbulent flow fluctuations, rather than average forces exerted on the bed material. He thereafter assumed that whether or not a particle moves can be decided by probability. The reasoning behind this was that grain movement is caused by the impulse force of near bed turbulent eddies. Einstein assumed that the actions of these eddies were non-uniform in space and time. The occurrence of an eddy capable of entraining a particular grain therefore, is a statistical function of time. Based on experimental work Einstein found that, during bedload transport, particles were exchanged between the bed surface and the bedload itself. He also found that particles moving as bedload tended to do so in jumps along the bed of length relative to the particle size. The transport rate can be taken as the number of grains per unit width of the bed to pass a given cross-section during a given period of time. This was taken as the product of the number of grains, in the surface layer bed area, and the probability that, at any time, a force is imposed on a grain that is great enough to set the grain in motion. The area considered was of

unit width, and length equal to the grain movement length. The probability that a grain is eroded during a time scale of observation is therefore a function of the immersed self-weight and fluid lift force acting on the grain.

2.1.4 Graded Sediment Behaviour

By definition, a graded bed is made up of particles of several different sizes. What makes graded sediment transport more complex and difficult to predict than uniform sediment transport is the interaction between these different sized grains. Basic theory suggests that larger grains are more stable than smaller grains due to their size and, in a graded bed, this allows the smaller grains to be sheltered from the entrainment forces (Einstein 1950, White and Day 1982, Proffitt and Sutherland 1983, Sutherland 1991, Kunhle 1992). This effects the mobility of each size fraction in the graded sediment relative to the mobility of uniform beds of material equal to each size fraction. The larger grains are more mobile in the graded sediment bed than in a uniform bed of large grain size. This is because in the graded bed they protrude further into the flow. They are therefore exposed to a greater percentage of the tractive forces, than in a bed where all the material is the same size. The opposite is true for the finer material. It is sheltered much more by particles of a larger size, in the graded bed, than it is by particles of the same size, in a uniform bed. It is therefore relatively less mobile in a graded bed. The case of a mixed grain size bed is complicated further by increasing the number of particle sizes present in the bed. This can lead to preferential transport of a middle size fraction leaving a bimodal mixture on the bed surface. Preferential transport occurs if the larger material sizes in the mix are too large to be entrained as bedload but the finer material is too well sheltered. This leaves the partially sheltered middle size material as the only size able to be entrained.

The interaction effect between particles of different sizes is known as hiding. Hiding itself is affected by the ability to shelter in the active layer of the bed and by the feedback effect of the bed surface geometry on the near-bed flow structure. Surface geometry can affect eddy shedding and the resulting generation of wakes,

turbulence and grain motion. It is therefore important to take account of bed surface characteristics when evaluating the affect of hiding on sediment transport.

In a uniform bed, changes in transport rate with time are linked to changes in bed forms and changes in the hydraulic conditions. For graded sediment beds, with all other applied conditions remaining equal, it is possible for the bed composition to control sediment transport rates. This occurs due to the development of an armoured bed surface layer. The composition and arrangement of the exposed surface material adjusts to prevent erosion by balancing the forces acting within the transport environment. Two kinds of armour layer have been reported in literature (Proffit and Sutherland 1983, Parker and Sutherland 1990).

2.1.4.1 Mobile Armour

The mobile armour surface that is formed during the transport of non-uniform material has been the subject of many publications (e.g. Parker et al 1982a, Parker 1990, Parker and Sutherland 1990, Wilcock and Southard 1989). Mobile armour has been found to occur in the presence of active gravel bedload transport, as a bed surface adjusts to the applied conditions (Parker 1990). Through selective transport and hiding processes an active armour layer is developed that is approximately one large grain size thick (Parker and Sutherland 1990, Sutherland 1991). This active layer of temporarily stored material acts as a buffer between the moving bedload and flow and the substrate, the composition of which is finer. The protection provided is such that in the presence of an active mobile armour layer the immediate substrate is only occasionally disturbed while deeper particles are hardly ever disturbed (Parker et al 1982a). The product of a mobile layer development is a condition of equilibrium transport, such that the quantity and composition of the sediment load entering a reach is matched by that leaving. The fact that the coarse surface layer condition is described as "mobile" and "active" illustrates the interaction between the bedload, the armoured layer and the substrate.

2.1.4.2 Static Armour

If the flow conditions applied to a graded sediment bed are insufficient to move the entire range of particles within the bed composition then the composition of the bed surface will evolve with time. The degree of coarsening that occurs on the bed surface is enhanced by the imbalance between the upstream sediment supply and the transporting capacity of the flow (Tait et al 1997). Thus, for the extreme non-equilibrium transport condition of zero upstream sediment supply the imbalance is at its greatest and the developing armour is said to be static rather than mobile. Mobile armour development and static armour development are closely related (Parker and Sutherland 1990). The same processes of selective transport and particle hiding occur during static armour development but, because the upstream sediment supply is nil, the evolution to a fully armoured state is more direct. No sediment is deposited into the armour layer to replace the eroded material and so the bed degrades, and the transport rate decreases as coarse, immobile material accumulates on the bed surface (Tait et al 1992). Willetts et al (1987) concluded that sediment transport behaviour was dependent on prior as well as contemporary flow conditions. This suggests that static armour stability is related to surface material arrangement as well as composition. Recent work published by Tait et al (1997) agree that this is the case. Other work by Tait and Willetts suggest that the composition of a static armoured surface stabilises early on in its evolution but that stability is continually increased by grain rearrangement (Tait and Willetts 1991; Tait and Willetts 1992; Tait et al 1992).

2.1.4.3 Equal Mobility

The theory of equal mobility is linked to the development of armoured surface layers (Parker et al 1982a; Parker et al 1982b; Parker and Sutherland 1990). By formation of an armour layer the fluvial system is attempting to equalise the relative mobilities of the different grain sizes (Parker and Sutherland 1990). The coarse material is intrinsically less mobile than the fine material. In an armour layer the coarse material is concentrated in larger quantities than the fine material, exposing a larger number of coarse grains to the flow. The availability for transport of the coarse

grains is therefore considerably greater than that for the fine grains. This attempts to balance the intrinsic lower mobility of the coarse grains and so render all the grains in the armour layer of near-equal mobility (Parker et al 1982a).

A further point relating to armour layer behaviour is the reaction to increased tractive forces. To break a developed armoured surface the applied hydraulic forces have to at least peak above the critical threshold value for the stable bed composition and arrangement. During this peak all the particles are able to be readily entrained and the bedload composition approximates that of the substrate bed material (Parker et al 1982b).

2.1.5 Graded Sediment Transport Prediction Methods

Those developing graded sediment transport prediction methods have used various approaches, as for the determination of incipient motion and the computation of sediment transport rates. Many of these are variations on the equations introduced previously in section 2.1.3. Again, more complete and comprehensive reviews are available in literature, of the methods introduced in the following sections (White et al 1973a,b; White et al 1975; Yang 1996).

2.1.5.1 Stream Power Approach

Yang (1972) reviewed the basic assumptions that were made during the formulation of conventional sediment transport equations. He concluded that it had been assumed that sediment transport rate was derivable from water discharge, average flow velocity, energy slope and boundary shear stress. He felt that these assumptions were questionable which in turn lead him to question the generality and application of the available transport equations. Instead, Yang approached the problem by defining unit stream power as the product of velocity and slope. Yang proposed that the rate of work done, by a unit weight of water in transporting sediment, must be directly related to the rate of work available to the unit weight of water. This lead to his

alternative assumption that the total sediment concentration must be directly related to unit stream power. Yang's assumption therefore stresses the availability of power per unit weight of fluid to transport sediments (Yang 1972, 1973). This approach is similar, but slightly different from that of Bagnold (1966). Bagnold's work assumed the stream power applied to a unit area of bed. Yang used dimensional analysis along with multiple regression analysis of laboratory data to investigate the proposed relationship between unit stream power and sediment transport. The basic form of the unit stream power equation offered by Yang was derived from well established theories in fluid mechanics and turbulence. The result of his work was predictions relating bedload, suspended load and total load concentrations directly to unit stream power (Yang 1996). Though Yang's approach is applicable to graded sediment it assumes that any sediment grading can be approximated by using the d_{50} value.

2.1.5.2 Probabilistic Approach

Einstein modified his approach to allow it to be applied to graded sediment transport (Einstein 1950). In the new approach the transport rate of each size fraction is computed individually. A hiding factor is then applied to define the influence of mutual interference between the particles of different sizes. The result is an estimation of not only the sediment transport rate, but also composition of the material transported. Unfortunately the method is complex to use and does not always produce comparisons with observed transport rates. However, Einstein's important contribution to the field remains the introduction of the probability concept. Authors have since attempted to developed Einstein's work further or use it as a starting point (Bishop et al 1965; Brown 1950). Bishop et al (1965) published work improving Einstein's equations for certain specific conditions by treating two of Einstein's original constants as variable quantities.

2.1.5.3 Equal Mobility Approach

Parker et al (1982b) proposed a hypothesis called equal mobility. It was first developed as part of a substrate-based bedload relation (Parker et al 1982b), and then as part of a surface-based relation (Parker 1990). The theory of equal mobility consists of two parts. The first is equal entrainment, which is defined as occurring when each particle in a graded sediment bed surface is equally likely to be entrained, see section 2.1.4.3. The second is equal transport mobility, defined as the state when all sizes are transported according to their relative proportions in the bed. This essentially means the bed and the transported load have the same size fraction composition.

Parker et al (1982b) define the pavement layer as the coarse surface layer present during periods of bedload movement during which all sizes of the bed material move. However, it has been found that both conditions of equal mobility do not necessarily occur together during transport conditions.

When Wilcock and Southard (1988) reported on their laboratory flume experiments with graded sediment beds they found this to be the case. All their experiments showed almost perfect equal entrainment, but only during their high flow strength experiments did the transported material approach the composition of the bed and therefore equal transport mobility. Wilcock and Southard (1988) further concluded from their work that incipient motion occurred at nearly the same critical conditions for all sizes within their gradings. This was true for all the ranges of unimodal and weakly bimodal mixed grain size beds tested. They also found a common trend between different beds. The critical conditions for the threshold of motion matched the critical conditions for motion of a uniform bed made up of material of approximate size to the d_{50} of the graded bed. However, it appears that this is not the case for strong bimodal mixes. The work of Kunhle (1992), at Goodwin Creek, Mississippi, concluded that the size independence of the fractional critical shear stress is no longer maintained. In the case of strongly bimodal beds the larger grains

in the sediment mix require a larger shear stress to move them than the smaller grains.

Discussion regarding the validity of the equal mobility hypothesis continues. However, the work of Parker et al (1982b) enabled the development of an empirical gravel transport function based solely on field data. The function relates two groups of parameters defined as the dimensionless bedload transport function and the dimensionless shear stress parameter. Because of the theory of equal mobility of all sizes, only one grain size is used to characterise the bedload discharge as a function of the dimensionless shear stress. The grain size used is the d_{50} size of the substrate material.

2.1.6 Hiding Functions

The processes of graded sediment transport are more complex than the processes of uniform sediment transport. This is due to the interaction between different sized particles within a graded sediment bed. Often this in turn leads to inaccurate predictions of transport rate based on a single representative grain size and using a uniform sediment transport prediction model (Pender et al 1993; Li 1995).

In an attempt to improve the prediction of graded sediment transport hiding functions have been developed for use with existing sediment transport predictors. Hiding functions are used to account for the interaction between size fractions in graded sediment. In order that hiding functions can reproduce this phenomenon, within a transport calculation, the sediment composition is separated into a number of different size fractions. Each size fraction is then represented by a single grain size. The empirical hiding function then modifies the critical shear stress of each size fraction to account for the existence of the other sizes within the mix. For examples of this see Einstein (1950), Parker (1990), Proffitt and Sutherland (1983), Sutherland (1991) and White and Day (1982). A key element of this theory is the assumption that all particles within a defined fraction size behave in the same way or demonstrate equal mobility (Kirchner et al 1990). Threshold evaluation for each

fraction within the graded sediment is critical in estimating graded sediment transport rates (Li 1995).

Two forms of hiding functions are presented and defined in literature (Li 1995). The first was published by Einstein (1950) and an alternative introduced by Parker (1990). Einstein's hiding function is defined as the ratio of: the critical threshold condition for a particular grain size within a graded bed, to the critical threshold condition of that grain size relating solely to the Reynolds number of that grain size and the Shields diagram. As a result, the hiding function can be said to be dependent on the three parameters of: relative particle size within the bed, the deviation of the bed grain size distribution and the Froude number of the flow conditions imposed.

Parker's reduced hiding function is similar in form to the function proposed by Einstein and is defined as the ratio of: the threshold condition from Shields' diagram relating to the Reynolds number for the geometric mean size of the graded bed, to the threshold condition for a particular grain size within the graded bed. Therefore, Parker's reduced hiding function is also dependent on: the relative particle size within the bed, the geometric standard deviation of the bed composition and the Froude number of the flow.

The two definitions are clearly not independent of each other. Einstein's function essentially relates the mobility of a size fraction within the graded bed, to the mobility of a uniform bed of that size fraction. Parker's function however, relates the mobility of a size fraction within the graded bed, to the mobility of a uniform bed of a size equal to the geometric mean of the graded bed.

The evaluation of different hiding functions for the use with different non-uniform sediment transport formula depends largely on good quality experimental data. The derivation of a function assumes that all the complex interactions taking place in graded sediment transport are contained within the observed data. It is then assumed that the resulting hiding function will faithfully reproduce these interactions when applied to independent analysis. A number of hiding functions have been developed

and published for use with various different equations (e.g. Einstein 1950; Parker 1990; Proffitt and Sutherland 1983; White and Day 1982). Of the two proposed forms for hiding functions presented in literature the reduced hiding function has shown advantages over the alternative form (Pender and Li 1995). However, this study only considered the two forms developed for the sediment transport formula of van Rijn (1984a,b).

The two commonly used approaches to graded sediment transport prediction are hiding functions and the approximation of equal mobility. It is suggested that of the two, a hiding function related to particle size, grain size distribution and flow conditions will provide better results over a wider range of conditions (Li 1995). However, even the best hiding functions developed for use with the best of the uniform sediment transport models are still limited in their application and accuracy (Bennett and Bridge 1995).

2.1.7 Requirement for a New Approach to Graded Sediment Transport

It is now thought to be the case that small scale physical processes play a more dominant role, in determining the global evolution of mobile bed rivers, than previously appreciated (Pender and Li 1996). It may be that graded sediment transport has behaviour patterns in common with the now widely discussed chaos theory (Gleick 1987). Many of the existing approaches have only dealt with macro scale parameters which may in part explain their limitations. Over the last two decades this has become increasingly apparent and researchers have begun to investigate individual areas of the problem more closely.

The effects of relative protrusion, pivoting angles and bed topography on the threshold of entrainment for individual size fraction within a bed have been examined by Fenton and Abbott (1977), Kirchner et al (1990) and James (1990) and (1993). The role of turbulence in mixed grain size sediment entrainment and subsequent transport was addressed by Grass (1983) and Thorne et al (1989). The nature of the transport of individual size fractions over a mixed grain size bed has

been discussed by Diplas (1987), Wilcock and Southard (1989), Wilcock (1992, 1997) and Wilcock and McArdell (1993, 1997).

Traditionally engineers have numerically modelled sediment transport problems by simplifying conditions and defining them in one-dimension. One-dimensional dynamic processes in mobile bed channels can then be described mathematically by sets of partial differential equations (Holly and Rahuel 1990; Pender and Li 1996). The equations derived describe: water volume conservation, water momentum conservation, suspended load transport, bed load transport, bed material conservation and bed material sorting. The limitation to one-dimension implies that the values of the dependent variables are averaged over a cross-section. This means that these approaches take no account of parameter variation across a channel, no account of bends in the channel and no account of any effects caused by bends. Consequently one of the limitations is that no predictions about changes in planform can be made.

If improvements are to be made in graded sediment transport prediction, the author believes that, small scale processes must be taken into account in prediction formulae. This may require a new approach not necessarily based on existing formulae or theories of equal mobility and hiding. However, the small scale processes are highly complex. It is therefore essential to understand the influence of the controlling parameters involved, rather than trying to produce regression based predictions. Some of the topics thought to influence graded sediment transport are discussed below.

The capacity of a set of flow conditions to transport plays an important role in controlling graded sediment transport rate. The capacity defines the maximum transport rate that can occur. Adequate quantification of this is therefore central to any prediction method. All other influences will then control how close to this capacity the actual transport is and how the capacity and the transport vary with time.

The varying levels of interaction between grains of different sizes in both the bed and the bedload is important to understand, and quantify, if improvements are to be

made. To date hiding functions have been used to address this problem. However, small scale changes in interaction may not be described sufficiently by this existing approach.

The texture of the bed plays a part in the control of sediment transport in that it influences the hydraulic resistance and the near-bed flow structures. It is known that for material with a mean grain size diameter greater than 2 mm the dominant influence on flow resistance is grain size composition or grain roughness. The resistance can therefore be determined from a representative grain size. For beds with a mean grain size less than 2 mm, flow resistance is also partly controlled by bed form roughness. The evaluation techniques for hydraulic resistance of Engelund and Hanson (1967), White et al (1980) and Van Rijn (1984a) have all been found to give reasonable results for flume and river data (Van Rijn 1984b).

The characteristic length for suspended load and the travel length for bed load should also be considered in any new approach to graded sediment transport prediction. The characteristic length of suspended load has been used in the past to describe temporal and spatial lags in transport rates due to unsteady flow. The same temporal and spatial lag reactions have been found to occur in bedload by Bell and Sutherland (1983), in steady flows, under non-equilibrium conditions, with zero upstream bedload input. Knowledge of the travel length of bedload under given conditions would help to describe such reactions.

Particle fall velocity has an influence on the transport of material in suspension and should therefore be considered in any total sediment transport prediction approach. A significant amount of work has already been done in this area and reasonable estimates are believed to be available. The fall velocity for particles smaller than 0.1mm in clear still fluid can be derived from Stokes' law, while two relationships are provided by Van Rijn (1984b) for larger particles. A correction has also been provided for situations involving large concentrations of particles (Yalin 1977).

The mean velocity of the bedload has an influence on transport rate. Bagnold assumed that for steady continuous saltation, the fluid velocity causes a mean fluid drag on the particle which is in equilibrium with the mean bed frictional force (Bagnold 1973). This led Bagnold to suggest a relationship for calculating the mean velocity of the bedload partly based on the premise that saltation height is a function of sediment size.

The bottom layer is defined as the height above the bed surface in which bedload transport takes place. Evaluation of the layer thickness may therefore enable better predictions of transport to be made. Garcia and Parker (1991) summarised the choices for defining bottom layer thickness. These included defining it; as a function of flow depth, as proportional to sediment grain size, as a function of bed form height or as the elevation of the top of the saltation layer. All these approaches have there relative merits, and further investigation may outline a clear choice.

Another influence on sediment transport rates and compositions is the thickness of the active layer. The concept of the active layer differs between degradational and aggradational conditions. For aggradation it is easy to define, in that it is the depth of deposited stratum accumulated during each given time increment. For the case of degradation the boundaries are less clear. The active layer is defined as the depth of bed from which erosion takes place. Holly and Rahuel (1990) used empirical conceptualisation to evaluate the active layer thickness, while Armanini and Di Silvio (1988) set the thickness as equal to the bottom layer depth, with a minimum limit of 0.05h.

The discussion above is by no means exhaustive in terms of small scale influences on sediment transport behaviour. It demonstrates however, that a new approach to sediment transport would need to be based on more than the macro scale influences of shear stress or stream power used before. This approach should, in some way or form, quantify the influence of these and other small scale influences, as without doing so may yield methods no better than the techniques available at present.

If such a new approach may is thought to be overly complicated it may be worth remembering once more the extreme complexity of the natural phenomenon. Reid et al (1985) have reported that natural beds can show different conditions for the incidence of bedload transport, for successive floods, while having essentially the same composition. They suggest that long periods of low or no transport cause the beds of natural rivers to consolidate. Consequently, when the next significant flood event comes along, it takes a more extreme flow to initiate transport and the transport is often confined to the recession limb of the event. They also reported that initial motion in a natural bed, caused by the earlier stages of a flood event, may occur at a higher shear stress than that at which motion ceases.

Such a new approach taking account of many small scale processes is beyond the present study. Indeed it may be beyond the current knowledge of the subject today. In order to advance towards the goal of an accurate prediction method for the behaviour of natural channel evolution, more basic research is required. The research can be divided into two categories. Firstly, more complete data sets studying graded sediment transport need to be made available. These must include a wide range of parameter measurements at clearly recorded conditions. This will allow calibration and testing of any theories put forward. Secondly, research into the small scale processes needs to continue. With the further understanding of the influences of such processes the foundations for a better prediction method will be laid.

2.1.8 Research into the Behaviour of Graded Sediment

This section is by no means meant to review or discuss the research cited, rather, it is meant to illustrate to the reader the wide range of research published on the general topic of graded sediment behaviour. The section will be split into four sub-sections, covering three centres of research in the UK and a selection of researchers from the rest of the world. Many other researchers have produced interesting and useful publications but are not referenced here for the sake of brevity.

2.1.8.1 HR Wallingford Ltd.

HR Wallingford Ltd. (HR), previously the UK government Hydraulic Research Station, has for many years been a centre of research into graded sediment transport. One of the most commonly used transport prediction methods. the Ackers and White Theory, was derived and revised by researchers associated with HR (Ackers and White 1973, 1990).

As well as playing a key role in the development of large scale, physical modelling, research projects at HR (Bettess 1994, 1997) Bettess has also published work on the initiation of sediment transport in gravel streams (Bettess 1984).

Day, although normally associated with the Geological Survey of Canada, did spend some time at HR and has published co-authored papers with White (White and Day 1980, 1982; Day 1980). All three papers examine the characteristics of transport for graded sediments with reference to the behaviour of different size fractions. Some experimental results are presented.

Other work published by White in association with HR includes reviews of existing sediment transport prediction methods and their performance (White et al 1973a, 1973b, 1975). Later work, included in a conference paper, examined the interaction between engineering projects and fluvial morphology (White 1987). In this White identified considerations for the river engineer along with important river processes and characteristics.

In more recent years, research undertaken by HR has tended to be numerically based, due to the greater expense associated with physical modelling. A recent report published by HR examines the possibility of numerically modelling lateral variations in sediment transport (Seed 1996).

2.1.8.2 The University of Aberdeen

A succession of research grants awarded to the university have meant that research into graded sediment behaviour has been active in Aberdeen for over a decade. The most recent grants, one of which resulted in the work presented in this thesis, have been held jointly with the University of Glasgow.

Tait spent several years at Aberdeen, before moving to Sheffield, and published several papers and a Ph.D thesis as a result of physical and numerical experiments examining bed armouring processes (Tait and Willetts 1991, 1992; Tait et al 1992; Tait 1993). More recent work by Tait has included a conference paper on the adjustment of the turbulent flow over a stabilising gravel bed (Tait and Willetts 1995). Another, from the Series C work, examined the re-arrangement of particles on the bed during sediment feed conditions (Tait et al 1997).

Willetts has published work on several aspects of graded sediment transport. Earlier work included numerical simulation of armour development, which was compared to experimental results gained by other researchers (Willetts et al 1987). Hardwick and Willetts (1991) devised a novel sediment trap that allowed examination of changes in sediment transport rates and bedload composition during the early stages of bed armouring in small scale experiments. Wheeler and Willetts (1994) used the same laboratory flume to examine the effects of upstream sediment feed upon the movement of graded sediment. The examination included a study of the feed effects on near bed velocities through the use of a laser doppler anemometer (LDA) velocity profiler. More recently Willetts' involvement in the Series C programme has lead to two conference papers. The first examines bedload transport rates and compositions, for bankfull and overbank flow, over a gravel bed, with and without upstream sediment feed (Willetts et al 1997). The second, co-written with the author, compares transport rates, bedload compositions and final bed compositions associated with degradation from man-made and water worked beds (Pender et al 1997).

2.1.8.3 The University of Sheffield

Researchers associated with the University of Sheffield have produced several papers relating to the behaviour of graded sediment beds. The majority of the published work has related to field studies and attempts to numerically model the observed behaviour.

Ferguson and Ashworth (1992) published a discussion of field techniques for the measurement of spatial patterns of bedload transport and the non-uniform characteristics of natural channel flow. Results from field studies were presented and estimates of mean transport rates, and streamwise variations in transport, from within-reach stream budgeting were discussed. Ferguson (1994) showed that, the effect of relative grain size on entrainment from a graded sediment bed can be included in a semi-theoretical equation for critical unit discharge. He concluded that results using the derived equation match well the sensitivity to grain size and the absolute levels of critical discharge reported by others. Wathen et al (1995) used results from field studies to examine size fraction mobility during several flow events in a weakly bimodal sediment bed river. In a paper published by Ferguson et al (1996) field data is presented that provides evidence of downstream fining due to selective transport, rather than due abrasion. The researchers state that the strong downstream fining is linked to the river system's tendency to minimise downstream variation in bedload transport rates.

Hoey (1992) proposed spatial and temporal classifications for the variation in bedload transport and sediment storage reported in previous published work. Three scales were suggested, each containing a wide range of processes acting to produce the observed bedload fluctuations. The development of a numerical model to simulate downstream fining by selective transport, observed in previous field studies, was reported by Hoey and Ferguson (1994). Within the model the simulated channel was free to adjust in longitudinal profile and bed surface composition. More recently sensitivity tests on the model have been reported (Hoey and Ferguson 1997).

2.1.8.4 The Rest of the World

An introduction to some of the graded sediment work published by a selection of commonly referenced researchers from the UK has been presented above. Of course, graded sediment research is by no means limited to the UK, as can be seen from the references cited previously in this chapter. For completeness the work of some of the more referenced researchers from the rest of the world is included in this sub-section. This is again intended purely to illustrate the depth of work published on graded sediment behaviour.

Gomez (1983) used field studies to examine the effects of progressive bed armouring on the temporal variations in bedload transport caused by the limitation of material available for transport. A decade later he published work examining grain roughness of stable armoured beds formed in a laboratory flume (Gomez 1993). This work was followed by more experimental results evaluating the effects of particle shape and grain mobility, on the development of stable armour layers (Gomez 1994).

Four years of field studies, located on Goodwin Creek, lead to a paper by Kuhnle (1992), which examined the different fractional transport rates observed. Using his field data he also proposed a technique for calculating bedload transport by separating the sand and gravel fractions. The work on fractional transport was furthered by a paper examining the initiation of motion and fractional transport rates of bimodal sediments using laboratory flume and natural channel data (Kuhnle 1993). More recent work associated with Goodwin Creek, examined the effects of a reduction in the area of cultivated land in the channel catchment area, on the concentrations of sediment in the flow (Kuhnle et al 1996).

Parker has been one of the most prolific authors of papers dealing with issues of graded sediment transport. Parker et al (1982a) used laboratory experiments to model channels with a graded sediment bed and examine the phenomenon of mobile bed armour. In the same year Parker et al (1982b) used field data to study the size distribution of the bedload in armoured gravel bed channels. The paper also included

the development of a substrate-based graded sediment transport relation. In a later paper Parker (1990) converted the existing substrate-based relation, developed solely with reference to field data, to a surface-based relation. Again in the same year, Parker and Sutherland (1990) published a paper examining the ability of two numerical models, designed to predict the transport of non-uniform sediment, to be used to predict the development of fluvial armour. In Parker (1991), he presented a framework for the simultaneous treatment of selective transport and abrasion which is believed to account for the process of downstream fining. While in Parker and Wilcock (1993), the researchers examined the different equilibrium conditions produced by graded sediment flume experiments operating recirculation and sediment feed conditions.

Sutherland has also been the author of a significant amount of work relating to graded sediment processes. Proffitt and Sutherland (1983) modified two existing transport rate formulae based on laboratory experiment data. The result allowed both the transport rates and the size distribution of the transported material to be predicted, knowing the hydraulic conditions and bed material grain size distribution. Bell and Sutherland (1983) examined the transient gravel bed response to steady non-equilibrium flow conditions for reaches of different lengths. They also reviewed previous research and general numerical models associated with non-equilibrium alluvial conditions. Phillips and Sutherland (1985) describe a one-dimensional unsteady flow and sediment transport model, able to simulate spatial and temporal lag effects, and test it against experimental results. They then went on to examine the temporal lag effects on bedload transport, caused by changing flow conditions, using laboratory experiments (Phillips and Sutherland 1990). A temporal model was also developed and tested against measured data. A selection of empirical and analytical hiding functions were presented by Sutherland (1991). Several significant issues relating to the use of the presented functions were then discussed with reference to work on grain mobilities by Kirchner et al (1990). Hoey and Sutherland (1991) presented results of an experimental study examining the relationship between bedload pulses and channel morphology.

One researcher in particular, from outside the UK, who has devoted a considerable amount of time to studying graded sediment transport related problems is Wilcock. In Wilcock (1988) he examined two commonly used methods for estimating the critical shear stress of individual size fractions within a graded sediment. He went on to describe a general definition for initial motion which allowed the characteristics between the methods to be explained in terms of sampling and scaling considerations. Wilcock and Southard (1988) followed this with a study of the critical shear stress, for incipient motion, of individual size fractions in graded sediment beds, using five laboratory flume experiments. A year later, Wilcock and Southard (1989) published a paper examining fractional transport rates, bed forms and the development of a coarse surface layer during graded sediment, bedload transport using a recirculating laboratory flume. Wilcock (1992) examined, through an experimental investigation, the effects on sediment transport dynamics of graded sediment properties. The now famous "bed of many colours" allowed Wilcock and McArdell (1993) to investigate mobilisation thresholds and the resulting partial transport, of a bimodal bed, in relation to surface-based transport rates. While Wilcock et al (1996) reported on field measurements which relate flow characteristics to sediment entrainment for a large gravel-bed river. In a sister paper, Wilcock et al (1996b) develop a basis for evaluating a sufficient discharge for sediment maintenance flows in the same large gravel-bed river. In the same year Wilcock (1996) reviewed and evaluated, using replicate field velocity profiles, three methods of estimating local bed shear from velocity observations. In the following year Wilcock and McArdell (1997) demonstrated the existence, and limits, of partial transport, using flume experiments with graded sediment, while Wilcock (1997) examined the components of fractional transport rate.

2.1.9 Existing Extensive Graded Sediment Transport Data Sets

The previous sub-sections and the work already referenced in this chapter, demonstrate the large amount of published research concerning graded sediment behaviour. However, complete data sets of a significant size are still very limited in number. In this context, the term "complete" is being used to describe data sets that

provide descriptions of size fraction transport rates and hydraulic conditions, in sufficient detail to facilitate use in new research. Li (1995) reviewed the literature for such data sets in order to allow the calibration and verification of hiding functions developed for used with Van Rijn's transport formula (Van Rijn 1984a, b). Three such extensive data sets were found.

The United States Waterway Experimental Station (USWES) (1935) published the results of an extensive series of experiments into graded sediment transport. The work covered nine different bed material mixes with each mix being tested for a variety of different conditions. However, a full range of information relating to the conditions is only available for three of the nine gradings. The grading details are listed in table 2.1.

Table 2.1 Grading Details for USWES (1935) Experiments

Grading Number	Range of D_i (mm)	D_{50} Size (mm)	σ_g Value
1	0.153 - 2.86	0.42	1.82
2	0.153 - 2.03	0.44	1.51
9	0.925 - 5.56	4.10	1.45

Three slopes were tested for each of the three gradings. For the finer gradings 1 and 2, the slopes tested were 0.001, 0.0015 and 0.002 while steeper test slopes of 0.003, 0.004, and 0.0045 were used for the coarser grading 9.

All the experiments were carried out in a tilting flume 18.89 m long and 0.9 m wide which had a sediment trap positioned at the downstream end of the flume to allow for transport rate measurement. At the upstream end of the flume an automatic sand feeding device was used to feed material into the channel at a rate approximately equal to that leaving the channel. A constant discharge was imposed down the channel, while bed and water surface levels were measured using pointer gauges positioned on instrument rails. This allowed the section averaged velocities to be calculated from the discharge and cross-sectional areas. The elevation at the downstream end of the flume and therefore the flow profile was controlled by a vertical sliding tailgate. Visual identification was used to judge the intensity of sand

movement and to classify the bed forms occurring. Unfortunately, during each run only one measurement of sediment transport was made making it impossible to establish the precision of the measured transport data. Between the three gradings 53 experimental runs were carried out. Seventeen runs were carried out with each of gradings 1 and 9 while nineteen runs were carried out with grading number 2.

Gibbs and Neill (1972, 1973) evaluated basket-type bedload samplers. In the presentation of their work they provided an extensive data set covering two series of experiments. The same bed material composition, outlined in table 2.2, was used in all the experimental runs.

Table 2.2 Grading Details for Gibbs and Niell (1972, 1973)

Grading Title	Range of D_i (mm)	D_{50} Size (mm)	σ_g Value
G&N	1.02 - 14.2	4.75	2.28

The grading had a similar median size to that of the USWES grading 9, but had larger σ_g value. A nearly constant flow depth was used for all the experiments along with a narrow range of mean velocities. The shear stress was varied between the different experimental runs by varying the flume slope.

Only six transport measurements are available, however each of these represents the average of a detailed study of the variations in transport rates. During each experimental run 50 transport measurements were taken using a slot sampler in the flume bed. The length of each sample varied while the interval between each of the samples was kept constant.

The third data set was the result of two series of experiments carried out at HR Wallingford (Day 1980). For both sets of experiments the bed material was made up of a natural mixture obtained from a local gravel pit. The first series was called HRS-A and the bed material was widely graded and bimodal. The second series was called HRS-B and the bed material comprised of a selection of fractions extracted from the

HRS-A bed mix. The resulting bed composition had a similar mean size but a narrower grading. Both bed mixes are detailed in table 2.3 below.

Table 2.3 Grading Details for Day (1980)

Grading Title	Range of D_i (mm)	D_{50} Size (mm)	σ_g Value
HRS-A	0.153-14.2	1.75	4.28
HRS-B	0.153-5.56	1.55	3.24

The same flume was used in the two sets of experiments as was used in the work presented in this thesis. A more complete description is given later in Chapter 3. Briefly, the flume was 2.46 m wide and 25 m long, with a re-circulation system for the water discharge. During the two sets of experiments HRS-A and HRS-B a sediment transport return system was also used. The sediment returned to the upstream end re-entered the flume downstream of the main pump discharge vents but upstream of the start of the original bed. Initially a 0.2 m deep sediment bed was laid in the flume for all the experiments. This was levelled off using a template. After each run of series HRS-A the top few centimetres of the bed were removed and replaced by fresh material so that the new experiment would not be affected by vertical sorting. The new material was then levelled using the same template. For the HRS-B series of experiment each new bed was formed from 0.1 m thick layer of fresh material placed on top of a sheet of plywood on top of the previous bed.

Within each run there were several tests. Each test consisted of measurements of sediment transport rate, discharge, water surface elevation and flow depth. The sediment transport measurements were taken as the material was returned to the upstream end of the flume and were measured in parts per million by weight. The water surface was derived using regression analysis of the collected surface elevation data, while the mean flow velocities were calculated assuming continuity. Twenty runs in total were carried out, 11 during series HRS-A and 9 during series HRS-B.

2.2 An Introduction to Compound Channel Flow

One important consideration that should be taken into account, when assessing further developments in graded sediment transport prediction, is applicability to overbank flows. To date, the data used in development of sediment transport predictors has been from in-channel flow experiments. It is therefore, unknown whether predictors in there present form will apply to overbank flow conditions found in compound channel cross-sections.

Historically society has been dependent on rivers for irrigation, transport and power. This has led to the tradition for centres of population to be cited on river flood plains. The continued urbanisation of our catchment and floodplain landscapes has increased the problems associated with flooding, caused by larger rainfall events. Flood plains are a natural part of the river channel and are utilised for larger flows once or twice a year, but society still wishes to be protected from inundation. Many solutions have been offered by engineers through the years. However, judging from global and local examples, such as practically the whole of Bangladesh in 1989, the Mississippi in 1993, the Tay in January 1993 and the Clyde in December 1994, complete protection has not yet been achieved.

Traditional flood alleviation or protection methods have contributed to the demise of many natural riverine habitats and environments (Purseglove 1989). These traditional methods include re-sectioning, re-alignment and bankside levees (Hey et al 1994). Re-sectioning of channels by dredging increases the channel discharge capacity within the existing channel width dimensions, but destroys the existing channel environment. Re-alignment of the channel course reduces the resistance to flow caused by bends, thus allowing the flood event to pass more quickly through the reach. This obviously damages both channel and bankside environments. Bankside levees prevent inundation of adjacent flood plains by enclosing the existing channel within high flood banks. This can result in diminished flood plain habitat.

Recently an environmentally educated society has demonstrated its awareness of the detrimental effects of some of the previously implemented flood prevention schemes. In doing so it has begun to demand environmentally sensitive flood alleviation schemes. Practising engineers have therefore been encouraged to conserve and enhance natural river environments, wherever possible, in the design of these schemes. One of the better options now being widely promoted is the use of two or multi-stage compound channels (Hey et al 1994; Reeve and Bettess 1990). A multi-stage channel is created by placing artificial limits such as flood banks on the flood plain set 3 to 6 main channel widths back from the main channel / floodplain interface. Another way of creating a two-stage channel is by removing a section from the bankside flood plain to make the upper half of the existing main channel significantly wider. The former of these two approaches is preferable due to the lack of destruction of existing channel form, environment and habitat.

A compound channel can be defined as a simple main channel, in which normal low flows are wholly contained, with either one or two flood plains or berms at either side. These flood plains are dry for most of the time, but convey discharge during periods of high flow. One common characteristic of compound channels is that the flow depth over the main channel is much greater than the flow depth over the flood plains. Another is that the boundary roughness of the flood plains is usually considerably rougher than that of the main channel. These aspects mean that the velocity distribution and the lateral distribution of boundary shear stress are both non-uniform across any given cross-section. This makes the calculation of the stage / discharge relationship for compound channels more difficult. Recently this has been highlighted by various authors who have concluded that simple channel techniques are not sufficient to produce accurate estimates (Myres and Brennan 1990; Knight and Shiono 1990; Ackers 1991, 1992a).

To calculate compound channel discharge capacity it is recommended that the channel is divided into individual flood plains and main channel zones (Chadwick and Morfett 1986; Ackers 1992a). Each of the zones is then treated as a single channel before summing the zone discharge estimates to obtain the total channel

discharge. The vertical division lines between zones are not included in the wetted perimeter during the individual section calculations. The method is more applicable than treating the whole channel as a single unit and is justified by the assumption that within each zone the velocities are fairly uniform. However, the method takes no account of flow interaction between adjacent zones and therefore over-predicts channel conveyances (Chow 1959; Henderson 1966; Chadwick and Morfett 1986).

2.2.1 Research into Compound Channel Flows

Research into compound channel behaviour began several decades ago with the examination of the intense interaction between the main channel and flood plain flows. Sellin (1964) was the first to publish photographs illustrating the vortices occurring at the main channel flood plain intersection. These are responsible for the dissipation of turbulent energy and the transfer of momentum from the main channel flow to the flood plain.

Myres and Elsawy (1975) examined the distribution of boundary shear stress and the distribution of discharge in the simplified case of a main channel with only one flood plain. By running tests, with and without an impermeable barrier between the main channel and the flood plain, they were able to assess the significance of the interaction between the main channel and the flood plain. They also assessed the effect of the interactions on the bed shear distribution. When flow was allowed onto the flood plain they found that the bed shear stress in the main channel was less than when flow was restricted to the main channel itself. This difference between the two cases was greatest for small overbank flow depths.

One suggested way of taking account of the effects of flow interaction mechanisms, is the use of an apparent shear stress on the imaginary vertical division lines between zones (Myres 1978; Baird and Ervine 1982, 1984; Knight et al 1983; Wormleaton and Merrett 1990). Apparent shear forces retard main channel flow and enhance flood plain flow and are a convenient way of parameterising the complex interaction.

All of the above authors have derived equations relating the apparent shear stress to the channel's geometry and the flow variables.

A further investigation into the distribution of velocities and bed shear stress in straight compound channels was carried out by Rajaratnam and Ahmadi (1979, 1981). In an asymmetric compound channel (only a flood plain on one side) the researchers measured longitudinal velocities and bed shear stresses. They discovered that the normal single channel distribution of point velocities in the vertical was disturbed by the interaction effects within the shear layer width. The strength of the effects within the shear layer and the width of the shear layer itself appeared to be a function of the main channel and flood plain flow depths. The behaviour of the mixing of the main channel flow and flood plain flow was more complex.

The relative effect of different channel geometry and boundary conditions has also been a popular area of research concerning compound channels. James and Brown (1977) investigated the effects of various flood plain widths and roughnesses on the stage-discharge relationship for the channel and the distribution of depth-averaged velocity. Wormleaton and Hadjipanos (1985) also examined the effects of various flood plain roughnesses. They concluded that the apparent shear stress on the plane of division, between the main channel and flood plain, was strongly dependent on the velocity differential between the two. It was also concluded that the apparent shear stress was a function of the width and depth ratios of the compound channel as a whole. Work published by Myres (1987) suggests that the ratios of velocity and discharge between the main channel and flood plain are independent of the channel gradient. Instead it is suggested that they are dependent on channel geometry and flow depth. This work was based on small scale laboratory flume data and theoretical considerations. The compound channel used had hydraulically smooth boundaries.

Up until the late 1980's the majority of the published work on experimental investigations into the behaviour of compound channel flow was carried out in small scale facilities. The question over whether the mechanics of flow, and therefore the overall behaviour of such channels, is the same when scaled to such an extent led to

the call for more field data or appropriate scale investigations. Within the UK the economic need for better discharge estimating potential for compound channels was strong enough to justify the funding of a series of large scale projects (Knight and Sellin 1987). The Flood Channel Facility was constructed in 1985 by the then Science and Engineering Research Council (now the Engineering and Physical Science Research Council) and HR Wallingford Ltd. It was built at HR Wallingford's site in Oxfordshire, England. The first two series of investigations involved fixed bed channels. Series A ran from 1986 until 1989 and focused on straight and skewed compound channel flows. Series B ran from 1989 until 1992 and examined the flow behaviour of meandering compound channels. Both series of work were supplemented by smaller scale work in various university laboratories.

It is the Series A work with straight main channels that is of most relevance to the work presented in this thesis. It is therefore briefly reviewed here.

Wormleaton and Merrett (1990) investigated the effectiveness of dividing the compound channel into zones, which are then treated as simple channels, in order to estimate the total discharge capacity. They found that this approach produced errors for hydraulically smooth channels and bigger errors (up to 60%) for channels with roughened flood plains.

Myres and Brennan (1990) investigated flow resistance. They did this by first demonstrating that the trowelled mortar finish to the channel was hydraulically smooth. They then treated the channel as a single unit for the computation of boundary roughness at different discharges or depths of flow. By comparing the variation of the predicted roughnesses they confirmed that a compound channel cannot be treated as a single channel. The variations in the predicted friction parameters were due solely to the compound channel geometry at the various depths as the friction characteristics of the bed remained unchanged.

Similar results to those obtained by Rajaratnam and Ahmadi (1979) were gained by Knight and Shiono (1990) when they examined the characteristics of turbulence in

the shear layer. They used a laser doppler anemometer to measure the three components of the primary and fluctuating velocity from which they derived the turbulent intensities and Reynolds stresses. They found that, as for single channels, the primary velocities were logarithmic in the vertical and the corresponding Reynolds stresses linear, out with the shear layer. Regions where high lateral turbulence was imposed on the bed generated turbulence, resulted in lateral Reynolds stresses that were not linear, and included the effects of secondary circulation. It was also concluded that the lateral variation in local friction factors was such that compound channels could be modelled using constant friction factors in each zone of flow. Lastly they showed that the interaction between the main channel and the flood plain flows caused a redistribution of bed shear stresses. A reduction was observed within the main channel shear layer and an increase in the flood plain shear layer.

Elliot and Sellin (1990) investigated the discharge capacity of compound channels in which the main channel was skewed to the direction of the flood plain boundaries. This is considered by most as an intermediate form of compound channel between the straight and the meandering cases. They discovered that a skewed main channel passes less discharge than a straight main channel and that the reduction in capacity increases with increasing angle of skew. The amount by which the capacity is reduced varies with overbank flow depth and is a maximum at low relative depths.

The work from Series A and B addressed the problem of predicting the total discharge carried by a given compound channel, or alternatively the question, what channel dimensions are required for a given design flood event? For straight compound channels two design methods have been developed. The first, by Wark et al (1991), is in the form of a numerical model using a lateral distribution method to predict unit discharges across the channel (Wark 1993). The second is a hand-calculation methodology developed by Ackers (1991).

Most lowland rivers, prone to flooding, are predominantly meandering in plan. The development of a prediction technique for such channels by James and Wark (1992) is therefore particularly useful to practising engineers (Wark 1993). Both the design

techniques for straight channels, by Ackers, and for meandering channels, by James and Wark, have been incorporated into an easily followed design manual (Wark et al 1994).

The Series C work currently underway (started 1994). is an extension of the already completed compound channel program. This time the research is examining mobile bed straight and meandering channels (Bettess 1997). The additional facility of the Tilting Flume has been made available to allow examination of the effect of bed slope on the aspects of sediment transport in compound channels being examined.

The work was motivated by a requirement to further understand the behaviour of more natural river channels. As a result of Series A and B work Ackers (1992a) developed a method for predicting flow conditions in two-stage channels. When the predicted flow resulting is used to further predict sediment transport rates the results suggest that the sediment transport rate decreases for the transition between inbank and overbank flow. Seed (1996) has concluded that sediment transport capacity predicted using section averaged values is significantly different than that predicted using a summation of point predictions across the section. This is particularly true for channels with significantly varying flow depth across the cross-section, such as compound channels.

2.2.2 Published Series C Work

Much of the experimental work from the first three years of the series is still under analysis. However, several international conference papers and reports have been written and presented from the Mixed Grain Group alone, three of these co-written by the author. These cover several topics including; bed surface composition and grain re-arrangement, the evolution of bedload composition and sediment transport during overbank flows (Marion 1996; Brown and Willetts 1997; Ervine et al 1997; Hoey et al 1997; Marion et al 1997; Pender et al 1997; Tait et al 1997; Willetts et al 1997). The conference papers were presented at the 27th IAHR Congress in San

Francisco, USA and the 3rd International Conference on River Flood Hydraulics in Stellenbosch, South Africa.

2.3 Conclusions

In this chapter a literature review has been carried out. It has covered several topics including; uniform and graded sediment transport, existing common prediction methods for both, a general discussion of a new approach to transport prediction, existing extensive graded sediment data sets and previous work examining compound channel flow.

From the chapter the following conclusions have been drawn.

1. The transport of sediment in an open channel is a complex phenomenon. It can involve different types of material, graded and uniform, and different mechanisms of transport, bedload and suspended load. The initiation of movement is difficult to define and the processes influencing transport rates are many and varying.

2. Existing transport rate prediction techniques are sufficiently inaccurate to cause continued resources to be spent on investigation of basic transport processes. Indeed the accuracy of many existing techniques is such that results are considered good if they fall within a factor of two of the correct value. Many existing graded sediment transport predictors are based on uniform sediment formulae with the application of an empirically derived hiding function.

3. In addition to conclusion 2, existing predictive techniques were derived using simple, single channel flows. They therefore take no account of the effect of overbank flows on predicted transport rates.

4. Macro parameters, such as shear stress, velocity and unit stream power, may not be sufficient on their own to predict transport rates. The influences of small scale

physical processes on the overall transport mechanisms appear to be more important than previously thought.

5. It is therefore suggested that a new approach is required to produce accurate predictions of graded sediment transport rates. Such an approach is outside the scope of this study and may be beyond current knowledge of the subject. However, any new prediction methods proposed should include estimates of influence from small scale physical processes.

6. In order to proceed towards such an approach further research is required. Further detailed studies of graded sediment transport need to be undertaken to develop greater understanding of the physical processes involved. More extensive data sets relating to graded sediment transport also need to be completed and made available. These should include detailed measurements of flow conditions and transport rates to allow any transport predictors to be compared to measured results.

7. A further limitation of the existing approaches to sediment transport prediction is that they were derived using simple, single channel data. They therefore take no account of the more complex flow structures involved in overbank flow and the effects of such structures on transport rates. Any new work in the area of transport prediction should review the published work on overbank flow and assess its affect on sediment transport.

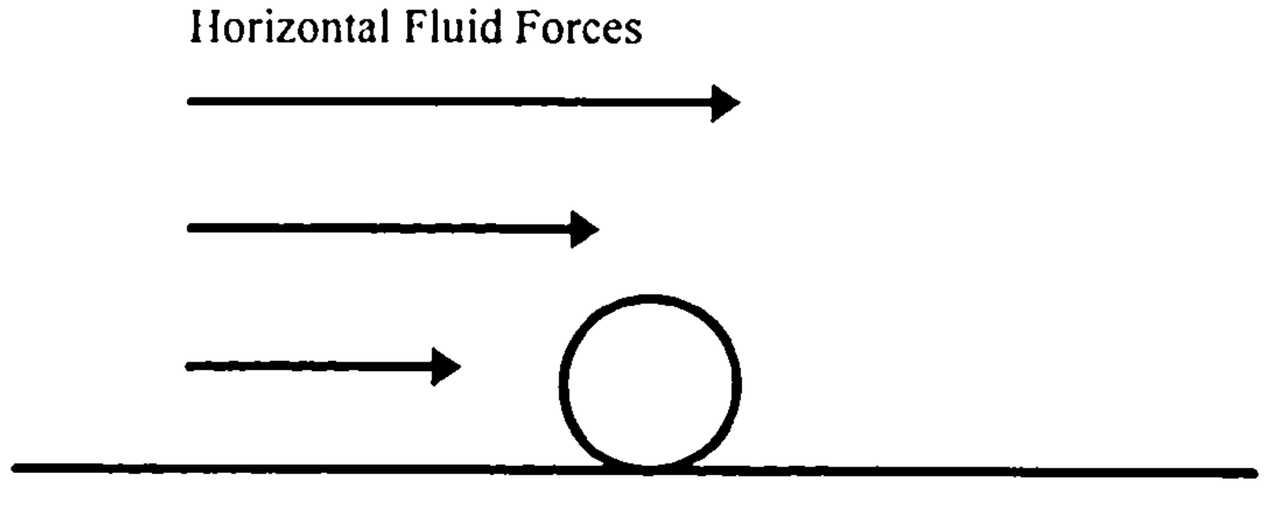

Elevation - Marble on Horizontal Surface

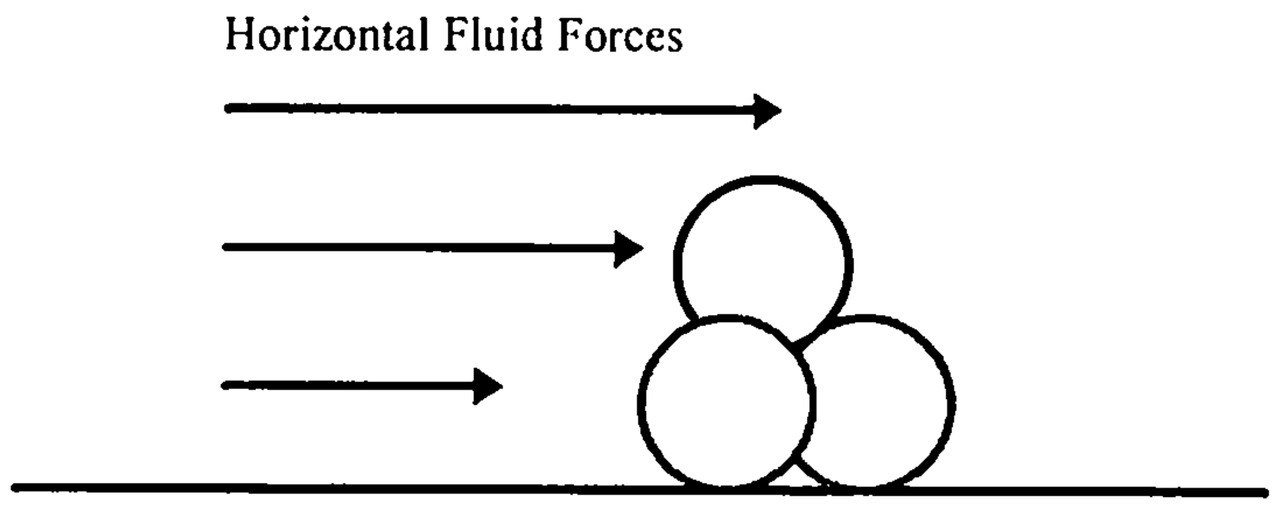

Elevation - Marble on Bed of Marbles

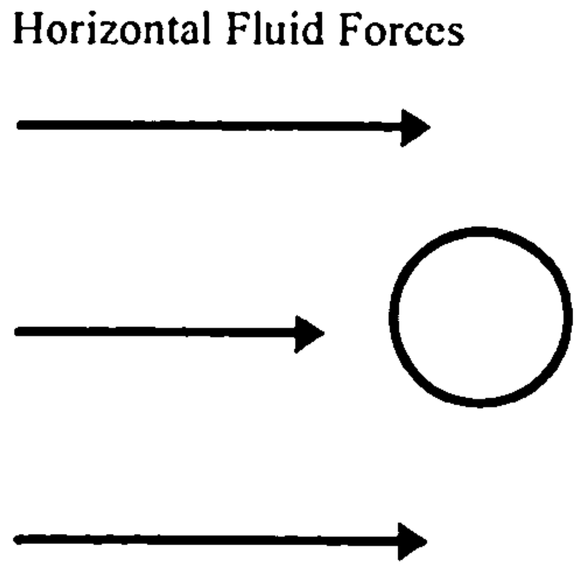

Plan - Marble on Horizontal Surface

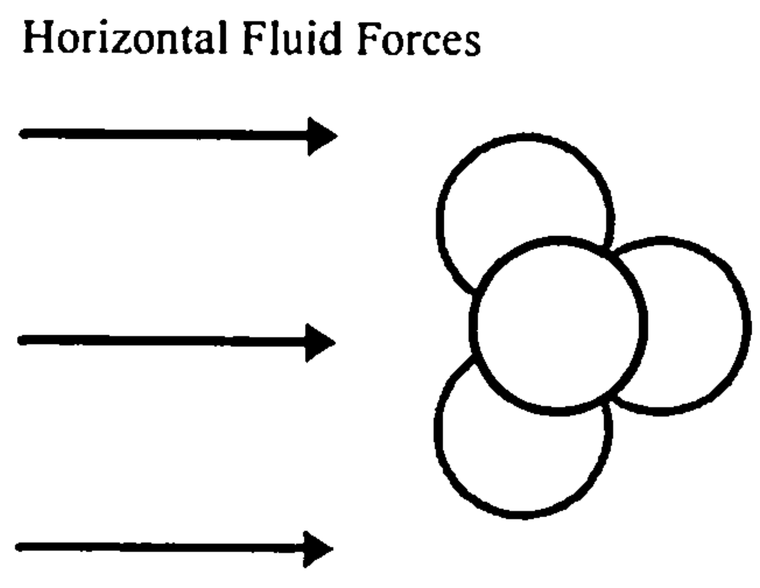

Plan - Marble on Bed of Marbles

Figure 2.1 Threshold of Movement

Chapter 3

Experimental Programme, Apparatus and Procedures

3.1 Experimental Programme

The series of experiments referred to in this volume of work were carried out using the Tilting Flume research facility at HR Wallingford Ltd. England. The research was funded by the Engineering and Physical Science Research Council (EPSRC), and the European Union, Human Capital Mobility (HCM) fund as part of Series C.

Two sets of experiments examining graded sediment transport, in a straight compound channel, were carried out between August 1994 and August 1997. The first set of experiments were completed during the period between January 1995 and March 1996. This included a five month period spent commissioning all of the experimental apparatus used. The second set ran between February 1997 and May 1997. Both sets are outlined in table 3.1 below.

Only results from the first set of experiments (Experiments 2 to 12) are presented in this thesis. The analysis and work involving the second set (Experiments 13 to 16) is ongoing.

The variables investigated during both sets were: initial bed slope, stage level, feed conditions and composition of the bed and feed material. The experiments completed during the experimental programme allows for the grouping of experiments in three ways. The eleven experiments (Experiments 2 to 12) can be examined in groups in order to assess the effects of, initial bed slope, initial flood plain depth and sediment feed rate.

Table 3.1 Experiments undertaken.

Experiment No.	Initial Bed Slope	Initial Flood Plain Depth (mm)	Bed Mix	Sediment Feed Rate (g/s)	Feed Mix	Feed Duration (mins.)	Experiment Duration (mins.)
2	0.0026	20	B	0	--	--	4162
3	0.0026	65	B	0	--	--	3788
4	0.0026	0	B	0	--	--	5555
5	0.0029	0	B	0	--	--	5134
6	0.0024	0	B	0	--	--	4800
7	0.0024	20	B	0	--	--	4810
8	0.0024	0	B	2.5	B_f	4020	5220
9	0.0024	0	B	5.0	B_f	2953	4172
10	0.0024	20	B	5.0	B_f	2575	3775
11	0.0026	0	B	5.0	B_f	1920	3633
12	0.0026	20	B	5.0	B_f	1954	4380
13	0.0026	0	C	0	--	--	5160
14	0.0026	0	C	5.0	C	4230	4230
15	0.0026	20	C	5.0	C	2100	2314
16	0.0026	0	C	0	--	--	3650

3.1.1 Variable Initial Slope

Variation in the initial slope was designed to produce different boundary shear stresses for essentially the same flow depth. The programme undertaken allowed for four groupings under this heading, of bankfull with no feed, overbank with no feed, bankfull with feed and overbank with feed (table 3.2).

Table 3.2 Groupings for variable initial bed slope.

Experiment No.	Initial Bed Slope	Initial Flood Plain Depth (mm)	Sediment Feed Rate (g/s)	Feed Duration (mins.)	Experiment Duration (mins.)
6	0.0024	0	0	--	4800
4	0.0026	0	0	--	5555
5	0.0029	0	0	--	5134
7	0.0024	20	0	--	4810
2	0.0026	20	0	--	4162
9	0.0024	0	5.0	2953	4172
11	0.0026	0	5.0	1920	3633
10	0.0024	20	5.0	2575	3775
12	0.0026	20	5.0	1954	4380

3.1.2 Variable Initial Stage Level

The variations in initial stage level were also designed to produce different boundary shear stresses, but this time due to the different hydraulic flow structures. The experiment groupings resulting allow examination of. the different effects of bankfull and overbank flow, on the sediment transport processes occurring in the main channel. The groups of shallow slope with no feed. shallow slope with feed. steeper slope with no feed and steeper slope with feed are outlined in table 3.3 below.

Table 3.3 Groupings for variable initial stage levels.

Experiment No.	Initial Bed Slope	Initial Flood Plain Depth (mm)	Sediment Feed Rate (g/s)	Feed Duration (mins.)	Experiment Duration (mins.)
6	0.0024	0	0	--	4800
7	0.0024	20	0	--	4810
9	0.0024	0	5.0	2953	4172
10	0.0024	20	5.0	2575	3775
4	0.0026	0	0	--	5555
2	0.0026	20	0	--	4162
3	0.0026	65	0	--	3788
11	0.0026	0	5.0	1920	3633
12	0.0026	20	5.0	1954	4380

3.1.3 Variable Upstream Feed Rates

By undertaking experiments with the same initial slopes and stage levels. but with different upstream feed conditions, groupings of experiments were produced to allow the examination of the effect of feeding material into the channel. The four groups produced are shallow bed slope experiments with bankfull flow. shallow slope with overbank flow, steeper slope with bankfull flow and steeper slope with overbank flow (table 3.4).

Table 3.4 Groupings for variable upstream feed rates.

Experiment No.	Initial Bed Slope	Initial Flood Plain Depth (mm)	Sediment Feed Rate (g/s)	Feed Duration (mins.)	Experiment Duration (mins.)
6	0.0024	0	0	--	4800
8	0.0024	0	2.5	4020	5220
9	0.0024	0	5.0	2953	4172
7	0.0024	20	0	--	4810
10	0.0024	20	5.0	2575	3775
4	0.0026	0	0	--	5555
11	0.0026	0	5.0	1920	3633
2	0.0026	20	0	--	4162
12	0.0026	20	5.0	1954	4380

3.2 Experimental Apparatus

The flume was made available by HR Wallingford Ltd.. with additional equipment financed by the EPSRC. The equipment was commissioned by the Universities of Aberdeen and Glasgow, and by the HCM participants involved in the research.

3.2.1 Tilting Flume Facility (TFF)

The flume is rectangular in cross-section and 25 metres long by 2.46 metres wide (figure 3.1). It can be tilted by mechanical jacks operated by two electrically driven shafts. A calibrated revolution counter, on the electric motor, enabled the flume slope to be set. Level surveying was then used to check the slope setting.

The original instrument rails were replaced by box section rails prior to the start of the first series of experiments. This ensured the rails were linear, parallel to each other and parallel to the flume bed.

Water was re-circulated through the flume using three electrically powered pumps. Two of the pumps had a maximum discharge of 100 litres per second and the third, smaller pump, a maximum discharge of 10 litres per second. The pumps were located at the downstream end of the flume, downstream of the sump. Water was pumped from the sump to the upstream end of the flume through a pipe network beneath the flume. Each return pipe contains an orifice plate of British Standard dimensions to

allow the measurement of discharge through the network. At the upstream end of the flume the two larger pump discharges were split, and entered the flume symmetrically either side of the flume centre line. The small pump discharge entered along the centre line (figure 3.2).

The area where the discharges entered the flume was separated from the rest of the flume by a woven fibre (hairlock) barrier, in order to provide a stilling basin and some dampening of the flow turbulence entering the flume. The flow then passed down the flume, through the test section, and over the downstream tailgate before returning to the sump. The sump was kept at a constant head level by inflow to the recirculation circuit from the top-up inlet valve opened into the sump.

Prior to the start of each series of experiments the hairlock was replaced at the upstream end of the flume. This was done to prevent clogging by very fine material, circulating in suspension.

A steel measuring tape was attached to each of the rails with 0.0 m chainage at the upstream end of the flume. This enabled the identification of areas of the flume, and bed, by rail chainage.

At the downstream end of the flume a tailgate was placed across the full width of the flume and was operated as a cable draw bridge with a crank handle (figure 3.3). This was used to control the water surface profile and establish uniform flow at the start of each experiment.

Within the rectangular cross-section of the flume two flood plains were cast. These gave a main channel geometry similar those used in the Series A and B experiments (Myres and Brennan 1990; Wormleaton and Merrett 1990; Knight and Shiono 1990; Elliott and Sellin 1990; Sellin et al 1993), (figure 3.4). The flood plains were cast relative to the flume centre-line in order to produce a channel with a top width of 1.1 m, bank side walls sloping at a 45^{o}, to a width of 0.65 m, and then moulded vertically to the base of the flume. The flood plains were moulded in cement mortar with the

flume in a horizontal position and were levelled to the horizontal. The upstream end transition section was bell mouth shaped. Rough non-transportable material was placed on the bed in this area to accelerate the development of a turbulent boundary layer in the flow. The upstream end of the transition section began immediately downstream of the hairlock barrier, upstream of chainage 0.0 m. The transition to the linear section was complete by chainage 0.2 m.

A concrete block was cast across the channel just downstream of the chainage at which the sediment traps were positioned. The block was slightly lower in height than the upstream bed level so that it would cause minimal disturbance to the flow around the trap location. The purpose of positioning a fixed object at this location was to allow in-channel measurements to be related to a common datum. These measurements are discussed later in this chapter where the block is referred to as the concrete datum block.

Pressure tappings were moulded into the flood plains at various chainages down the channel. The channel ends of these were 100 mm below the flood plain level and the outer flume ends all connected to stilling pots. From the stilling pots the water surface changes were monitored using digital pointer gauges.

For experimental runs carried out with a flow depth greater than bankfull, flood plain roughness elements were used. These were of similar relative size, shape and geometry as the roughness elements used in Series A and B to approximate flood plain vegetation (figure 3.5).

3.2.2 Mobile Bed Material

Freshly mixed material was placed in the main channel section of the flume before the start of each experiment. Two mixes were used for the bed and a third used as feed material only.

During the first set of experiments mix B was used as the bed material and mix B_f (essentially mix B without the coarsest size fraction) was used as the feed material. Mixes B and B_f were both unimodal sediments made up of material carefully selected to be non-crushed and of a suitable colour, shape, density and durability. Their grading parameters can be seen in table 3.5 and their grading curves in figure 3.6. For the second set of experiments mix C was used as both the bed material and the feed material. Again the mix was made up of carefully selected material, but this time the fractions used produced a bimodal composition (table 3.5, figure 3.6).

Table 3.5 Grading parameters for mixes B, B_f and C.

Mix	D_5 (mm)	D_{16} (mm)	D_{50} (mm)	D_{84} (mm)	D_{95} (mm)	σ_g
Mix B	0.26	0.83	4.04	7.09	10.60	2.92
Mix B_f	0.25	0.62	3.64	5.86	7.88	3.07
Mix C	0.38	1.07	3.70	8.46	10.41	2.81

All three of the mixes were designed to have natural grading and sediment characteristics. In addition the series of experiments were designed to examine conditions of marginal transport, i.e. where some size fractions are mobile while others are not. To this end the bed mixes used where designed so that the range of critical shear stresses for the individual size fractions straddled the range of applied shear stresses (figure 3.7).

3.2.3 Bedload Transport Traps

Bedload sediment transport was sampled at chainage 16.5 m using a trap system developed from the system proposed by Hardwick and Willetts (1991). The trap sampled from the left, centre and right of the bed, combining to completely span the width of the bed (figure 3.8). The streamwise length of the trap was 30 mm, just larger than the largest grain sizes in the bed material used. Sampling was controlled by barrel valves near the top of the traps, below the base of the flume, and sliding guillotines at the bottom of the traps. Below the guillotines was a waste box to allow material collected during non-continuous sampling to be stored. The section above

the barrel valves was flooded at all times during an experimental run. The lower sections had to be bled from below each time the trap section was changed.

3.2.4 Instrument Carriage

An instrument carriage was used, running along the full length of the experimental bed on the instrument rails. This allowed various measurements to be recorded at almost any position along or across the channel or flood plains. The design of the instrument carriage was based on a bridge truss. The carriage was built out of aluminium angles and gusset plates, and ran along the instrument rails on roller bearings (figure 3.9). From the instrument carriage velocity profiles of the flow, water surface profiles, longitudinal bed slope profiles and bed surface topography measurements were all taken.

3.2.4.1 Velocity Profiling Apparatus

Attached to the upstream side of the instrument carriage, for the first set of experiments, was a frame with a beam spanning almost the full internal width of the flume. The beam could be driven up and down over the height of the frame by a electronic stepper motor. The motor was controlled by a Personal Computer (PC) via a terminal emulator and the PC serial port. At marked positions across the beam, referring to specific vertical profiles in the channel, miniature propellers were clamped. The centre of each propeller was at the same horizontal level across the channel (figure 3.9). For Experiments 2 to 11 a bank of three mini propellers were used and in Experiment 12 eight were used. Velocity data was produced by the miniature propellers and streamflo instruments as an analogue voltage. The voltage was then recorded by the PC after being converted by the PC Analogue to Digital Conversion Card (A/D card). Calibration of the propellers allowed the program, specifically written to control the movement and the data acquisition for the velocity profiles, to convert the data from A/D units to velocities.

For the second set of experiments the miniature propellers were replaced by a 3-D Acoustic Doppler Velocimeter (ADV).

3.2.4.2 Water Surface Profile Apparatus

During the first set of experiments water surface profiles were taken using the tapping points and stilling pots (figure 3.10). Data was also collected over the main channel, and the flood plains during overbank experiments, with pointer gauges attached to the same beam as the miniature propellers (figure 3.9). The stilling pots allowed more accurate measurement, but measurements from the instrument carriage could be taken at chainages other than the five locations of tapping points. Measurements from the instrument carriage were taken while the beam was at its datum position.

As velocity profiles were only taken at one chainage during the second set of experiments, and that chainage was at one of the tapping points, water surface data was recorded using the stilling pots only.

3.2.4.3 Longitudinal Bed Slope Profile Apparatus

Using three lasers and a wire potentiometer, all mounted on the instrument carriage, longitudinal bed slope profiles were taken. LAS-8010V lasers were used with a datum range of 100 mm +/- 1 mm, a measurement range of +/- 40 mm, a resolution of 50 μm, an ellipsoid spot diameter less than 1mm at reference distance and a response time of 20 ms. The three lasers were housed in stream lined farings attached to a frame on the downstream side of the instrument carriage. This frame was driven by an electric motor to position the lasers within reading distance of the bed (figure 3.11). The wire from the potentiometer, attached to the instrument carriage, was fixed to the upstream end of the flume. This allowed readings, recorded from the lasers, to be related to a potentiometer reading, and therefore a chainage, as the instrument carriage was pushed along the flume. A program written specifically for the experiments, by Aberdeen University, allowed readings from all four instruments

to be recorded through an A/D card in a PC. By starting each longitudinal bed slope profile with a series of readings taken over the concrete block datum it was possible to relate bed profiles to each other, the water surface and the flood plain levels. This equipment was used in all but the first two experiments (Experiments 2 and 3). Prior to Experiment 4 no wire potentiometer was in place and 250 mm longitudinal sections were profiled every metre, using the bed surface texturing laser and positioning frame.

Both the water surface profiles and the longitudinal bed surface profiles have to be adjusted to take account of the fact that the profiles taken were relative to the slope of the flume.

3.2.4.4 Bed Surface Texturing Apparatus

A fourth laser was used to collect data on bed topography, or texture, from a positioning frame on the instrument carriage. For bed surface texturing an LC 2450 laser was used with a datum range of 60 mm, a measurement range of +/- 8 mm, a resolution of 0.5 μm, a spot diameter of 45 μm and a response time of 100 μs. The laser was again housed in a waterproof faring and was moved in 0.5 mm steps over a 256 mm by 256 mm grid by a 3-D positioning frame (figure 3.12). The instrument carriage was able to be locked in position at the same chainage for each texture plot. This allowed detailed data to be collected on the bed texture at this location for different periods throughout the experiment. Texture data was only able to be collected in the periods of overnight shut down as the data took 13 hours to collect and a completely static bed was required. The output voltage from the laser was again converted to a digital recording by the PC A/D card and then converted to levels using the laser calibration. The same PC also controlled the positioning frame from a serial port. The instrumentation was again commissioned by Aberdeen University.

3.2.5 Photography Frame and Carriage

A second smaller instrument carriage, in the form of a flat bridge across the flume, was used as a base for taking detailed photographs of the bed (figure 3.13). A glass plate suspended from the photographic frame enabled photographs to be taken through the water surface without reflection. The plate level was adjustable and it was able to be lifted clear of the water surface as soon as the photographs had been taken. Photographs were taken at several chainages, with a record kept of each exposed frame. Most of the photographs taken were done so to record visually the bed area examined by the texturing laser.

3.2.6 Bed Surface and Substrate Sampling Apparatus

During the first set of experiments two types of physical sediment samples were taken of the initial and final beds. The first, only carried out on the initial screeded bed, was bulk sampling. A volumetric sample was removed from the bed and bagged for sieve analysis. The second was areal, surface layer, wax sampling and was carried out on both the initial and final beds. The areal surface wax sample was taken by placing a square frame, 15 cm by 15 cm internally, on the drained bed over the area to be sampled. Wax, of a consistent temperature, was then poured over the area within the frame. The wax cools as it touches the sediment and, when set, the whole frame can be lifted from the bed taking with it a sample of the surface layer material (figure 3.14).

For the second set of experiments the initial bulk volumetric bed samples were still taken at the start of each experiment. The areal wax samples however, were replaced by a more elaborate bulk wax sample, which sampled deeper into the bed. The technique, designed and carried out by collaborators from Aberdeen University, involved establishing a water table at a depth to which the sample was to be taken. Then a wide cylinder was driven into the bed to the base of the flume. Into the cylinder was poured a mix of boiling water and molten wax to ensure full wax

penetration to the water table depth where it cooled and solidified. Once the whole sample had set it was removed from the flume and the wax melted from the bottom, in layers, so as to enable the analysis of any vertical sorting. Only the central core of the wide cylinder was used, for composition analysis, to avoid any side wall effects from driving the wide cylinder into the bed (figure 3.15).

3.2.7 Orifice Plates and Pressure Transducer

The discharge during each experimental run was measured using the orifice plates inserted into the recirculation pipe network beneath the flume. By measuring the head loss across the orifice plates it was possible to calculate the discharge through the network. Measurement of the head difference was taken using a pressure transducer and the voltage output was converted using an A/D conversion card in the PC (figure 3.16). Discharge through each of the pipes in use was monitored for a period of time and averaged, at a number of times throughout each experiment. A program written specifically for the task recorded the A/D card output and converted it to head loss.

3.2.8 Temperature

The water temperature and surrounding air temperature were measured periodically throughout the experimental series. This was done using an electronic temperature probe recording the temperature to 0.1 ^{o}C with an accuracy of +/- 0.4 ^{o}C. Water and air temperature were measured one after each other to enable a comparison.

3.3 Experimental Procedures

The experiments were designed so that they would all be run in a similar fashion, with the appropriate initial variable change in either bed material, discharge, slope or feed rate. Although, in some of the very first runs not all the procedures had been standardised, they were carried out in a constant and careful manner.

For each of the experiments a record of all measurements and occurrences was kept in the events sheets. The event sheets were kept with the flume at all times during the two series of runs and now provide record of how each experiment progressed. Each entry comprised of a date, a time and the event.

The following is a brief description of the methods used in the setting up and running of an experiment.

3.3.1 Bed Preparation

The first stage of every experiment was to mix, place and prepare the bed material to be examined. The bed material was mixed using hand measured quantities of each component and a small, clean mixer. This allowed small amounts of the material to be mixed at a time and reduced the likelihood of a badly mixed bed. The mixed material was then placed in the channel in such a way as to avoid segregation, by spreading or settling. When the flume was approximately filled to the correct level, the material was carefully moved about to make a roughly level bed. This was then screeded level using two screeder boards, of successively lower levels, each run once down the flume, to minimise any longitudinal sorting this may cause. Both screeder boards rested on the flood plains so the initial prepared bed for each experiment was at the same level below the flood plains.

3.3.2 Flume Slope and Rail Adjustment

Once the bed material was in place the flume was tilted to the correct slope using the revolutions counter on the jacks motor and successive level surveys of the rails. Adjustment of the flume slope was carried out after the placing of the bed, in case the changes in load on the jacks, caused by the removal and replacement of the bed material, caused a distortion of the set slope. As far as possible, throughout the experimental program, experiments with the same slope were run one after the other.

This minimised the changes required to the slope and avoided any difficulties caused by having to return to specific slopes.

3.3.3 Initial Sampling of the Bed Material

To check the consistency of initial bed conditions, the bed prior to the start of each experiment was sampled using the bulk and areal apparatus and methods described in section 3.2.6. Once the sample had been removed the bed was reinstated, with material from the same batch used to fill the bed initially, and the local area to each sample re-screeded. Throughout the series of experiments between 2 and 6 areal samples were taken from each initial bed as well as between 2 and 4 bulk samples. All the initial bed samples collected from all the experiments conducted were used in the statistical analysis of bed similarity described in Section 6.5, Chapter 6.

If there was sufficient time available a texture survey was carried out in the dry to compare with the initial texture survey carried out in the wet.

3.3.4 Placement of Roughness Elements

If the experiment involved overbank flow then the roughness elements required to be positioned on the flood plains. This was done in such a way as to make the pattern of rods breaking the water surface continuous, down both concrete flood plains, and so that the flood plains were symmetrical.

3.3.5 Preparation of Feed Material and Conveyor Belt

Before an experiment involving an initial period of sediment feed could begin the speed of the conveyor belt had to be calibrated. The belt required to be set to the speed that would feed the material into the channel at the correct rate. This was done by timing marked sections of the feed belt past a certain point, and then multiplying the time in seconds by the required feed rate. This gave the weight of material to be

placed in each of the marked sections. Bags of material were then made up to the correct weight, for ease of loading during the experiment. and the first load placed on the belt. The material used for feeding was mixed in the same way as that used for the bed.

3.3.6 Flooding of the Bed

The flume was then trickle filled very slowly from the downstream end, so as to avoid disturbing the screeded bed surface and positions of the grains in the initial bed. Once sufficient volume of water was contained in the channel a flow was established, below the threshold of movement or entrainment. This made sure there were no perched grains or pockets of air in the bed which might affect the transport rates at the start of the experimental run. The sub-threshold flow was allowed to recirculate for a couple of hours.

3.3.7 Initial Bed Measurements

The flow in the flume was then ponded, by raising the tail gate and reducing the flow, to allow for some initial data to be collected on the texture and gradient of the bed. A texture survey of the area to be monitored throughout the experiment, was completed in the wet, and then the same area photographed. A longitudinal profile was also taken of the bed, to allow comparison with the other experiments and the development of the bed throughout the experiment in progress.

3.3.8 Setting Datum Level for Water Surface Profiles

During the two sets of experiments two forms of water surface profile data were collected, as described in section 3.2.4.2.

Setting the datum water level for the tapping point data was done by using a ponded, horizontal water level within the channel. The stilling pots connected to each

of the tapping points were bled and the water level allowed to settle. The water level was then marked on the side of the stilling pots, which were fixed in position, and the pointer gauges set to zero with their points at this marked water level. The level of the ponded water surface was then measured relative to the concrete block datum.

Two different levels were used to set the datum levels of the pointers attached to the instrument carriage. The first level, corresponding to bankfull flow experiments, was established by placing a strip of dexion section across the channel from flood plain to flood plain, at the same chainage for all experiments. The pointer tips were then lowered onto its surface and the gauges set to zero. The second level, corresponding to overbank flow experiments, was generated by placing a strip of marine plywood across the tops of the roughness elements, again at the same chainage for all experiments.

3.3.9 Establishment of Uniform Flow

The first task was to establish uniform flow of the correct depth for the particular run in hand. This was done using the iterative technique of adjusting the discharge and tailgate settings while measuring the flow depth at several chainages down the channel. Essentially this was the same technique as that described by Lorena (1992), but less involved due to the restriction of a mobile bed. Ideally uniform flow was established from a backwater profile rather than a drawdown profile as it was less likely to disturb the bed. The whole process was done as quickly as possible, while still allowing time for the water surface profile to react to changes in discharge or tailgate settings. Once uniform flow of the correct depth had been established the clock measuring experimental elapsed time was started.

3.3.10 Cyclic Data Acquisition

Once the experimental run had begun the procedure became a cyclic routine. Although data was not always collected in the same order, it was attempted to keep

measurements close together. This allowed the different data sets to be examined with respect to each other.

Typically a cycle of data collection would begin with the initiation of a sediment transport sample collection. Depending on the transport rate this may have had to be completed straight away or allowed to continue collecting until some point throughout, or at the end of, the data collection cycle. Next, a discharge measurement would be taken and recorded, followed by a water surface profile. As close to the water surface profile recording as possible was taken a longitudinal bed slope profile, which itself would be followed by a velocity profile. Finally, within the regular cycle of readings, would be a recording of the air and water temperatures. Occasionally a series of photographs of the bed, including the area which was surveyed by the laser, was included in the cycle for completion of the data set.

This cycle was carried out periodically throughout the experimental runs and at a frequency that was relative to the activity shown by the bed.

3.3.10.1 Discharge Measurement Procedure

In order to get an accurate reading of the pressure drop across the orifice plates, all the air had to be bled from the downstream side of the orifice plates. Air also had to be bled from the pipes connecting the two sides of the orifice plates to the pressure transducer and the pressure transducer itself. This was done using bleed valves on the pipe networks and the through flow facility on both sides of the pressure transducer. Once all the air was removed from the system it was possible to take an average of the head loss across the orifice plates using the Visual Basic program written for the task. The resulting head loss was then converted to a discharge, using the head loss discharge relation for British Standard orifice plates.

3.3.10.2 Water Surface Profiling Procedures

Water surface profiling inside the channel, using pointer gauges attached to the instrument carriage, began by setting the datum levels on the pointer or pointers, as described in section 3.3.8. For Bankfull flow only one pointer gauge was used, to the left of the centre-line. For Overbank flow the same main channel pointer gauge was used but an additional one was attached to the instrument carriage above the centre of the left flood plain. Once the datum levels were set, or checked and found to be correct, the instrument carriage was moved down the channel at 1 metre intervals. In this way the water surface level was recorded at chainages between 2.5m and 16.5 m. As the water surface within the flume was not static a certain amount of averaging was required to obtain a reading. The water surface level was taken as the point where the pointer gauge broke the water surface for approximately half the time of sampling.

Water surface profiling using the tapping points and stilling pots also required that the datum levels of the pointer gauges be checked. The tapping points and tapping point stilling pot connecting pipes required bleeding before measurements were taken. This ensured there were no blockages causing a difference in pressure. Once this was done the water surface was recorded as the level at which the pointer just broke the still water. This gave a more accurate water surface level at fewer chainages than the pointers attached to the instrument carriage.

3.3.10.3 Temperature Measurement Procedure

Temperature measurement was very simple. It involved holding the electronic temperature probe steady in the air or in the water flow, until the temperature had reached a steady value. This temperature was then recorded in the data sheets.

3.3.10.4 Velocity Profile Procedures

Miniature propellers were used to measure flow velocity in the streamwise direction. The propellers required to be rinsed with de-scaling solution and water at least once each experiment. There was no way of checking the propeller calibration. other than re-calibration. It was assumed the calibration was constant with time. The propellers were therefore used as long as they were clean and in good working order. If they received a knock, or showed signs of being worn or damaged. then they were replaced with freshly calibrated propellers.

Velocity profiles were taken at four chainages corresponding to tapping points 2, 3. 4 and 5. The instrument carriage was positioned so the propellers were in line with the relevant tapping point and the instrument carriage locked in position. The streamflo instruments, which convert the signal frequency produced by the miniature propellers to an analogue voltage, were switched on and the data acquisition program started. The program, running on the laptop PC, controlled both the positioning of, and the sampling from, the propellers throughout the flow. The bank of propellers were driven down through the flow, stopping at specific levels, relative to the flood plain level, to record flow velocities. The bottom position of the profile was close to the bed, but not so close as to disturb it. Once the profile was finished, the instrument carriage was moved to the next tapping point and the process repeated. All the data was saved as velocities at levels relative to the bankfull level, in a file generated by the data acquisition program.

3.3.10.5 Longitudinal Profile Procedure

Taking a longitudinal profile, for all experiments except 2 and 3, involved initially positioning the instrument carriage at the downstream end of the flume. The instrument carriage was positioned with the profiling lasers located over the concrete datum block downstream of the traps. The lasers were then lowered, so that the bed was within their range of measurement, and the wire potentiometer attached to the upstream end of the flume. The data acquisition program was then started which

recorded readings from the three lasers and the wire potentiometer, at a set frequency, as the instrument was pushed slowly up the channel. When the top of the channel had been reached the data acquisition program was stopped and the lasers raised out of the water again.

For the first two experiments a single laser was attached to the bed texturing positioning frame and the instrument carriage positioned at successive positions down the channel. At each position, one metre apart, the laser was driven along three longitudinal profiles, at the left, centre and right of the bed, for a length of 250 mm.

3.3.10.6 Sediment Transport Sampling Procedures

The three sediment traps were all operated in the same way, and at the same time, to collect data relating to the transport rate down the left, centre and right of the channel. Before a trap cycle could be started the whole trap system had to be bled of air from the bleed pipe entering the waste box. Air was bled out using bleed screws just below the barrel valves at the top of the trap units. The penetrator unit was flooded from the flow down the flume above. Once the system was clear of air the barrel valves were opened and any material collected in the penetrator unit during the period of no sampling, was allowed to fall into the waste box. The guillotines were then slid into place to start collection by preventing material falling through the traps into the waste box. At this point the real time, elapsed time and cycle number were recorded on the sediment sample labels that would be stored with the collected samples.

When the samples were to be stopped the elapsed time was recorded again and the top barrel valves shut, stopping material falling through the penetrator unit and into the traps. The waste box was then lowered and the trap units removed with the material contained inside by the guillotine valves. Empty trap units, without guillotine valves in place, were then attached to the penetrator unit, the waste box raised, to create a seal, and the traps bled of air once again.

The samples were transferred from the trap units to sediment drying trays by washing with a low flow hosepipe. They were then allowed to stand for at least 24 hours to let some of the water drip away. After this draining period the samples were sealed in heavy duty plastic bags, along with the labels, and returned to the sediment labs. The samples were then oven dried and sieved, using a standard set of sieves. Larger samples were split using a riffle box prior to sieving.

Initially there were concerns that the finer material might be saltating over the traps and that the collected material may therefore not fully represent the actual bedload material. To check that significant volumes of fine material did not escape the trap through saltation Karolyi samplers were used immediately downstream of the trap. The samplers did not collect any significant volume of material suggesting that fine bedload material was not escaping the traps. The Karolyi samplers were supplied by Aberdeen University and worked on the principle of flow expansion. When a sampler was placed on the bed it allowed a cross-section of the flow to enter the sampler chamber through the upstream opening. The cross-sectional area of the sampler increased in the downstream direction causing the velocity of the sampled flow to decrease before exiting the sampler through the mesh at the downstream opening. As the velocity of the sampled flow decreases the material carried is deposited and retained in the sampler by the downstream mesh.

During the second series of experiments some Karolyi samples were taken at chainages 3, 6 and 9m and at the left, centre and right of the channel. The samples were taken by holding a Karolyi sampler on the bed for a period of time and then comparing the wet weight of the sampler and the sample with the wet weight of the sampler when it was empty. This technique was not intended to give any detailed data on sediment transport, but to provide a crude indication of whether there was any significant difference in transport down the length of the flume.

3.3.10.7 Photographic Procedure

After each laser texture survey, and at other periods of interest throughout the experiments, photographs of the bed were taken. The photographic bridge was positioned at the point which was to be photographed and the position noted relative to the chainage of the flume. The photographic frame was then lowered, so that the horizontal glass plate was just in contact with the water surface. This allowed a clear photograph of the bed to be taken without reflection from the water surface itself. If the water surface had changed level then the height of the glass plate below the photographic plate could be adjusted. A flash unit was also used to ensure that a clear, well lit photograph was produced.

3.3.11 Overnight Shutdown

At the end of a working day the experimental run was temporarily shutdown, by raising the tailgate and lowering the discharge, to bring the flow conditions to a sub-threshold state. If appropriate, sediment feed was also switched off. This allowed for the continuous monitoring of the experimental run throughout its elapsed time. It also allowed the bed texture surveying (a 13 hour process) to be carried out at an effectively instantaneous elapsed time.

At periods in an experimental run, when there was little movement of the bed, overnight runs were undertaken. This was done only when it was deemed more important to examine parameters at a later elapsed time than to have continuous monitoring and regular bed texture surveys. The traps were closed and the penetrator units allowed to overflow, as the experiment ran unmonitored throughout the night. Overnight runs were only completed in experiments with no feed taking place, due to the necessity for manual loading of the feed conveyor belt.

3.3.12 Bed Texture Survey Procedure

The bed texture surveys took place during overnight shutdown periods as they required a static bed for approximately 13 hours. The survey was carried out over the same area of the bed each time to enable comparison of developing texture throughout the different phases of the experiments. The instrument carriage was located at the same chainage using studs screwed into the instrument rails. The instrument carriage was then locked off at this position. The laser was then positioned over the bed using a 3-dimensional positioning frame, controlled by a desktop PC, which also collected the survey data. The survey recorded levels within a 256 mm by 256 mm grid, at 0.5 mm intervals, and to an accuracy of 0.1 mm in height. Results of the survey were stored in individual files created by the laser positioning and data acquisition program.

3.3.13 Material Feeding Shutoff at Equilibrium

The point at which the upstream feed was discontinued, and the degradational part of the experiment started, was judged visually for experiments involving upstream sediment feed conditions. The aim was to stop feeding material when the bedload transport at the downstream end was equivalent to the feed. In theory it should be equal both in terms of transport rate and composition. However, without analysing the sediment samples it was impossible to establish the weight and composition of the collected material. Equilibrium was therefore estimated using the volume collected in the sediment trap units, compared to the volume being fed into the flume, over a period of time. When the transport rate had remained reasonably constant, for a significant period of time, at a rate comparable to the feed rate, the feeding of material was stopped and the elapsed time recorded.

3.3.14 Experiment Final Shutdown

Once the level of bed activity was sufficiently low, it was judged that the experimental run was complete. A final cycle of readings were taken before the tailgate was raised and the discharge lowered, to a flow level well below threshold. At this point the final elapsed time was recorded on the data sheets and a final bed texture survey carried out.

3.3.15 Final Bed Procedure

After the final bed surface texture survey had been completed, the bed was drained slowly, avoiding disturbance of the final armoured bed, to allow for wax sampling. No volumetric bulk sample was taken of the final bed due to the vertical sorting of material through depth. Areal and bulk wax sampling were carried out using apparatus and procedures described in section 3.2.6.

All the top layer material was then removed, to a depth which was judged to be unaffected by the flow and sorting of the experiment. The flume was then ready for preparation for the next experiment.

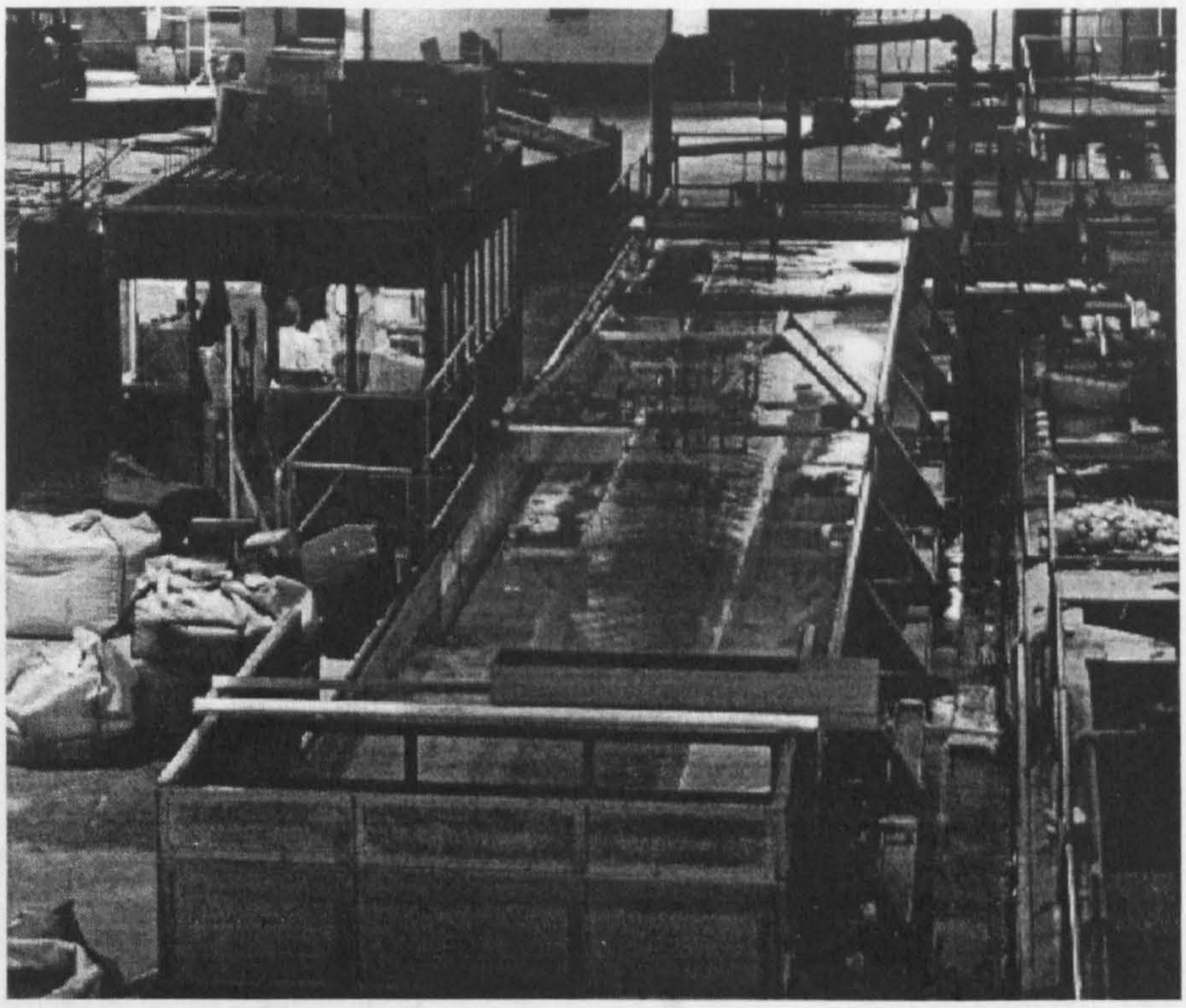

Figure 3.1a HR Wallingford Tilting Flume Facility, Looking Downstream

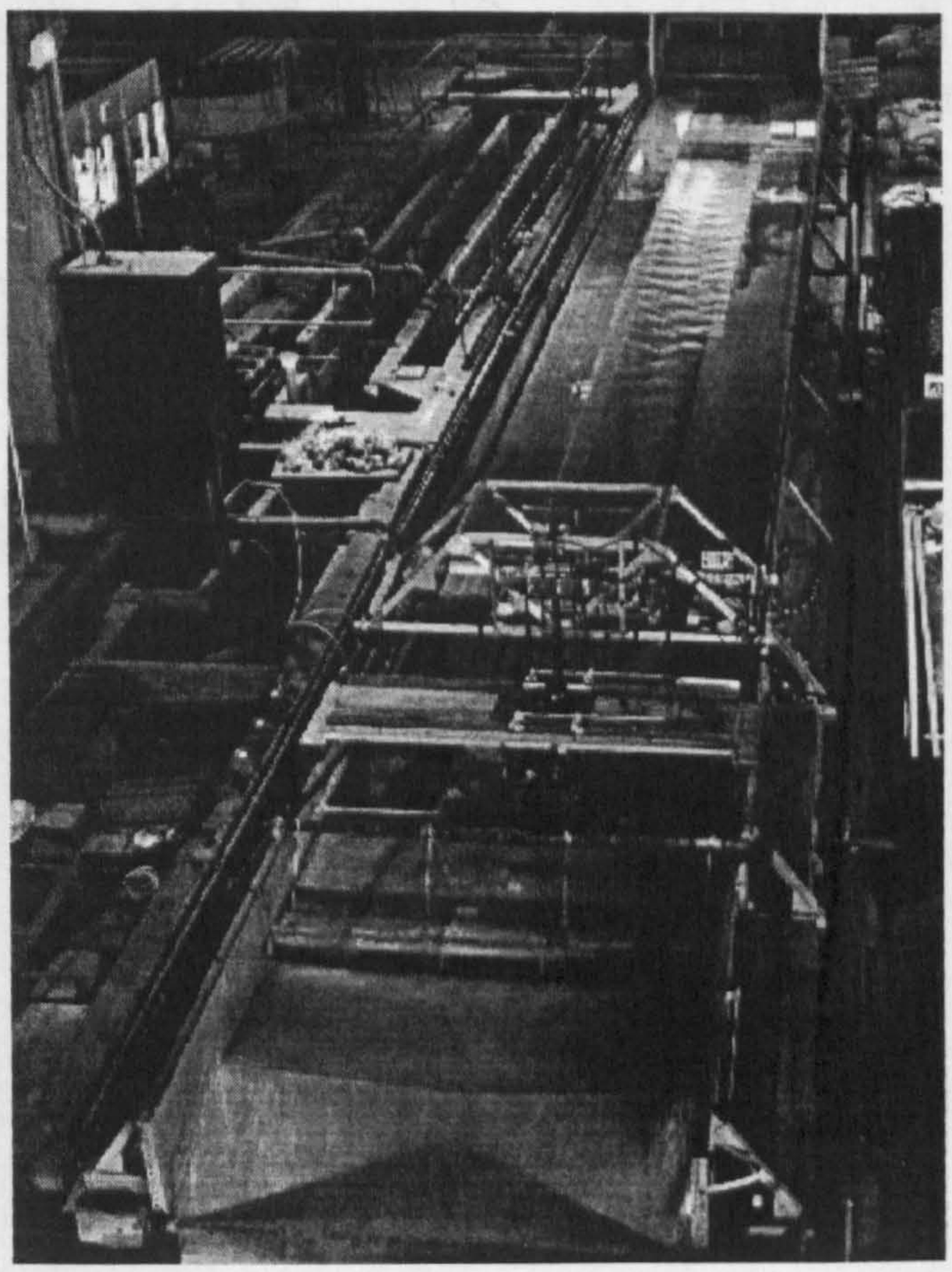

Figure 3.1b HR Wallingford Tilting Flume Facility, Looking Upstream

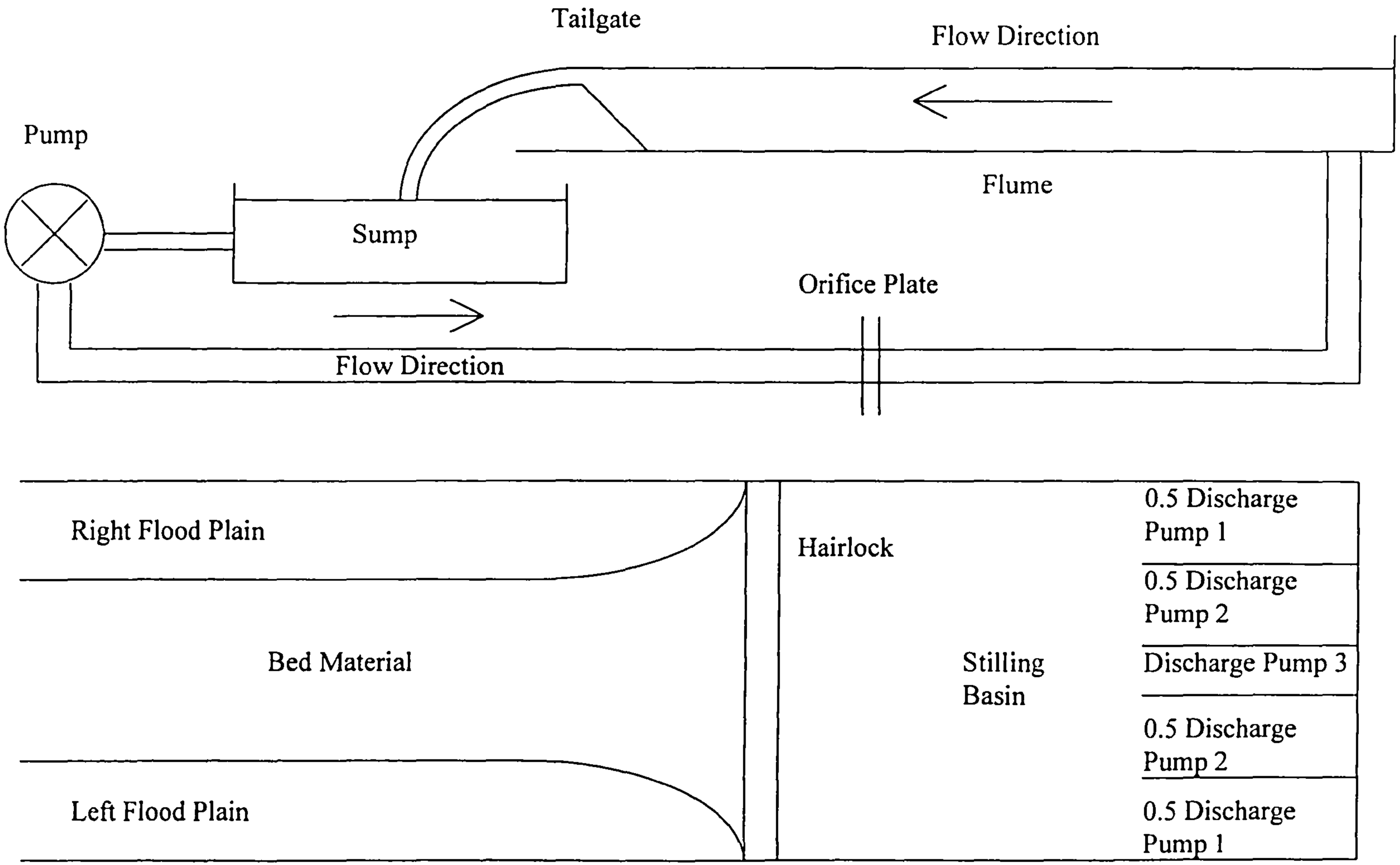

Figure 3.2 Schematic Diagram of the Pipe Network and the Upstream End of the Flume.

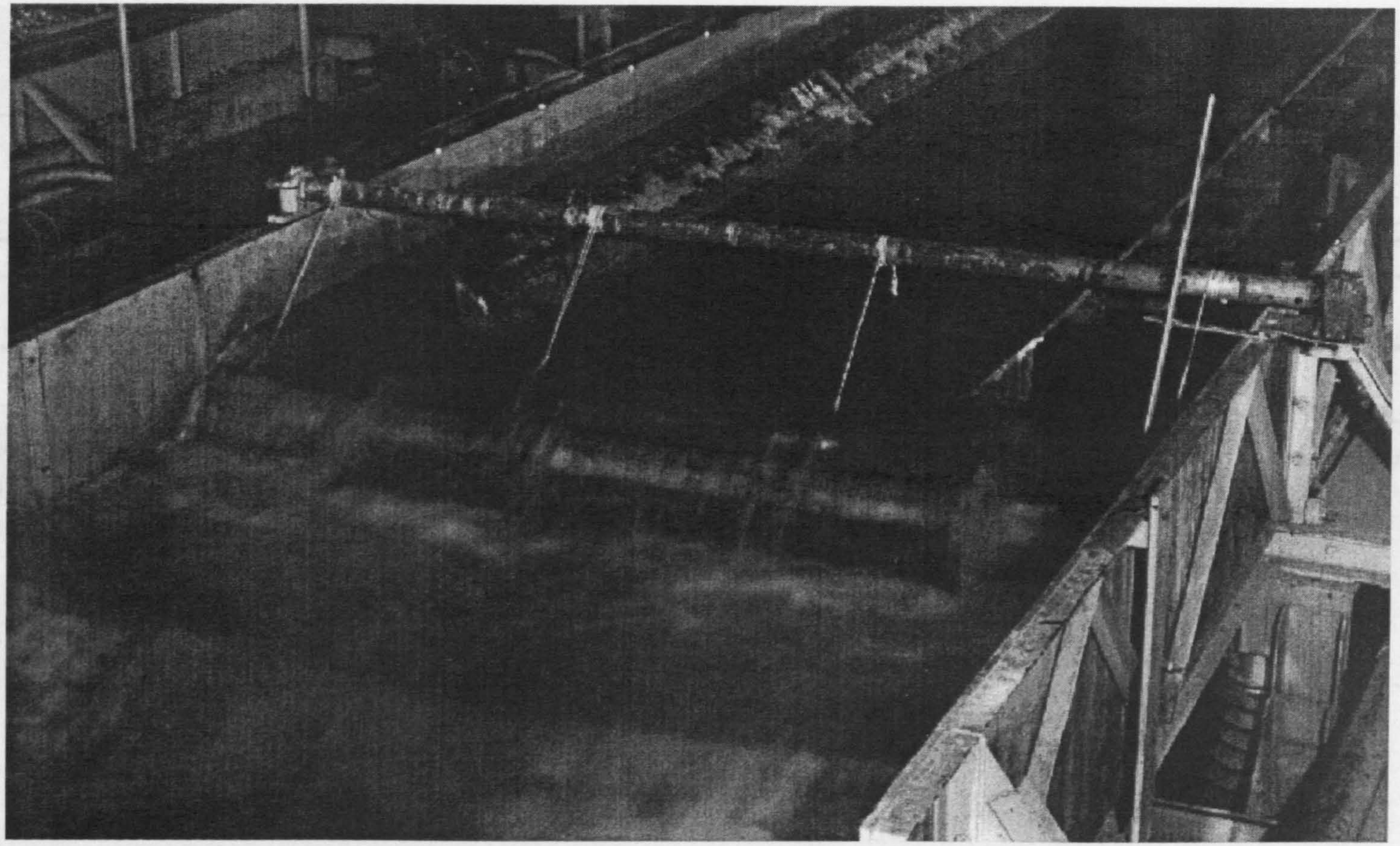

Figure 3.3 Crank Handle and Cable Operated Tailgate

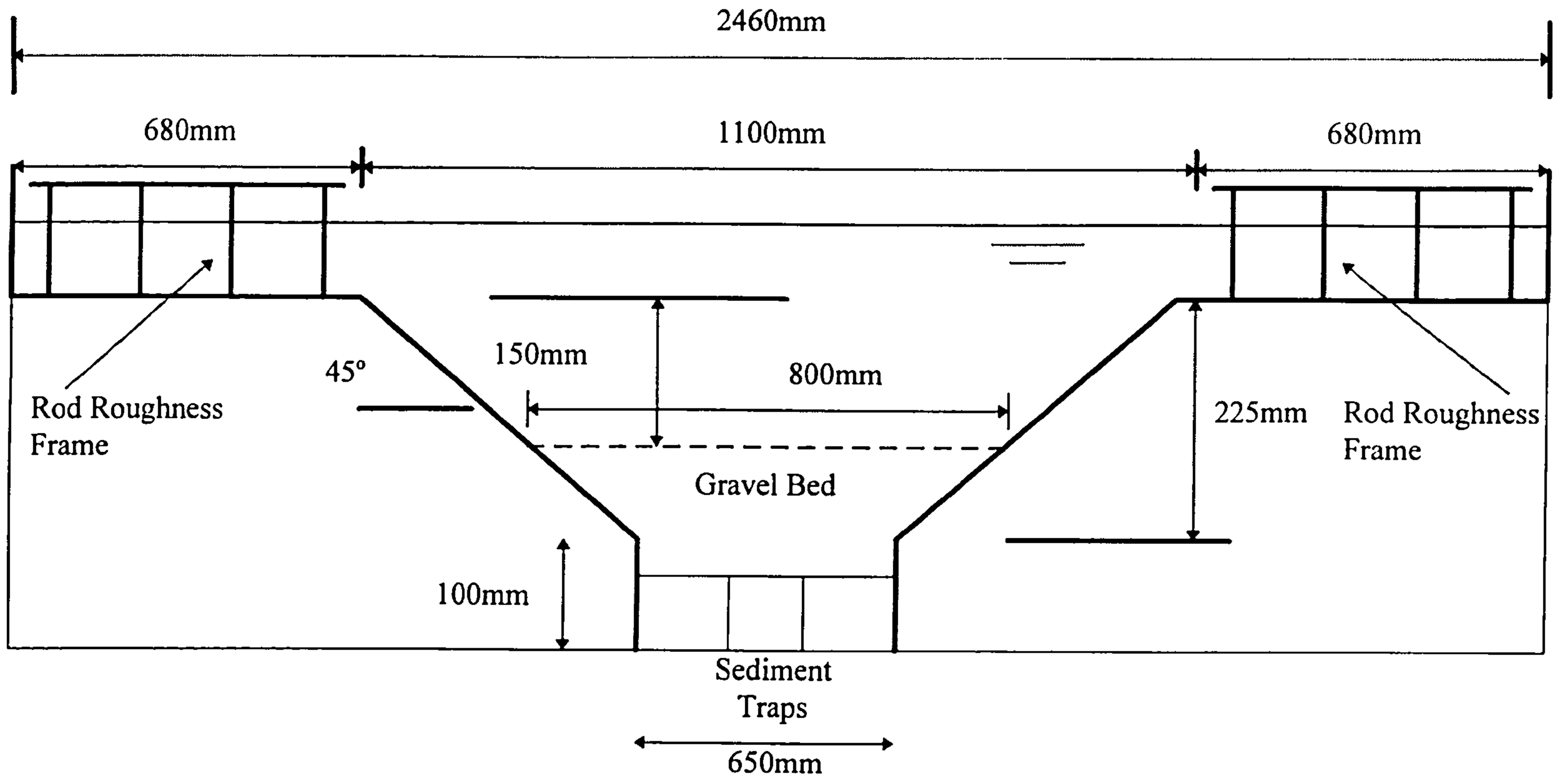

Figure 3.4 Flume Cross-Section Showing Overbank Flow

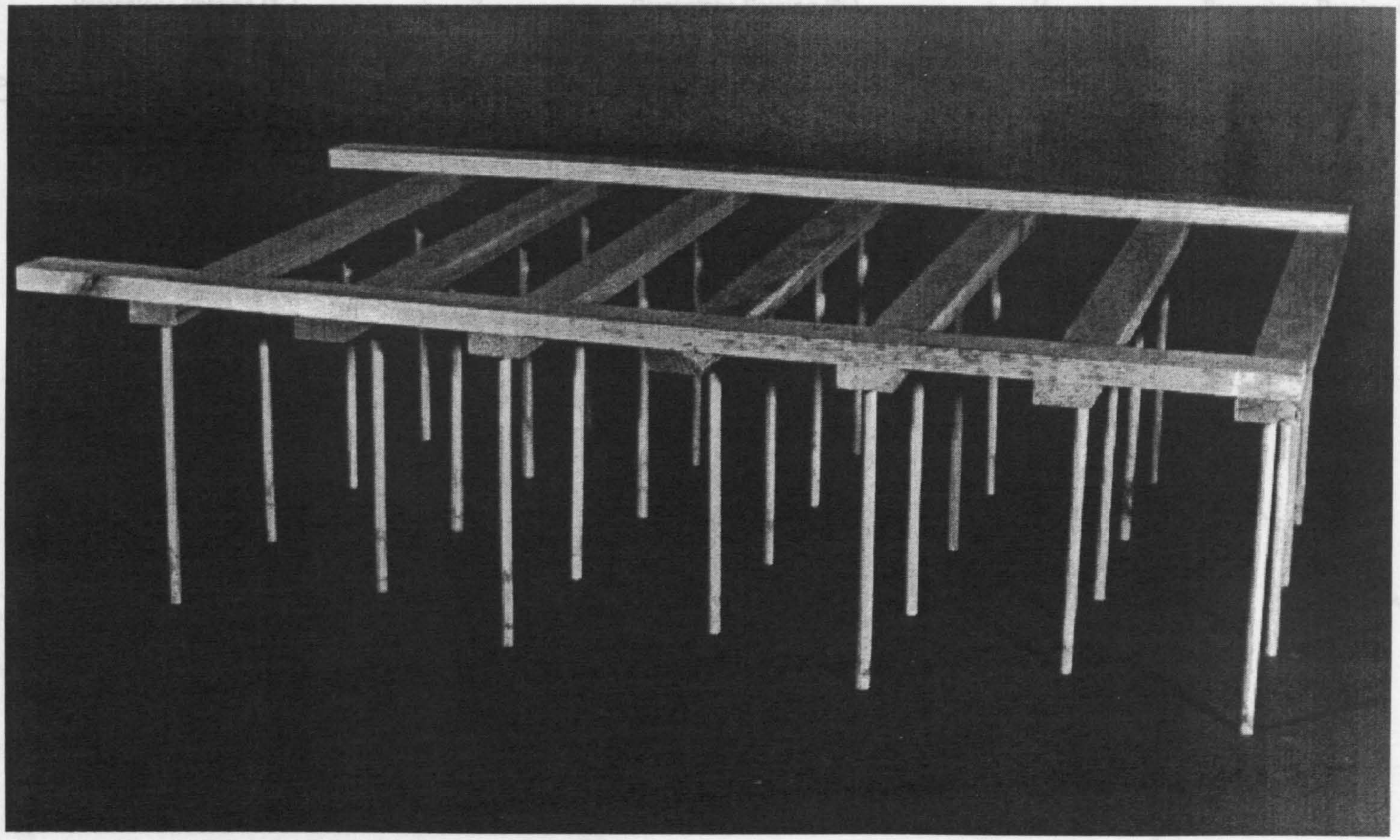

Figure 3.5 Flood Plain Roughness Element

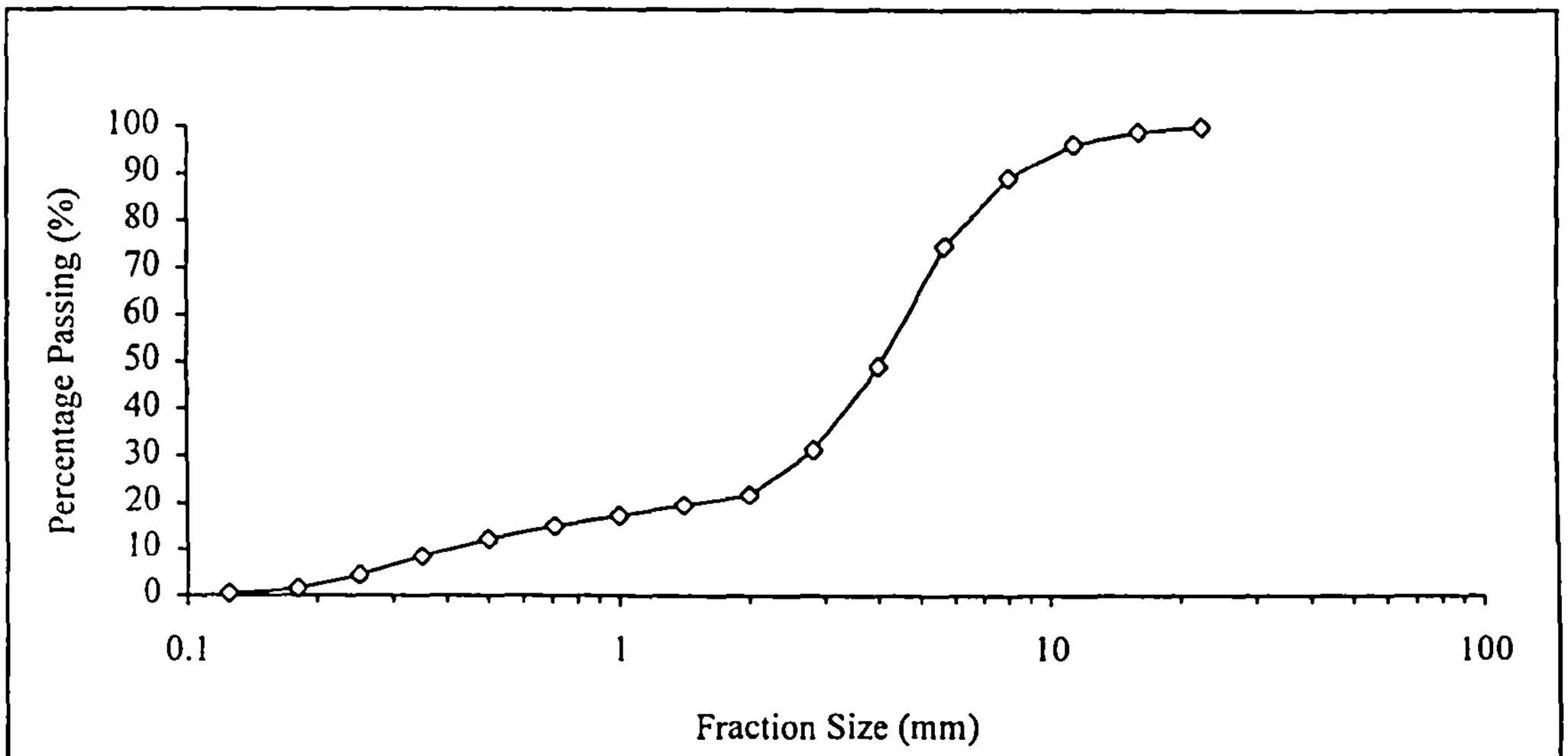

Figure 3.6a Cumulative Grading Curve for Design Mix B

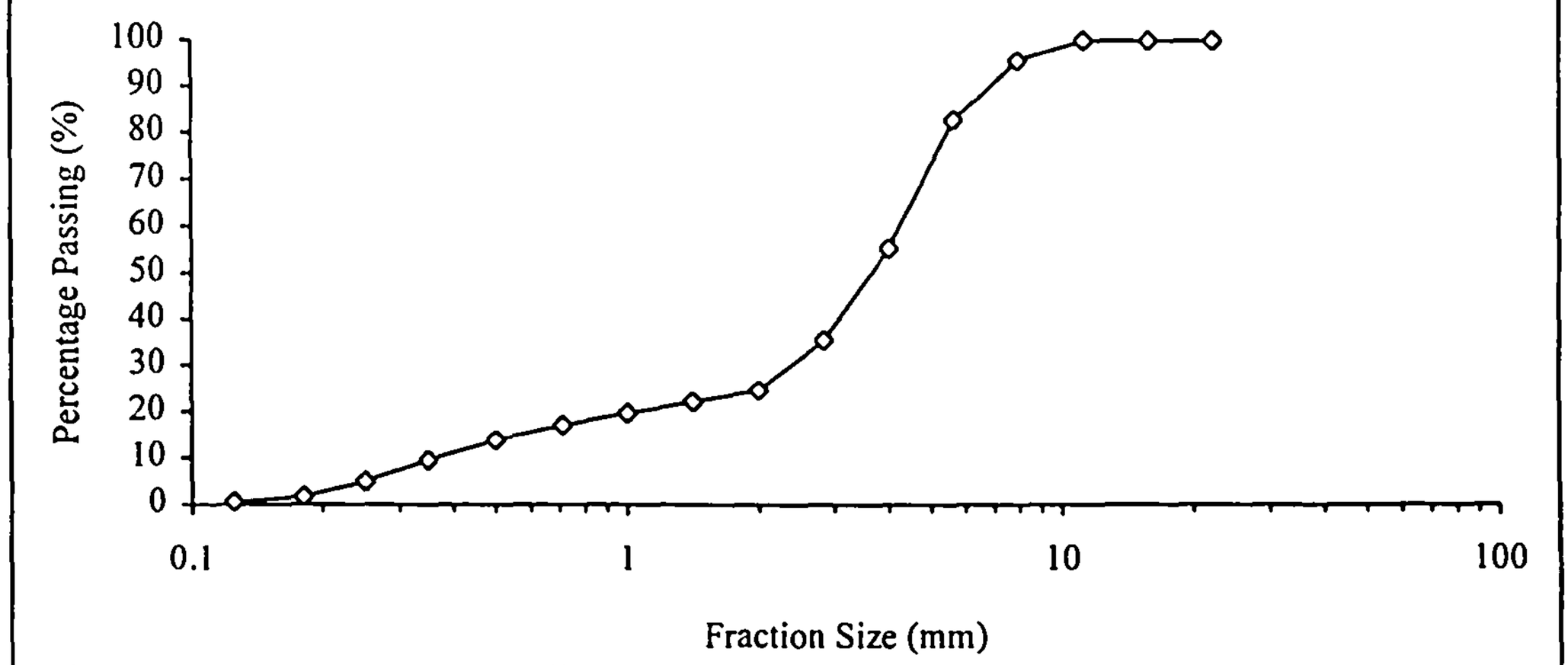

Figure 3.6b Cumulative Grading Curve for Design Mix B_f

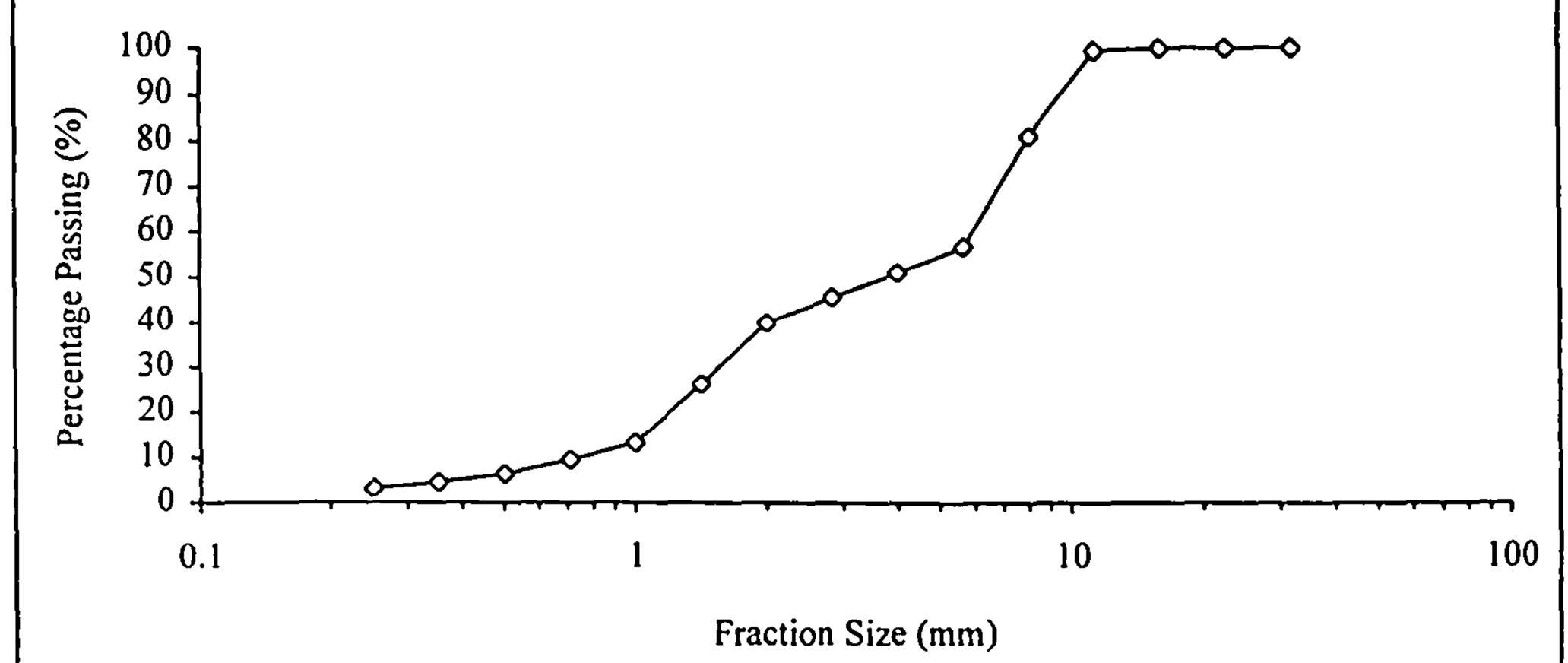

Figure 3.6c Cumulative Grading Curve for Design Mix C

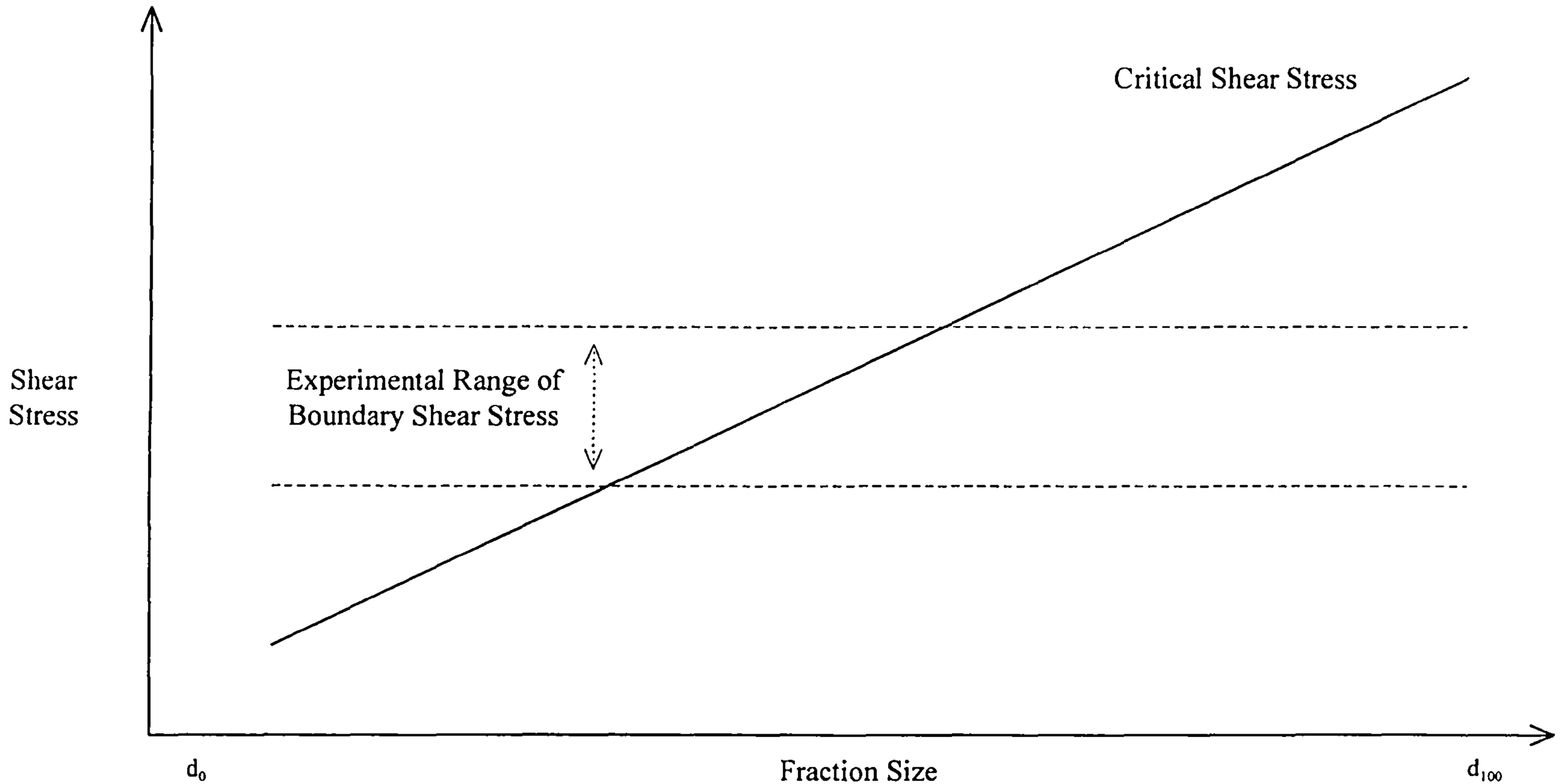

Figure 3.7 Theoretical Relationship Between Critical Shear Stresses of Individual Fractions and Experimental Range of Boundary Shear Stresses

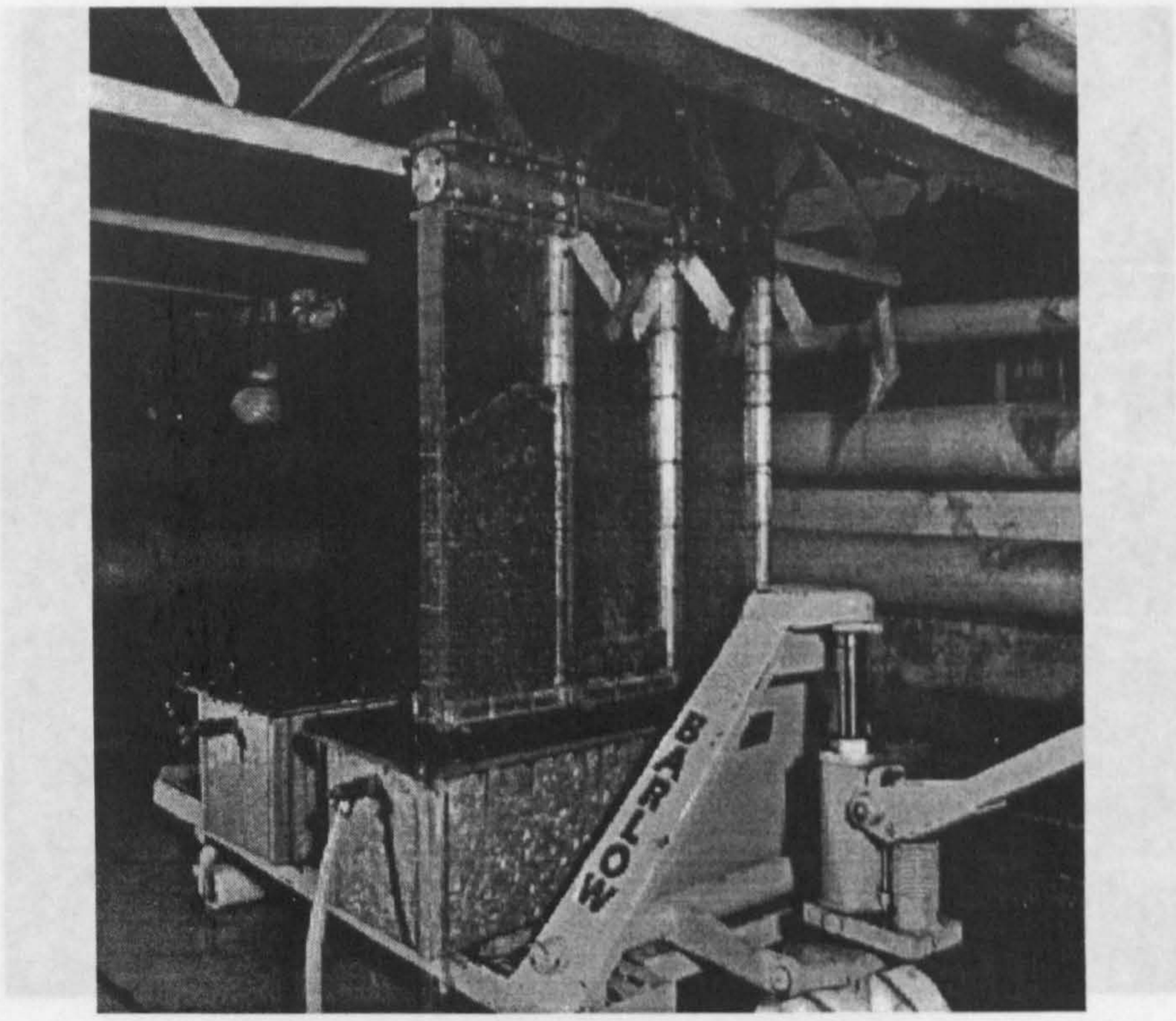

Figure 3.8 Bedload Sediment Transport Traps

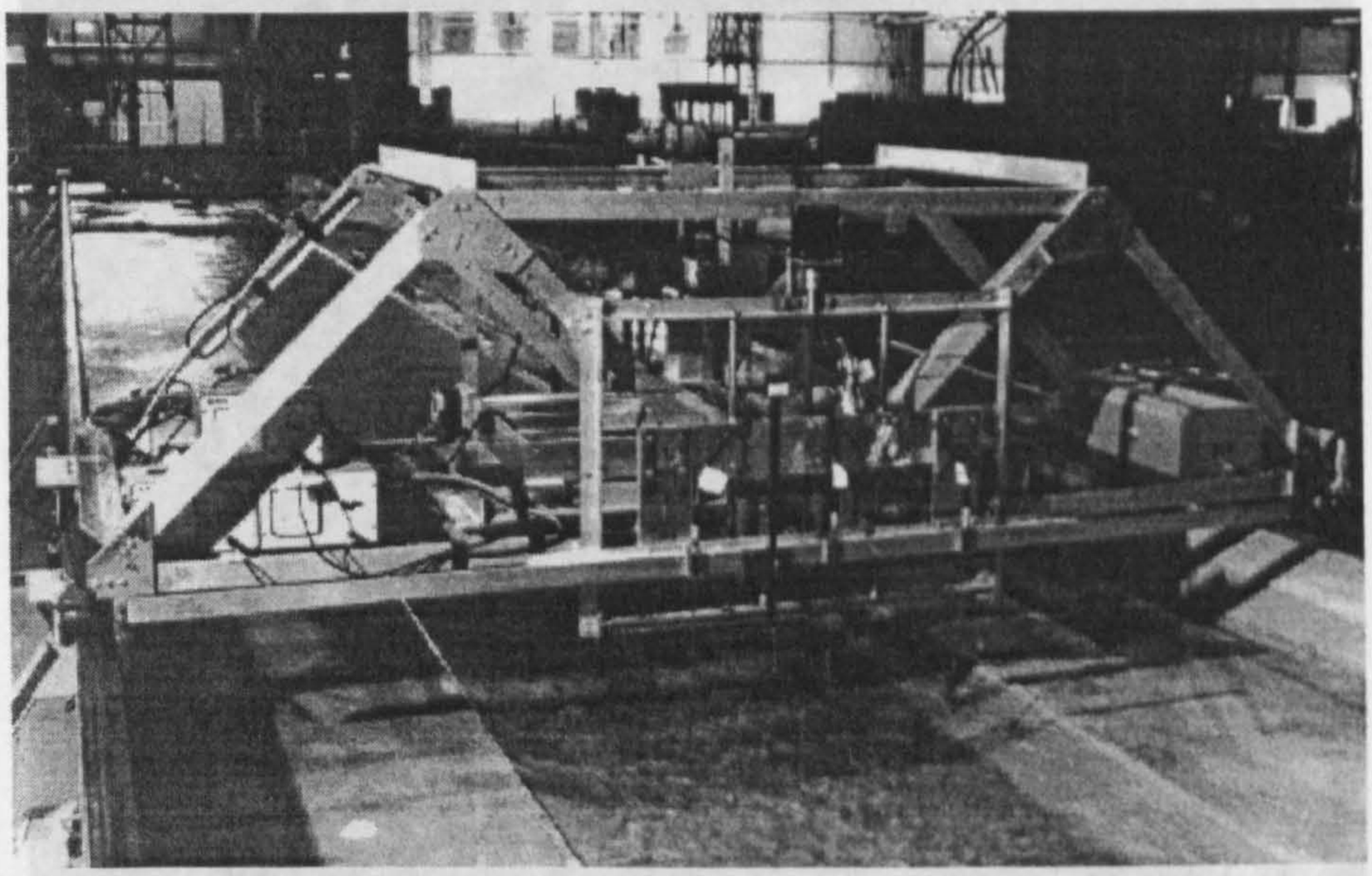

Figure 3.9 Instrument Carriage, Miniature Propellers and Main Channel Water Surface Pointer Gauge

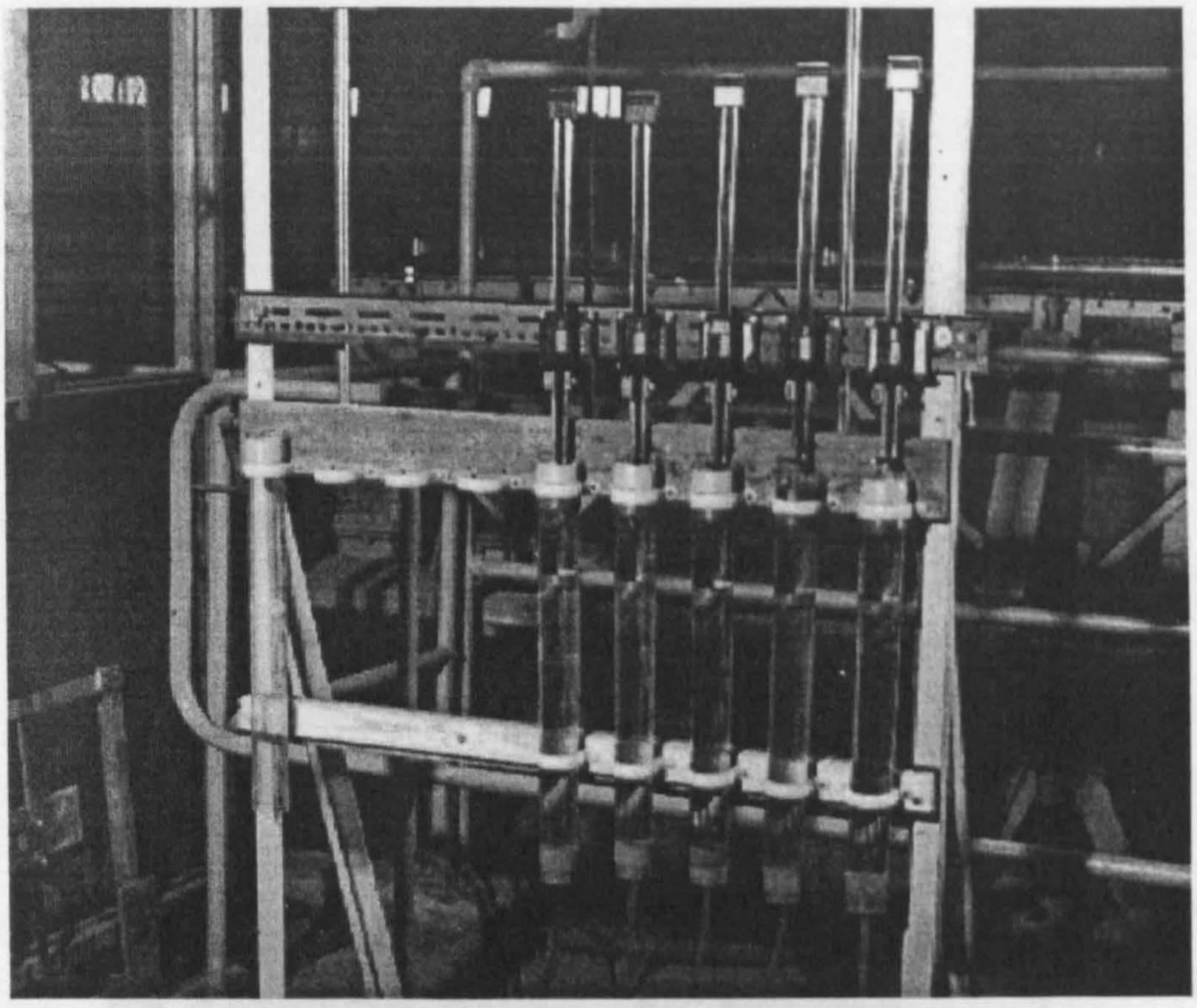

Figure 3.10 Pointer Gauges with Stilling Pots Attached to Main Channel Tapping Points

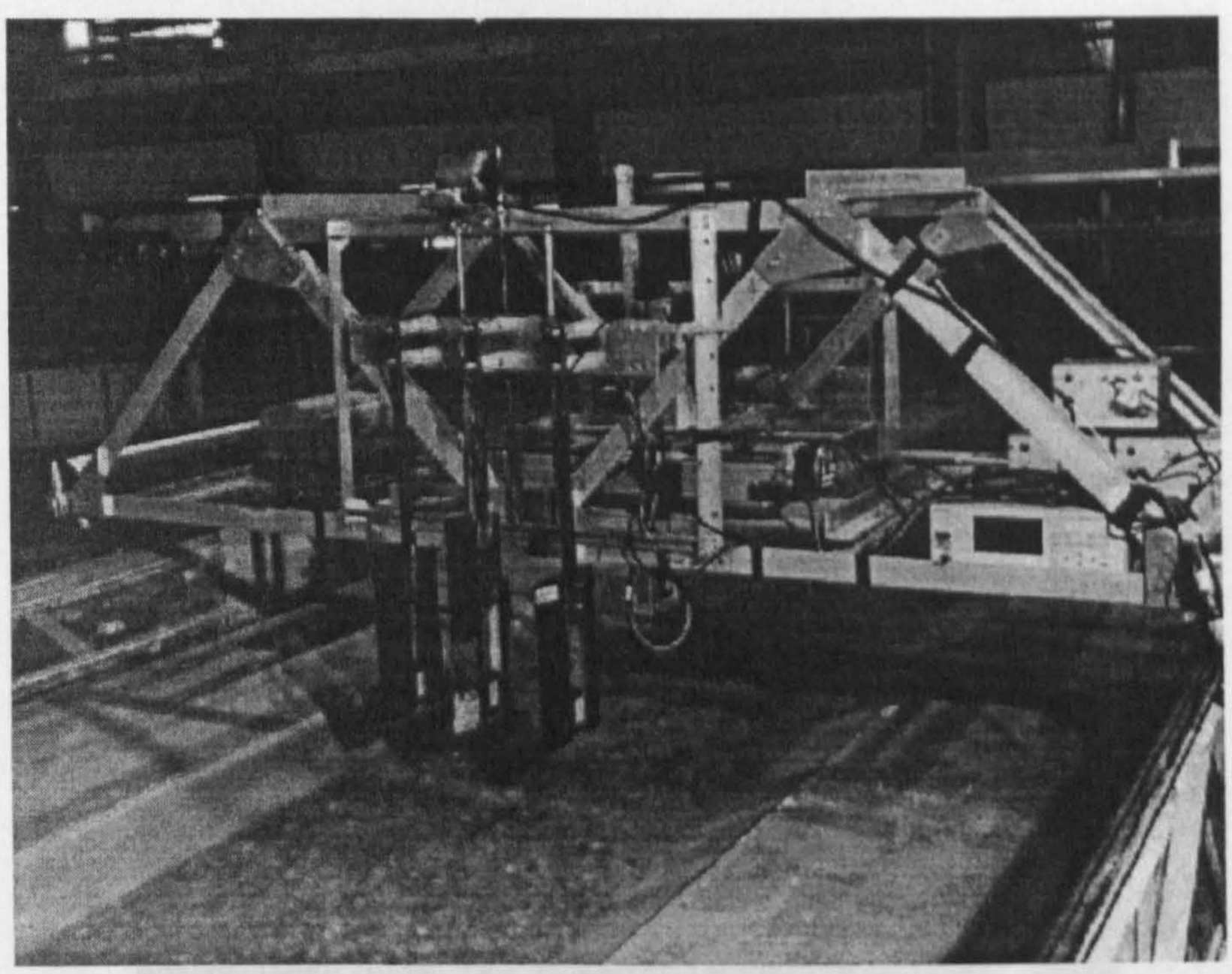

Figure 3.11 Longitudinal Lasers in Stream Lined Farings Attached to Vertical Positioning Frame

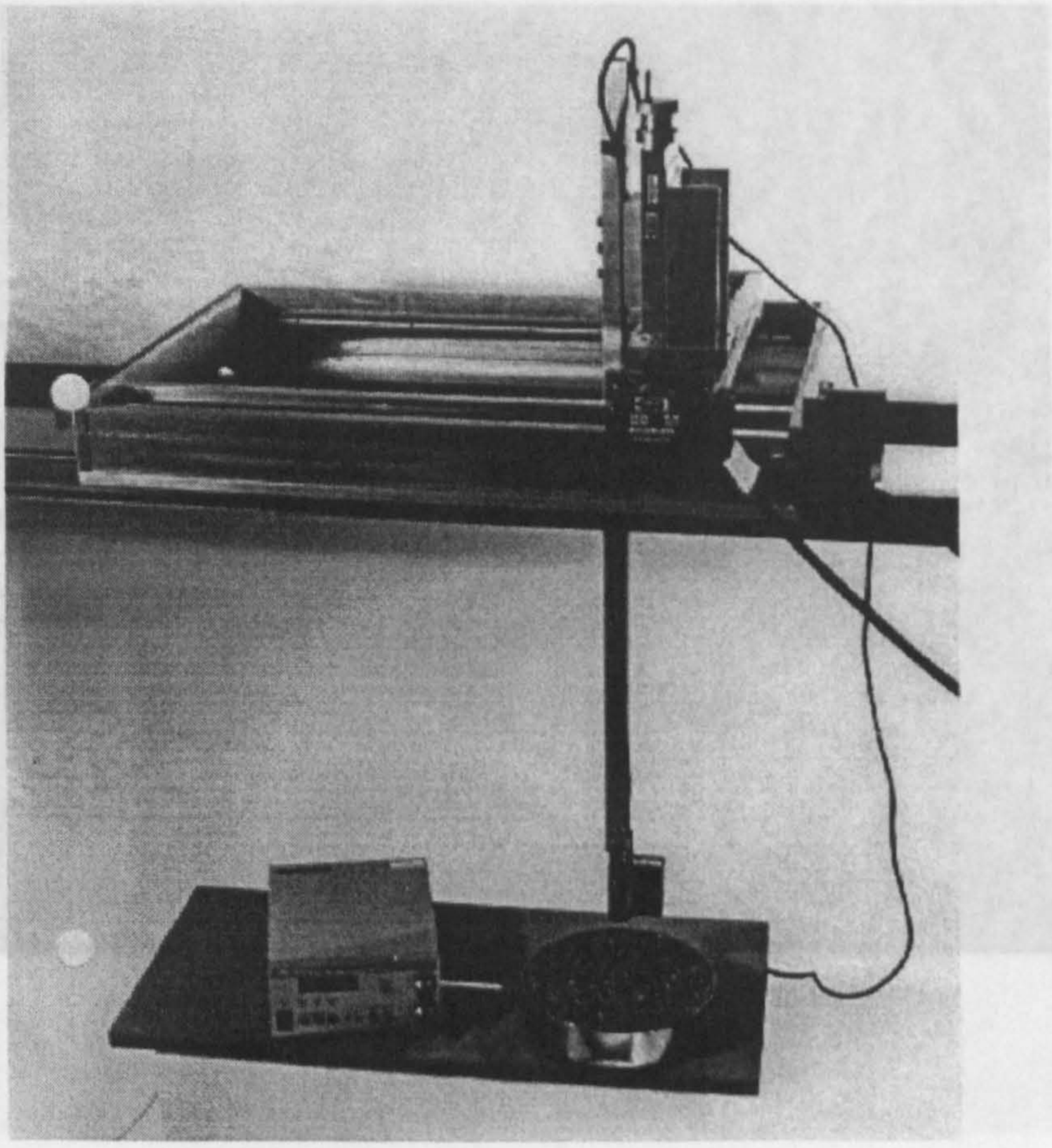

Figure 3.12 Bed Texture Laser and Positioning Frame

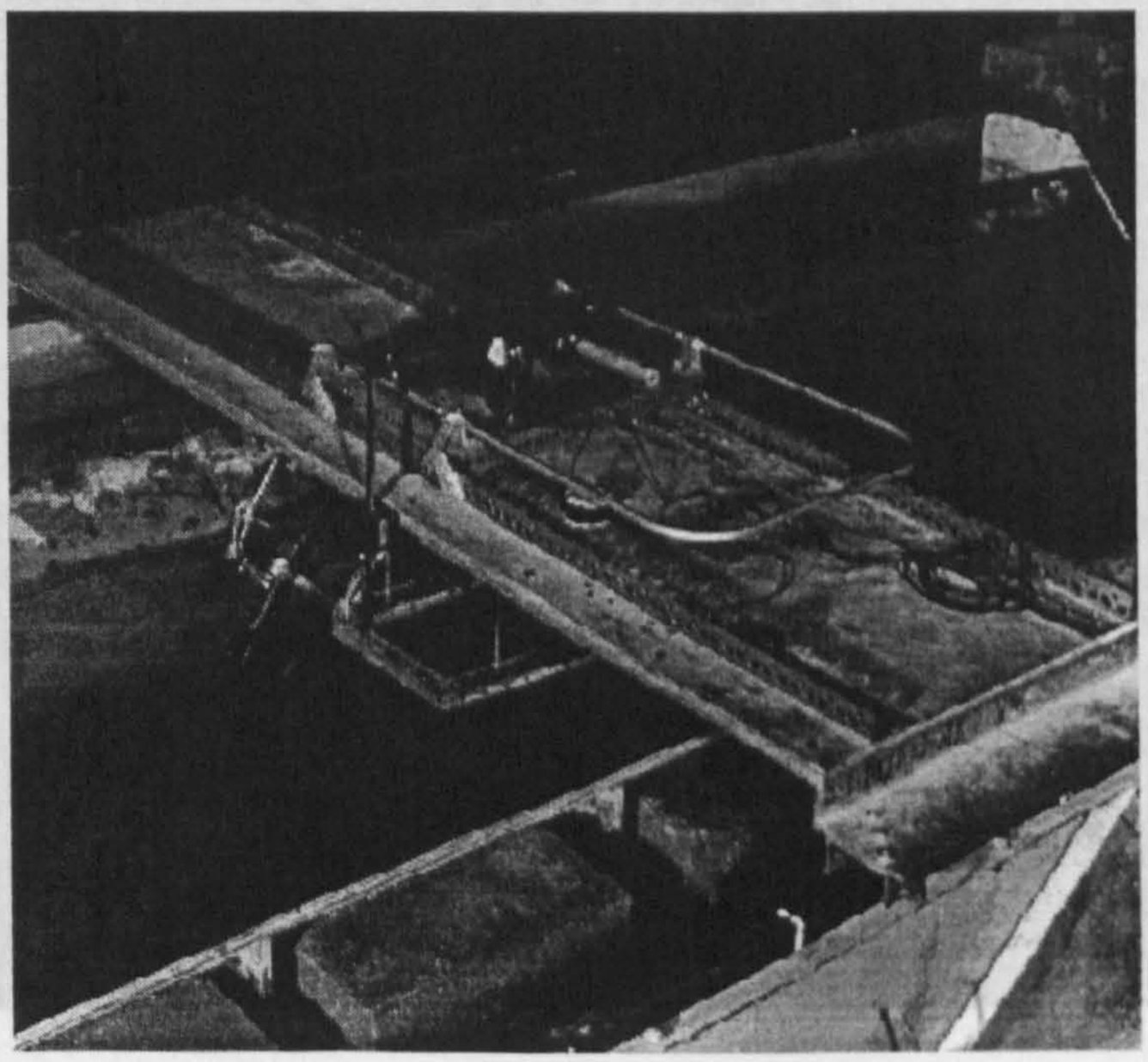

Figure 3.13 Photographic Instrument Carriage and Photographic Frame

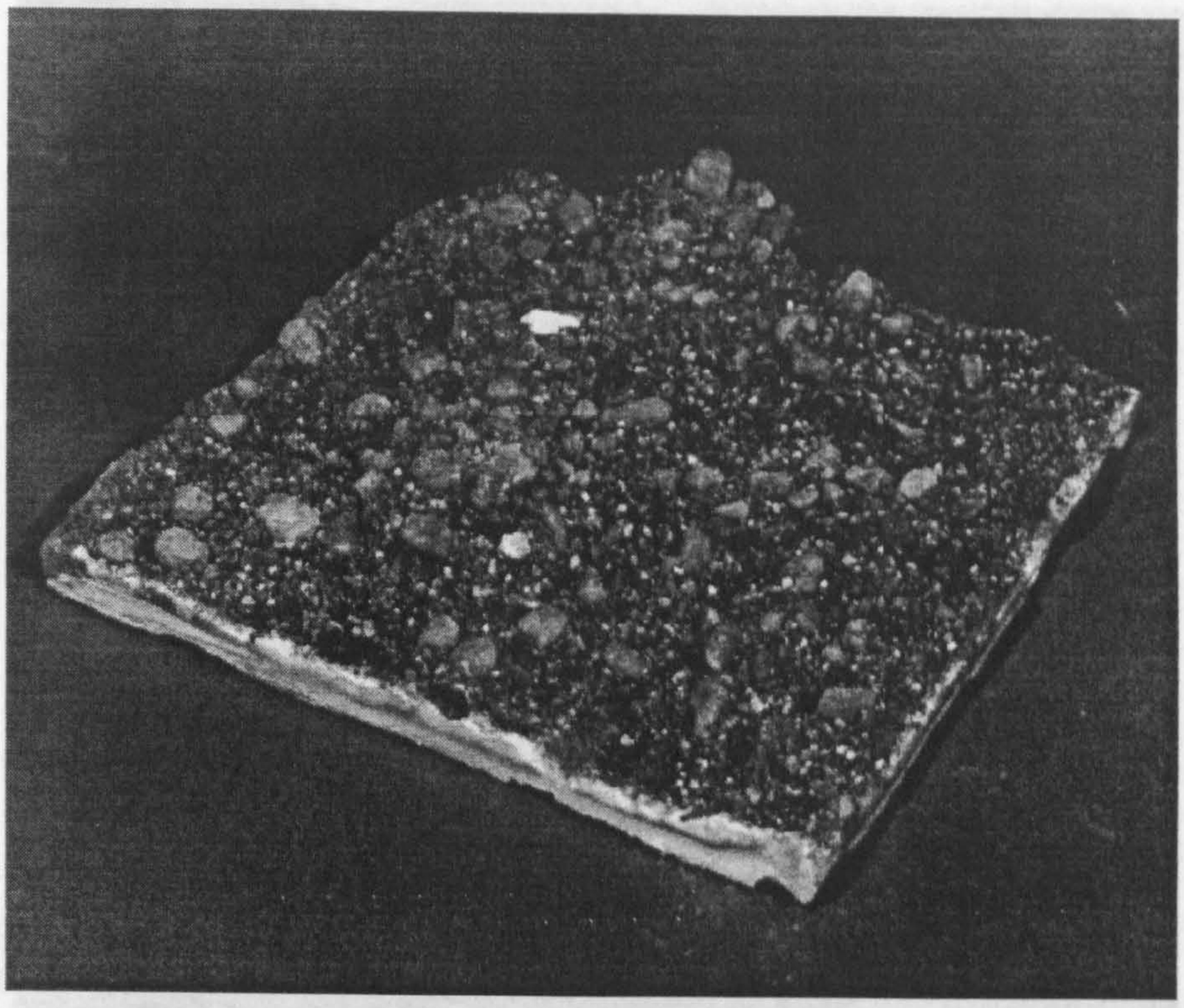

Figure 3.14 Areal Wax Surface Sample

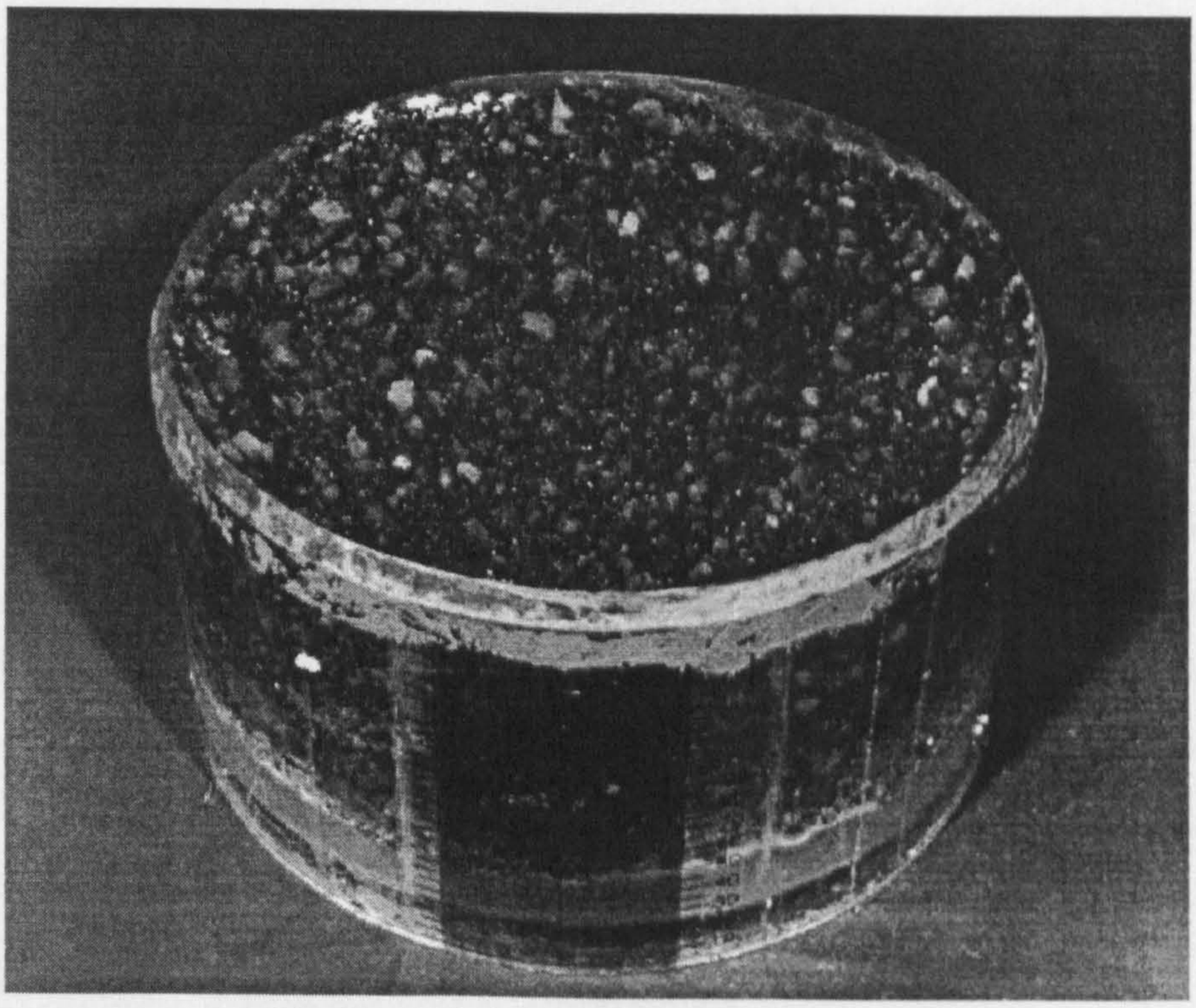

Figure 3.15 Bulk Wax Volumetric Sample

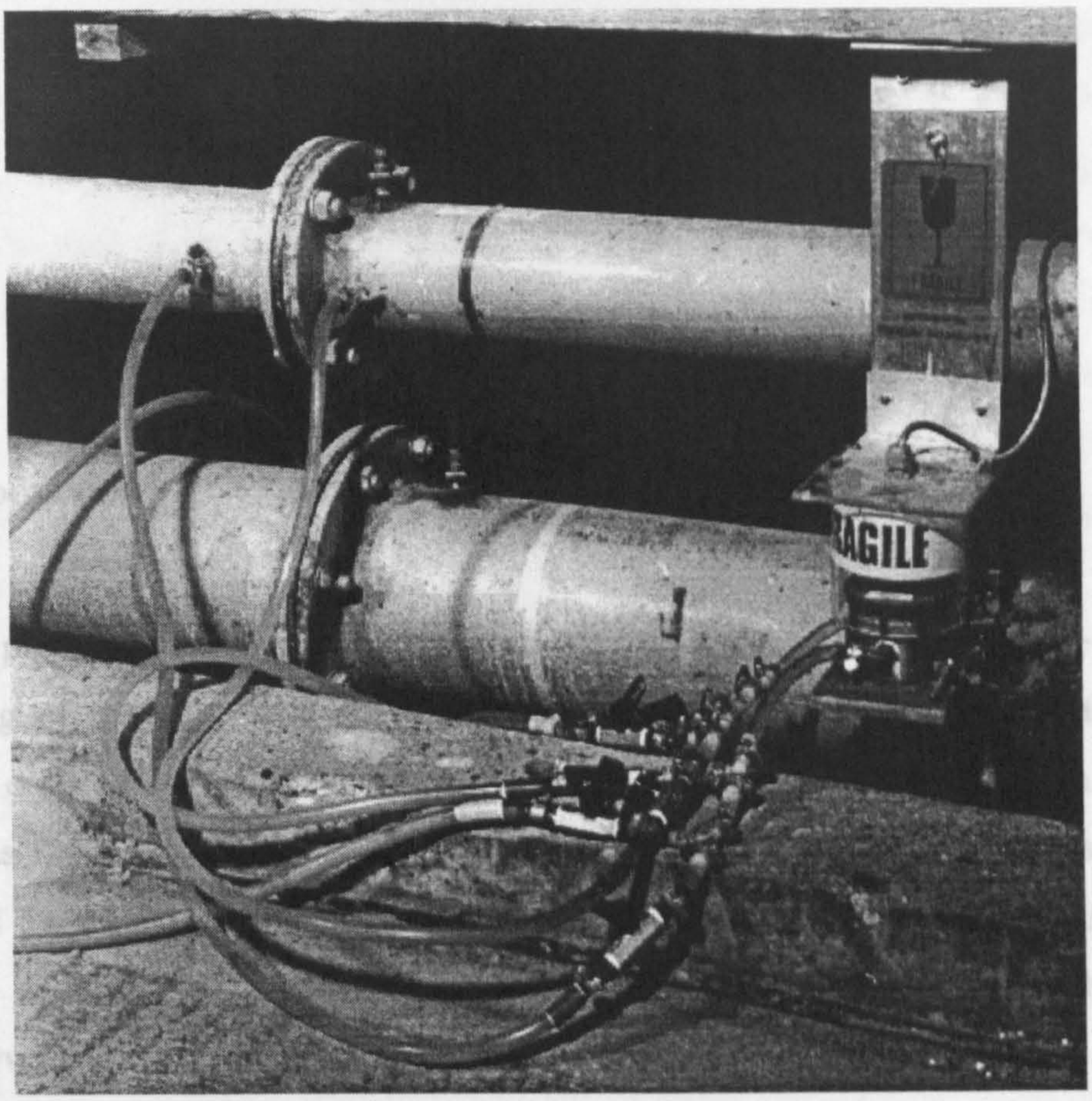

Figure 3.16 Pressure Transducer Connected Across Pipe Orifice Plate

Chapter 4

Data Processing

4.1 Introduction

Before presenting any results of analysis it is useful to briefly describe the processing of the raw data. The assumptions made and processes involved are therefore outlined below. Some samples of the processed data are presented in this chapter as illustrations. On the whole the basic data from the experiments is not presented for the sake of brevity. However, the data sets from the experiments are available and can be downloaded from the internet at the following address: http://www.civil.gla.ac.uk/research/GSRP.

4.2 Bed Mixes, Feed Mixes and Bed Surface Compositions

Two pieces of processing were undertaken on the compositions gained from sieve analysis of the bed, feed and bed surface material. The first of these was used on the results of the areal wax sampling, in an attempt to account for the bias towards coarser material created by the sampling technique. Because only grains with an exposed surface in contact with the wax are removed by the sampling technique, large grains are sampled from a deeper layer than small grains. Therefore, within the sample volume, the large grains are over represented relative to their number in the bed surface layer. The adjustment technique employed is that described by Marion and Fraccarollo (1997). The model is based on the statistical properties of homogeneous mixtures, rather than being an empirical exponential formula. The new model includes an evaluation of the sample layer thickness.

The second process was necessary due to the logistics of sieve analysis. The amount of sieving required meant that it was necessary to undertake this at three sites: Aberdeen, Glasgow and Wallingford. For practical reasons different sizes of sieves were used at each of the sites. The standard used was the half Phi range employed extensively in analysis of mixed size sediment. Conversion, of any sieve analysis results from sieves of a non-half Phi range, was carried out by linear interpolation of the points on the cumulative grading curve against the Phi scale. The resulting cumulative grading curve was then converted back to percentage composition on each sieve size in mm.

The results of these processes were descriptions of the graded materials sampled in terms of an equivalent bulk composition. In the first instance these results take the form shown in figures 4.1a and 4.1b.

4.3 Instrument Rail Survey

The survey data was reduced to an arbitrary datum using standard surveying procedures. The difference between left and right rail levels at any particular chainage was found to be no more than 4mm. At each chainage the levels of the left and right rails were averaged. A linear regression was then fitted to the average level values and the gradient of this was taken as the slope of the flume. The levels were then adjusted (each point by the same amount) so that the average of the left and right rail levels produced a regression passing through a level of zero at the datum chainage of 16.7 m. The derived linear regression was also important as it was used, to adjust the levels of readings taken from the instrument carriage, to produce data relative to a horizontal datum. An example of the reduced rail survey values and the linear regression are shown in figure 4.2.

4.4 Discharges

The output, in metres of head loss across the orifice plates, from the pressure transducer was converted to a discharge, in litres per second, at the time of

measurement. This was achieved using orifice plate calibration curves provided by HR Wallingford. No other processing was required, other than calculating an average discharge and checking the variation throughout the experiment, and between related experiments.

4.5 Air and Water Temperatures

Again no processing was required other than checking the variation throughout the experiments. The water temperature was found to be approximately constant throughout the year, while the air temperature varied.

4.6 Bedload Data

This was the first of the data sections which required a considerable amount of processing in order to produce useful values for analysis. From the raw sieve analysis data, cumulative grading curves were converted, where appropriate, using the technique described in section 4.2. The resulting data was then entered into an Excel workbook for each experiment. Within the workbook each sheet related to a single cycle and contained data from the left, centre and right traps, as well as a section combining all three to produce total transport data. An Excel macro, contained within each workbook, allowed for the derivation of the grading parameters. The values of the D_{16}, D_{50} and D_{84} sizes, along with the σ_g value, for each trap sample, and the total bedload, were calculated. The workbook also produced basic cumulative grading curves and percentage composition charts for left, centre, right and total samples. Plots of bedload sample grading parameters, compared with the original bed or feed material parameters (figures 4.3a and 4.3b) could then be produced.

To calculate the transport rate for each trap, and for the total channel, the weight of the sample collected was divided by the time over which the sample was collected. The unit transport rate was then calculated by dividing these values by the effective width of the channel bed across which the trap sampled. For the centre trap the

effective width was the width of the trap, as any material to either side was collected by the left and right traps. For these traps the effective width was greater than the width of the trap, as the total width of all three traps was less than the width of the mobile bed. However any material to the outside of the outer traps would slide down the sloping side walls and enter the traps from the side. In this way the full width of transport was sampled. Any slight variations in mobile bed width, due to degradation or aggradation were ignored, and the total width of the bed was assumed to be 0.8 m. The physical width of the three traps was 650 mm. The effective width of the centre trap was therefore taken as (650 mm/3) = 216.6 mm, while the effective widths of the left and right traps were taken as ((800 mm - (650 mm/3))/2) = 291.6 mm. Examples of the resulting plots, both individual trap and total unit transport rates, are shown in figures 4.4a and 4.4b.

4.7 Longitudinal Bed Level Profiles

Although two slightly different methods were used to collect the data, on longitudinal bed level variation throughout the experiments, the results were processed in the same way. This involved four steps to get from the recorded output of the A/D card, to data relating bed levels at chainages along the flume to a common horizontal datum.

Step 1: The digital units recorded were converted to chainages in metres and distances between bed and laser in millimetres. This involved using calibration equations relating the output of the wire potentiometer to positions along the flume, and the output from the lasers to distances between the bed and the lasers.

Step 2: The distance values gained from the lasers then had to be inverted to produce levels. Without this step a large reading of distance gained, due to the bed being low and far away from the lasers, would produce a result appearing to be a high point in the bed.

Step 3: Once inverted, the resulting profile had to be adjusted to take account of the lasers not being at the same level above datum every time a profile was recorded. This was why data was recorded over the concrete block. Its absolute level didn't change and therefore each profile could be related to that level. To make the adjustment the levels over a narrow range of chainages above the block were averaged and the result subtracted from every level recorded in the profile. This made the levels over the block zero and allowed comparison between profiles.

For Experiments 2 and 3 no readings over the block were made as the wire potentiometer was not in place. The laser, attached to the bed texturing positioning frame, was at the same level for each profile. The longitudinal profiles were therefore relative to each other. To relate them to the block all levels in profiles from Experiments 2 and 3 were adjusted so that the initial profile from each experiment matched the initial profile of an experiment with the same initial bed slope (Experiment 4).

Step 4: This step accounted for all the levels being related to a sloping datum with the same gradient as the rails. In order to produce a profile related to a horizontal datum the equation of the linear regression of the rail survey was employed to add a value to each level dependent on its chainage.

From this processed data three more stages were implemented to produce useful information. All points recorded at chainages less than 6 m and greater than 16 m were disregarded. The remaining data was then scanned by eye and any readings that were obviously spurious removed. The criteria for being spurious was that either a chainage was out of sequence or the bed level between two readings increased by a value greater than approximately twice D_{84}. Finally the levels at each chainage were averaged to produce an average bed level across the width of the channel at each chainage. The result was longitudinal bed level profiles, at times throughout all the experiments, related to the same horizontal datum level of the concrete block.

The initial and final bed level profiles for Experiment 4 are shown in figure 4.5.

4.8 Water Surface Profiles

The pointer gauges used to measure the water surface were zeroed to constant datum positions throughout each of the experiments. This enabled checks on the consistency of the data to be made during an experiment. The pointer gauges attached to the stilling pots were outside the flume and their datum was a horizontal water level marked on the stilling pots. The data collected from them therefore required no adjustment for the slope of the flume. However, the data collected from the instrument carriage pointer gauges required to be reduced using the linear regression of the rail survey as described in Step 4, section 4.7. Both sets of profiles were then adjusted to take account of the difference between the profile datum levels and the concrete block level.

The result are water surface profiles related to the same datum level as the bed profiles, and which illustrate the changes in surface slope with time. An example of the final water surface profile data, which could be plotted on the same figure as the relevant bed level profiles, is shown in figure 4.6.

4.9 Flow Velocity Profiles

Velocities were recorded at chainages relating to the tapping points, and at levels through the flow depth, relative to the bankfull level. It is possible to relate velocity readings to both height above the bed and depth below the water surface, due to all the data being related to the fixed levels of the block or flood plains. However, this is a time consuming process and so it has only been carried out where the analysis undertaken has required it.

Step 1 : For the known chainage at which the velocity has been recorded the bed level is calculated using a linear regression. The regression employs the average of the left, centre and right profiles collected or an average of the reading collected around the chainage in question, depending on the profile of the bed.

Step 2 : The water surface level is calculated similarly.

Step 3 : The level at which the individual velocities were recorded is then converted from being related to the bankfull level to a level, above the concrete block.

Once all the levels of velocity readings are converted, and the levels of the bed and water surface are known, it is possible to compare velocity profiles at different times. This is done by relating the velocity levels to either the bed or the water surface, by subtraction of the greater level from the lesser level (figure 4.7).

4.10 Bed Surface Texture Laser Surveys

The initial stages of post-experimental processing for the texture data were carried out by Aberdeen University. The texture data contained a periodic accuracy check, throughout each survey, which involved the laser returning to the same point over the bed and repeating the reading. This happened several times, spaced evenly throughout the survey, and the values recorded were called home values.

The processing included the following steps.

Step 1: Removal of all data beyond the point when the home values cease to be consistent.

Step 2: Removal of all points with an out of range value and replacement with an average of the two adjacent values.

Step 3: Conversion from A/D units to X and Y co-ordinates and levels (in mm), using calibration equations derived during the experimental programme.

Step 4: Arranging the data into files, for each survey, containing X and Y co-ordinates and corresponding levels.

It is not yet possible to derive a composition for the bed surface material from the topography data collected. However, the non-destructive recording of detailed bed topography is an important measurement not previously possible. Continuing work at Aberdeen University is attempting to identify individual grains from the texture survey data which would then lead to an estimate of composition (figure 4.8).

4.11 Bed Surface Photographs

Details of the chainage and the elapsed time were recorded, at which each photographic frame, on each roll of film, had been taken. The post experimental processing then included labelling the photographs with an identification code and then sorting them into adjacent frames. This was necessary as the area surveyed, by the bed texturing laser, was greater than a single frame size. Often two or three photographic frames were used to cover the full textured area (figure 4.9).

4.12 Event Sheets

For each experiment undertaken the relevant period of event sheets were examined and edited to remove information not relevant to the results or information recorded elsewhere. A table of events was then produced for each experiment containing only data about the running of that experiment and details of events that might have effected the experimental results. A table of events for each of the experiments analysed in this thesis is presented in Appendix A.

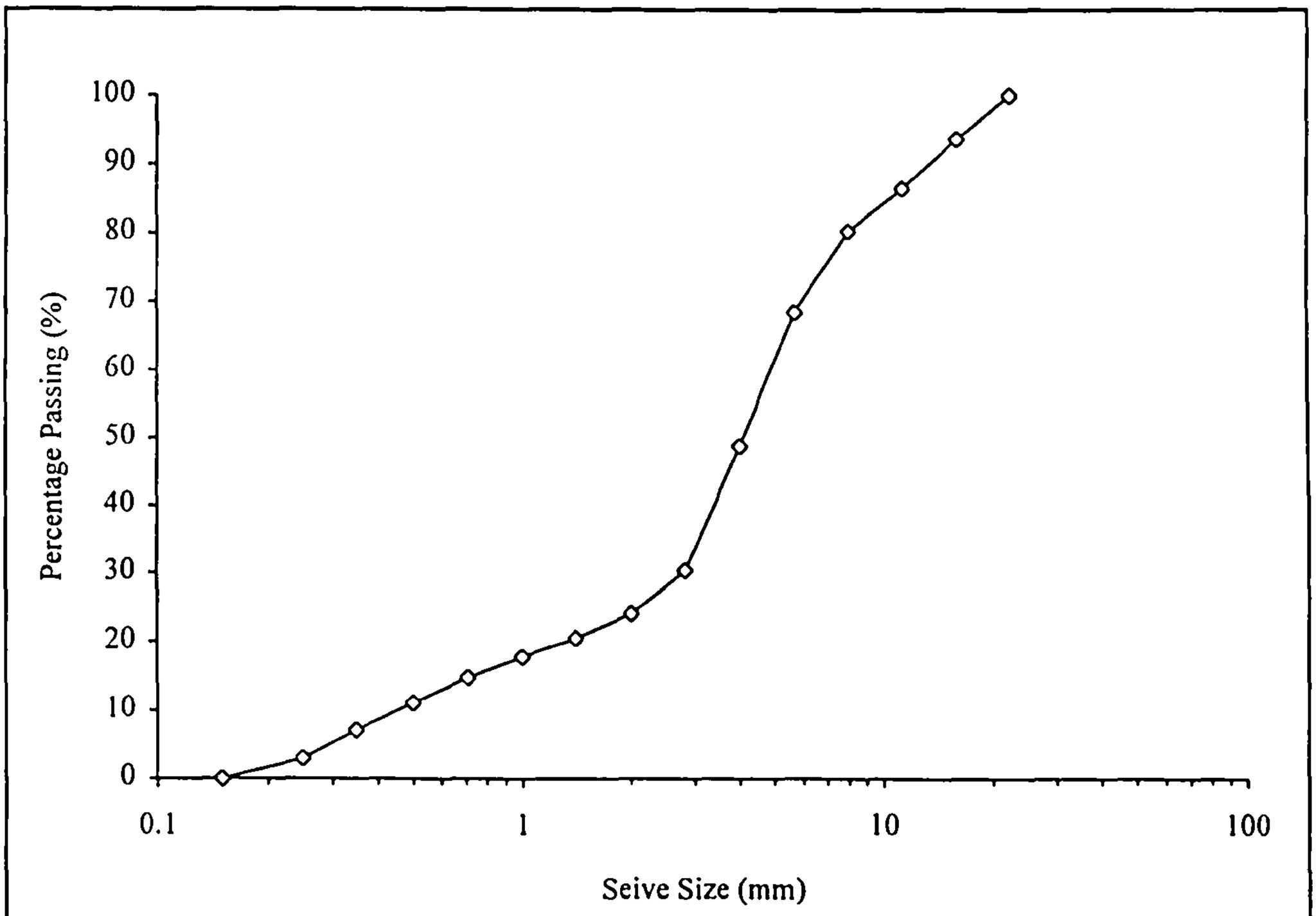

Figure 4.1a Cumulative Grading Curve, Experiment 4 Final Bed Surface Sample

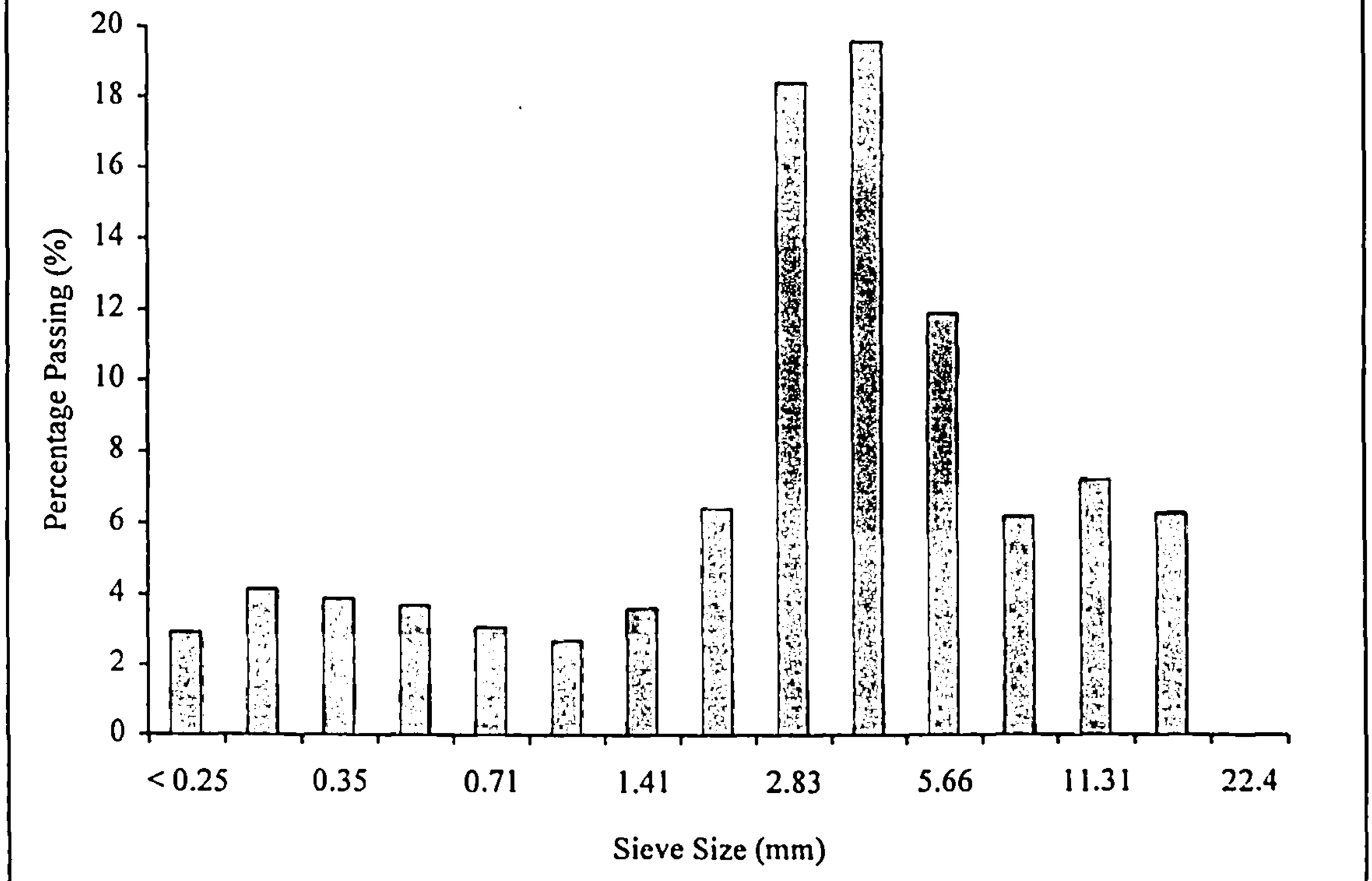

Figure 4.1b Fraction Composition Bar Chart, Experiment 4 Final Bed Surface Sample

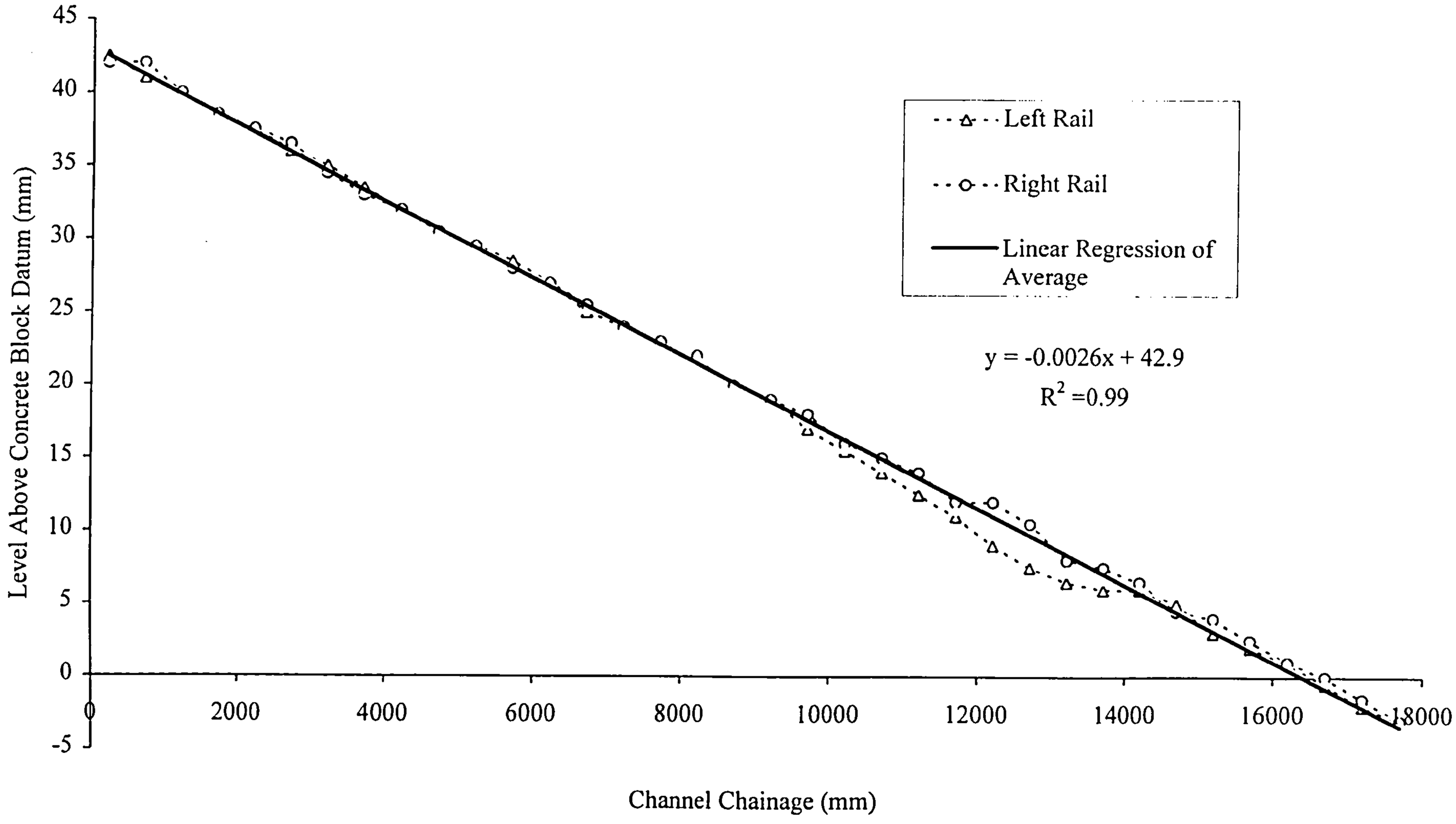

Figure 4.2 Rail Survey and Linear Regression, Experiment 4

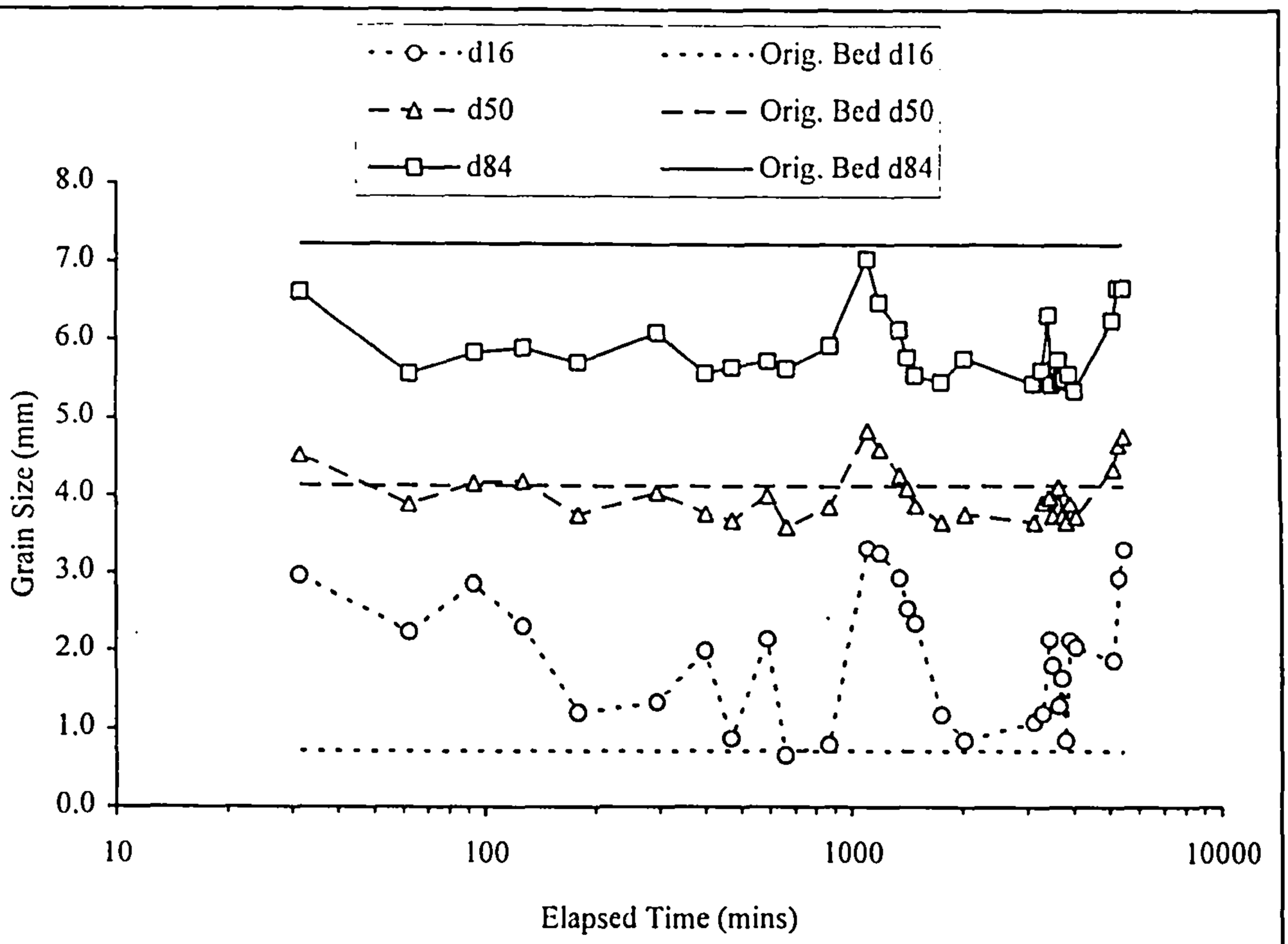

Figure 4.3a Comparison Between Bedload Sample Grading Parameters and Original Bed Material Parameters, Experiment 4

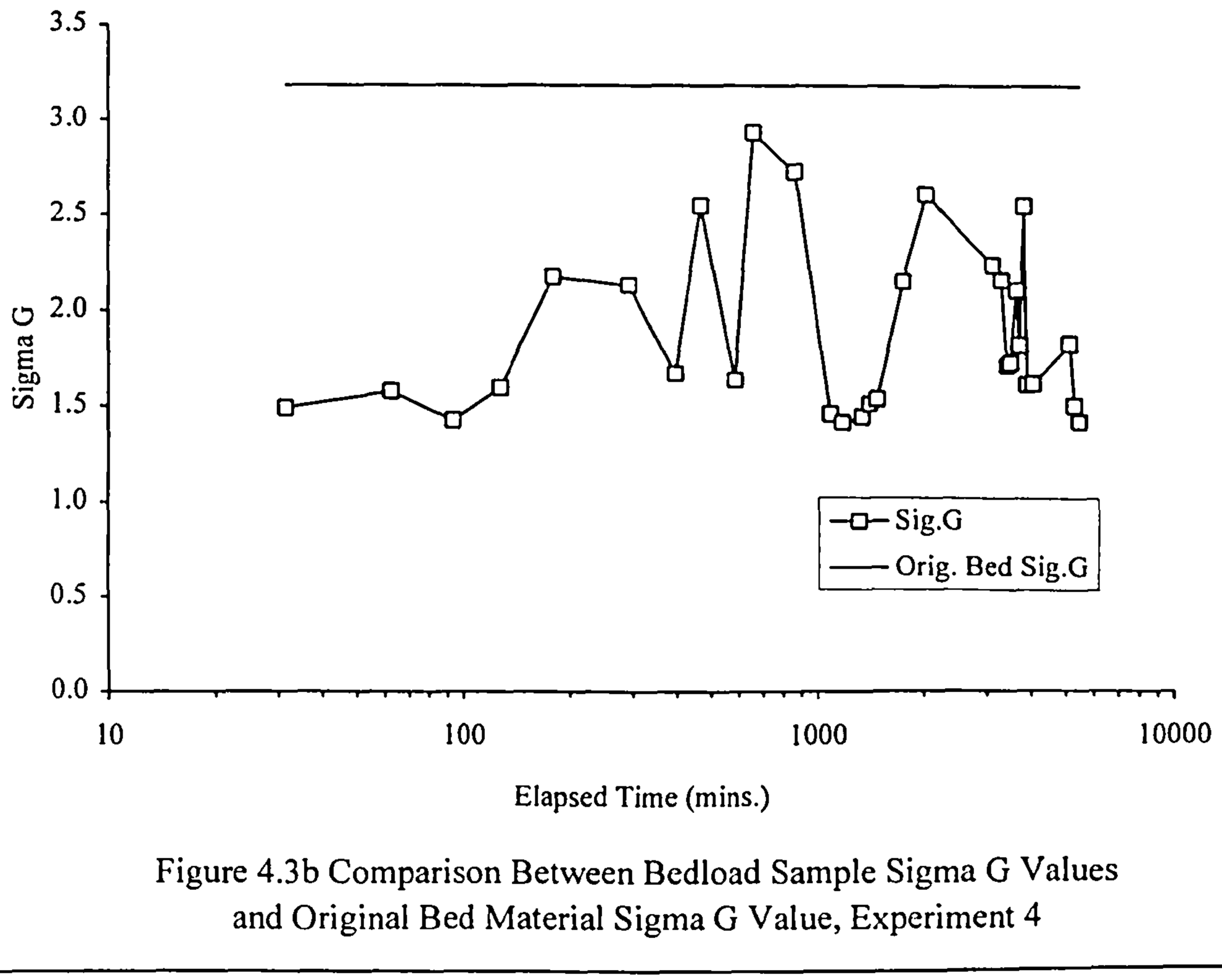

Figure 4.3b Comparison Between Bedload Sample Sigma G Values and Original Bed Material Sigma G Value, Experiment 4

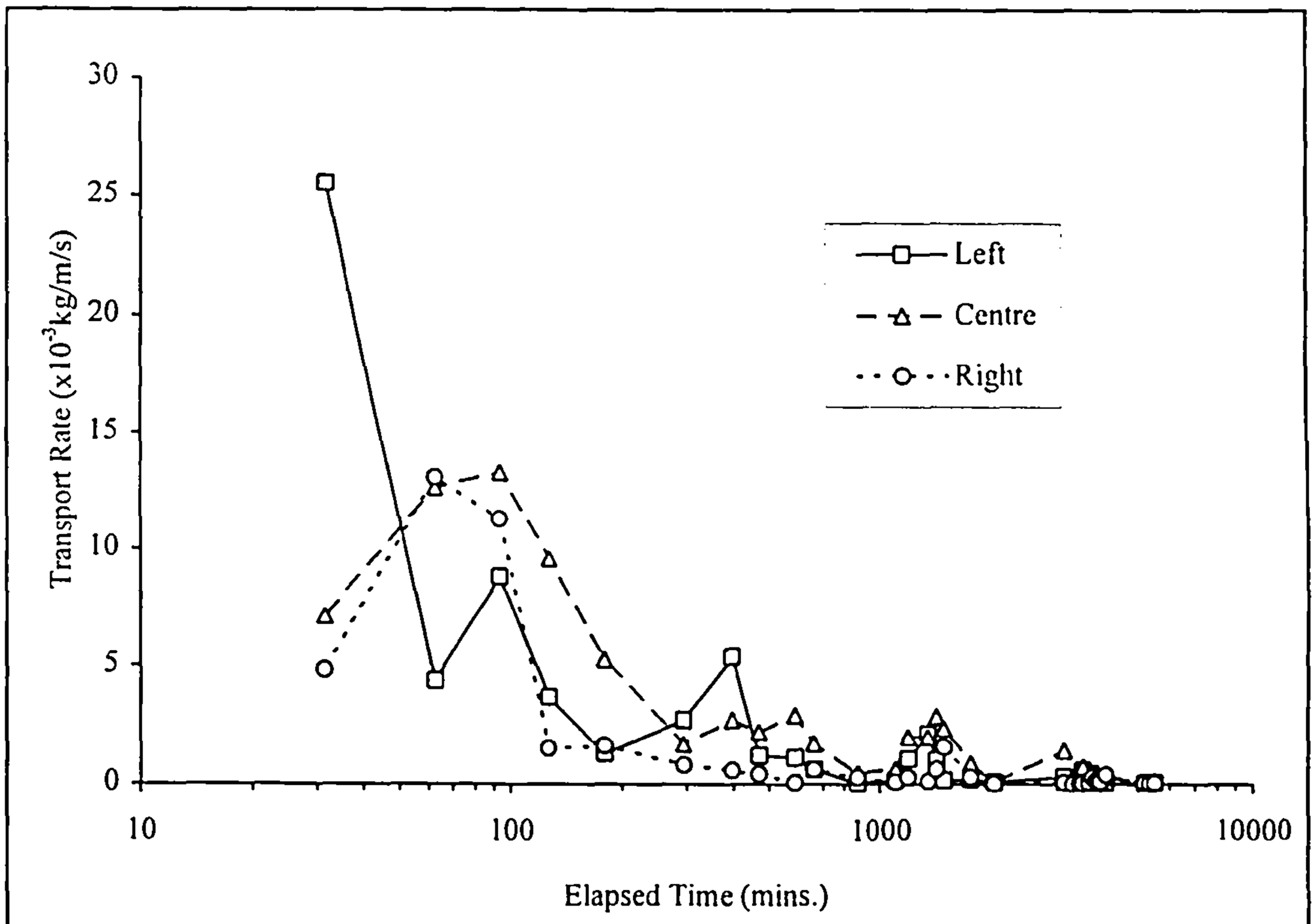

Figure 4.4a Individual Unit Transport Rates For the Left, Centre and Right Traps, Experiment 4

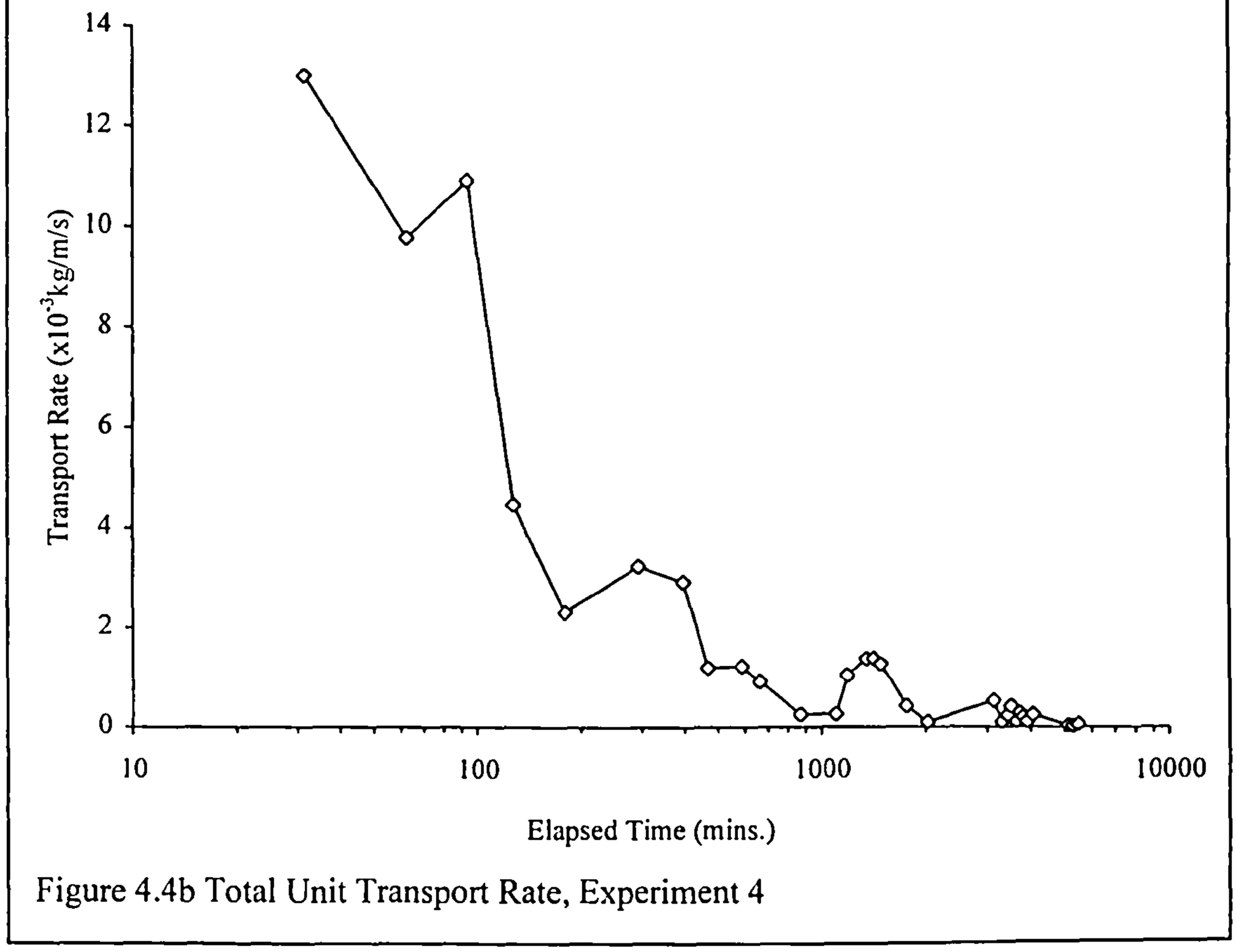

Figure 4.4b Total Unit Transport Rate, Experiment 4

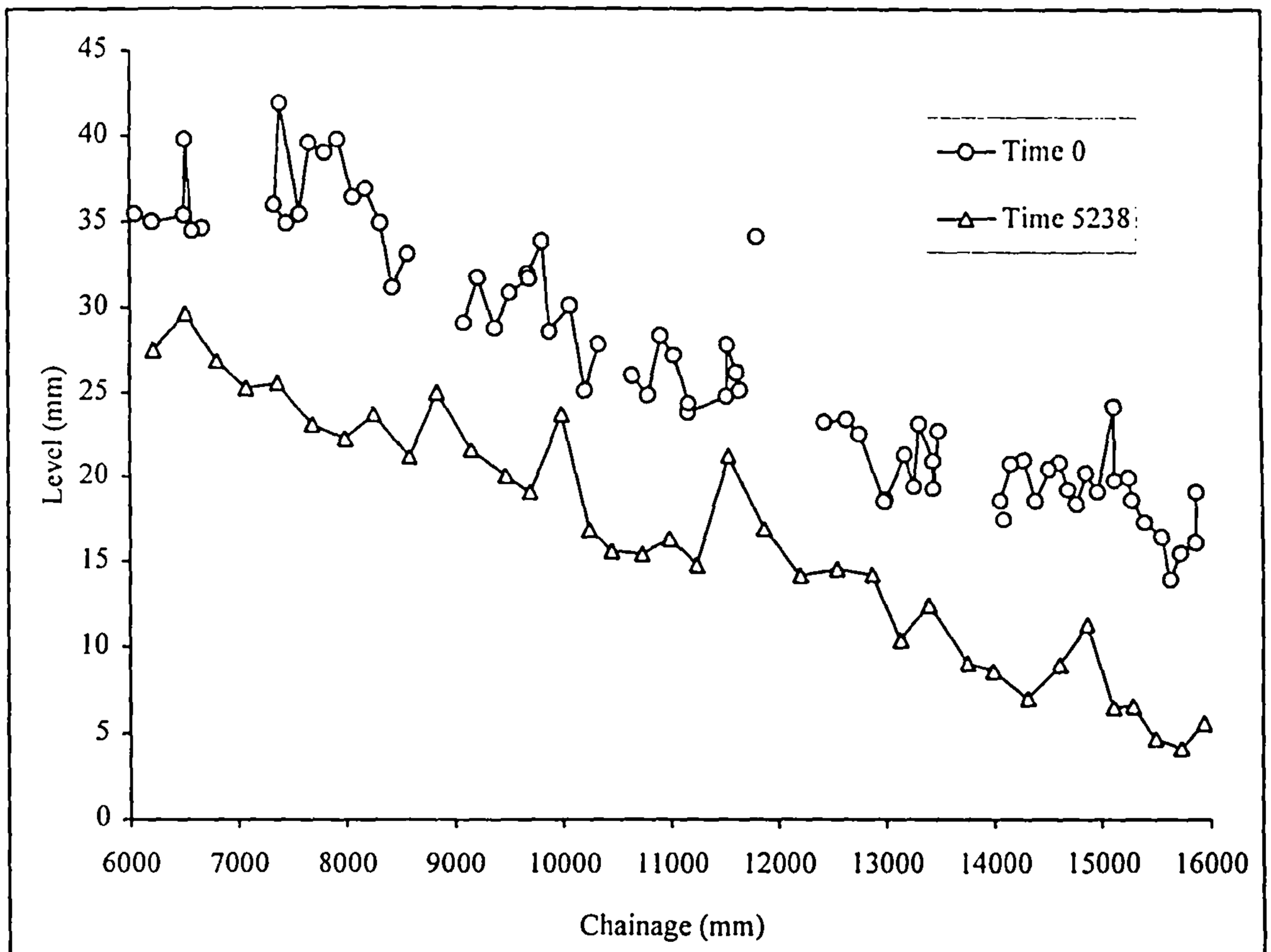

Figure 4.5 Initial and Final Bed Level Profiles, Experiment 4

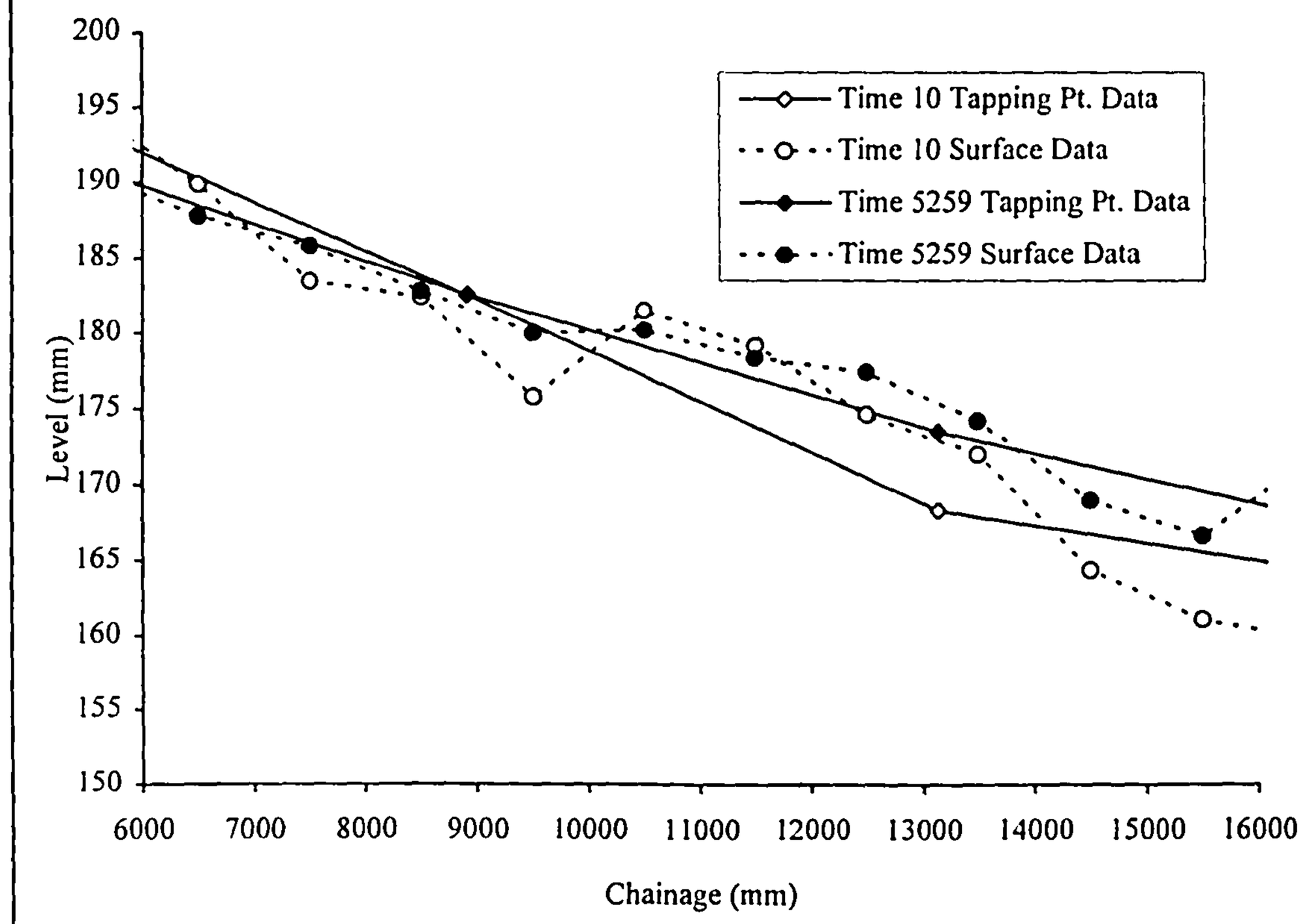

Figure 4.6 Water Surface Profiles From Tapping Point and Within Channal Pointer Gauges, Experiment 4

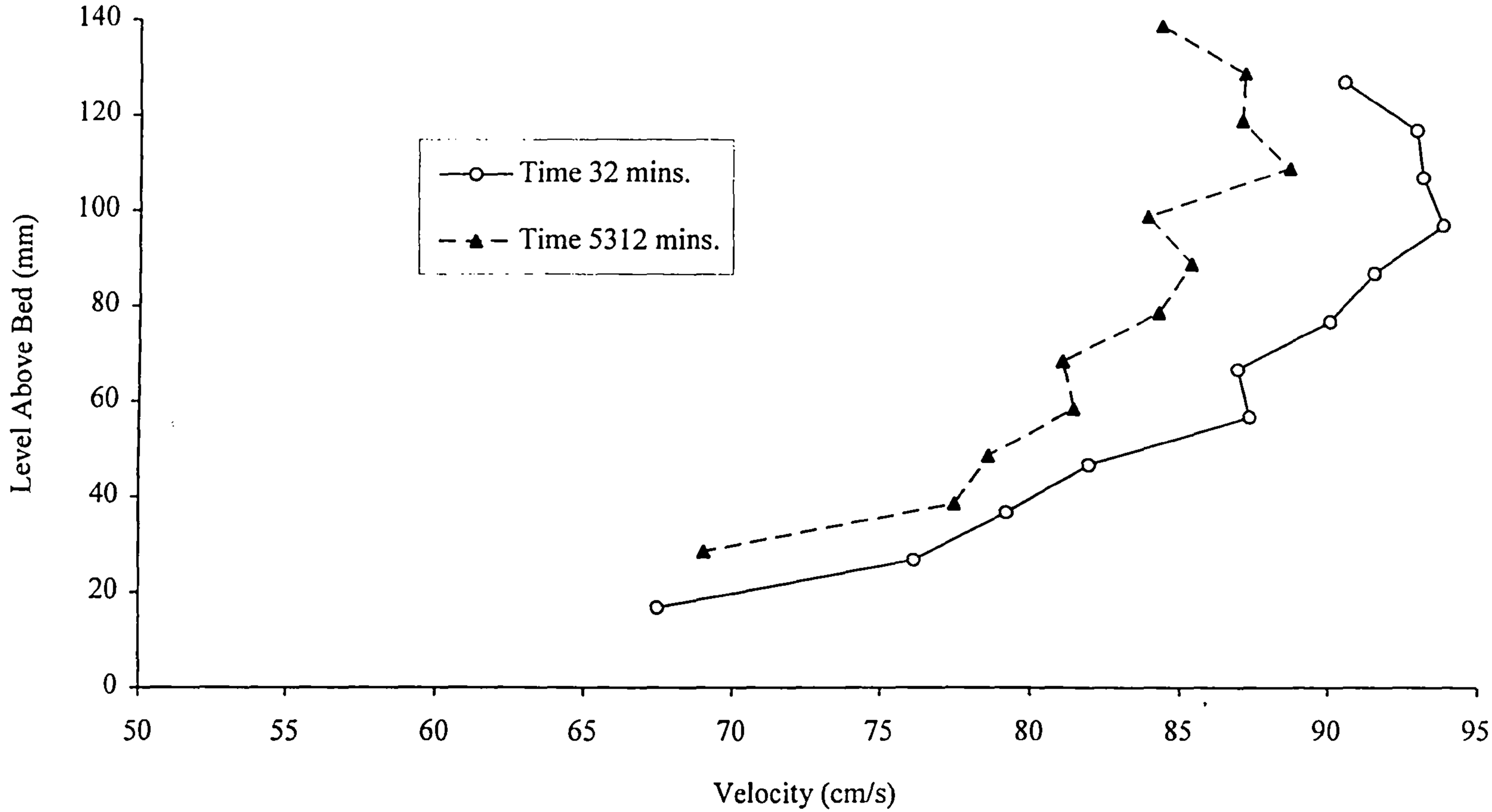

Figure 4.7 Velocity Profiles Related to the Bed Level,
Experiment 4, Tapping Point 4 (ch. 13.14m)

Figure 4.8 Detailed Bed Topography Data, Greyscale Plot

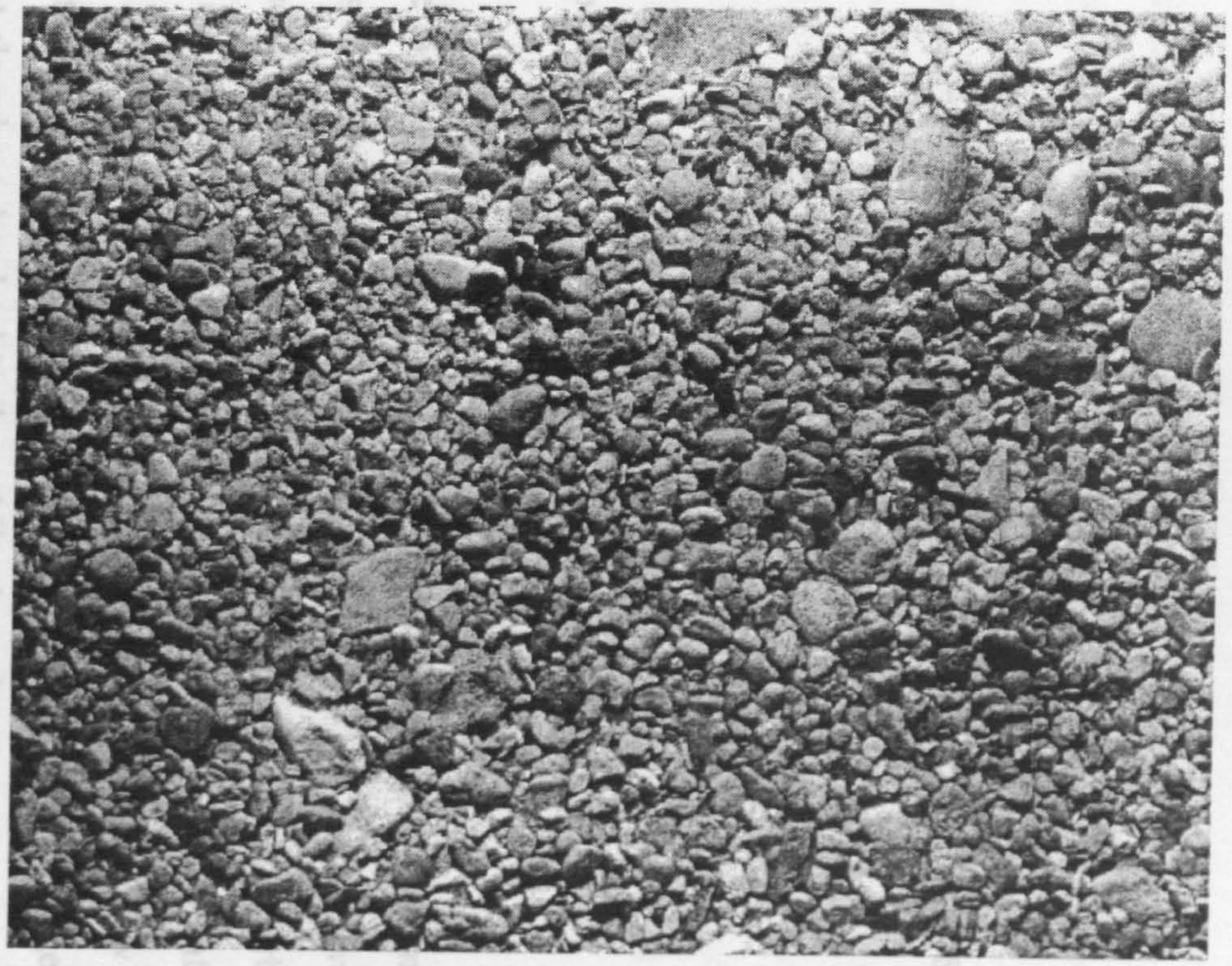

Figure 4.9 Photograph of the Bed Surface

Chapter 5

Comparisons of Sediment Transport Rates: Bankfull and Overbank Flow

5.1 Introduction

Over the last 10 to 15 years much research has been carried out investigating the hydraulics of overbank flow in compound channels. EPSRC funded work in the U.K. has produced extensive data sets from large scale modelling of overbank flow. The work has examined channels with both straight and meandering planform geometry. Research has focused on conveyance characteristics, turbulent flow structures and lateral distribution of boundary shear stress. Analysis of this data, together with work carried out elsewhere, has lead to the publication of design manuals for straight and meandering compound channels (Ackers 1991; James and Wark 1992). Numerical models have also been developed to predict the lateral distribution of both depth-averaged velocity and boundary shear stress (Knight and Abril 1996; Wark 1993).

Most of the work to date relates to channels with fixed boundaries and uniform roughness. A significant set of such work was the first series experiments funded by SERC (now EPSRC) and carried out at HR Wallingford between 1986 and 1989. As part of the research carried out in the series, the lateral distribution of boundary shear stress was measured, for various discharges and therefore stage levels (Shiono and Knight 1991). Researchers have since postulated how sediment transport in a channel would vary with inbank to overbank variations in stage level (Ackers 1992b; Knight and Abril 1996; Knight and Shiono 1996). The variation in sediment transport in a hypothetical river channel suggested by Ackers (1992b) can be seen in figure 5.1. The research presented in this chapter investigates if the proposed decrease in transport rate at shallow overbank depths is supported by our experimental data. The

experimental data to be examined relates to the specific condition of no sediment feed, no sediment recirculation, degradational graded sediment transport.

What makes this work novel is that, research into graded sediment transport has to date concentrated on inbank flow conditions. For example, Wilcock and Southard (1989) have published work on varying mobility between size fractions; Sutherland (1991) on hiding functions; Parker et al (1982a,b) on bedload, active layer and substrate interaction; and Parker (1990) and Tait and Willetts (1991) work on static and mobile armour layer development.

Earlier analysis by the author, of bankfull / overbank transport rates, has been published in the proceedings of the 27th IAHR Congress (Ervine et al 1997). Within the paper a similar approach was taken to gain values of boundary shear stress but less attention was paid to the related unit transport rates. An earlier line of research was also included, examining the difference in predicted boundary shear stress and critical bed shear stress. This area of work has since been discarded. Of the two conclusions presented the first still hold true and is included in this volume while the second related to the discarded work. The paper was limited in its length and was written during the early stages of the work presented in this chapter. Consequently the completed work presented here is more extensive in its analysis and more conclusive in its results.

5.2 Experimental Range

The experiments used to carry out the investigation were a sub-group of those shown in Table 3.3, Chapter 3. Five experiments were examined, as shown in table 5.1 below. As with the entire range of experiments, the five presented here were designed to cover a range of bankfull and overbank stage levels. In doing so this allows for the examination of boundary shear stress variation with stage level. In particular it affords the comparison of the recorded experimental results with the variation proposed form Series A work and supported by Ackers (1992b) and Knight and Abril (1996). An idealised variation of boundary shear stress with stage level is

presented in figure 5.2. The region of particular interest is that just above bankfull where a reduction in the main channel boundary shear stress has been proposed for an increase in discharge and therefore stage level. The experiments also allowed examination of the effects of initial bed slope and stage level changes on transport rate.

Table 5.1 Experiments used in bankfull / overbank transport analysis

Experiment No.	Initial Bed Slope	Initial Flood Plain Depth (mm)	Stage Level Description	Experiment Duration (mins.)
4	0.0026	0	Bankfull or Inbank	5555
2	0.0026	20	Shallow Overbank	4162
3	0.0026	65	Deep Overbank	3788
6	0.0024	0	Bankfull or Inbank	4800
7	0.0024	20	Shallow Overbank	4810

As described in section 3.2.2 all the initial bed compositions are the same. For the five experiments examined some size fractions were mobile while others were immobile. The division between mobile and immobile fractions was not clearly defined and varied with the experimental conditions applied.

Ideally, more experiments with different stage levels would have been completed at these two slopes, however, due to the extensive nature of the experimental programme, time was limited.

5.3 Idealised Transport Rate Decline in Degradational Experiments

All five experiments examined were non-feed experiments, without sediment recirculation and therefore produced bed degradation. Previous work with such experiments, and graded sediment bed material, have shown that the bedload decreases with time from the initial high (Proffitt and Sutherland 1983; Tait et al 1992; Tait and Willetts 1995).

Using experiments of a similar nature in a simple channel, but at a much smaller scale to those presented here, Tait et al (1992) and Tait and Willetts (1995) proposed

a basic pattern of decline behaviour. From their results they concluded that the decline in bedload transport rate with time during a degradational experiment is approximated by the generalised trend shown in figure 5.3. Within figure 5.3 four distinct periods are identified throughout the transport rate decline. Each of these idealised periods of behaviour are introduced below. It should be noted that these are generalised descriptions of behaviour based on existing understanding of degradation transport. A detailed examination of the evolution of bed surface and bedload compositions is included in Chapter 6.

Period A

The initial period within the overall decline is characterised by its high value of transport rate. The value of the transport rate during this period is related to the equilibrium value for the initial bed composition and arrangement, and the applied hydraulic conditions. It is assumed that the bedload transport rate is being sampled at the downstream end of the channel. The longevity of period A is therefore dependent upon the applied conditions and the length of the channel. An initially screeded bed will begin to armour from the upstream end of the channel and the bed will stabilise progressively down the channel length (Tait et al 1992). Only when the bed is stable up to and including the area immediately upstream of the bedload trap will the transport rate recorded significantly decline. This identifies the end of period A. For all other variables being equal, longer channels will produce a longer duration of period A. During this period Tait et al (1992) suggest that the bed surface composition coarsens rapidly while the bedload modal size remains relatively constant. The modal grain size of the bedload is the grain size which is most populous, by weight, in the bedload. The bedload modal grain size remains constant as it is the small-medium sized material that is being transported leaving the coarser material to rearrange itself on the bed surface.

Period B

During period B a dramatic drop in sediment transport rate is observed. The period begins when the armouring process is active along the full length of the channel bed. The reduction in transport rate is due to the rearrangement of the bed surface grains into a more stable lattice structure, which occurs during the armouring process (Tait and Willetts 1991). Due to the rapid decline in sediment transport activity the composition of the bed surface remains relatively constant throughout this period. The transport that does occur is due to the destruction of stable grain arrangements on the bed surface by bursts of turbulence. This causes the bedload transport composition to vary during the period as material escapes from the stable arrangement. The frequency of disturbance decreases with time as the bed rearranges into an ever more stable structure and thus the transport rate declines.

Period C

During this third period the transport rate is low but still shows sporadic peaks of higher transport rates. The bed surface is relatively stable in its rearranged form and the low transport rate is due to the winnowing of finer material out from within the stable matrix. The peaks of higher transport are again caused by periodic disruption of the stable grain arrangement by bursts of turbulence. The frequency of disruption continues to progressively decline. The bed composition is stable during this period while the bedload composition varies with the disruption of the bed surface by turbulence.

Period D

During the final period identified in figure 5.3 the bed arrangement is very stable and able to resist even the largest bursts of near bed turbulence. Therefore the transport rate that is still present is due solely to the winnowing of fine material from the stable bed surface arrangement. Again as the sediment activity on the bed surface is low the bed surface composition remains stable throughout the period. The

composition of the small amount of bedload occurring is likely to be finer than that during higher peaks of transport in previous periods.

Gessler (1990) and Tait and Willetts (1991) point out that the hydraulic resistance of a bed is not solely dependent on bed surface composition. Indeed, Gessler (1990) found the friction factor of an armoured surface to be independent of the maximum grain size of the bed surface. Tait and Willetts (1991) concluded that to characterise a bed surface information was needed on both the grain size distribution and some measurement of bed topography. This is because, during all the periods outlined above, rearrangement of surface grains is taking place whether significant transport, and therefore bed surface composition modification, is occurring or not. The hydraulic roughness therefore increases throughout all four periods of the transport rate decline identified in figure 5.3.

5.4 Observed Transport Rate Decline

The transport rates observed during the five experiments are plotted on linear axes in figures 5.4a and 5.4b and are plotted all together, on shortened axes, in figure 5.5. All five experiments produced the same pattern of transport rate decline similar to the idealised pattern described in the previous section. The most notable difference between the observed and idealised patterns is the lack of a stable period of initial high transport, period A. The observed transport rate declines right from the start of each of the experiments. This difference is due to the initial bed composition, the applied hydraulic conditions and the length of the experimental channel upstream of the bedload trap. As the conditions were designed to examine marginal transport processes the initial bed material was very close to a stable composition for those applied conditions. The amount of rearrangement therefore required to stabilise the bed was very small and so the length of idealised period A was practically zero.

In other respects the pattern of transport rate decline matched the proposed idealised pattern very well. The initial value of high transport rate varied between experiments and was related to the stage level and the initial bed slope applied. The steeper initial

bed slope experiments produced higher initial transport rates as did the deeper stage level experiments. This means that for the five experiments the highest initial transport rate occurs for Experiment 3, the deep overbank flow experiment at the steepest slope. The lowest initial transport rate was observed for Experiment 6, the bankfull flow experiment at the shallowest slope. All five experiments clearly show the dramatic decline in transport rate of period B, followed by a period of low but fluctuating transport and then by a period of low but more stable transport, (periods C and D above).

The analytical research carried out required that the transition between the period of active bedload transport and marginal bedload activity be established. This can be taken as the transition between period B and C in figure 5.3. For this work the transition was defined as the point at which the transport first fell to below 5% of the initial transport rate measurement. For future reference within this thesis idealised periods A and B are examined together and referred to as phase 1, while periods C and D are referred to as phase 2 and are also examined together. The two phases can be identified by plotting each transport rate data point as a percentage of the first data point. The resulting plot for Experiment 4 is presented for illustration in figure 5.6.

5.5 Relative Depth Ratios

The relative depth ratio was employed to quantify the different stage levels between and during experiments. The relative depth ratio of a compound channel is taken as the ratio of the flow depth over the horizontal flood plain to the flow depth over the main channel bed, (H-h)/H, as shown in figure 5.7.

The bed and water surface level data available throughout each experiment allowed the calculation of relative depth ratios. The bed and water surface levels mid-way down the reach, at chainage 11 m, were derived relative to the concrete block datum (figure 5.8). The results reproduced here are for Experiment 7 but all five of the experiments show the same general trends. The bed level would decrease initially

and then stabilise and the water surface level would remain almost constant throughout the experiment. Based on visual observation the slight variations from these trends were probably caused by small transport events on the bed. For example, the break up of an area of armoured surface, or the collapse of a shallow bed form, causing a small wave of bedload. Using linear interpolation, between times with known water and bed levels, the levels of the water and bed surfaces at chainage 11 m were established for four specific experimental elapsed times. Using these values and the known bankfull level, relative to the concrete block datum, the relative depth ratio was calculated for the specific times. The relative depth ratio results for Experiment 7 are also shown graphically in figure 5.8 while the numerical values are contained in table 5.2 below, along with the values for the other experiments.

The four specific experimental elapsed times chosen were 0, 60, 180 and 600 minutes. Throughout this chapter the collected data will be examined at these specific times, and also occasionally at time 1000 minutes. These times were chosen in order to assess and compare the changes in relative depth, boundary shear stress, sediment transport and unit stream power throughout phase 1.

Table 5.2 Relative depth ratios at times 0, 60, 180 and 600 minutes.

	Relative Depth Ratio			
Experiment No.	0 minutes	60 minutes	180 minutes	600 minutes
4	0	0	0	0
2	0.095	0.094	0.092	0.106
3	0.284	0.284	0.299	0.288
6	0	0	0	0
7	0.112	0.109	0.098	0.102

5.6 Boundary Shear Stress

Many researchers regard boundary shear stress as a key variable for the comparison of transport capacity between different applied flow conditions (Shiono and Knight 1991; Ferguson and Ashworth 1992; Knight and Abril 1996). Consequently, sediment transport predictors are often based on the premise that sediment transport rates can be calculated solely from knowledge of the boundary shear stress. Some of

these prediction techniques have proven reasonably reliable and have been widely used in practice. Most transport predictors however, are based on laboratory or field observations of inbank transport. This chapter will examine the relationship between boundary shear stress and sediment transport during bankfull and, the more complex, overbank flow conditions.

It was not possible to measure boundary shear stress directly due to the existence of the mobile bed. A pitot tube, for example, would have disturbed the bed and risked influencing the bedload transport processes occurring. However, methods are available, from published literature, to predict estimates of boundary shear stress using data that was collected non-intrusively.

5.6.1 Estimating Boundary Shear Stress Using Velocity Profiles

Three possible methods for predicting boundary shear stress values using velocity observations were outlined by Wilcock (1996). Each method has a different range of application and a different level of accuracy. All three are based on the commonly used relationship between bed shear velocity and the logarithmic variation of flow velocity with height above the bed, presented below.

$$\frac{u}{u_*} = \frac{1}{\kappa} \ln\left(\frac{z}{z_0}\right) \qquad \text{Equation 5.1}$$

In equation 5.1 u is the local velocity, u_* is the bed shear velocity, κ is the von Karman constant which is taken as 0.4, z is the height above the bed and z_0 is the roughness height of the bed corresponding to u = 0. The zero plane displacement (zpd) is an optional length that may be added to or subtracted from z if the datum for z is believed to be inappropriate. Local boundary shear stress is related to bed shear velocity by

$$u_* = \sqrt{\frac{\tau_{0l}}{\rho}} \quad \text{Equation 5.2}$$

in which τ_{0l} is the local boundary shear stress and ρ is the fluid density. Equation 5.1 applies within the near bed region, above the local influence of grains and well below the free surface. The region can be approximated by $3D_{84} < z < h/5$ and is small or non-existent when $h/D_{84} < 15$, where h is the flow depth (Wilcock 1996). In the application of the logarithmic "law of the wall" it is assumed that the conditions of flow are steady, uniform and sub-critical in a wide straight channel. Within such a channel the roughness should be dominated by grain surface roughness. The theoretical experimental conditions were designed to be steady, uniform and sub-critical. In addition no bed forms were apparent and so attempts were made to apply the methods outlined by Wilcock (1996) to the collected velocity data.

All three methods are presented in more detail by Wilcock (1996), but are summarised below for completeness. The applicability of each to the experiments presented is also discussed.

Method 1

Equation 5.1 is applied to a single data point of (u,z) recorded in the region of application for the logarithmic law. This requires an estimate of the bed roughness height z_0 in order to gain an estimate of the shear velocity u_* and hence a value of bed shear stress τ_{0l} from equation 5.2. Both Ferguson and Ashworth (1992) and Wilcock (1996) suggest that the bed roughness height in a poorly sorted gravel bed can be estimated from

$$z_0 = 0.1D_{84} \quad \text{Equation 5.3.}$$

When investigation of the range of application was carried out, using the initial bed grading parameter D_{84} and the depth of flow h, it was found that often the range was

small, 21 mm < z < 30 mm ($3D_{84}$ < z < h/5). In turn this meant that the velocity profile data points, when related to the bed level (see Chapter 4), often fell outside this range application. The method was therefore discarded.

Method 2

From the derivative of equation 5.1 the shear velocity may be calculated by fitting a least-squares regression of u on ln(z) in the form

$$\frac{u_*}{\kappa} = \frac{du}{d(\ln z)} \qquad \text{Equation 5.4.}$$

Bed shear stress τ_{0l} can then, once again, be calculated from equation 5.2. This method has been described in a paper by Ferguson and Ashworth (1992) which included a discussion on its applicability by R.A. Kuhnle.

The defined region of application is again small, due to the near bed flow distortion by local large particles and far bed flow distortion by secondary circulation (Ferguson and Ashworth 1992). However, there is some published work which suggests that in steady, uniform, sub-critical flow conditions the logarithmic profile extends almost to the surface with minimal deviation (Yalin 1977; Cardoso et al 1989). An extended range of the collected velocity profile data was therefore used, applying the method in a spreadsheet written by Dr. T.B. Hoey of the University of Glasgow. Although the method itself does not require an estimate of z_0 a value was used in conjunction with the correlation coefficient r^2 to evaluate the resulting estimate of τ_{0l}. The coefficient r^2 being a function of the correlation between the logarithmic profile and the velocity data. For a resulting estimate of τ_{0l} to be considered as satisfactory the correlation of the velocity data points with the logarithmic profile had to be greater than 0.75. At the same time the resulting z_0 had to be around $0.1D_{84}$ and not greater than $0.5D_{50}$ (Ferguson and Ashworth 1992). It proved impossible to gain an acceptably high correlation coefficient for many of the

profiles collected, without the value of z_0 being outside the prescribed range. As a result method 2 was also discarded.

Method 3

The depth averaged velocity U can also be used to estimate τ_{0t} using a friction factor or drag coefficient expression $C_D \propto (u_*/U)^2$ (Wilcock 1996). For nearly uniform or uniform flow in a wide channel, in which only grain scale roughness is dominant, the depth integrated form of equation 5.1 is

$$\frac{U}{u_*} = \frac{1}{\kappa} \ln\left(\frac{h}{ez_0}\right) \quad \text{Equation 5.5.}$$

In equation 5.5, e is the base of the natural logarithms. If both grain and bed form roughness exist then the estimate of u_* refers to the total drag due to bed surface friction and bed form drag.

The depth averaged velocity was calculated from the recorded velocity profiles and the known bed and water surface levels. Estimates of u_* were therefore made for the bankfull experiments. The results for Experiment 4 are included in table 5.3. When these are compared to the estimates of bed shear stress using the theoretical weight of the fluid acting down the channel gradient they are seen to be considerably greater.

Table 5.3 Estimated values of bed shear stress for the initial conditions during Experiment 4.

	Local Bed Shear Estimates (N/m^2)			
Chainage	From Velocity Data			From Energy
(m)	Left Profile	Centre Profile	Right Profile	Gradient
4.64	4.69	5.58	4.70	3.82
8.91	5.62	7.21	6.25	3.82
13.14	5.47	6.80	6.58	3.82

As a check on the quality of the velocity data the velocity profiles were integrated over the cross-section area and compared to the measured discharge. Using this technique the velocity profiles over-predicted the discharge during Experiment 4 by

about 10%. When the effect of a reduction in the depth-averaged velocity of around 10% was examined it was found to decrease the estimated bed shear by around 20%. This brought the values estimated using the velocity data closer to the estimate of the bed shear stress from the energy gradient.

After this analysis it was felt that the resolution and quality of the velocity data collected was not sufficient to allow estimates of bed shear stress to be made using any of the three methods. Instead, it was decided to use two predictive techniques designed specifically for compound channels. The first technique examined was the area averaged Ackers 1-D method (Ackers 1991; Ackers 1992a; Wark et al 1994); the second was the depth averaged Wark 2-D Lateral Distribution Method (LDM) (Wark et al 1991; Wark 1993).

5.6.2 The Ackers 1-D Method

The Ackers 1-D method is an empirical conveyance calculation technique which estimates the main channel / flood plain interaction, and was developed using the FCF Series A data. It predicts area-averaged velocity and average boundary shear stress values, for the main channel and flood plain regions separately (Ackers 1991; Ackers 1992a; Wark et al 1994).

Conventional textbook advice recommends splitting compound channels into sub-sections and then dealing with each sub-section as a single channel before summing the results (figure 5.9). The Ackers method recognises the failure of this technique to account for the interaction between the generally slower flood plain flow and the main channel flow. The traditional method therefore over predicts the capacity of compound channels by more than an acceptable amount. The Ackers method proposes a correction to overcome this limitation.

The method attempts to take account of the main channel flood plain interaction. The controlling parameters are listed by Ackers (1992a) as: the relative depth ratio; the relative magnitude of the roughness of the flood plains and the main channel; the

ratio of the flood plain width to the main channel width; the number of flood plains; the side slope of the main channel and the aspect ratio of the main channel. All of these parameters combine to control the difference in average velocity between the flood plain and the main channel. It is this difference that determines the degree of main channel / flood plain interaction.

Ackers (1992a) presents a suite of functions which assess the overall channel conveyance. In doing so the method calculates the discharge adjustment factor, DISADF, and the channel coherence, COH. DISADF is defined as the ratio of actual discharge to nominal discharge, where the latter is derived as the sum of flows estimated separately for the main channel and flood plain zones. COH is a measure of the degree to which the separate zones exhibit flow similarity. Single channel conveyance and COH are described in detail by Chow (1959) and Ackers (1991b). The use of these ratios allow a performance region for the channel to be assessed. Four regions of overbank flow performance are described by Ackers (1992a). They cover from just above bankfull, Region 1 (coherence is low) to very deep overbank flow, Region 4 (coherence is approaching unity) (figure 5.10). In Region 4 the energy loss is dominated by bed friction and it is acceptable to treat the section as a single channel.

In estimating the capacity of a compound channel the Ackers 1-D method estimates the flow depth for a given total discharge and the discharge distribution between the main channel and the flood plains. The method then allows the estimation of main channel boundary shear stress from an initial estimation of the shear stress, ignoring interaction effects, and the discharge adjustment factor, calculated using the discharge distribution results.

5.6.3 The Wark 2-D Lateral Distribution Method (LDM)

Wark's LDM was designed to be used in natural rivers with overbank flows (Wark et al 1991; Wark 1993). The model is based on steady flow theory and uses a finite difference technique to solve the depth-averaged steady flow equation of motion. The

equation also includes a term for lateral turbulent shear stress. The result is a two-dimensional numerical simulation of the flow pattern at a cross-section. Lateral shear is included through a lateral shear stress term, which requires the use of a simple turbulence model for solution. The model provides the lateral distribution of unit discharge and flow velocity, and estimates the stage-discharge relationship and conveyance of the cross-section above bankfull water level.

The model is based on the shallow water equations used by several authors for the same purpose (e.g. Keller and Rodi 1985; Samuels 1985; Shiono and Knight 1989; Wormleaton 1988; Wark 1993). For a straight channel with steady uniform flow and the x-axis aligned to the channel centreline, the two-dimensional equations reduce to a single one-dimensional equation. This describes lateral variation in depth-averaged velocity and unit discharge across the channel (equation 5.6 below).

$$\left(gDS_{xf}\right)-\left(\frac{Bfq^2}{8D^2}\right)+\frac{\partial}{\partial y}\left[v_t\frac{\partial q}{\partial y}\right]=0 \qquad \text{Equation 5.6}$$

Where g is the acceleration due to gravity, D is the local flow depth, S_{xf} is the longitudinal friction slope, B is a factor relating to the side slope of the domain, f is the Darcy friction factor, q is the longitudinal unit flow and ν_t is the depth averaged lateral turbulent viscosity. The three terms in this equation represent: the weight of fluid acting down the slope in the longitudinal direction, the bed friction and the lateral shear stresses. The effects of the secondary currents are deemed to be included in the lateral shear stress term. The equation is expressed in terms of unit discharge rate q, rather than depth-averaged velocity U. This is based on the assumption that the distribution of unit discharge q is smooth and continuous across the channel (Samuels 1985). The method then uses finite differences as the solution technique. The flow domain is split into a number of nodes, N, and the variables are expressed as their values at the individual nodes, assuming that the variation between nodes is linear. The differential terms, $\partial F/\partial y$, can then be expressed as $\delta F/\delta y$, δF being the

difference between the F values at successive nodes and δy being the grid spacing. Wark applied central differences in his solution

$$\frac{\partial F}{\partial y} = \frac{(F_{i+1} - F_{i-1})}{2\delta y} \qquad \text{Equation 5.7.}$$

Applying the boundary conditions at nodes i = 1 and i = N produces N-2 equations with N-2 unknowns in terms of the solution vector F_i. Finally, Newton's iteration method was used to linearize the equations and allow a solution to be obtained. The non-dimensional eddy viscosity was used to approximate the variation of interaction effects across the compound channel. Non-dimensional eddy viscosity relates viscosity to bed roughness, flow depth and local flow or velocity (Wark 1993).

The above numerical technique has been coded into a FORTRAN computer program which allows the user to define: the channel cross-section geometry; the boundary roughness values for the channel; the non-dimensional eddy viscosities; the discharge and stage levels to be modelled. There is also an option as to which friction law the model uses. The user can tailor the output to their requirements. Options include the output of initial and final values, iteration details, convergence behaviour, and stage-discharge data. However, the main output is the lateral distribution of depth-averaged velocities and unit discharges.

The predicted depth-averaged velocities along with the predicted flow depths and the user specified boundary roughness could then be used to calculate a prediction of the boundary shear stress. This process is described in more detail within the following section (also see Equations 5.12 to 5.15).

Figure 5.11 shows the distribution of boundary shear stress, related to the channel cross-section, predicted from the lateral distribution of depth-averaged velocity.

5.6.4 Boundary Shear Stress Predictions

Both the methods were designed to allow them to be used with steady, uniform flow in straight channels. The experimental conditions remained close to uniform flow throughout (figures 5.12 and 5.13). The above methods were therefore considered adequate for estimating boundary shear stress.

As previously mentioned, the experimental length of the channel was from chainage 6 m to chainage 16 m. This allows for the full development of the boundary shear layer and prevents any disturbance of the experimental readings from the entry conditions or from the sediment traps and tailgate weir. To simplify the analysis changes in cross-sectional properties were obtained by examining conditions midway along the experimental reach at chainage 11 m.

For bed elevation this involved averaging the left, centre and right laser readings to obtain the average bed level across the channel for each longitudinal bed profile. The level at chainage 11 m was then calculated from levels at adjacent chainages. Linear interpolation was used to calculate the bed level at the times required. The same techniques were used for the water surface profiles.

The floodplain levels were known from the pre-experiment surveys. The main channel top width, the flood plain width and the main channel side slopes were all constant along the full length of the channel. This meant the channel cross-sections could be defined for each time required, in each experiment. The lateral and vertical co-ordinates used to define the channel cross-sections in the Ackers and Wark models, for Experiment 4, are presented in table 5.4 as an example.

Table 5.4 Cross-sectional data for Experiment 4. All levels relative to concrete block datum.

Experiment	4	4	4	4
Time (mins.)	0	60	180	600
Channel X-Section Co-ordinates (mm) Lateral, Vertical	0.000, 0.500	0.000, 0.500	0.000, 0.500	0.000, 0.500
	0.000, 0.179	0.000, 0.179	0.000, 0.179	0.000, 0.179
	0.770, 0.179	0.770, 0.179	0.770, 0.179	0.770, 0.179
	0.921, 0.028	0.928, 0.021	0.928, 0.021	0.929, 0.020
	1.719, 0.028	1.712, 0.021	1.712, 0.021	1.711, 0.020
	1.870, 0.179	1.870, 0.179	1.870, 0.179	1.870, 0.179
	2.640, 0.179	2.640, 0.179	2.640, 0.179	2.640, 0.179
	2.640, 0.500	2.640, 0.500	2.640, 0.500	2.640, 0.500
Water Surface Level (mm)	0.177	0.177	0.177	0.179
Relative Depth	0	0	0	0

In addition, to channel cross-sections and longitudinal slopes, the two boundary shear stress methods required estimates of lateral variation of boundary roughness across the channel. The three different roughness values that existed across the channel related to the flood plain section, the main channel side slope section and the main channel gravel bed section.

Prior to the start of any of the experiments a series of flood plain roughness measurements were taken, with the flood plains isolated from the main channel. Uniform flow was achieved at various stage levels, and a stage-discharge curve derived for the isolated flood plains. The flood plain cross-section dimensions, uniform flow depths, flume slope and discharge down the floodplains were therefore all known. Manning's equation was then used to produce the variation of Manning's n value with depth shown in figure 5.14

The Manning's n value of boundary roughness for the main channel side slopes was taken as 0.012. The side slopes were a brushed mortar finish and the value was chosen after a review of published values in literature (Chadwick and Morfett 1986; French 1986; Chow 1959).

Manning's equation was employed to estimate the main channel composite roughness using the three experiments with bankfull flow. (Experiments 4, 5 and 6). The energy line level was calculated for each metre between chainage 6 m and

chainage 16 m. This was done using the bed and water level data from when the flow was initially set to a uniform depth, and the discharge recorded. The main channel boundary roughness was then calculated, along the experimental length of the channel, using the gradients of the energy line.

The main channel roughness calculated was a composite of the side slope and gravel bed roughness. Several formulas from the literature were used to separate the gravel bed roughness from the main channel composite or equivalent roughness.

$$n_e = \left[\frac{\sum\left(P_i n_i^{\frac{3}{2}} \right)}{P} \right]^{\frac{2}{3}}$$ Horton (1933), Equation 5.8

$$n_e = \frac{\left[\sum\left(P_i n_i^2\right)\right]^{0.5}}{P^{0.5}}$$ Einstein and Banks (1950), Equation 5.9

$$n_e = \frac{\sum n_i A_i}{A}$$ Cox (1973), Equation 5.10

$$n_e = \left[\frac{\sum A_i n_i^{\frac{3}{2}}}{A} \right]^{\frac{2}{3}}$$ Cox (1973), Equation 5.11

In the above equations n is the Manning's roughness coefficient, P is the wetted perimeter and A is the cross-sectional area.

The results were then averaged and the initial estimate of the gravel bed roughness at time 0 was calculated as n = 0.01716. This value may appear low compared to published estimates of bed roughness in gravel bed rivers. However, the channel was

straight and there was no added roughness from bends. cross-section variations or riverine vegetation.

The next step was the application of the Wark LDM technique to the data for the various times throughout the five experiments. The model required an estimate to be made of the non-dimensional eddy viscosity (NEV). This takes account of the main channel / flood plain flow interaction and consequential energy loss.

Wark (1993) discussed the effect of varying NEV on the model's predictions. He concluded the effect is not significant and a value of 0.16 is recommended as being suitable for most trapezoidal compound channels. However, a further review of his results shows that NEV does vary with relative depth as one might expect. From the tests carried out in the FCF, reported in Wark (1993), the NEV value is low for low values of relative depth. It then increases with relative depth to a point before further increase in relative depth causes a decrease in NEV. This result therefore agrees with Ackers' theory that as the relative depth increases, the channel coherence approaches unity.

Three values of NEV were used for the three values of relative depth. These enabled the sum of the boundary shear stress across the channel to be matched to the weight of the fluid acting down the slope (table 5.5).

The values above were derived through an iterative process. This involved adjusting the value of the gravel bed roughness in order that the discharge, predicted by the LDM model, matched the discharge recorded during the experiments. This iteration was carried out until the difference between the predicted and measured discharge was +/-0.1% or less. The result is a prediction of the gravel bed roughness development through time, based on the measured hydraulic data and assumed values of NEV. The resulting values of Manning's n are tabulated in table 5.6, where the composite main channel roughness values are presented for completeness. All five experiments show an increase in bed roughness with time.

Table 5.5 Comparison between weight of fluid acting down the slope and the predicted boundary shear stress for the NEV values used.

Experiment No.	Time (minutes)	NEV Value	Weight Of Fluid Acting Down Slope, $\rho g A S_0$ (N/m)	Predicted Boundary Shear Stress, $\Sigma \tau_0 \times X$ (N/m)
4	0	0.12	3.52	3.26
4	60	0.12	3.74	3.33
4	180	0.12	3.74	3.33
4	600	0.12	3.81	3.39
2	0	0.22	4.76	4.62
2	60	0.22	4.79	4.67
2	180	0.22	4.88	4.72
2	600	0.22	5.11	4.99
3	0	0.16	7.82	7.70
3	60	0.16	7.82	7.70
3	180	0.16	8.18	8.08
3	600	0.16	8.34	8.16
6	0	0.12	3.23	2.98
6	60	0.12	3.36	3.03
6	180	0.12	3.43	3.09
6	600	0.12	3.41	3.07
7	0	0.22	4.55	4.46
7	60	0.22	4.63	4.56
7	180	0.22	4.54	4.41
7	600	0.22	4.64	4.48

Table 5.6 Boundary roughness values from literature and analysis for the three different boundaries.

Experiment No.	Time (minutes)	Manning's n Boundary Roughness Value			
		Flood Plain n_f	Side Slopes n_{ss}	Gravel Bed n_b	Main Channel Composite n_{mc}
4	0	0.012	0.012	0.01771	0.01596
4	60	0.012	0.012	0.01922	0.01697
4	180	0.012	0.012	0.01922	0.01697
4	600	0.012	0.012	0.02001	0.01751
2	0	0.01789	0.012	0.01446	0.01365
2	60	0.01789	0.012	0.0148	0.01387
2	180	0.01789	0.012	0.01546	0.01430
2	600	0.01858	0.012	0.01665	0.01511
3	0	0.02891	0.012	0.01901	0.01686
3	60	0.02891	0.012	0.01901	0.01686
3	180	0.02993	0.012	0.02064	0.01805
3	600	0.02968	0.012	0.02249	0.01918
6	0	0.012	0.012	0.01635	0.01500
6	60	0.012	0.012	0.01696	0.01541
6	180	0.012	0.012	0.0176	0.01584
6	600	0.012	0.012	0.01739	0.01570
7	0	0.01858	0.012	0.01565	0.01448
7	60	0.0186	0.012	0.01635	0.01495
7	180	0.0182	0.012	0.01607	0.01473
7	600	0.01841	0.012	0.0167	0.01515

The output from the analysis using the LDM model was depth-averaged velocities distributed laterally across the channel at 100 equally spaced nodal points. Estimates of the boundary shear stress could now be made at each nodal point over the cross-section.

By algebraic manipulation of Manning's equation

$$Q = \frac{1}{n} A R^{\frac{2}{3}} \sqrt{S} \qquad \text{Equation 5.12}$$

and

$$f = \frac{8gRS}{V^2} \qquad \text{Equation 5.13}$$

the Darcy-Weisbach friction factor can be derived from

$$f = \frac{8gn^2}{R^{1/3}} \qquad \text{Equation 5.14.}$$

As the velocity and flow depth was known at each node across the channel, equation 5.14 allowed the calculation of the friction factor at each node. This, in turn, allowed the estimate of boundary shear stress at each node from

$$\tau_0 = \frac{\rho \bar{u}^2 f}{8} \qquad \text{Equation 5.15.}$$

The values of boundary shear stress, compared to the weight of fluid acting down the slope, presented in table 5.5 were therefore gained by integrating the point values across the channel.

The same cross-sections and boundary roughness values used in the LDM model were used in the Ackers 1-D model. This produced estimates of average main channel and flood plain boundary shear stress.

The method is described clearly elsewhere in the compound channel design manual by Wark et al (1994). The manual provides a step-by-step guide, which was followed in this application, and so no further description of the technique is given here. Of the list of parameters controlling flow interaction that was given in section 5.6.2 only the discharge adjustment factor, DISADF and the channel coherence, COH had to be calculated specifically for use with the method (table 5.7). The other parameters required can be gained from the channel cross-section (figure 3.4) and table 5.6. The results for the COH clearly show that for all the overbank experiments the channel should be regarded as compound or two-stage.

Table 5.7 Relative depth ratios, main channel DISADFs, channel COHs, and predicted performance region for the overbank experiments.

Experiment No.	Time (minutes)	Relative Depth Ratio	Main Channel DISADF	Channel COH	Predicted Performance Region
2	0	0.095	0.9489	0.514	1
2	60	0.094	0.9501	0.519	1
2	180	0.092	0.9524	0.529	1
2	600	0.106	0.9443	0.547	1
3	0	0.284	0.8338	0.553	1
3	60	0.284	0.8338	0.553	1
3	180	0.299	0.8299	0.577	1
3	600	0.28	0.8485	0.596	1
7	0	0.112	0.9390	0.536	1
7	60	0.109	0.9416	0.546	1
7	180	0.098	0.9490	0.541	1
7	600	0.102	0.9471	0.550	1

The estimates of main channel shear stress resulting from use of both the Ackers model and the Wark model are presented in table 5.8 below.

Table 5.8 Main channel average boundary shear stresses calculated using Ackers 1-D method and Warks LDM.

Experiment No.	Time (minutes)	Measured Discharge Q_m (m^3/s)	Ackers 1-D Method		Warks LDM
			Predicted Discharge Q_p (m^3/s)	Average Main Channel Boundary Shear Stress τ_0 (N/m^2)	Average Main Channel Boundary Shear Stress τ_0 (N/m^2)
4	0	0.10553	0.10725	2.95	3.09
4	60	0.10553	0.10724	3.05	3.16
4	180	0.10553	0.10724	3.05	3.16
4	600	0.10553	0.10683	3.10	3.21
2	0	0.14676	0.15361	3.03	2.90
2	60	0.14676	0.15330	3.06	2.95
2	180	0.14676	0.15397	3.13	2.99
2	600	0.14676	0.15245	3.16	3.08
3	0	0.20809	0.19198	3.07	3.78
3	60	0.20809	0.19198	3.07	3.78
3	180	0.20809	0.19069	3.13	3.94
3	600	0.20809	0.19283	3.37	4.05
6	0	0.10712	0.10883	2.71	2.82
6	60	0.10712	0.10882	2.75	2.87
6	180	0.10712	0.10880	2.79	2.93
6	600	0.10712	0.10883	2.78	2.91
7	0	0.13802	0.14233	2.78	2.75
7	60	0.13802	0.14288	2.85	2.83
7	180	0.13802	0.14378	2.87	2.78
7	600	0.13802	0.14354	2.90	2.82

The results gained from the Wark LDM are averages of the predicted laterally distributed shear stress inside the main channel. The averages include values above the side slopes in order to allow comparison with the results from the Ackers method. The average main channel boundary shear stress values gained from both methods are plotted against the calculated relative depths, in figures 5.15a to 5.15d. The figures illustrate the results based on the hydraulic data at times 0, 60, 180 and 600 minutes.

It is clear that the Ackers method predicts only a small increase in boundary shear stress with increasing relative depth at any time throughout the experiments. As pure speculation this may be due to the method overestimating the flow interaction caused by overbank flow at the highest relative depth. This leads to the under-prediction of the deep overbank discharge, and the boundary shear stress is underestimated. For the shallow overbank case it is speculated that the opposite is occurring: the flow

interaction is underestimated, leading to an overestimation of the channel conveyance, and an overestimation of the boundary shear stress.

The results from the Wark LDM show similar trends to related results published by other authors (Ackers 1992b; Knight and Abril 1996). The boundary shear stress experienced in the main channel drops, from bankfull to shallow overbank conditions. This is due to the large increase in main channel flood plain flow interaction, and the strength of the main channel secondary cells. Comparing shallow overbank to deep overbank the boundary shear stress increases as the interaction effects, although larger again, are proportionally less important than bed friction. Again the pattern is consistent throughout the experiments. The results show a slight increase in estimated boundary shear stress with time, due to boundary roughness increasing with time, caused by the armouring gravel bed.

To summarise the results: the Ackers method shows little variation in boundary shear stress for increasing values of relative depth ratio, while the Wark LDM predicts a reduction in boundary shear stress for the shallow overbank condition compared to the bankfull condition. This is followed by a substantial increase in boundary shear stress for the deep overbank case. The greater detail included in the Wark LDM along with its similarity to other published work promoted it for use in the further investigation of the variation between bankfull and overbank sediment transport. The ability of the model to predict the lateral distribution of parameters was also thought to be desirable.

5.7 Transport Rate Regressions

The results presented so far in this chapter show that for the experiments conducted the estimated boundary shear stress during shallow overbank flow was less than during bankfull flow. This result appears to be in agreement with the predictions by Ackers (1992b) and Knight and Abril (1996), that for shallow overbank flow the sediment transport rate is less than for bankfull flow. The next logical step was

therefore to examine the recorded bedload transport rates to see if this was indeed the case.

The following analysis requires that the bedload transport rates are compared at the same elapsed times in each experiment. What is of interest therefore, is the general trend in transport rate decline and not the superimposed, sporadic fluctuations described in sections 5.3 and 5.4.

Least-squares regression was used to fit a smooth transport rate decline to each of the transport rate data sets. This enabled the comparison of transport rates at identical times, from different experiments. All the degradational experiments show the same pattern of decline and therefore the same form of regression was used on each data set.

To implement the regressions the Log_{10} values for time and transport rate at each of the data points in each of the experiments were calculated. These values were then plotted on linear axes and the statistical method of least-squares was used to fit a linear regression. The data for Experiment 4 is presented on linear axes and the regression detailed in figure 5.16. Using a statistical data analysis package the values of R^2, adjusted for the number of data observations, and the level of Significance (F-test) for each of the regressions were calculated. The results are presented in table 5.9 below.

Table 5.9 Results of statistical analysis of regressions

Experiment No.	3	2	4	7	6
Number of Observations	26	28	30	36	39
Adjusted R^2	0.806	0.693	0.812	0.844	0.787
Significance (F)	3.0×10^{-10}	2.3×10^{-8}	7.1×10^{-12}	1.7×10^{-15}	3.3×10^{-14}

The values of Significance are all much less than 0.01. The regressions can therefore be said to fit the collected data well and to give a good description of the

general trends of transport rate decline. Consequently it seems valid to use the regressions to interpolate transport rate values at the required specific times. Such regressions do not however, make any attempt to describe details of transport fluctuation due to sporadic movement of material into the traps.

The equation of the regression line can then be mathematically manipulated to convert it from the form

$$y = mx + c$$

in which $y = Log_{10} q_b$ and $x = Log_{10} t$ to the form

$$y = px^q$$

in which $y = q_b$, $x = t$ and p and q are the coefficient and power of the function. The conversion was made to allow the regression to be plotted on linear axes as in figure 5.17 for Experiment 4.

Included in the figure is the converted regression equation and the R^2 value unadjusted for the number of observations in Experiment 4. Predictions of the transport rates at the various times of interest can be seen in table 5.10 below.

Table 5.10 Transport rates predicted by the regressions

Experiment No.	4	2	3	6	7
Regression Equation	$y = 752.5x^{-1.02}$	$y = 235.9x^{-0.79}$	$y = 514.9x^{-0.82}$	$y = 60.2x^{-0.73}$	$y = 176.8x^{-0.83}$
Time (minutes)	Unit Transport Rate ($x10^{-3}$ kg/m/s)				
0	16.3	24.9	104.2	9.0	28.5
60	11.5	9.4	17.8	3.0	5.9
180	3.7	3.9	7.2	1.3	2.3
600	1.1	1.5	2.7	0.6	0.9
1000	0.7	1.0	1.8	0.4	0.6

The transport rate at time 0 minutes was estimated by extrapolating backwards the transport rate decline between the first two recorded data points. This approach is not as robust as the regression technique available for use with the other points. However, the result does predict, for the two different initial bed slopes, higher t = 0 transport rates for experiments with greater relative depths.

All the regressions are plotted together on the same set of axes in figure 5.18. The value of the initial transport rate, and transport rates in general throughout the experiments, increases with stage level and initial bed slope. The figure again shows Experiment 3, deep overbank at the steeper slope, with the highest transport rates. Experiment 6, bankfull at the shallower slope, possesses the lowest transport rates. The regression curves also show the same overall transport rate trend for degradational experiments of: initial high transport followed by a steep decline and a long phase of marginal transport.

5.8 Sediment Transport Rates and Boundary Shear Stress

The unit transport rates gained from the regressions in the previous section are plotted against the appropriate relative depth ratio in figures 5.19a and 5.19b. Each line has been constructed from experiments with the same initial slope but different relative depths. The figures show that for both slopes, and throughout the experiments, the tests with greater relative depths produced higher unit transport rates. Within the figures there is one line that is an exception to this and that is the plot for the steeper slope (0.0026) at time 60 minutes in figure 5.19a. A reduction in transport rate is shown between relative depths of 0 and approximately 0.1. This is a result of the regression function fitted to the measured data and used to predict the transport rate. For all the other data however, the sediment transport rate increases with relative depth ratio. Higher transport rates are produced by experiments with steeper initial bed slopes. This can be seen by comparing the transport rates at identical times between experiments with the same or similar relative depth ratios.

For the experiments presented, figures 5.19a and 5.19b show sediment transport rate to be greater for larger relative depth ratios. However, the results from section 5.6.4 show the estimated main channel boundary shear stress to be lower for a shallow overbank flow condition than for a comparable bankfull condition. This result contradicts the proposal by Ackers (1992b) and Knight and Abril (1996) that sediment transport will be less for a shallow overbank condition than for a bankfull condition.

To illustrate this point graphically it was decided to use boundary shear stress above the gravel bed plotted against the unit sediment transport rates. This was because it was only the boundary shear stress directly above the gravel bed that generated sediment movement. The previous average main channel boundary shear stress had included values above the main channel side slopes, to allow direct comparison with the results from the Ackers method. The two average boundary shear stresses from within the main channel are presented in table 5.11 below.

Table 5.11 Whole main channel and gravel bed only average boundary shear stresses as predicted by Warks LDM.

Experiment No.	Time (minutes)	Relative Depth	Whole Main Channel Ave. Shear τ_{0MC} (N/m^2)	Gravel Bed Only Average Shear τ_{0GB} (N/m^2)
4	0	0	3.09	3.38
4	60	0	3.16	3.64
4	180	0	3.16	3.64
4	600	0	3.21	3.73
2	0	0.095	2.90	3.01
2	60	0.094	2.95	3.07
2	180	0.092	2.99	3.25
2	600	0.106	3.08	3.43
3	0	0.284	3.78	4.37
3	60	0.284	3.78	4.37
3	180	0.299	3.94	4.63
3	600	0.28	4.05	5.02
6	0	0	2.82	3.05
6	60	0	2.87	3.12
6	180	0	2.93	3.19
6	600	0	2.91	3.17
7	0	0.112	2.75	2.93
7	60	0.109	2.83	3.03
7	180	0.098	2.78	3.07
7	600	0.102	2.82	3.14

The main channel boundary shear stresses, averaged above the gravel bed, are plotted against the unit transport rates for the chosen specific times in figure 5.20. Within the figure each line represents the results for a particular time, at a particular slope. The lines consist of points representing the individual experiments conducted at that particular slope. Even though the estimated boundary shear stress is less for

the shallow overbank case than for the bankfull case, the transport rate recorded is higher.

Consequently, some of the transport prediction methods introduced in sections 2.4 and 2.6 will predict lower transport for the shallow overbank case than for the bankfull case. Clearly such a prediction would conflict with the experimental results.

For bankfull flow it is suggested that boundary shear stress is the dominant factor affecting the transport rate. For this reason using boundary shear stress as the basis of a sediment transport prediction technique works reasonably well. However, for overbank flow it is understood that the flow mechanics are more complicated. It is suggested that for a given boundary shear stress, a case with overbank flow will produce higher transport rates than an bankfull case (with the same average boundary shear stress). This may be due to the turbulence generated by the main channel / flood plain flow interaction and the increase in secondary cell activity.

5.9 Weight of Material Transported

So far it has been shown that, although main channel boundary shear stress is less for the shallow overbank case, than for the bankfull case, the transport rate is higher, for the experiments conducted. However, the transport rates used for comparison were derived from regressional results. If the recorded transport rates are examined once again, in figures 5.4a, 5.4b and 5.5, it can be seen that the individual declines are very similar and in some cases overlap. It has been explained that this is due to sporadic activity associated with the rearrangement of surface material and the formation of a static armoured layer. A critic may however question if indeed the transport rates during a shallow overbank experiment were greater than those during an equivalent bankfull experiment. For this reason an alternative method of comparing the transport capacities of the five experiments was examined.

By numerically integrating the transport rate curve to obtain the weight transported, the different transport capacities of the experiments are more apparent. Integration is

necessary as the sediment trapping cycles were not continuous. Simply adding the weights of the samples together would have given a misleading estimate of capacity.

The weight of material transported over five time periods was examined. The time period of up to 1000 minutes was chosen as all five experiments appear to have reached the period of marginal transport by that time. Shorter periods, up to 60, 180 & 600 minutes were used also, along with integration of the area under the curve over the full length of each experiment. Integration was carried out using the recorded data transport rate curves, rather than the regression curves. Predictions had to be made of the transport rates at times 0, 60, 180, 600 and 1000 minutes, in order to do this, if recorded values at these times did not exist.

For time 0 minutes backwards extrapolation was used based on the first two data points collected for each experiment. Again, the use of backward extrapolation may seem hazardous, when the initial transport rate fluctuations described in sections 5.3 and 5.4 are considered. However, the order of magnitude of the estimated weight of material transported during the first time interval, matches the order shown when the other intervals are examined.

For all other times, which required an estimate to be made, linear interpolation was employed using the data points recorded either side of the time in question.

Trapezoids were created by using the recorded data points as internal nodes and the predicted data points as external nodes. Integration was then completed by summing the areas of the individual trapezoidal sections. The results of the integrations can be seen below in table 5.12.

Table 5.12 Weights of material transported during experiments, integration from time 0 mins.

	Experiment No. - All Weights in kg				
Time	3	2	4	7	6
60	123.6	43.3	37.9	30.7	15.5
180	172.6	73.3	75.5	57.1	28.1
600	265.3	140.0	120.6	88.4	43.2
1000	315.2	171.9	131.1	99.5	57.1
Final Data Point (In Brackets)	508.1 (3734.5)	251.5 (4074)	203.4 (5475)	164.5 (4753.5)	97.3 (4672)

The presented weights are represented graphically in figure 5.21. The curves representing the weight of material transported up until the various times throughout the experiments, diverge from one another for both sets of initial bed slope. This again indicates that the deep overbank experiment (Experiment 3), is transporting more sediment than the shallow overbank experiment (Experiment 2). Experiment 2 in turn is transporting more sediment than the bankfull experiment (Experiment 4). The shallower slope experiments also transported less sediment than their steeper initial bed slope equivalents.

The weights of material transported by the different experiments are plotted against the relative depth ratios in figures 5.22a and 5.22b. The figures illustrate the same trends as show between the relative depth ratios and the unit transport rates, namely: transport capacity increases with relative depth and with initial bed slope.

The difference between the weight of material transported by the bankfull and shallow overbank experiments, at the steeper initial bed slope, prior to the first two time points is almost negligible. This corresponds to a period when the transport rates of these two experiments were very similar and resulted in almost coincident regression curves for these experiments. However, the longer the duration of the experimental data that is examined, the less influence the initial fluctuations in sediment transport rate have. It is therefore reasonable to conclude that the experiments with larger relative depths and steeper bed slopes were able to move greater weights of material.

Figure 5.23 shows the values for the weight of material transported plotted against the estimates of the main channel boundary shear stress. The same negative gradient is apparent between the points representing the bankfull cases and the points representing the shallow overbank cases, as was seen in figure 5.20. Again it is illustrated that, for the experiments conducted, the transport capacity was greater for the shallow overbank cases than for the bankfull cases despite the lower boundary shear stress. This is again in conflict with the behaviour proposed by Ackers (1992b)

and Knight and Abril (1996) for sediment transport during shallow overbank flow conditions. It is suggested that boundary shear stress, as estimated here, may not be the only mechanism governing sediment transport during shallow overbank or low relative depth flow conditions.

5.10 Unit Stream Power

Boundary shear stress is not the only variable associated with applied flow conditions that has been used in attempts to predict transport rates. Indeed several prediction models based on other parameters are introduced in Chapter 2. Perhaps the main alternative to boundary shear stress is stream power (Ferguson and Ashworth 1992). To take the work one step further it was therefore decided to examine the relationship between sediment transport and unit stream power for the different relative depths.

The water in a channel exchanges potential energy for kinetic energy in moving from upstream to downstream. Part of the resulting energy is dissipated as friction against the bed and bank boundaries, due to the fluid viscosity. Another part is dissipated in transporting sediment. In these terms a fluid flow within a channel has the capacity to do work and that capacity can be defined as stream power. Stream power is therefore the time rate of energy change in a river or the mean rate of kinetic energy supply and dissipation per unit length of channel (Bagnold 1980, 1986). For the purposes of this work unit stream power is expressed as

$$\omega = \frac{\rho Q S}{stream\ width} \qquad \text{Equation 5.16}$$

or

$$\omega = \bar{\tau}\ \bar{u} \qquad \text{Equation 5.17}$$

in which ρ is the fluid density, Q the stream discharge rate, S the gravity gradient, $\bar{\tau}$ the mean distributed bed shear stress and $\bar{u}$ the mean flow velocity (Bagnold 1980).

It should be noted that the author has followed Bagnold in the description of stream power and omitted gravitational acceleration, g. In doing so the author's definition of unit stream power is dimensionally different to that of power ($kg.m^{-1}.s^{-1}$ vs. $W\ m^{-2}$). This means that compared to the dimensionally correct unit stream power values the values presented in the following tables and figures are out by an order of magnitude. However, this does not effect the correlations presented and Bagnold's definition of unit stream power has the advantage of being dimensionally equal to unit transport rate. In addition, the reader should be clear that this definition refers to stream power per unit bed area and not per unit water volume.

The unit discharge output files from the LDM model were used to calculate the stream power for each of the five experiments, at each of the times of interest. The model produces a lateral distribution of the unit discharge across the channel giving values at each of the one hundred evenly spaced nodes. It was therefore possible to calculate the unit stream power at each node by multiplying the unit discharge by the density of water and by the known slope of the experiment. The unit values were then integrated across the width of the gravel bed and the resulting value divided by the width of the gravel bed. In this way an average unit stream power was calculated for a specific experiment, at a specific time. The resulting values are presented in table 5.13 below.

Figures 5.24a and 5.24b show the variation of average unit stream power with relative depth and also with time throughout the experiments. From the figures it is clear that stream power shows little variation with time. This is due to there being little change in the channel cross-section, and therefore the depth-average flow velocity, even though the bed degrades marginally with time.

Figures 5.24a and 5.24b also show that the average unit stream power increases between the bankfull case and the shallow overbank case. It then increases again to the deep overbank case. This is clearly different from the variation of boundary shear stress between the different relative depths as seen previously in figures 5.15a to 5.15d. The result is more in line with the changes in sediment transport.

Table 5.13 Average stream power per unit width above gravel bed.

Experiment No.	Time (minutes)	Relative Depth Ratio	Average Shear Stress per Unit Width (N/m^2)	Average Stream Power per Unit Width ($x10^{-3}$ kg/m/s)	Unit Transport Rate ($x10^{-3}$ kg/m/s)
4	0	0	3.38	299.8	16.3
4	60	0	3.64	303.4	11.5
4	180	0	3.64	303.4	3.7
4	600	0	3.73	301.5	1.1
2	0	0.095	3.01	398.7	24.9
2	60	0.094	3.07	397.6	9.4
2	180	0.092	3.25	403.2	3.9
2	600	0.106	3.43	397.6	1.5
3	0	0.284	4.38	487.6	104.2
3	60	0.284	4.38	487.6	17.8
3	180	0.299	4.64	477.2	7.2
3	600	0.280	5.02	483.2	2.7
6	0	0	3.05	282.0	9.0
6	60	0	3.12	281.9	3
6	180	0	3.19	280.9	1.3
6	600	0	3.17	281.0	0.6
7	0	0.112	2.93	339.7	28.5
7	60	0.109	3.03	339.1	5.9
7	180	0.098	3.07	348.0	2.3
7	600	0.102	3.14	346.1	0.9

5.11 Sediment Transport Rates and Unit Stream Power

In figure 5.25 the relationship between the calculated unit stream power and the unit transport rates from the regression analysis is examined. Comparing figures 5.20 and 5.25 it can be seen that unit stream power has a simpler relationship with transport rate than boundary shear stress. There is a continuous increase in transport rate for an increase in unit stream power, during both sets of experiments presented, for all but one of the elapsed times examined. The exception is time 60 minutes at a slope of 0.0026, the reason for which has already been discussed in section 5.8.

The correlation between increasing transport and increasing unit stream power at increasing relative depth is confirmed in figure 5.26. The figure shows the weight of material transported, at various times throughout the five experiments, in relation to the unit stream power, averaged through time for each experiment. Clearly, the weight of material transported by the experiments increases with increasing unit stream power.

As a result of the data presented in figures 5.20, 5.23, 5.25 and 5.26 a speculation is made regarding sediment transport during overbank, degradational conditions. Unit stream power, as estimated here, may prove more useful than boundary shear stress, as estimated here, for predicting the behaviour of graded sediment transport during shallow overbank flow.

5.12 Conclusions

In this chapter the sediment transport rate decline of five degradational experiments have been examined. Estimates have been made of the boundary shear stress and the unit stream power associated with the experimental conditions. The variation in sediment transport rates between experiments of different relative depths has been found to be different to that postulated by others. An assessment has been made concerning the two key flow parameters examined, and which may be the better for predicting degradational sediment transport behaviour during overbank flow in straight compound channels.

It should be noted that the conclusions drawn from this chapter are based on the work described. They should therefore not be taken as general conclusions about graded sediment transport behaviour until further work examining a wider range of conditions has been completed.

1. The pattern of transport rate decline has been seen to be the same for all five degradational experiments examined. The pattern of an initial period of high

transport followed by a steep decline and then a long period of marginal transport is in agreement with other reported degradational experiments.

2. The sediment transport rates throughout an experiment depend on the applied conditions including that of the initial bed. Higher transport rates are produced by steeper initial bed slopes and by higher overbank flows (larger relative depths). Sporadic fluctuations in transport rate (caused by graded sediment bed processes) can mask the distinctions between experiments.

3. The weight of material transported also depends on the experimental conditions. Experiments with steeper initial bed slopes and deeper overbank flow conditions transport greater weights of material. Sporadic transport rate fluctuations are less significant when examining the weights of cumulative transported material.

4. Boundary shear stress, estimated from hydraulic measurements using Wark's LDM, was shown to vary with relative depth. It was found that the boundary shear stress experienced in the main channel was less during shallow overbank flow than it was during bankfull flow. Main channel boundary shear stress during deep overbank conditions was greater than during both shallow overbank or bankfull conditions.

5. Trends in bedload transport did not follow that of the predicted applied boundary shear stress. Both the sediment transport rates and the weights of material transported increased between the bankfull, shallow overbank and deep overbank experiments.

6. Unit stream power, estimated from hydraulic measurements using Bagnold's definition, increased monotonically with relative depth.

7. The relationships between unit stream power and relative depth and between sediment transport and relative depth show the same trend. It is therefore possible that unit stream power, as estimated here, would be a better predictor of degradational graded sediment transport behaviour during overbank flows, than bed shear stress, as estimated here.

5.13 Further Work

Several ideas are suggested as to how the work presented may be complemented by further research. These cover both areas touched on here and new areas highlighted by the results presented.

The results and conclusions presented in this chapter are specific to the case of non-equilibrium transport, of graded sediment, during degradation, in a straight compound channel. Before it can be stated whether these results are applicable to overbank transport more generally, further work will have to be done. This work should cover a wider range of conditions, such as transport during equilibrium and aggrading conditions. The use of a water-worked beds in recirculation experiments will no doubt have an effect on the transport rates.

In section 5.6.4 the implementation of Wark's LDM is described. Part of the process involved matching the measured hydraulic data to estimates of the non-dimensional eddy viscosity (NEV) and the hydraulic roughness of the gravel bed. The estimates of NEV values were obtained from literature and the estimates of the gravel bed roughness were thereafter obtained through iteration. The section describes the process for deriving an initial estimate of the bed roughness from the bankfull experimental data. Further work could focus on the development of bed roughness and its relationship with bed texture, grain arrangement or the evolution of bed surface composition.

More detailed analysis of the relationship between unit stream power and relative depth may also be justified. Figures 5.24a and 5.24b both show a diminishing increase in unit stream power for an increase in relative depth. The relationship will be dependent on the ratio of increase in discharge within the main channel compared to the increase in discharge over the flood plains, for an increase in relative depth. This will in turn be dependent on interaction between the main channel and flood plain flow caused by differences in relative roughnesses.

There is another trend identified within the results which cannot be examined with the current data. The change in transport rate or the weight of material transported is greater, for the same change in relative depth, at the shallower of the two slopes examined. This is true for almost all the data presented in figures 5.19a, 5.19b, 5.22a and 5.22b. One speculation is that this is a function of the relative transporting capacities of the experiments and thresholds of transport within the graded sediment mix. Further investigation may verify the trend and justify the speculation.

Although the LDM is a practical method for estimating channel properties it does have some limitations. The model appears to have difficulty modelling sudden changes in flow depth. These cases are usually found at the edges of vertical sided channels where there is a discontinuity in the flow depth with lateral co-ordinate y. The model correctly predicts decreases in unit discharge towards the side of the channel. If however, the flow depth is decreasing by a greater amount than the decrease in unit discharge then the result is an increase in predicted flow velocity. This has been discussed in a personal communication with Wark (1997). For this work it is not critical as the lateral boundaries of the main channel are sloping rather than vertical. The side slopes are also fixed boundaries and therefore predicted data above them is not included in the work relating to transport behaviour. Further examination of the Wark LDM model with a view to solving this anomaly may allow the model to be used for a wider range of conditions.

Further predictions of boundary shear stress using other lateral distribution models, such as that of Knight and Abril (1996), would also be welcome. This would allow further verification of the predictions made here and may also identify the best model to base further research on.

Perhaps the most obvious long term goal is to develop a prediction model for graded sediment transport behaviour, applicable to both bankfull and shallow overbank conditions. The largest barrier to achieving this goal is the present lack of data relating to graded sediment transport during overbank flow conditions. If further experiments were to be undertaken, they should be carried out at slopes and relative

depths aimed at filling in the gaps around the area of interest. This means significantly more data on sediment transport during low values of relative depth, as these are the most commonly occurring overbank flood levels. Running experiments with the re-circulation of sediment transport may also allow clearer assessment of transporting capabilities.

Finally, a personal communication with Dr. Roger Bettess (1997b), of HR Wallingford, raised the following point. Consultants, trying to predict sediment transport in natural channels, perceive that where existing predictive methods fail is in using section averaged values. It is believed this simplification leads to incorrect estimates of transport behaviour. If future predictions could be based on laterally distributed values of the key variables then more accurate results may be possible. This obviously adds another order of complexity to the problem. The predictions of boundary shear stress and stream power in this work did however come from a lateral distribution model. It may therefore be feasible produce a lateral distribution based predictor. But, before such a model could be attempted, more detailed data on the lateral distribution of sediment transport would need to be collected. As well as this more detailed measurements of the lateral distribution of unit stream power and boundary shear stress would be required during transporting conditions.

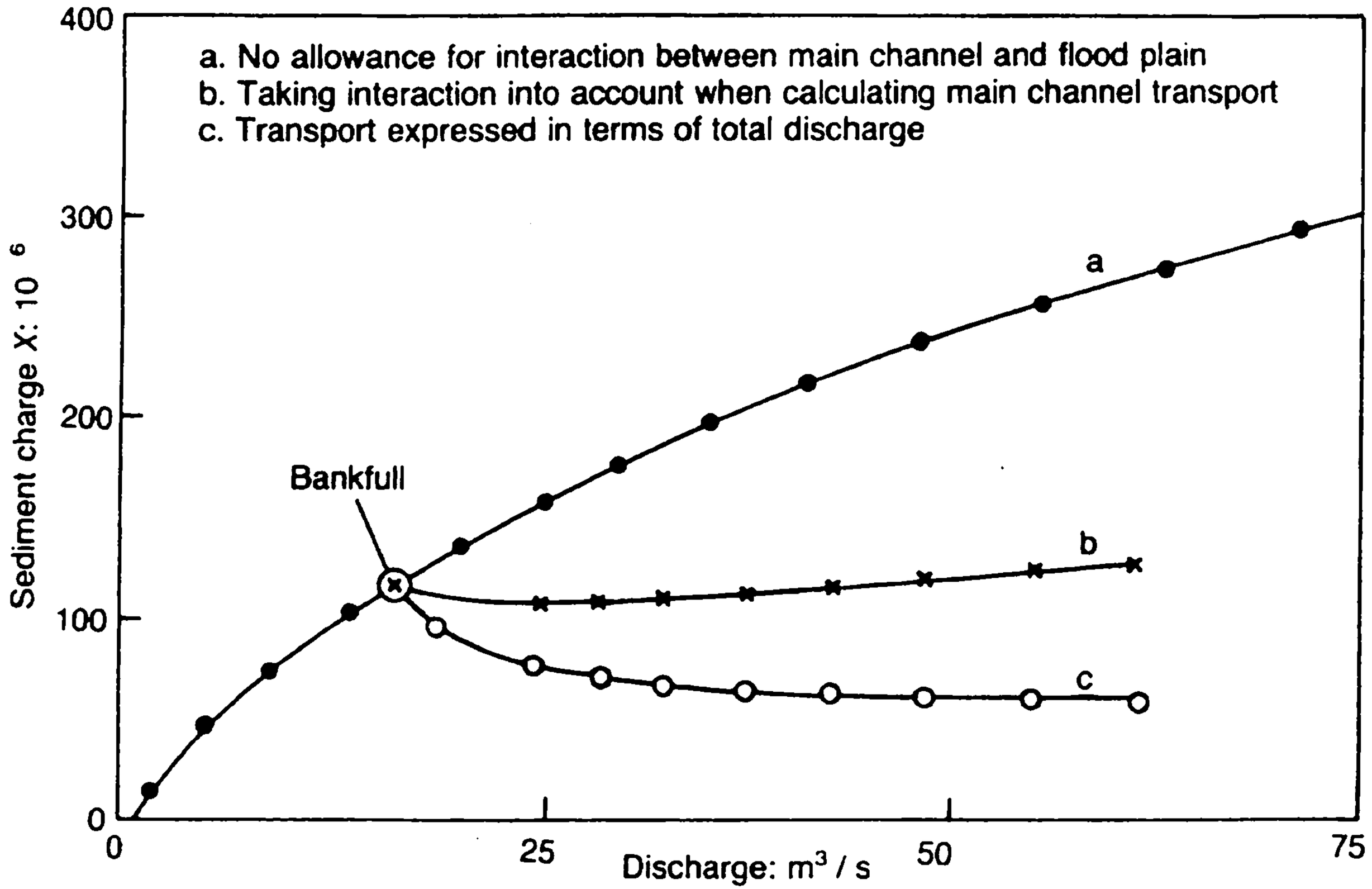

Figure 5.1 Variation in Sediment Transport with Discharge in a Hypothetical River Channel [Ackers (1992b) - fig.6a]

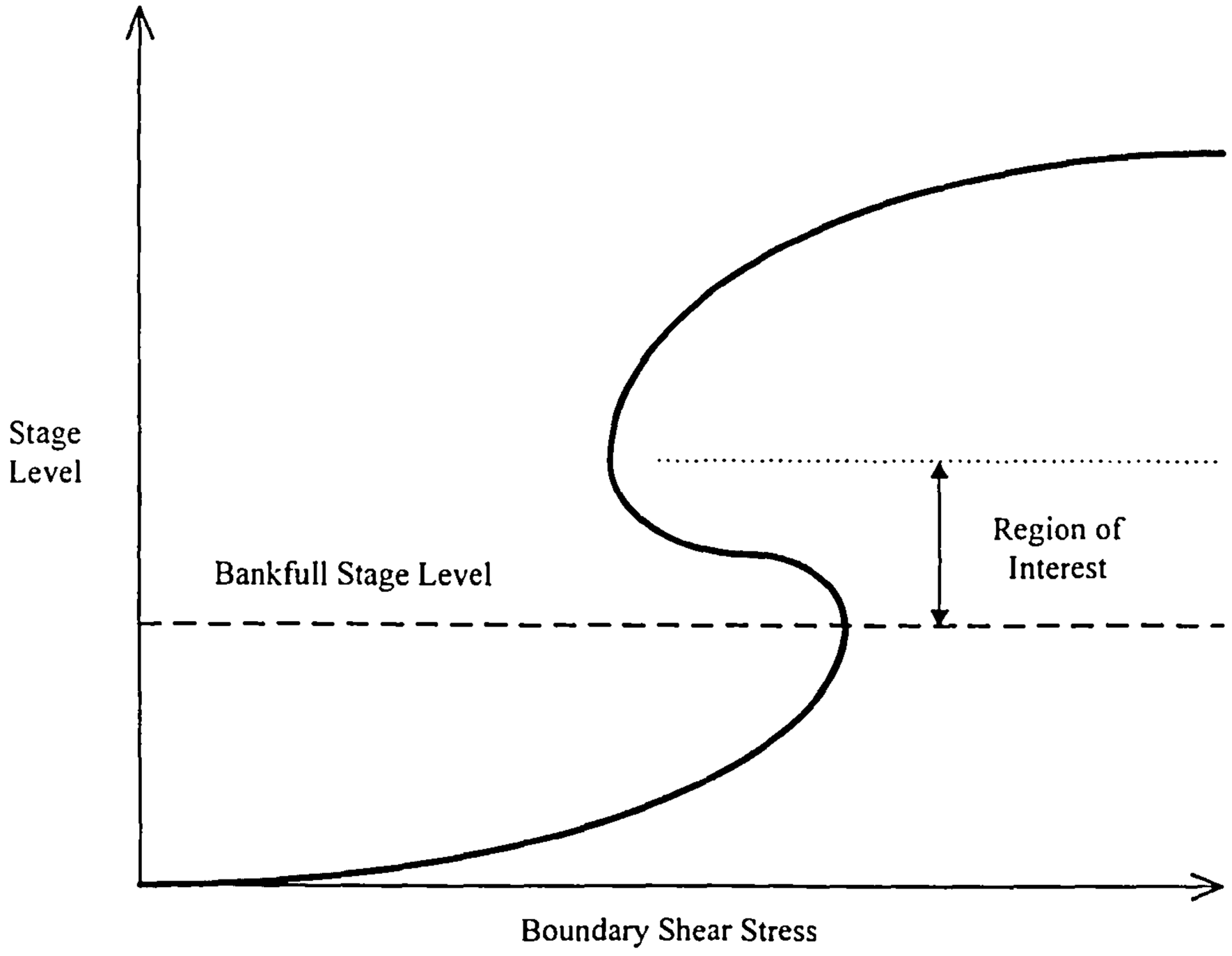

Figure 5.2 Idealised Variation of Boundary Shear Stress with Stage Level

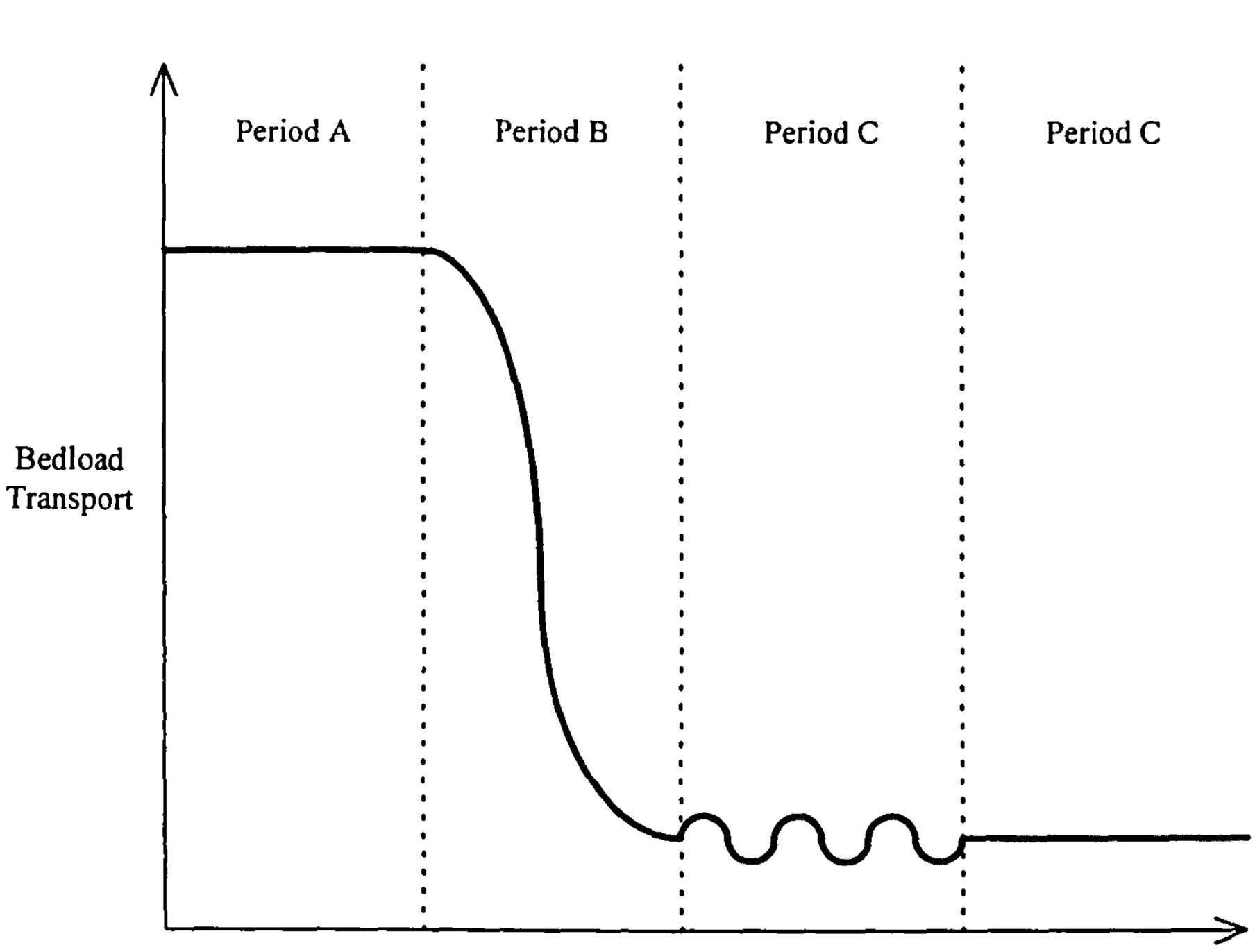

Figure 5.3 Generalised Trend of Degradational Behaviour Transport Rate Decline

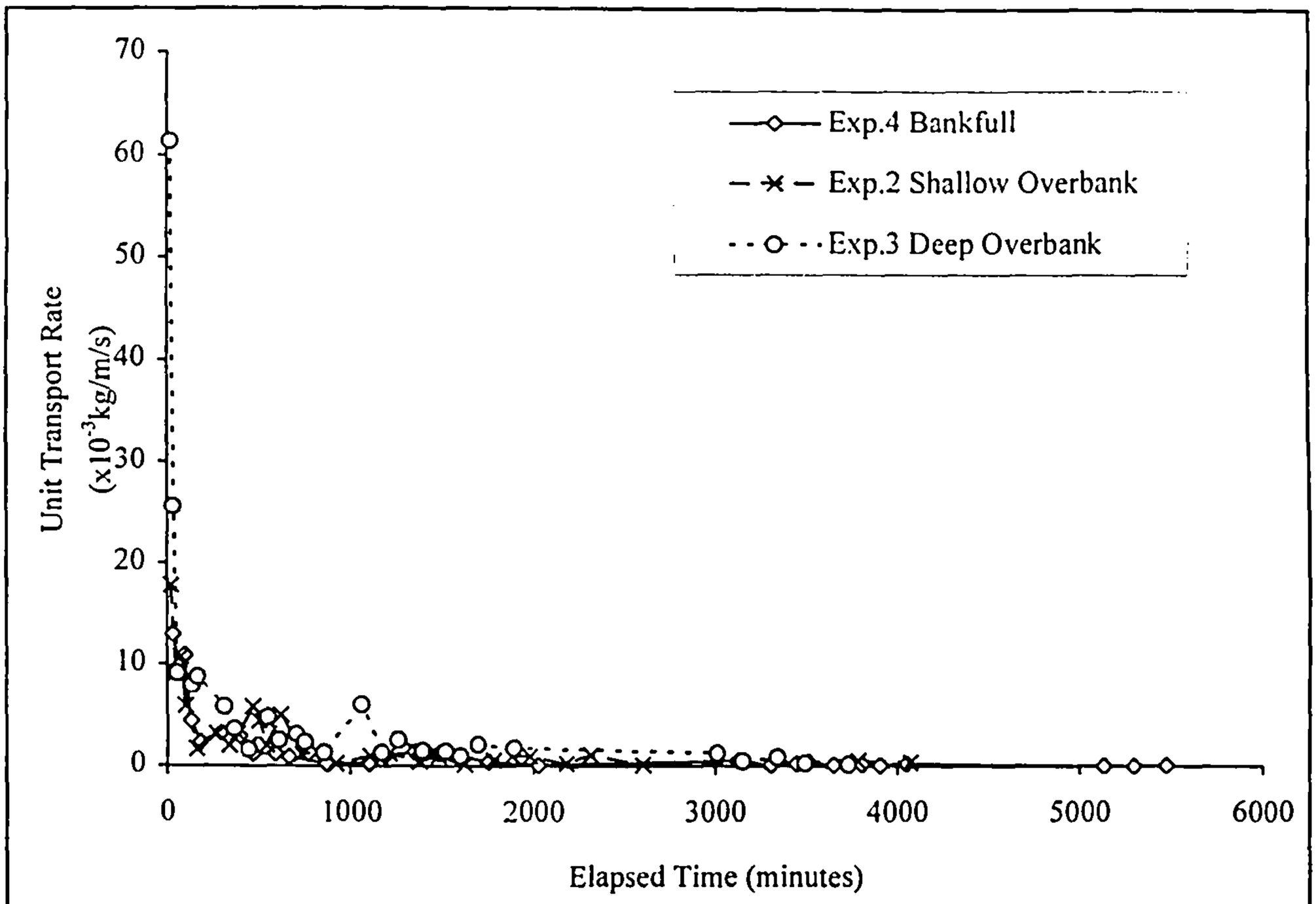

Figure 5.4a Unit Transport Rates for Experiments with Initial Slope of 0.0026

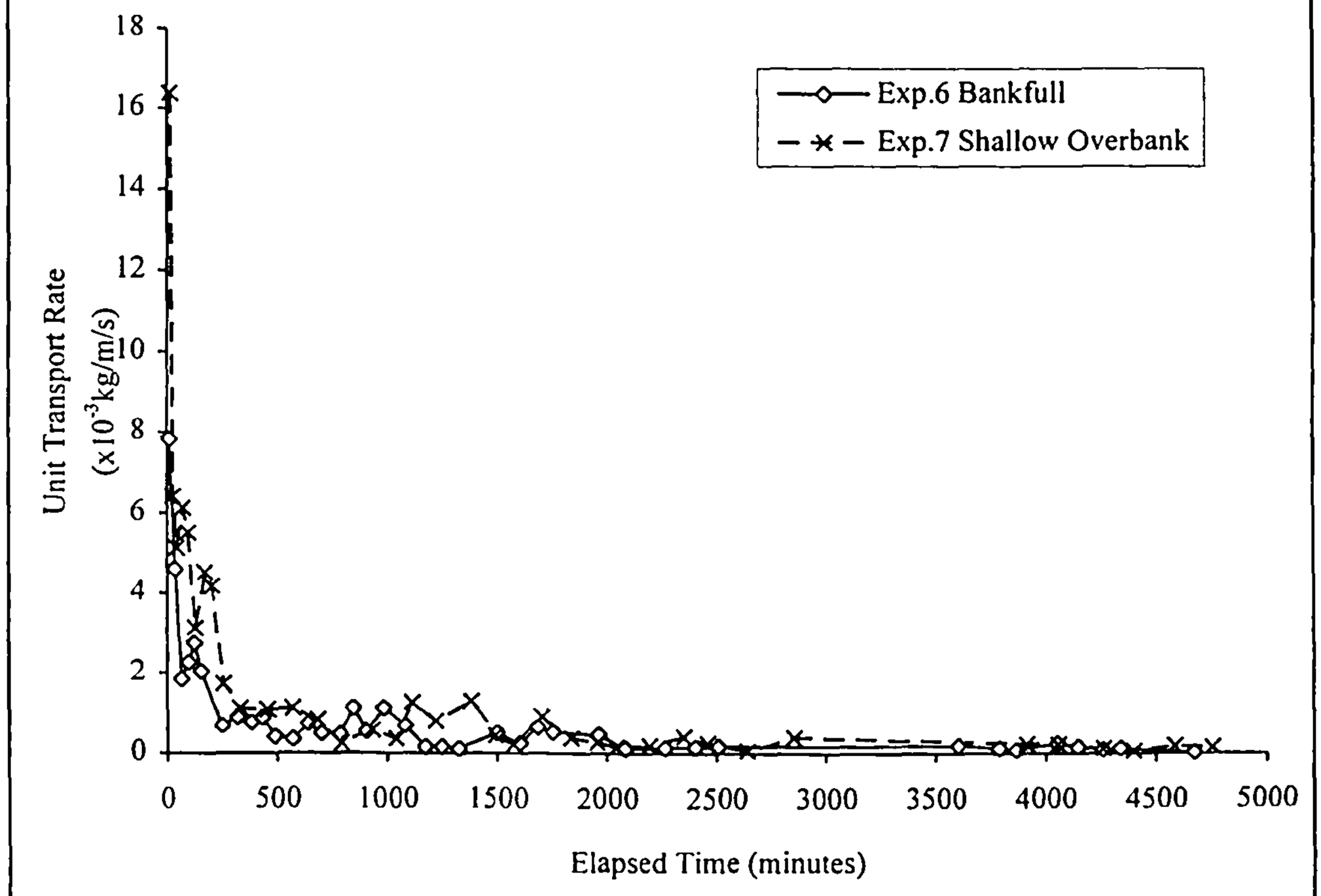

Figure 5.4b Unit Transport Rates for Experiments with Initial Slope of 0.0024

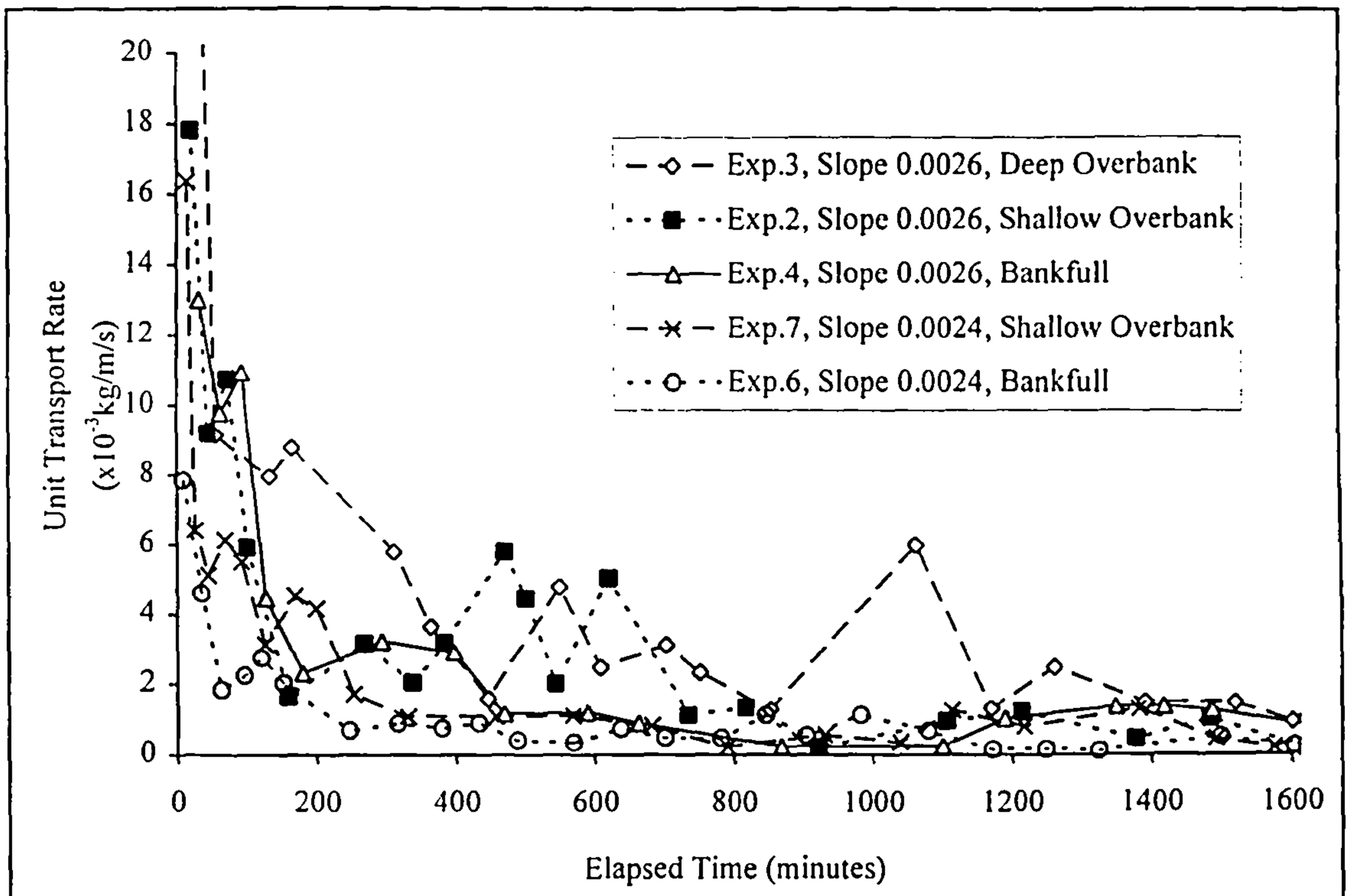

Figure 5.5 Unit Transport Rates for All Five Experiments on Shortened Axes

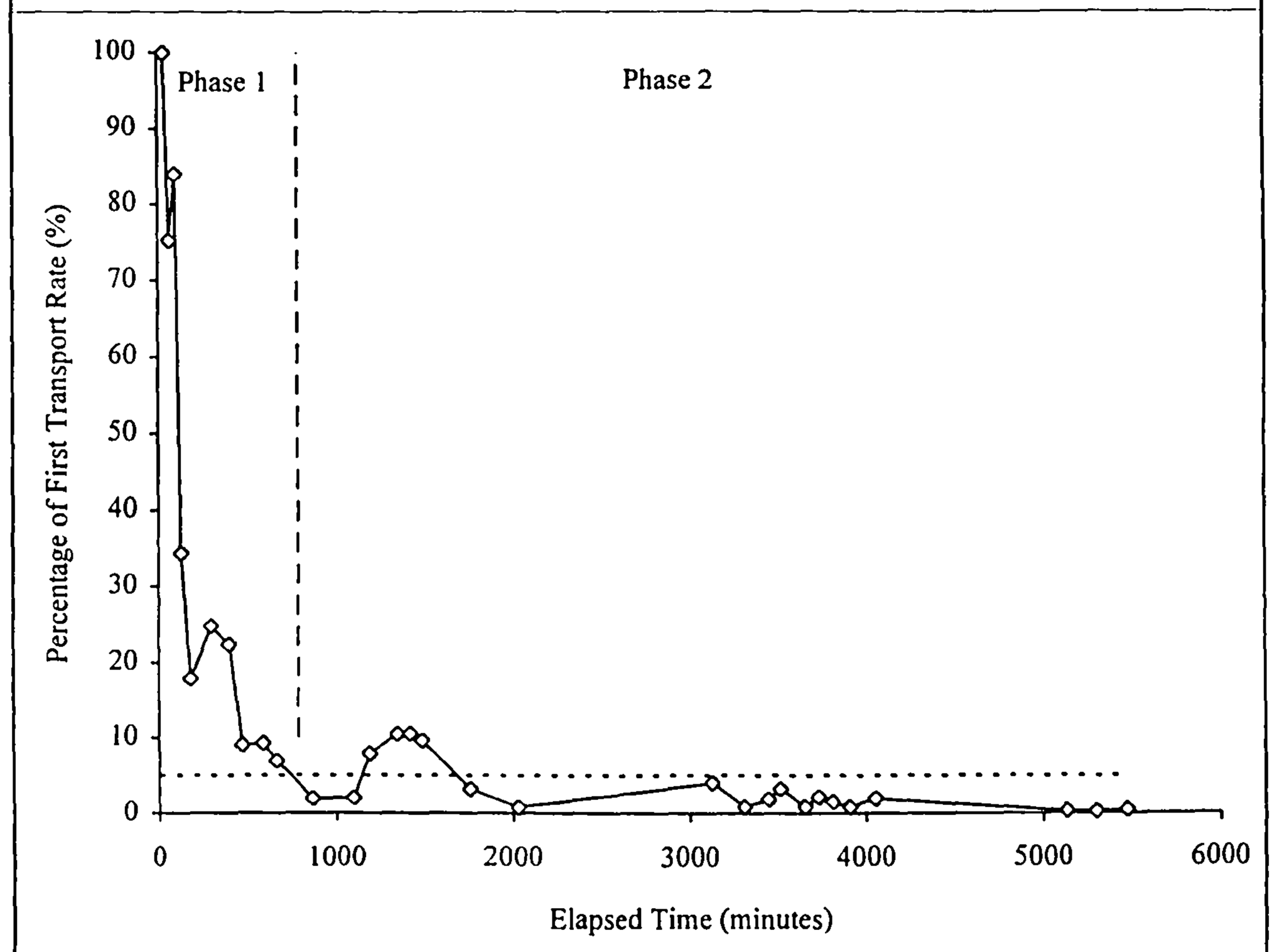

Figure 5.6 Unit Transport Rate as a Percentage of the First Transport Rate Recorded, Experiment 4.

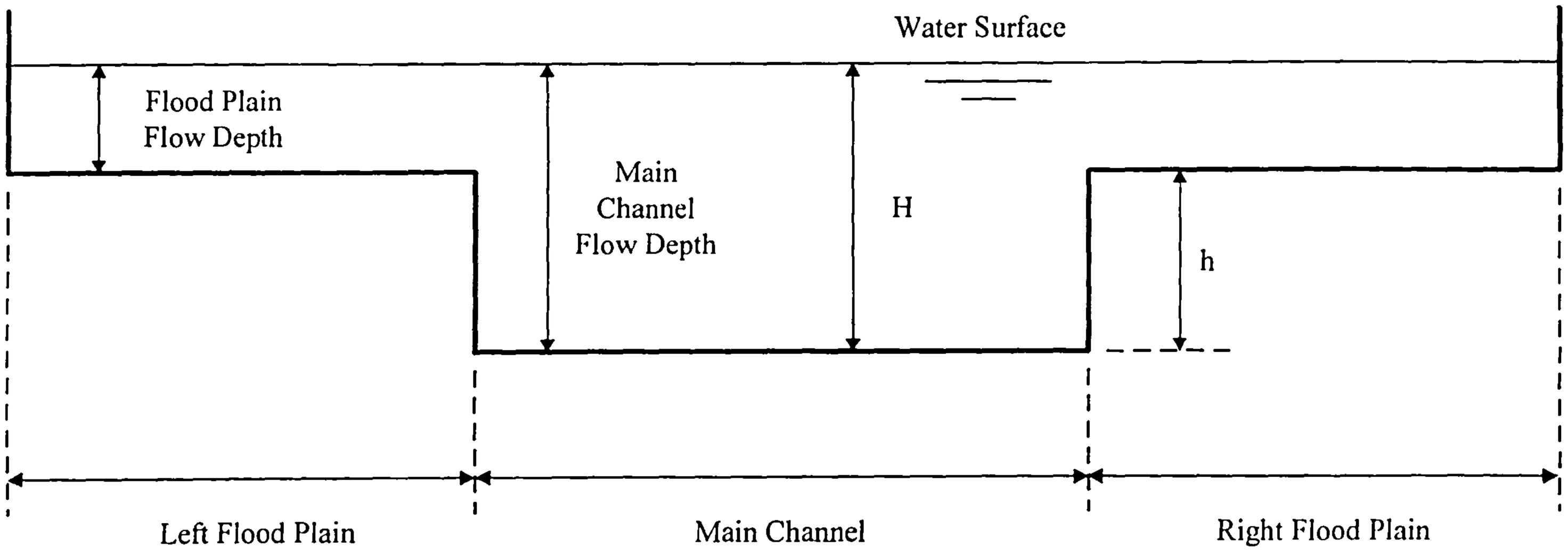

Relative Depth Ratio = (H-h)/H

Figure 5.7 Relative Depth Ratio of a Compound Channel

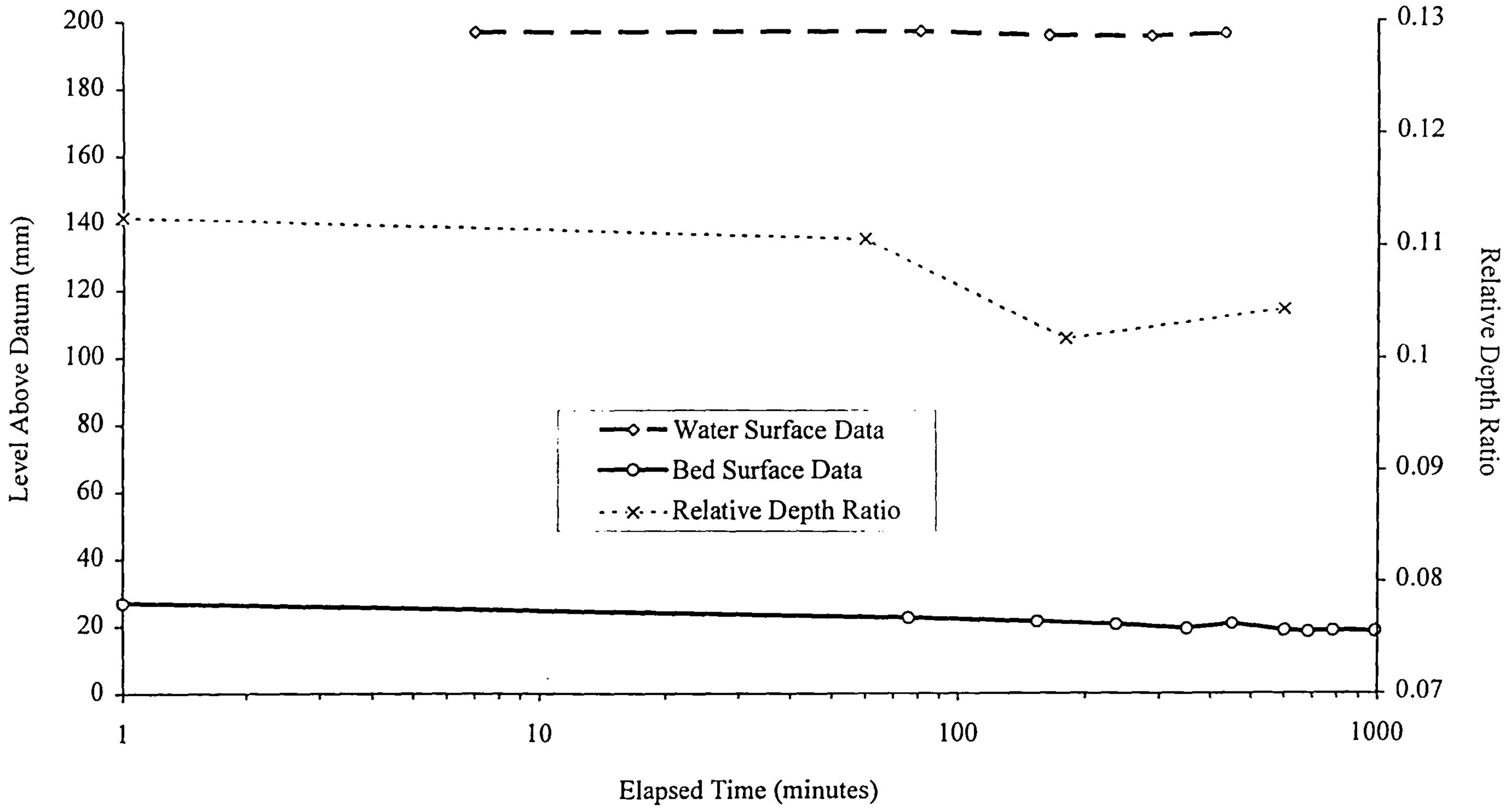

Figure 5.8 Experimental Trends in Water Surface Data, Bed Surface Data and Relative Depth Ratio, Experiment 7

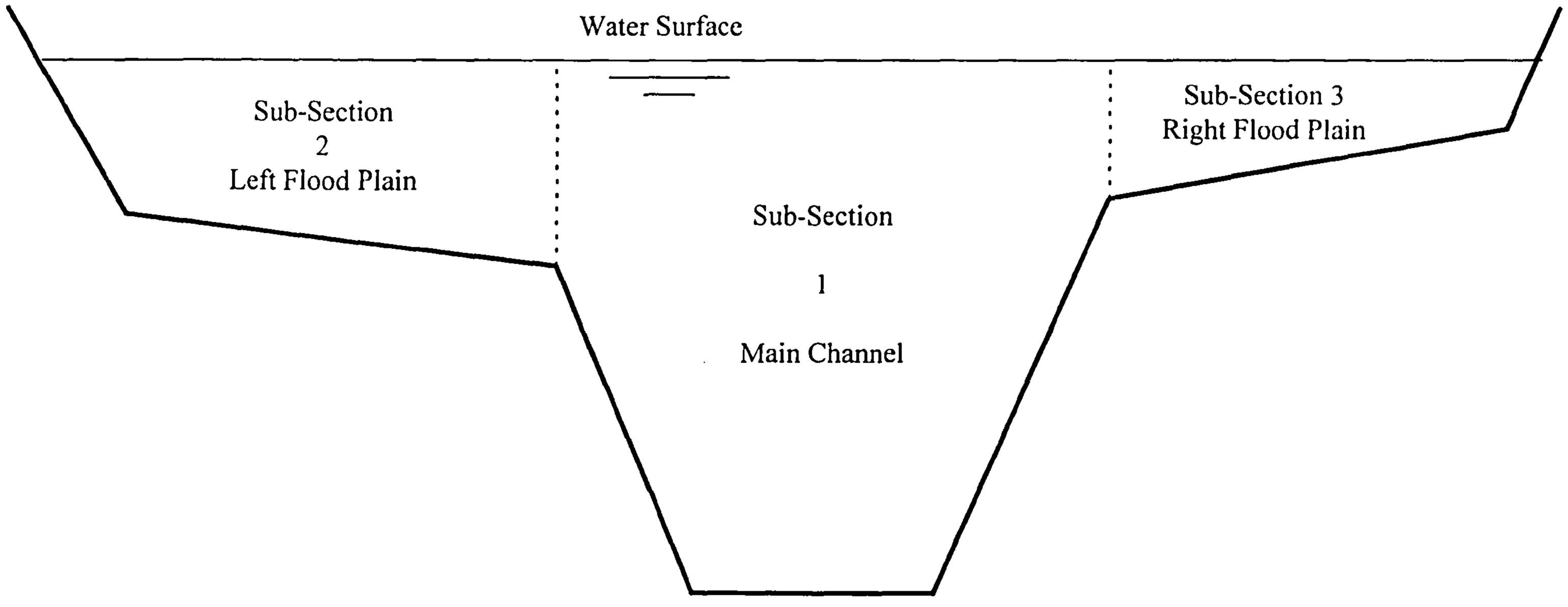

Figure 5.9 Conventional Sub-Section Approach to Compound Channel Discharge Assessment

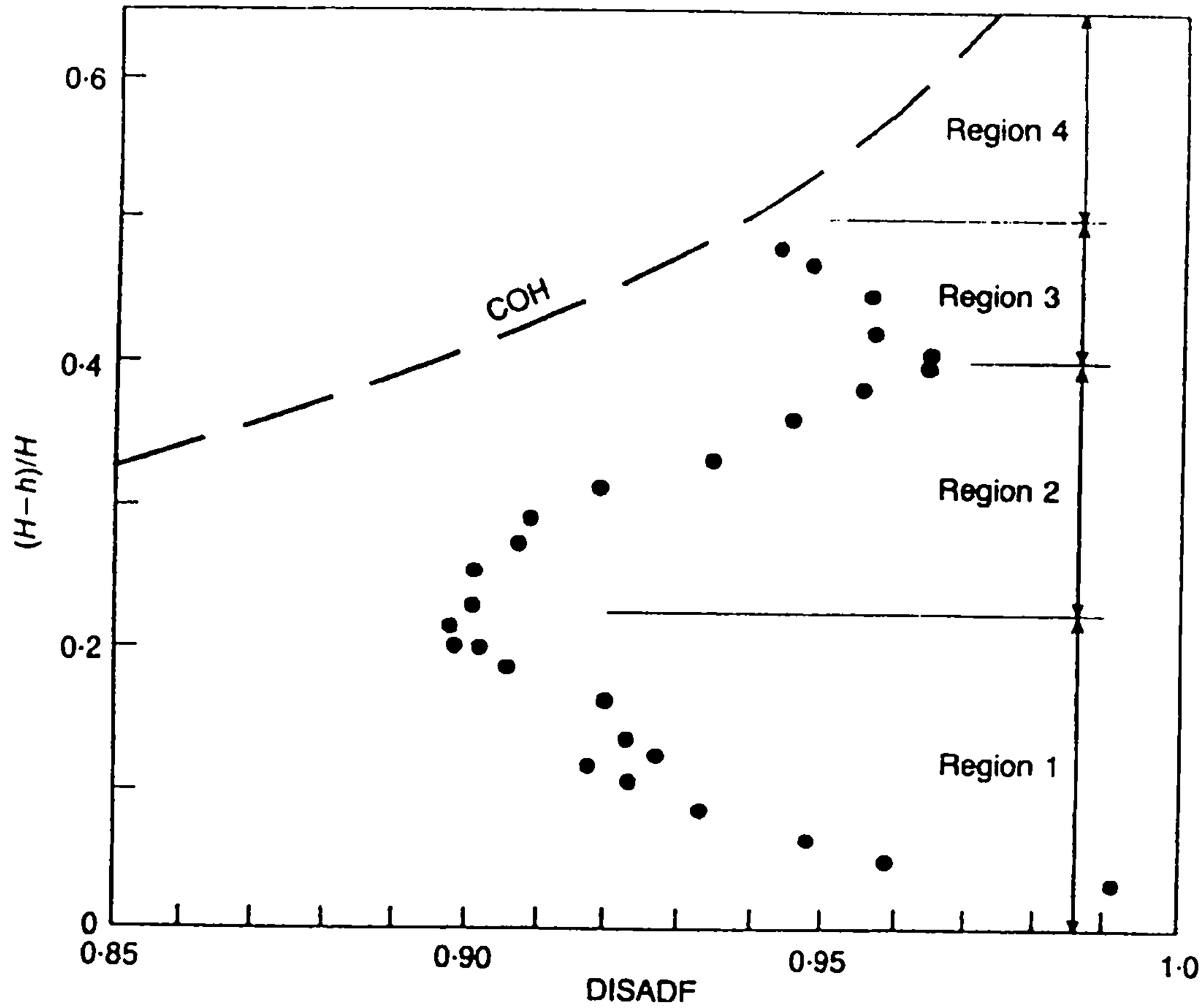

Figure 5.10 Variation of DISADF and COH with Relative Depth Ratio,
Sample Test Results from FCF [Ackers (1991) - fig.5]

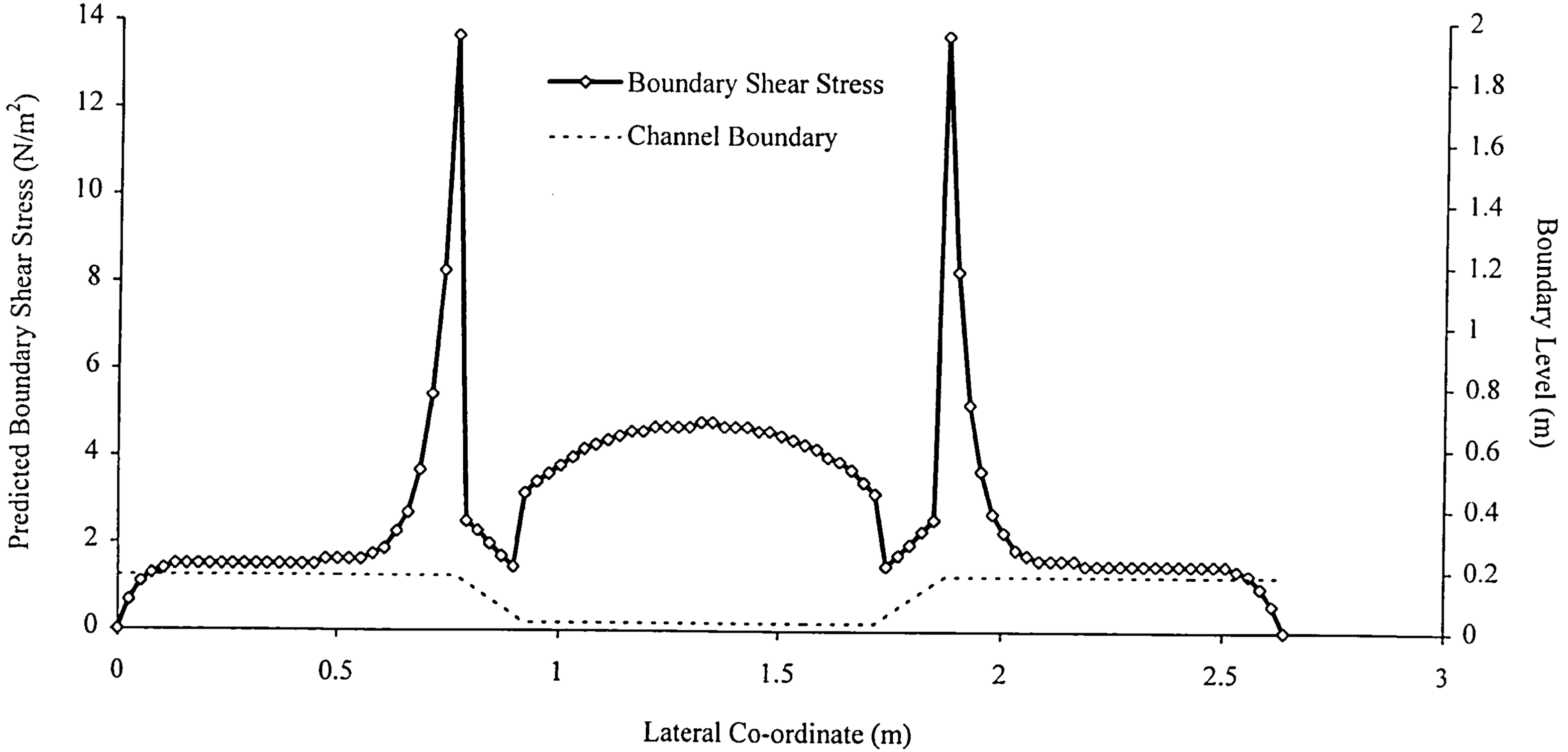

Figure 5.11 Results Showing the Lateral Distribution of Boundary Shear Stress, Predicted Using the Lateral Distribution Method (LDM)

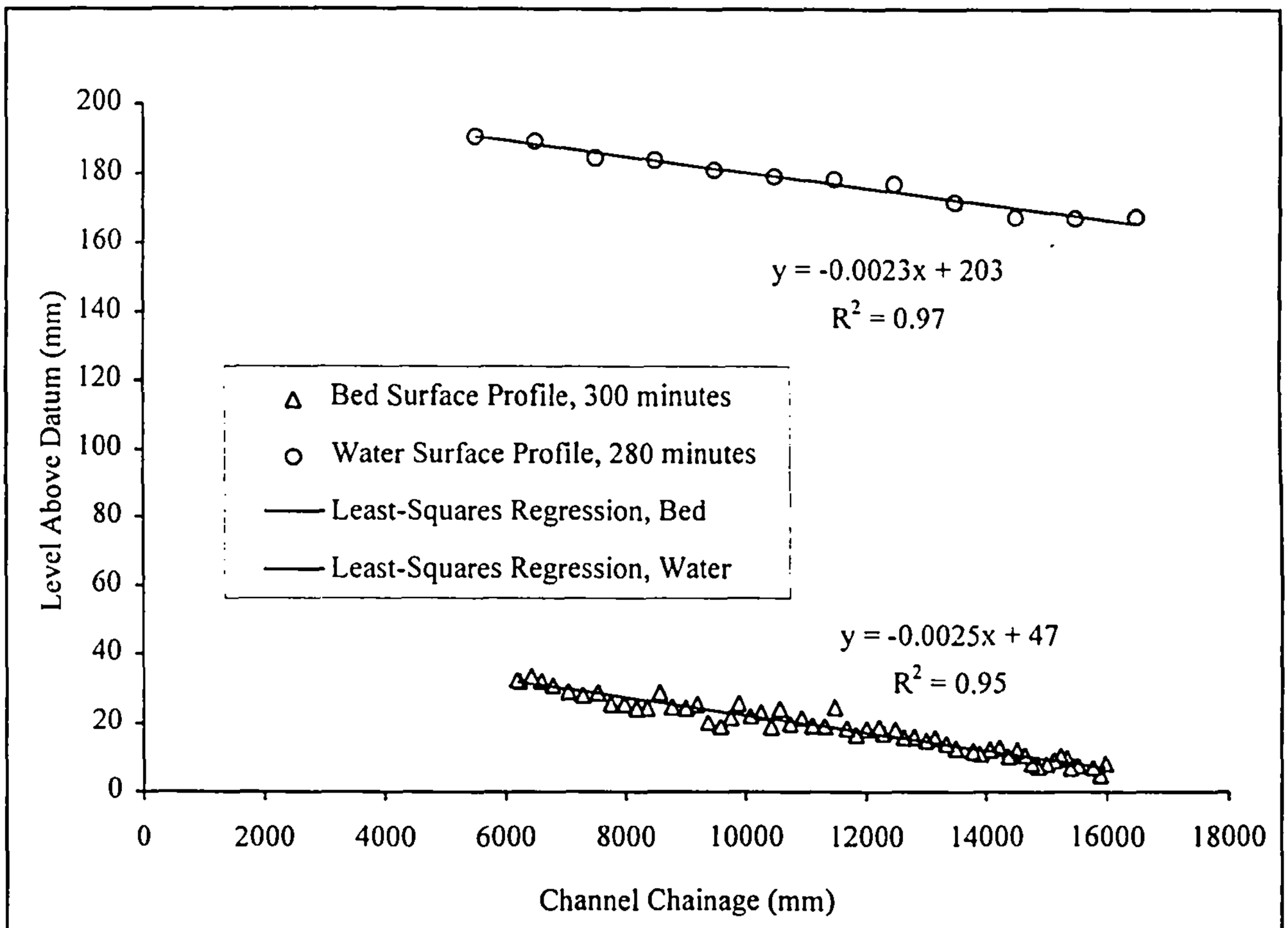

Figure 5.12 Bed and Water Surface Profiles,
Phase 1 of Experiment 4

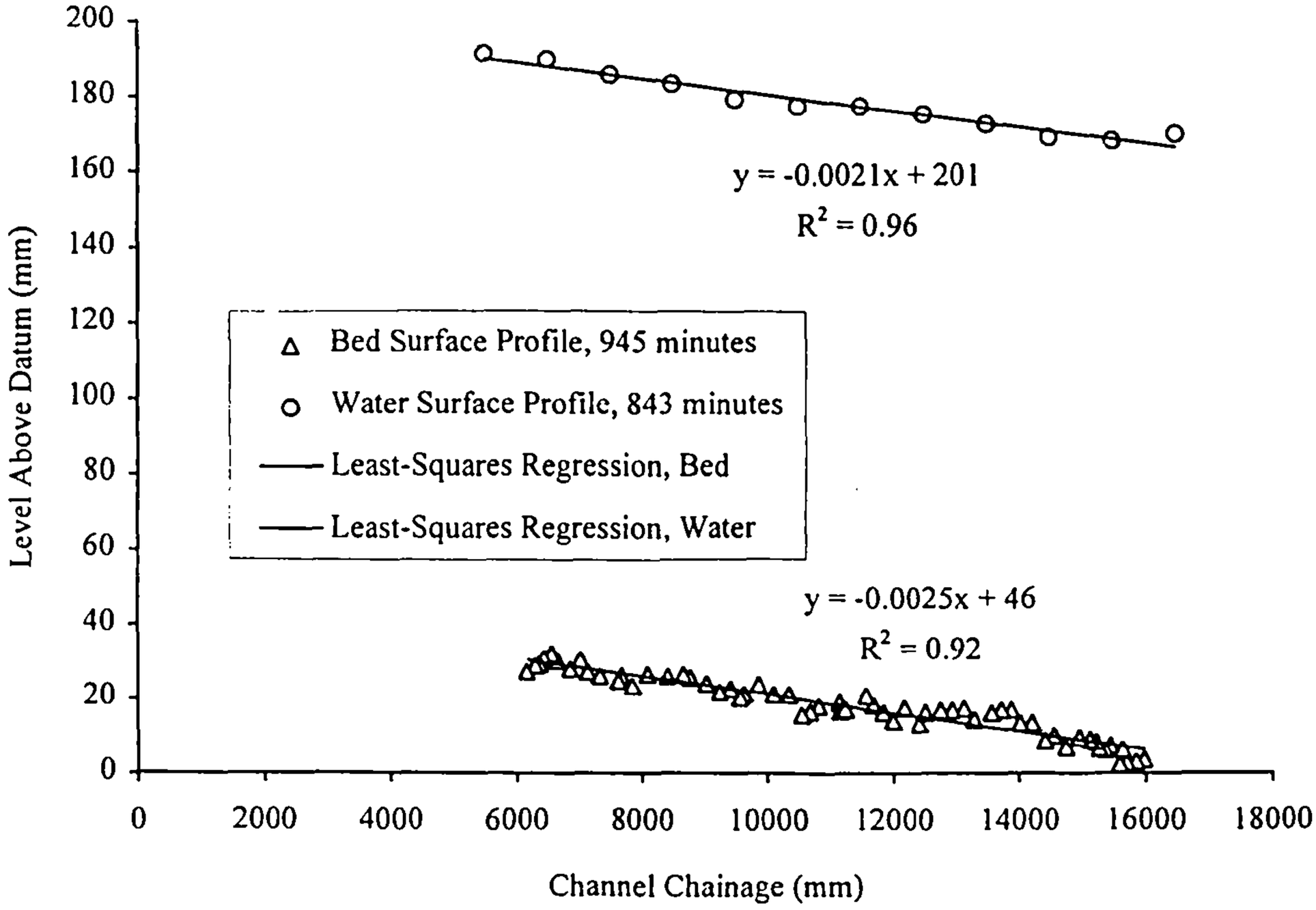

Figure 5.13 Bed and Water Surface Profiles,
Phase 2 of Experiment 4

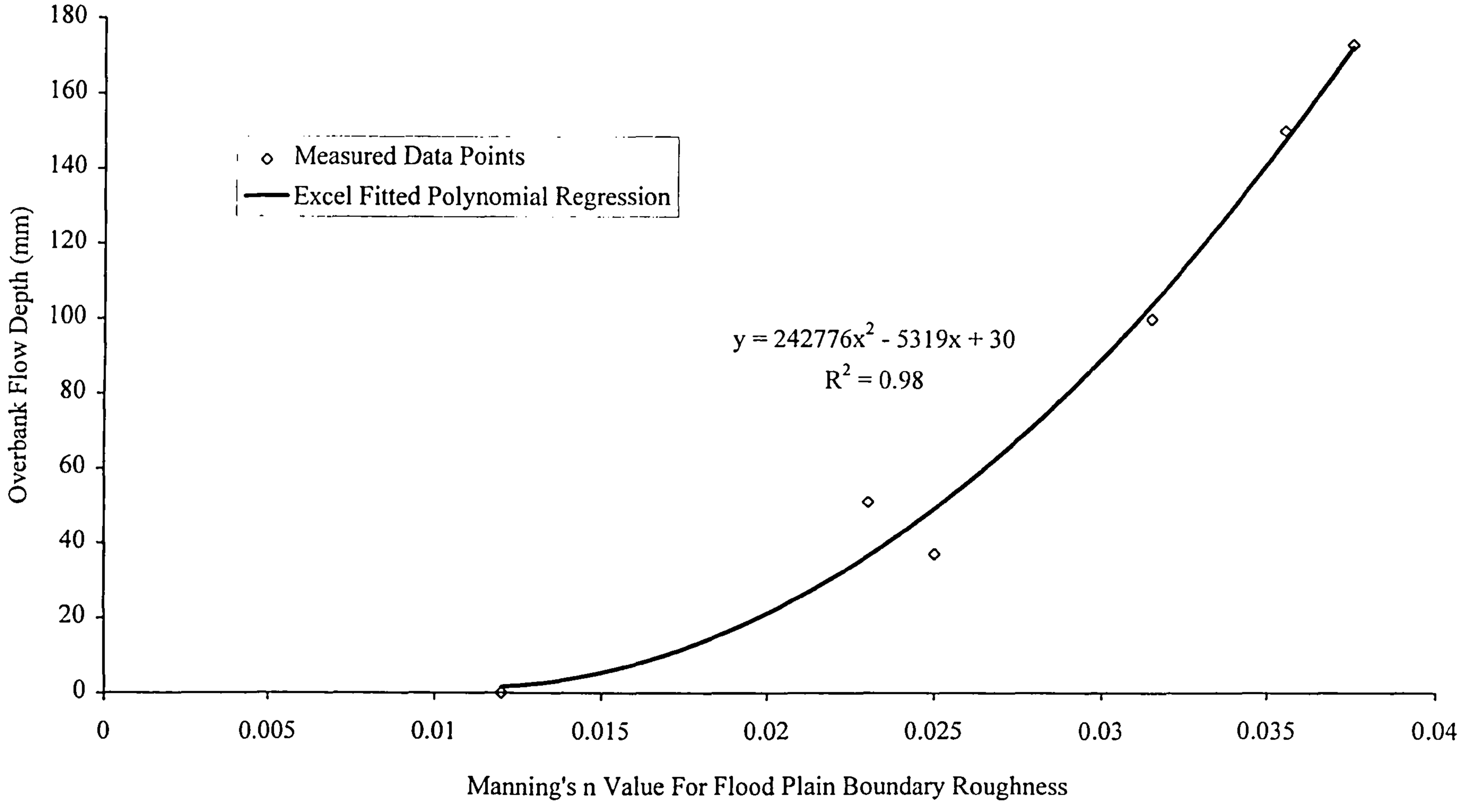

Figure 5.14 Variation in Manning's n Value with Overbank Flow Depth, for Flood Plain Boundary Roughness

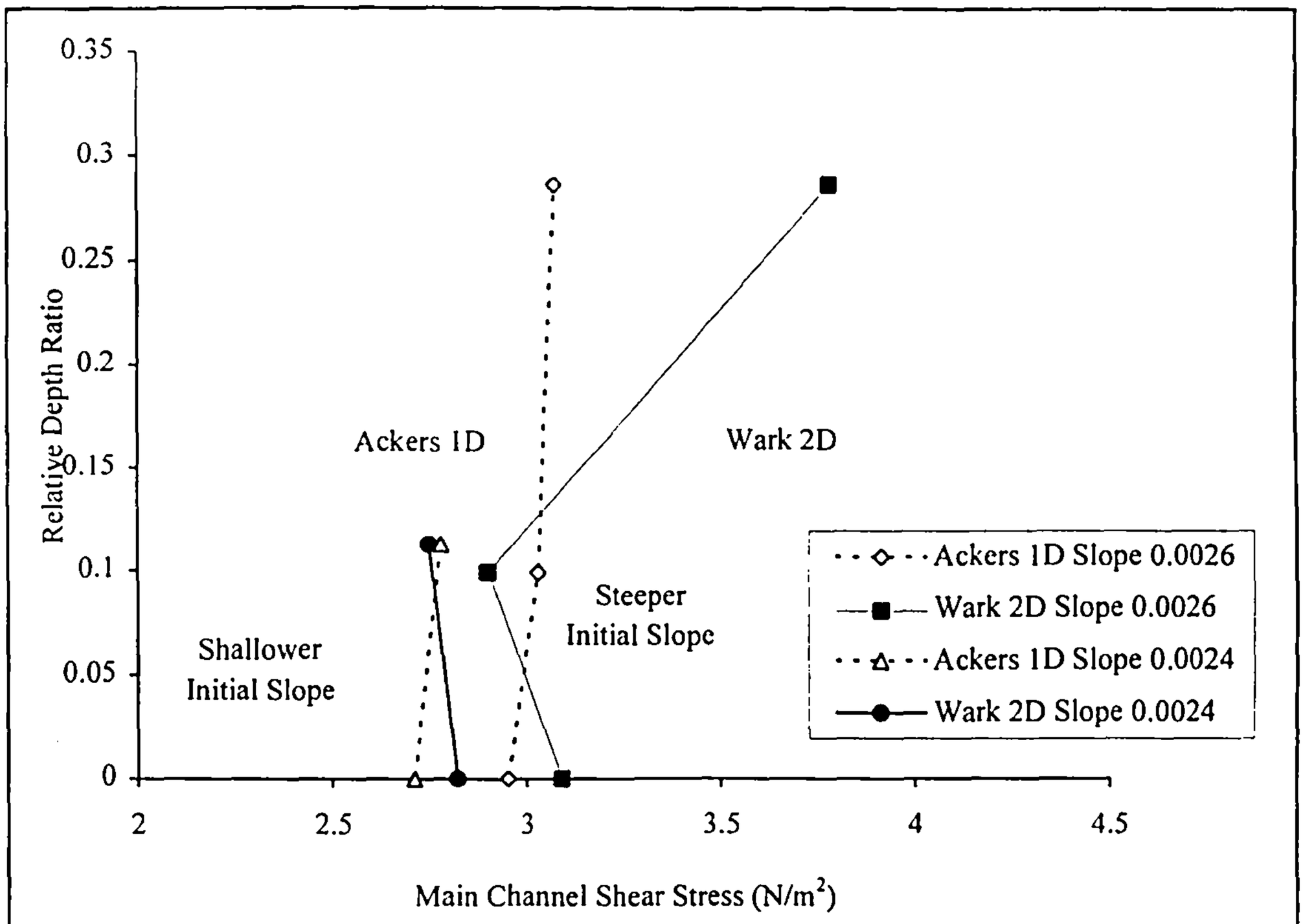

Figure 5.15a Results of Main Channel Boundary Shear Stress Predictions, Time 0 Minutes

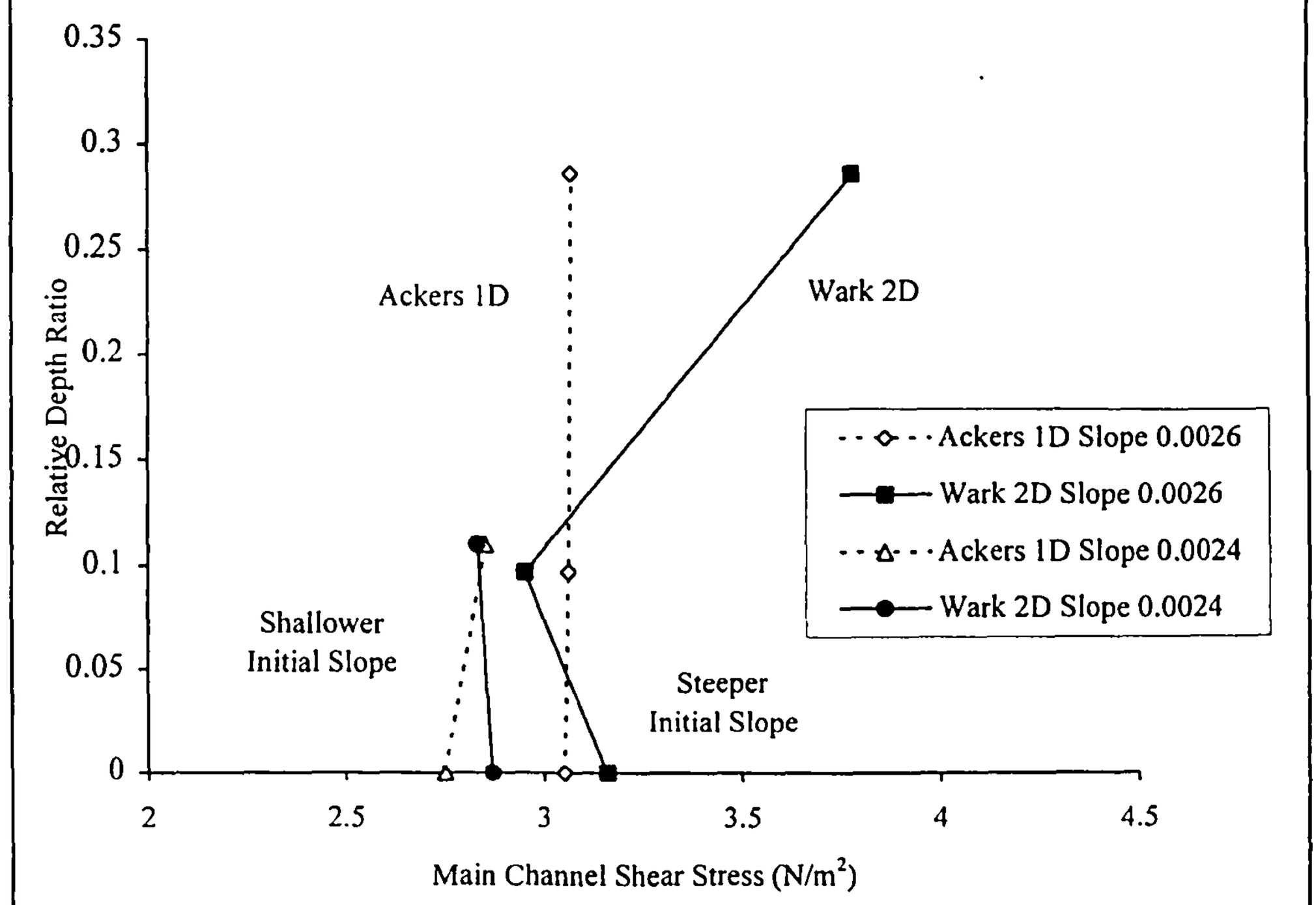

Figure 5.15b Results of Main Channel Boundary Shear Stress Predictions, Time 60 Minutes

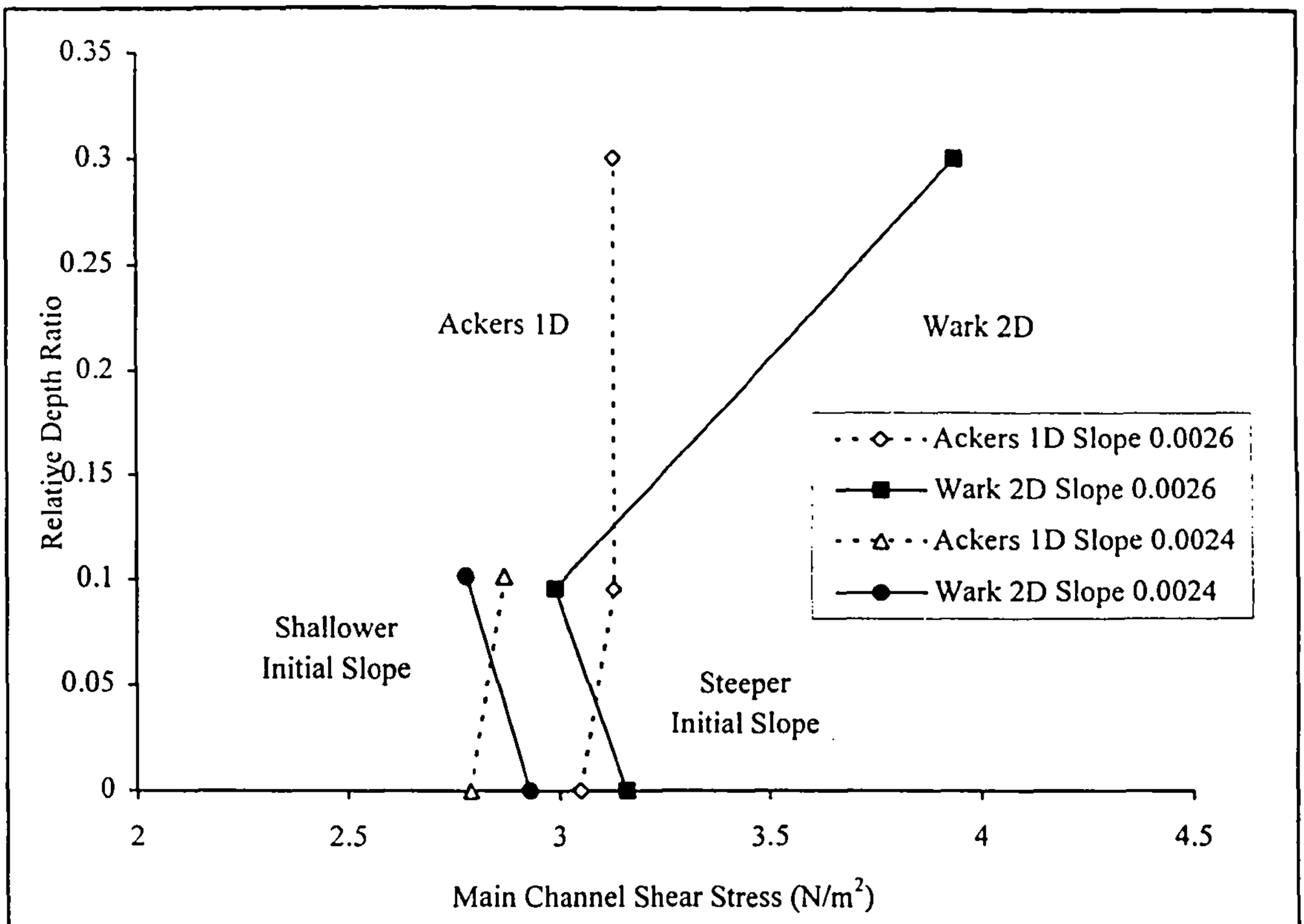

Figure 5.15c Results of Main Channel Boundary Shear Stress Predictions, Time 180 Minutes

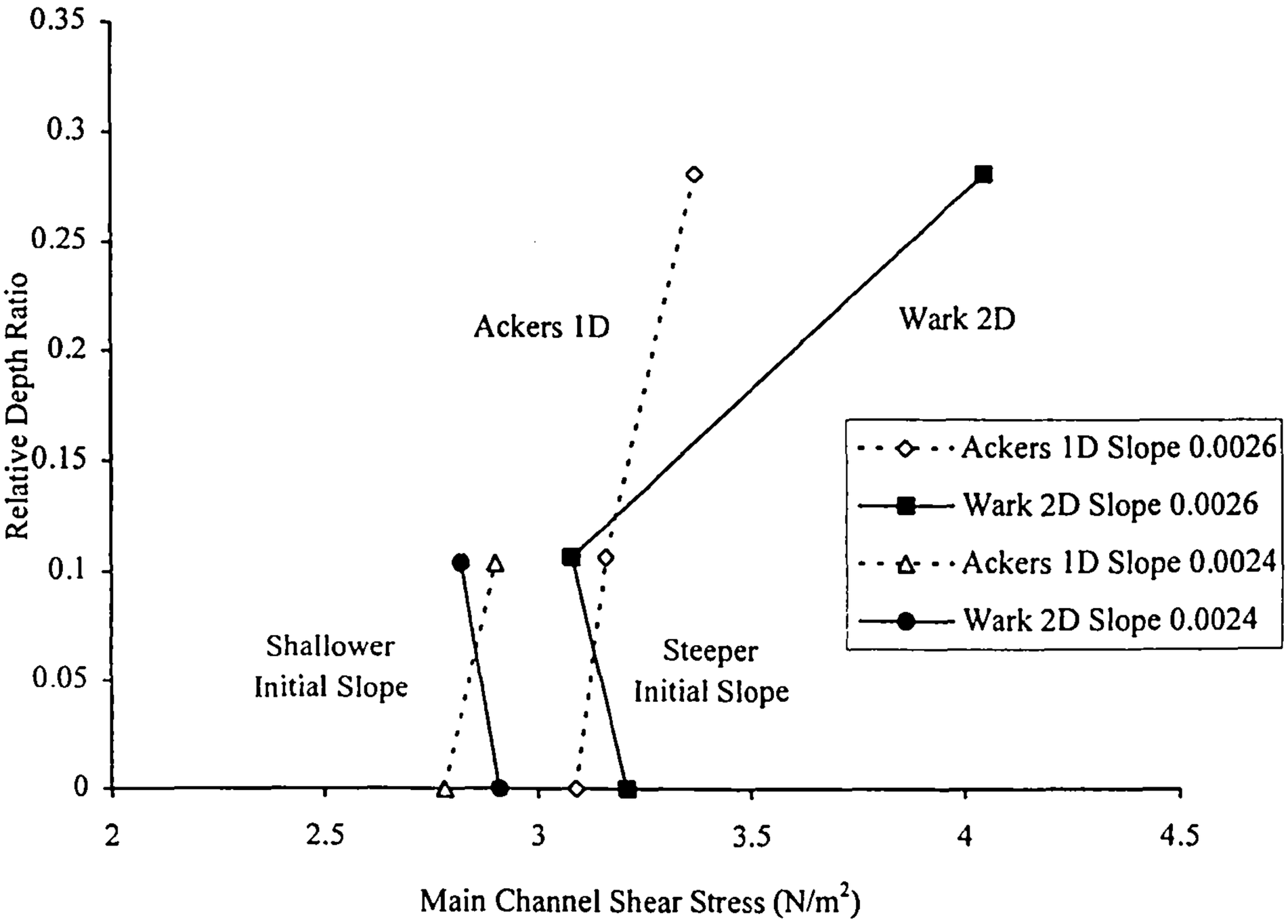

Figure 5.15d Results of Main Channel Boundary Shear Stress Predictions, Time 600 Minutes

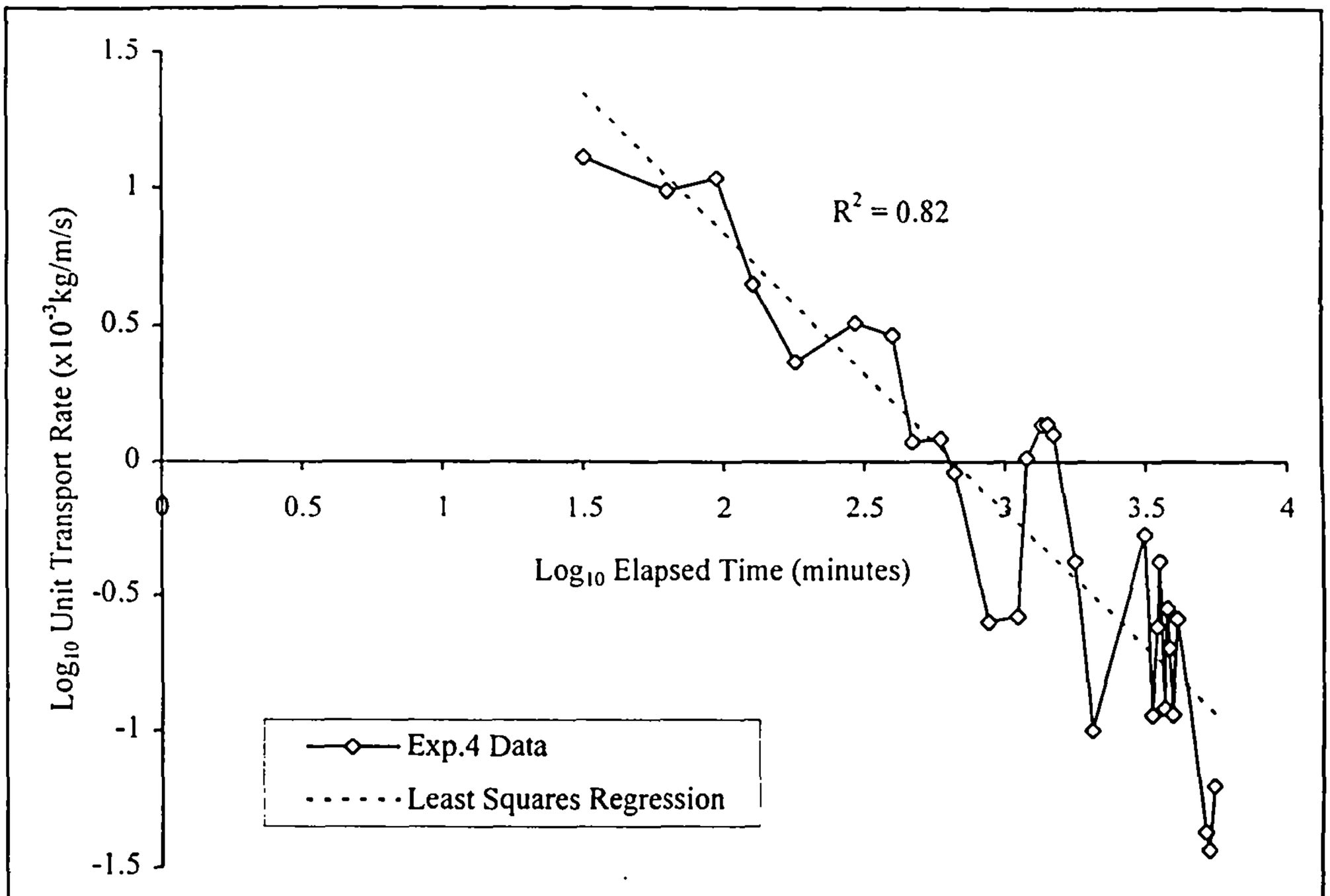

Figure 5.16 Plot of Log_{10} Transport Rate Against Log_{10} Elapsed Time

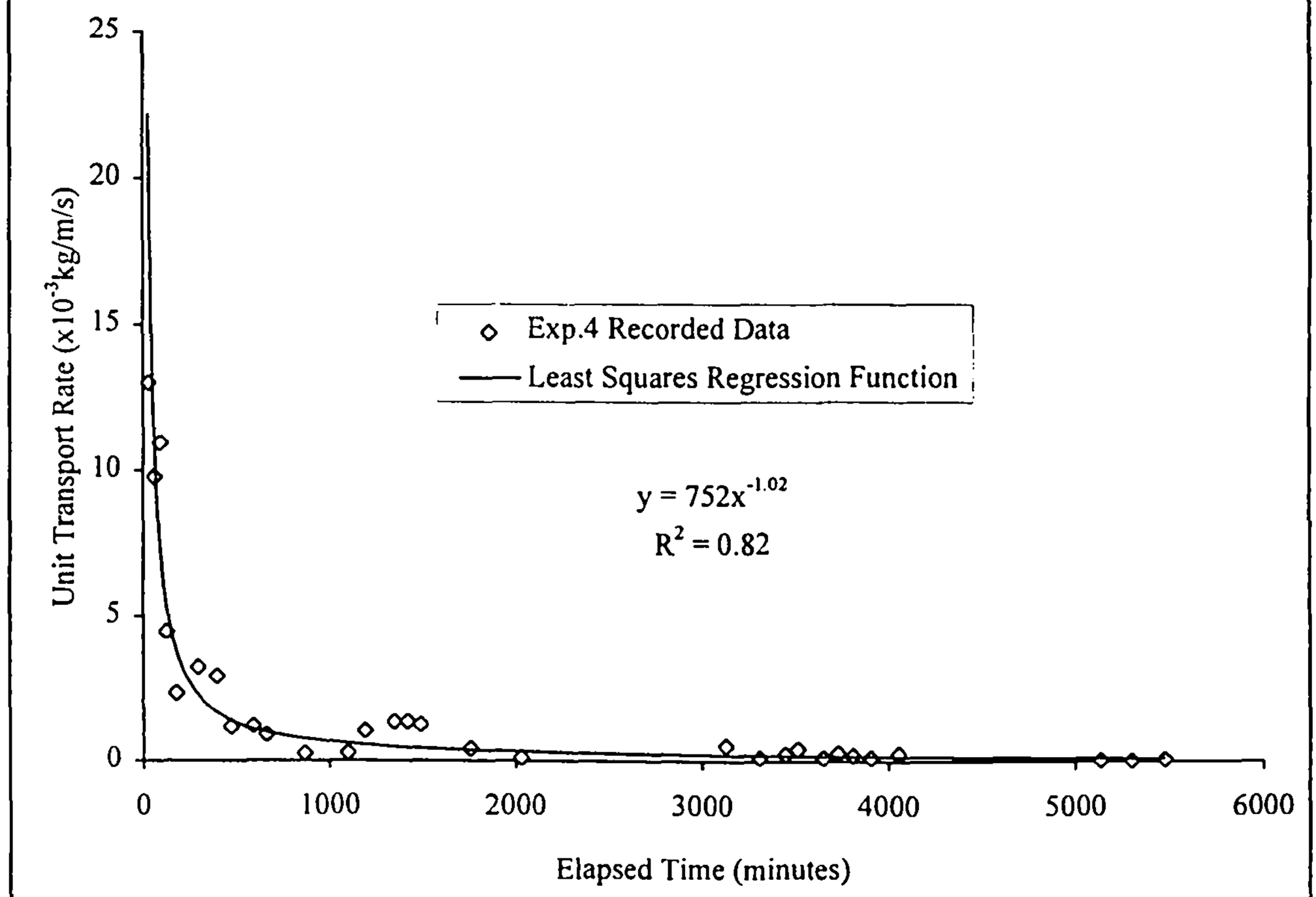

Figure 5.17 Transport Rate Data and Transport Rate Regression Function, Experiment 4

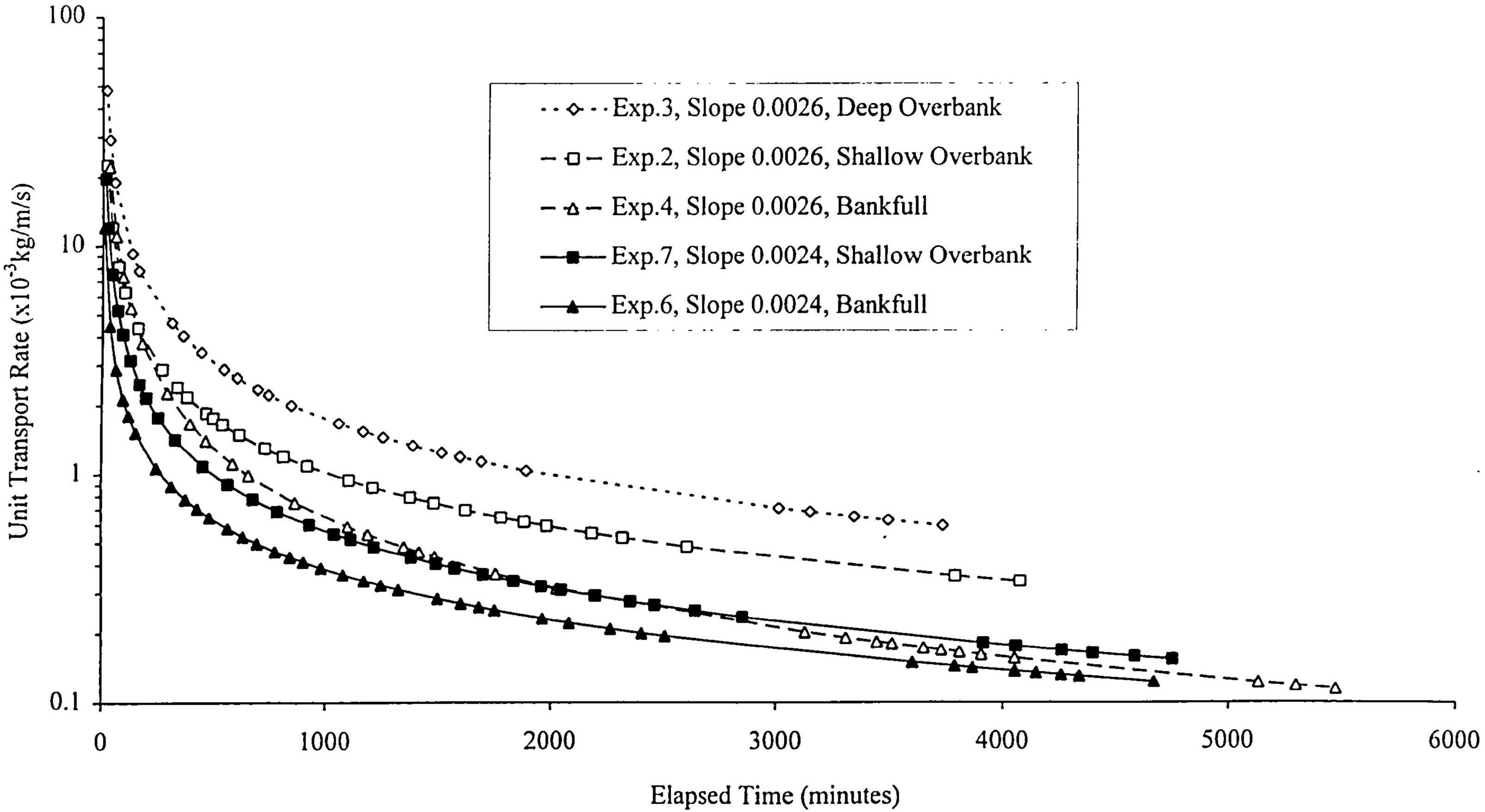

Figure 5.18 Results from Least-Squares Regressions, Experiments 2, 3, 4, 6 & 7

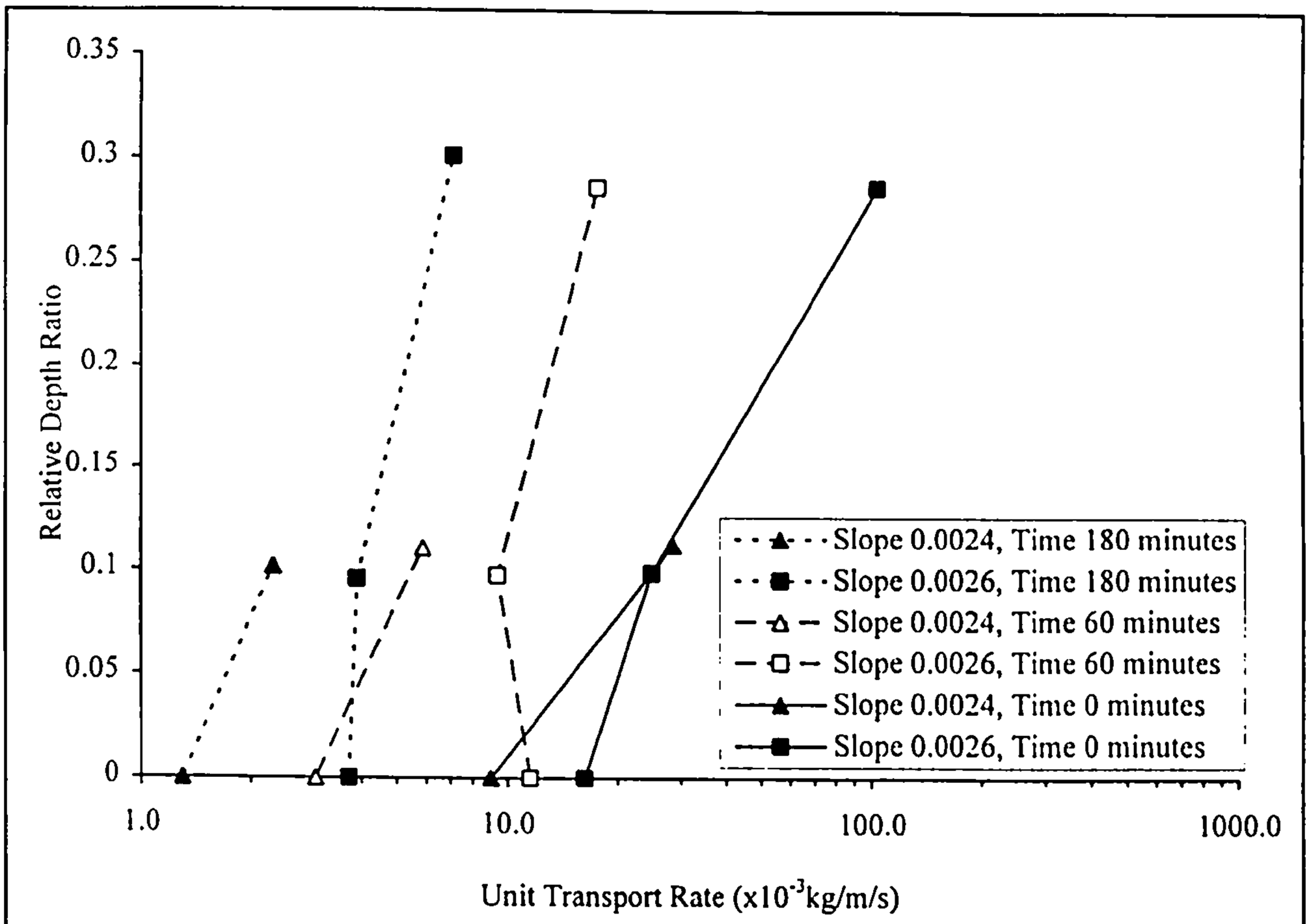

Figure 5.19a Unit Transport Rates at Different Times for Each Relative Depth Ratio, Times 0, 60 and 180 Minutes

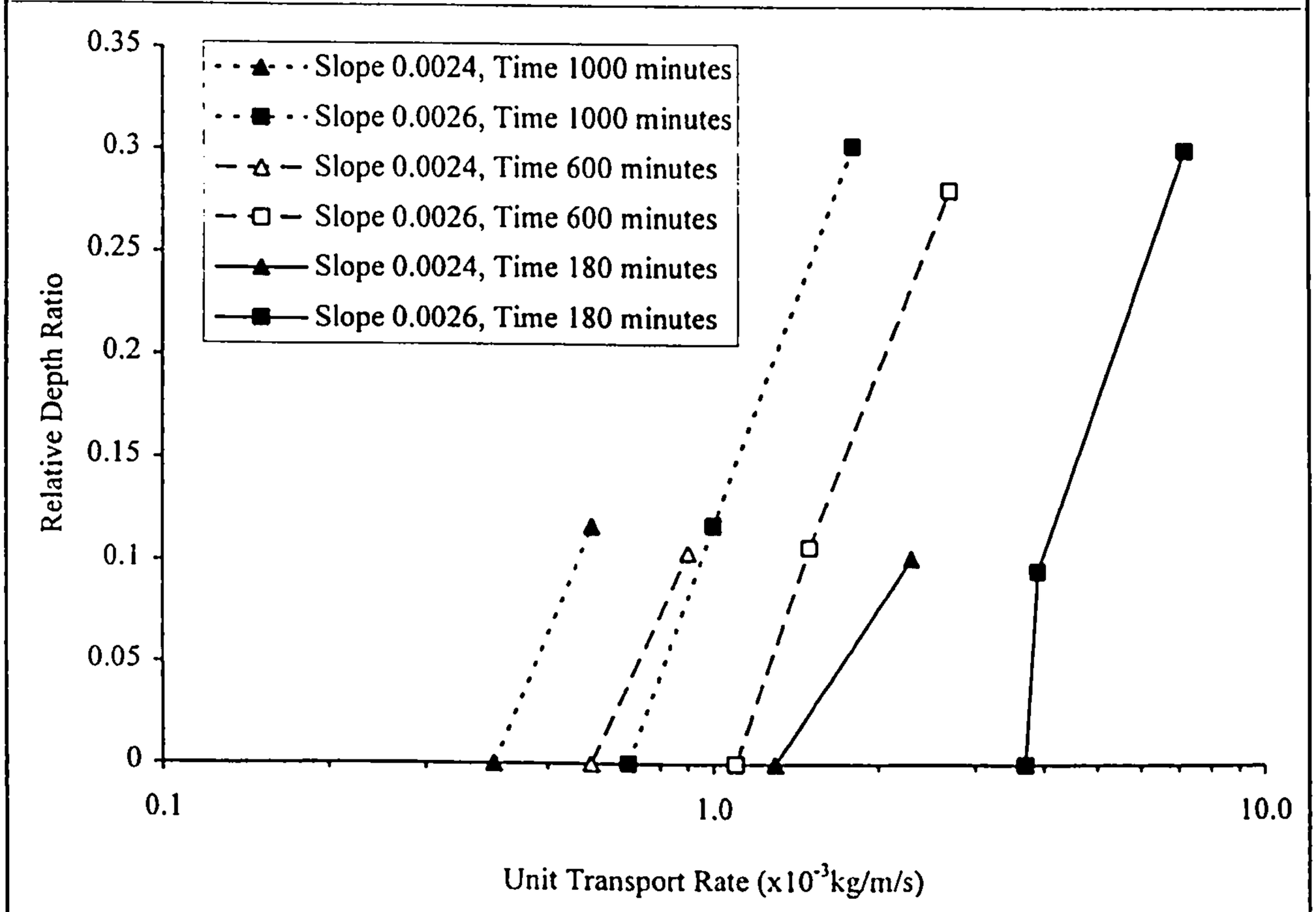

Figure 5.19b Unit Transport Rates at Different Times at Each Relative Depth Ratio, Times 180, 600 and 1000 Minutes

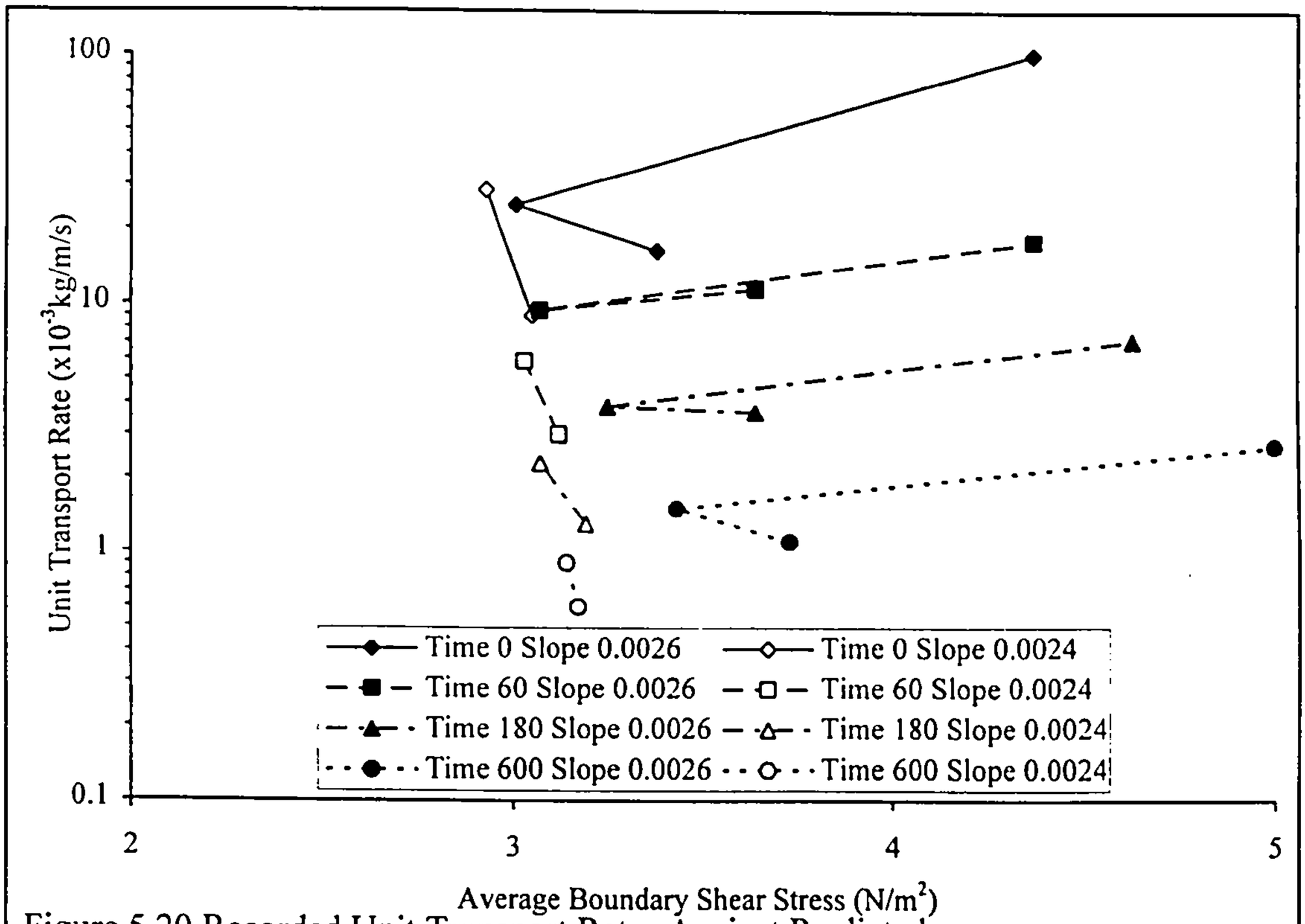

Figure 5.20 Recorded Unit Transport Rates Against Predicted Average Main Channel Boundary Shear Stress (Above Gravel Bed Only)

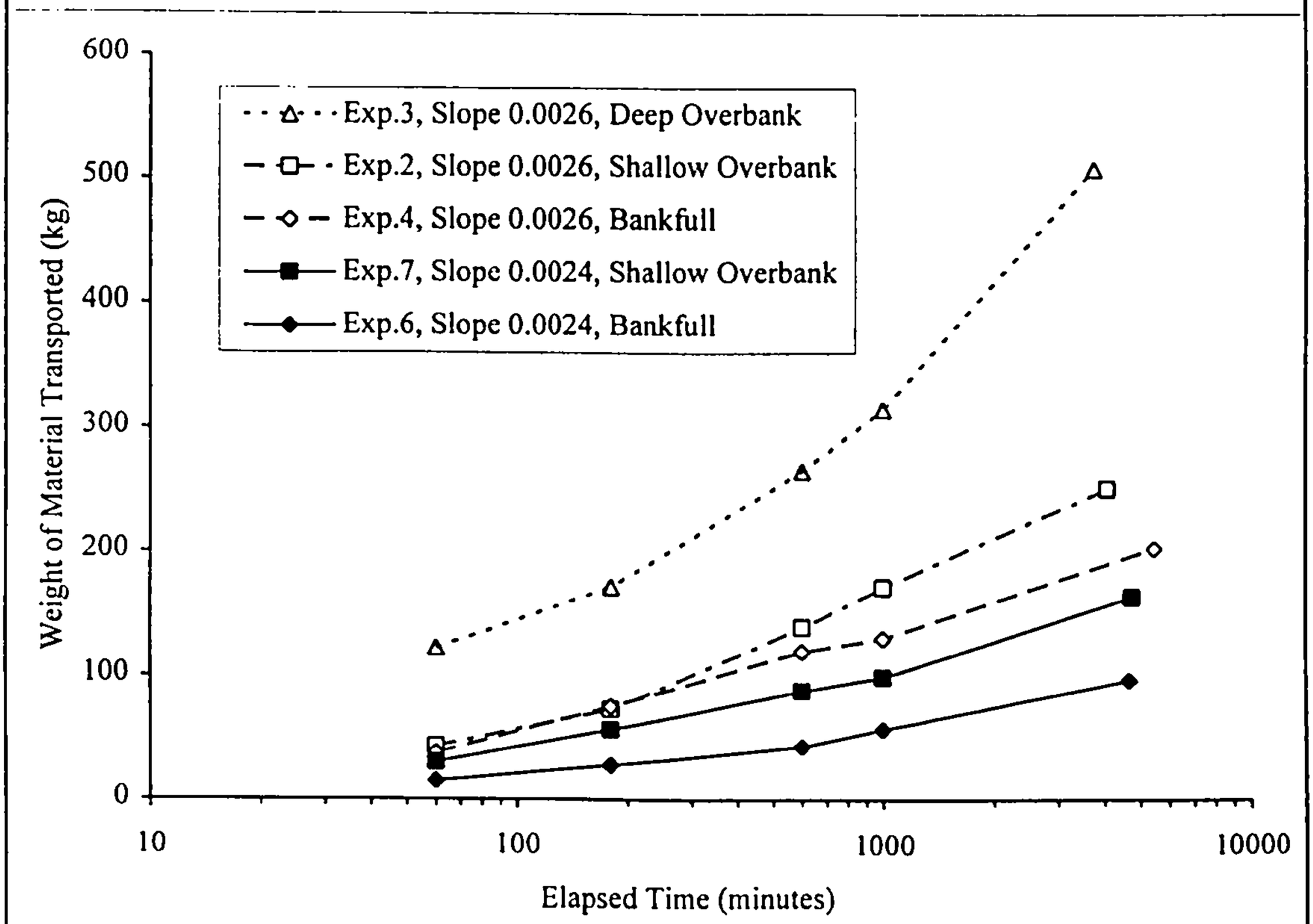

Figure 5.21 Weight of Material Transported Against Elapsed Time

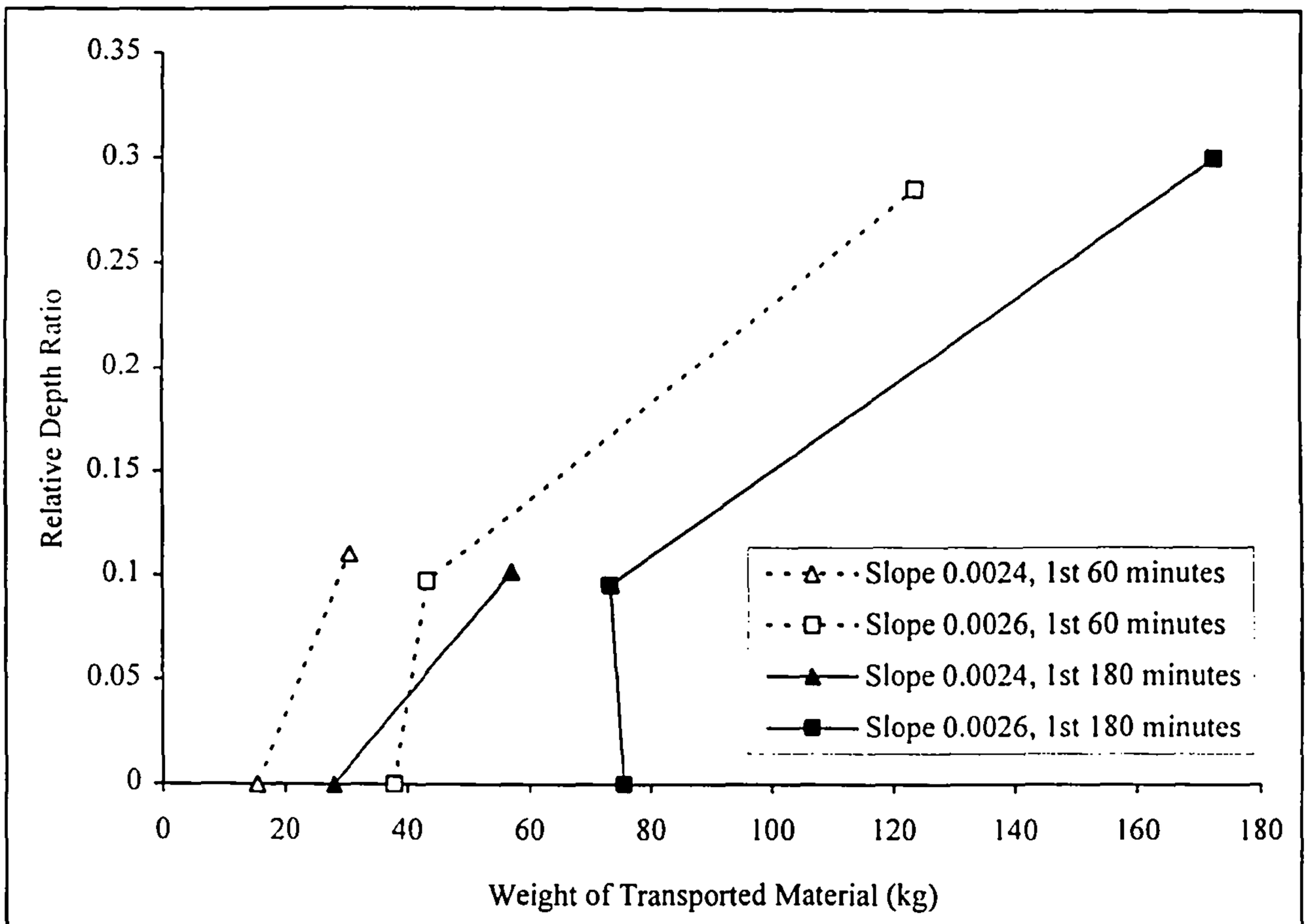

Figure 5.22a Relative Depth Ratio Against the Weight of Material Transported During the First 60 and 180 Minutes

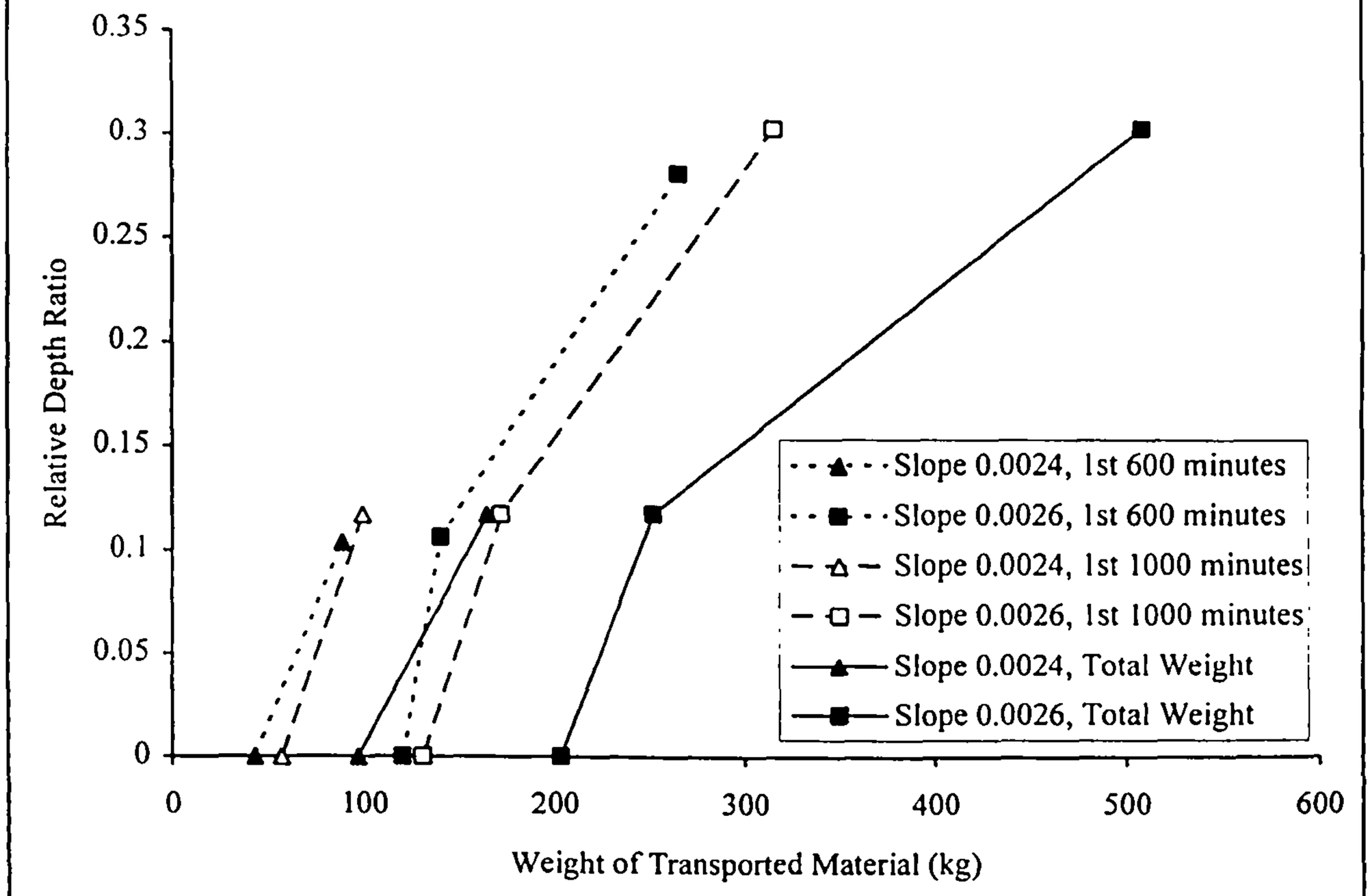

Figure 5.22b Relative Depth Ratio Against the Weight of Material Transported during the First 600 and 1000 Minutes, Plus the Total Weight Transported

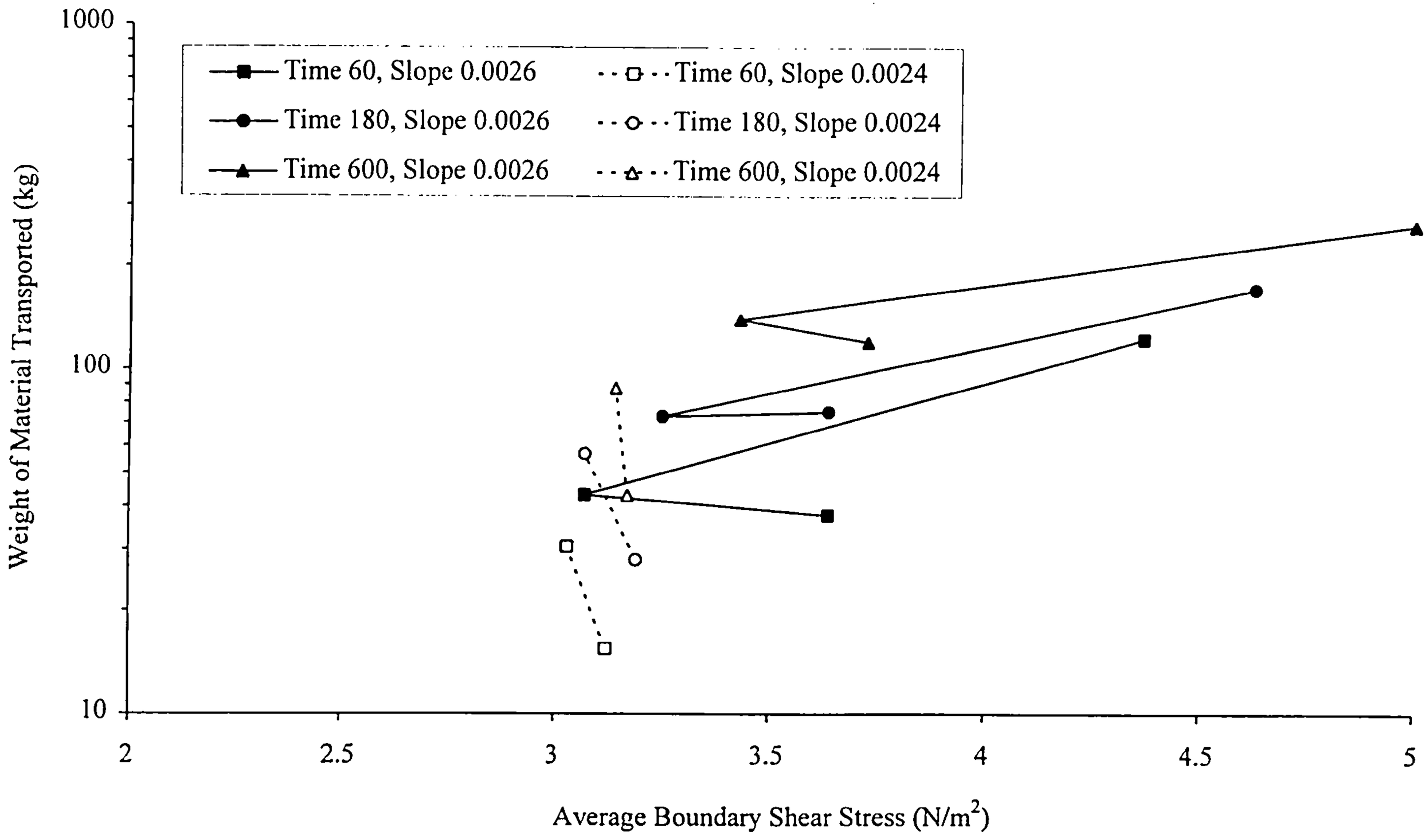

Figure 5.23 Weight of Material Transported Against Predicted Average Main Channel Boundary Shear Stress (Above Gravel Bed Only)

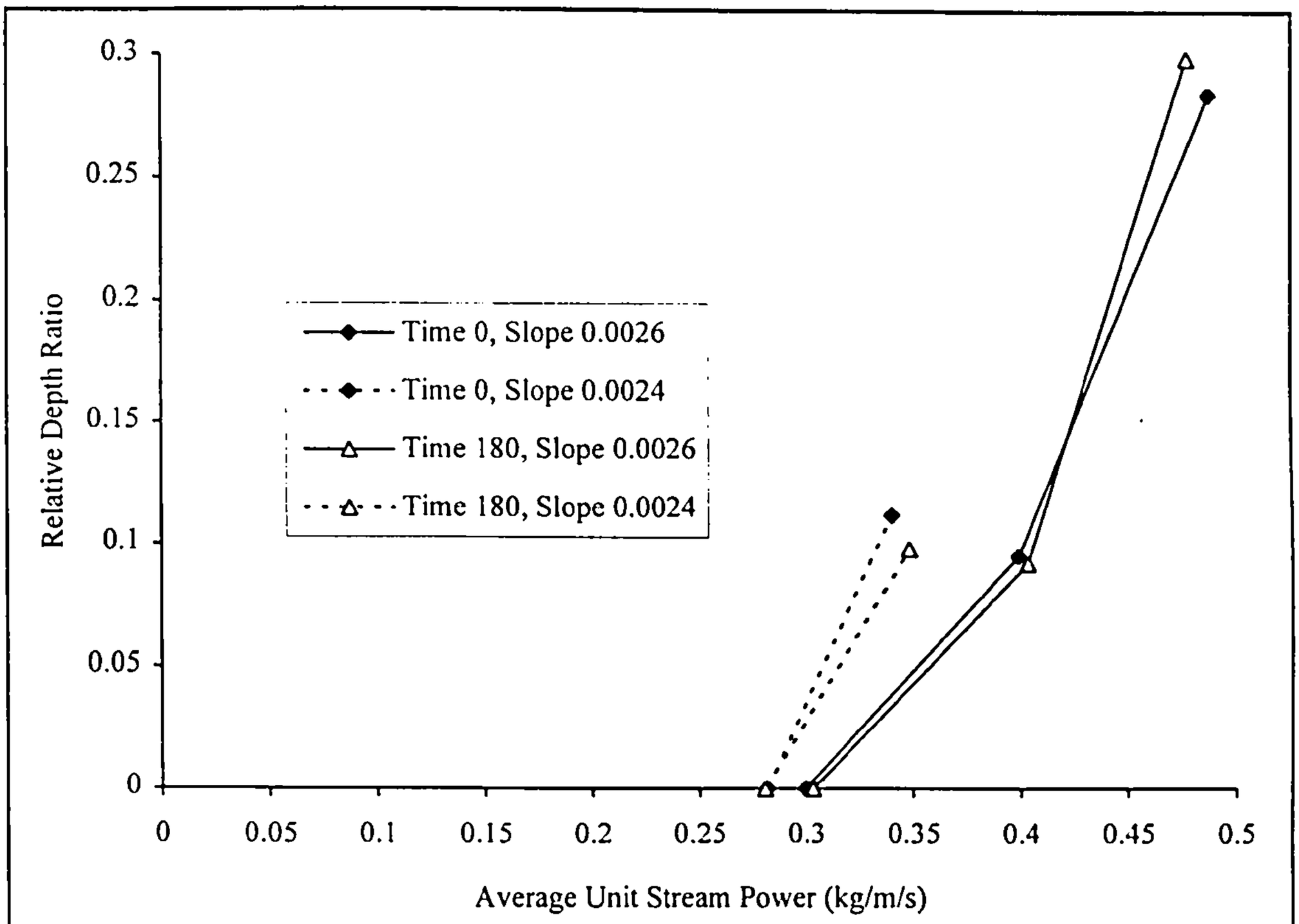

Figure 5.24a Relative Depth Ratio Against Predicted Average Unit Stream Power, Times 0 and 180 Minutes

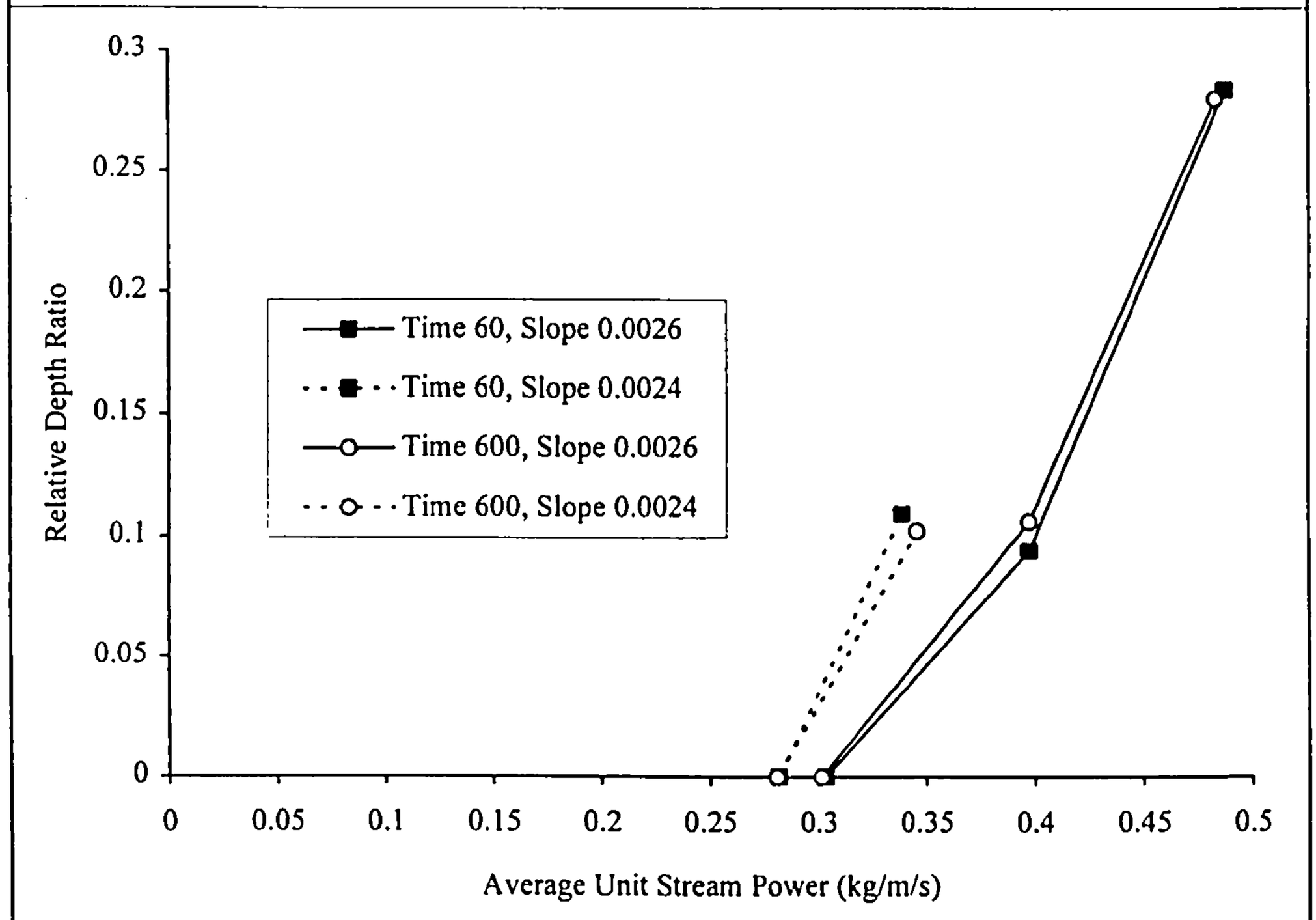

Figure 5.24b Relative Depth Ratio Against Predicted Average Unit Stream Power, Times 60 and 600 Minutes

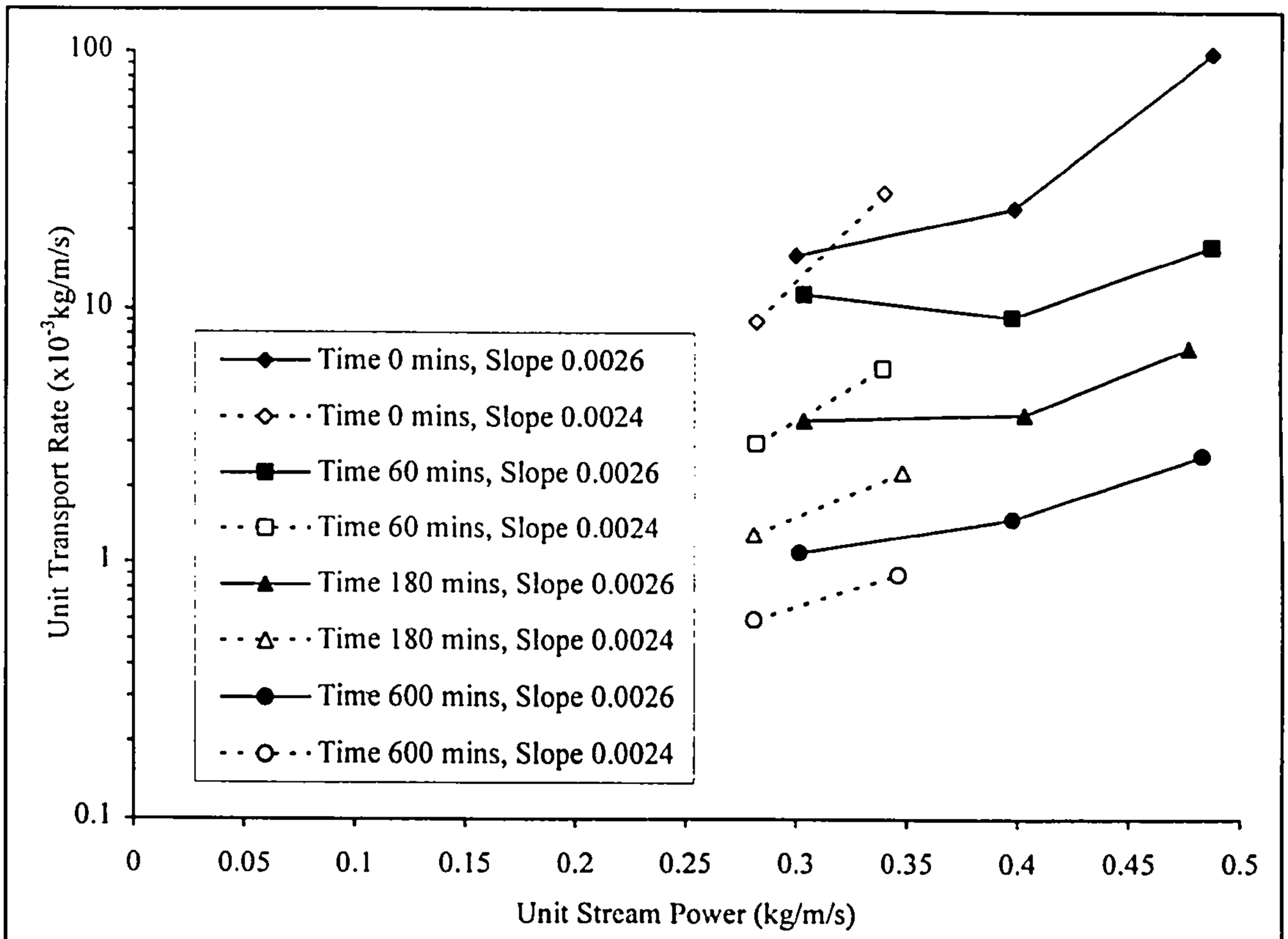

Figure 5.25 Unit Transport Rate Against Predicted Average Unit Stream Power

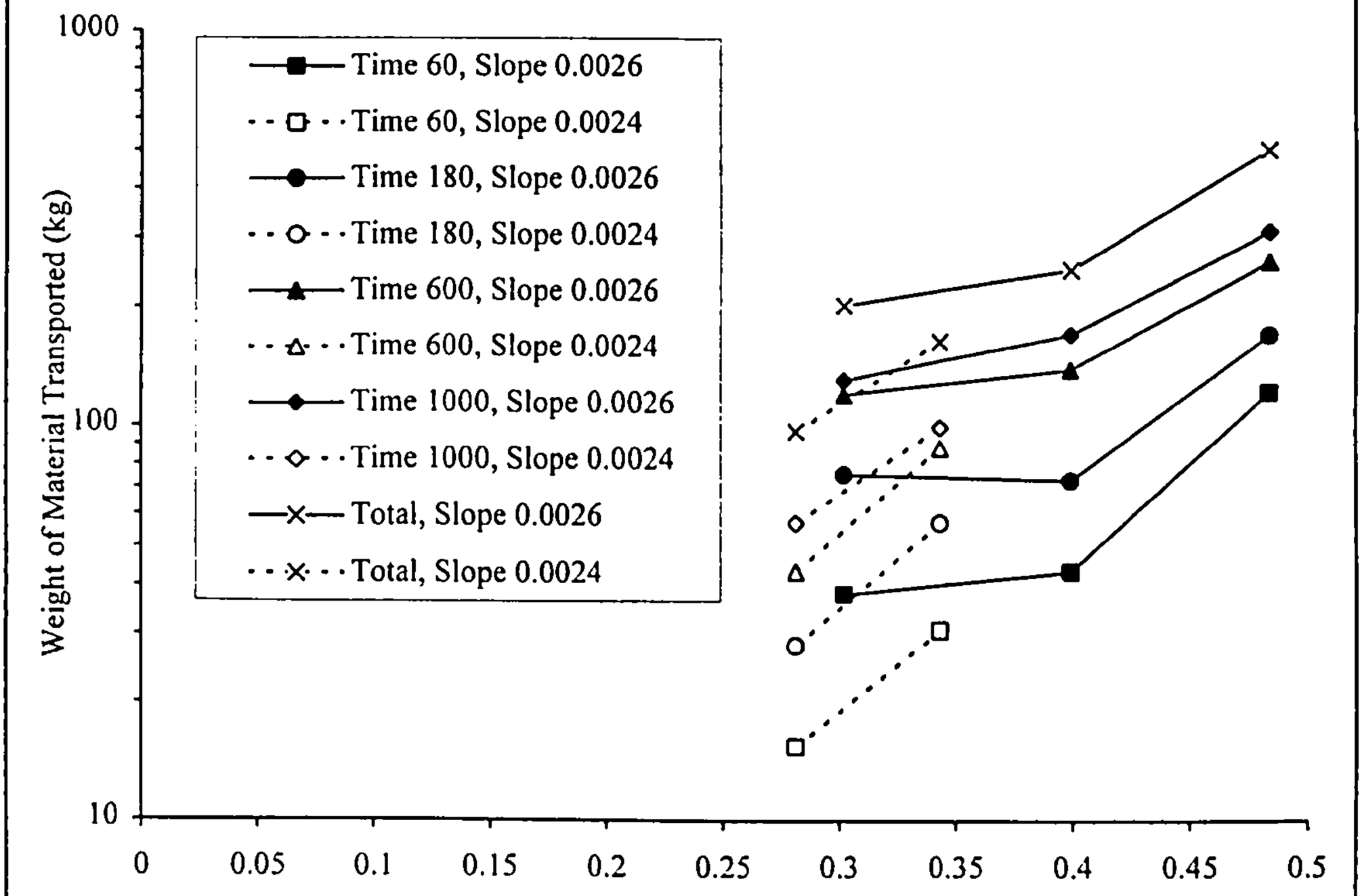

Figure 5.26 Weight of Material Transported Against Unit Stream Power Averaged Through Time

Chapter 6

Effects of Slope and Relative Depth on the Evolution of Bed Surface and Bedload Transport Compositions

6.1 Introduction

The large amount of interest in graded sediment behaviour can be quantified by the number of publications produced on the topic. Recent work has covered laboratory and field investigations and has included computer simulations (see for example Wilcock and Southard 1989; Parker 1990; Wilcock and McArdell 1993; Hoey and Ferguson 1994; Wathen et al 1995). Two aspects that have not been extensively covered are the effects of initial bed slope and overbank flow on degradational graded sediment transport.

Degradation is an important process in natural rivers. The resulting bed surface is significant in determining bed roughness at low flows, and in controlling sediment transport during the early phases of significant flow events. The study of degradational behaviour is also important as the resulting static armour layer closely resembles the mobile armour layers formed in equilibrium conditions (Parker and Sutherland 1990). Knowledge of the processes at work in degradational behaviour can therefore give insight into other coarse surface layer development (Hoey et al 1997).

The degradational experiments undertaken during this study were designed to produce marginal transport conditions. That is, the applied bed shear stress is only above threshold for part of the range of material sizes contained in the initial bed (see section 3.2.2). In a degradation experiment, where there was no upstream sediment supply, one would expect the bed to respond by establishing a static armour. Such

results have been gained by Proffitt (1980), Davies (1974), Little and Mayer (1976) and Gessler (1965), and have been cited by Parker and Sutherland (1990). Other work by Tait et al (1992) and Proffitt and Sutherland (1983) studied the general transport rate decline, while grain dynamics of surface coarsening was studied by Sutherland (1987). From this work it is clear that there is a relationship between bedload and bed compositions but further work is required to define that relationship (Tait et al 1992). Gomez (1994) and Wilcock and Southard (1989) have however, illustrated potential scope for using bedload size distributions and transport rates to further the understanding of the processes involved in bed surface armouring.

The development of an armoured layer has been found to be a phenomenon associated with unsteady mobile bed transport (Parker et al 1982b; Tait and Willetts 1992). Armour layers have been found to be coarser than the under-lying substrate and to coarsen as transport rate declines (Parker and Sutherland 1990). The layer protects the substrate, such that, immediate substrate material is only occasionally disturbed, while deeper particles are hardly ever moved (Parker et al 1982b). An armour layer itself acts to decrease the inherent difference in mobility between size fractions by over representing the percentage of larger grains exposed to the flow. In this way armouring has a pronounced influence on bed mobility (Willetts et al 1987). The final state of an armoured bed is still a matter of current research. To date though there is evidence to suggest that coarsening of the bed surface occurs through the mechanism of active transport (Parker et al 1982b; Parker 1990). It has also been suggested that the arrangement of the bed structure plays an important role in armour layer stability (Tait and Willetts 1991; Tait et al 1992; Tait et al 1997).

The work presented in this chapter attempts to add to the understanding of the processes involved in degradational graded sediment transport by:

1. Establishing a ranking order of transport potential between the different experiments presented.

2. By examining the effect of the initial bed slope on the bed surface and bedload composition development.

3. By examining the effect of the relative depth ratio on the bed surface and bedload composition development.

6.2 Experimental Range

This chapter analyses data obtained from Experiments 2, 3, 4, 5, 6 and 7. The main experimental parameters are detailed in table 6.1 below.

Table 6.1 Experiments used in bed surface and bedload transport composition analysis

Experiment No.	Initial Bed Slope	Nominal Flood Plain Depth (mm)	Initial Relative Depth (Theoretical)	Stage Level Description	Experiment Duration (mins.)
5	0.0029	0	0	Bankfull or Inbank	5134
4	0.0026	0	0	Bankfull or Inbank	5555
2	0.0026	20	0.118	Shallow Overbank	4162
3	0.0026	65	0.302	Deep Overbank	3788
6	0.0024	0	0	Bankfull or Inbank	4800
7	0.0024	20	0.118	Shallow Overbank	4810

The principal features of Experiments 2, 3, 4, 6 and 7 were discussed in Chapter 5. Experiment 5, however, was not and the following sections will briefly introduce its main characteristics.

An earlier analysis by the author examined only the three bankfull experiments. The work focused on the evolutions of the total transport rates, bed surface and bedload grain size distributions of the experiments. The results of the analysis have been published in a short conference paper co-written by the author (Hoey et al 1997).

6.2.1 Transport Rate Decline

Comparing figure 6.1 with figures 5.4a and 5.4b it can be seen that Experiment 5 shows the same pattern of decline. The initial transport rate for Experiment 5 is

relatively high reflecting the steeper initial bed slope. The relationship with the other experiments, during phase 1 and part of phase 2 (the period of decline and the first part of marginal transport), can be seen from figure 6.2.

6.2.2 Transport Rate Regression

As described in section 5.7 a least-squares fit was used to obtain a regression approximation to the recorded transport rate curve. The result was similar to those for the other experiments. The recorded data, including 48 transport rate observations, resulted in the regression line $y = 8.33x^{-1.01}$ with an adjusted R^2 value of 0.872 and a significance (F-test) of 2.2×10^{-22}. This compares well with the regressions obtained for the other five experiments, table 5.9. The regression equation predicts the transport rates in table 6.2, which are also compared with those from the other experiments.

Table 6.2 Transport rates predicted by the regression analysis

Time (minutes)	Unit Transport Rate (x10^{-3} kg/m/s)					
	Exp.6	Exp.7	Exp.4	Exp.2	Exp.3	Exp.5
0	9.0	28.5	16.3	24.9	104.2	68.5
60	3.0	5.9	11.5	9.4	17.8	13.3
180	1.3	2.3	3.7	3.9	7.2	4.4
600	0.6	0.9	1.1	1.5	2.7	1.3
1000	0.4	0.6	0.7	1.0	1.8	0.8

6.2.3 Weight of Material Transported

The same technique as described in section 5.9 was used to calculate the weights of material transported throughout the experiment. From table 6.3 it can be seen that Experiment 5 consistently transports more sediment than the other shallower initial gradient experiments with bankfull stage levels (Experiments 4 and 6).

Tables 6.2 and 6.3 also show that the magnitude of sediment transport increases with both slope, for a given stage level, and with stage level, for a given slope.

Table 6.3 Weights of material transported during the experiments, integration from time 0.

Time (minutes)	Weight of Material Transported (kg)					
	Exp.6	Exp.7	Exp.4	Exp.2	Exp.3	Exp.5
60	15.5	30.7	37.9	43.3	123.6	87.5
180	27.1	57.1	75.5	73.3	172.6	168.9
600	43.2	88.4	120.6	140.0	265.3	259.7
1000	57.1	99.5	131.1	171.9	315.2	280.7
Final Data Point. Time in Brackets	97.3 (4672)	164.5 (4753.5)	203.4 (5475)	251.5 (4074)	508.1 (3734.5)	343.3 (5082)

6.2.4 Boundary Shear Stress Predictions

Implementation of the Wark 2-D LDM, described in sections 5.6.3 and 5.6.4. produced predictions of bed shear stress for the times listed in table 6.4.

Table 6.4 Boundary shear stress predictions for the experiments, Warks LDM.

Experiment Number	Time (minutes)	Measured Discharge Q_m (m^3/s)	NEV Value	Manning's n Gravel Bed n_b	Average Main Channel Boundary Shear Stress τ_0 (N/m^2)	Gravel Bed Only Average Shear Stress τ_0 (N/m^2)
6	0	0.10712	0.12	0.01635	2.82	3.05
6	60	0.10712	0.12	0.01696	2.87	3.12
6	180	0.10712	0.12	0.0176	2.93	3.19
6	600	0.10712	0.12	0.01739	2.93	3.17
7	0	0.13802	0.22	0.01565	2.75	2.93
7	60	0.13802	0.22	0.01635	2.83	3.03
7	180	0.13802	0.22	0.01607	2.78	3.07
7	600	0.13802	0.22	0.0167	2.82	3.14
4	0	0.10553	0.12	0.01771	3.09	3.38
4	60	0.10553	0.12	0.01922	3.16	3.64
4	180	0.10553	0.12	0.01922	3.16	3.64
4	600	0.10553	0.12	0.02001	3.21	3.73
2	0	0.14676	0.22	0.01446	2.90	3.01
2	60	0.14676	0.22	0.0148	2.95	3.07
2	180	0.14676	0.22	0.01546	2.99	3.25
2	600	0.14676	0.22	0.01665	3.08	3.45
3	0	0.20809	0.16	0.01901	3.78	4.37
3	60	0.20809	0.16	0.01901	3.78	4.37
3	180	0.20809	0.16	0.02064	3.94	4.63
3	600	0.20809	0.16	0.02249	4.05	5.02
5	0	0.11682	0.12	0.01713	3.48	3.78
5	60	0.11682	0.12	0.01796	3.49	3.98
5	180	0.11682	0.12	0.01897	3.61	4.13
5	600	0.11682	0.12	0.01873	3.59	4.10

6.2.5 Unit Stream Power

Using the LDM, predictions of the average unit stream power above the mobile channel bed were made at times throughout the experiments (table 6.5). The same techniques were used as described in section 5.10 previously.

Table 6.5 Average unit stream power per unit width above gravel bed.

Experiment Number	Time (minutes)	Average Unit Stream Power per Unit Width ($x10^{-3}$ kg/m/s)
6	0	282.0
6	60	281.9
6	180	280.9
6	600	281.0
7	0	339.7
7	60	339.1
7	180	348.0
7	600	346.1
4	0	299.8
4	60	303.4
4	180	303.4
4	600	301.5
2	0	398.7
2	60	397.6
2	180	403.2
2	600	397.6
3	0	487.6
3	60	487.6
3	180	477.2
3	600	483.2
5	0	371.4
5	60	375.1
5	180	375.7
5	600	375.9

6.2.6 Transporting Potential Ranking Order of Experiments.

Implicit in the analysis within this chapter is the influence of predicted boundary shear stress and unit stream power on bed surface composition, bedload rate and bedload composition. It is therefore desirable to rank the experiments relative to their individual potentials to transport material.

Figure 6.3a shows an idealised plot of stage level against predicted bed shear stress, at time 0 minutes. Each line represents a different initial bed slope. It can be seen from this that the experimental ranking with regard to the applied shear stress (high to low) is 3, 5, 4, 6, 2 and then 7. The difference between 6 and 2 is very slight however, and these experiments swap ranked positions between 60 and 180 minutes (table 6.6).

Table 6.6 Ranked values of predicted boundary shear stress.

Time (minutes)	Experiment Order - Descending Shear Stress Left to Right Boundary Shear Stress τ_0 (N/m^2)					
0	4.37 (Exp.3)	3.78 (Exp.5)	3.38 (Exp.4)	3.05 (Exp.6)	3.01 (Exp.2)	2.93 (Exp.7)
60	4.37 (Exp.3)	3.98 (Exp.5)	3.64 (Exp.4)	3.12 (Exp.6)	3.07 (Exp.2)	3.03 (Exp.7)
180	4.63 (Exp.3)	4.13 (Exp.5)	3.64 (Exp.4)	3.25 (Exp.2)	3.19 (Exp.6)	3.07 (Exp.7)
600	5.02 (Exp.3)	4.10 (Exp.5)	3.73 (Exp.4)	3.45 (Exp.2)	3.17 (Exp.6)	3.14 (Exp.7)

Figure 6.3b shows an idealised plot of stage level against unit stream power, at time 0 minutes. Again each line represents a different initial bed slope. Unit stream power has been calculated as described in section 5.10 and therefore the values increase monotonically with stage. The relative ranking of the experiments with regard to unit stream power is therefore 3, 2, 5, 7, 4 and then 6, again high to low (table 6.7). The ranking order remains the same throughout the duration of the experiments.

Table 6.7 Ranked values of predicted unit stream power.

	Experiment Order - Descending Unit Stream Power Left to Right Unit Stream Power ω (x10^{-3}kg/m/s)					
Time (minutes)	3	2	5	7	4	6
0	487.6	398.7	371.4	339.7	299.8	282.0
60	487.6	397.6	375.1	339.1	303.4	281.9
180	477.2	403.2	375.7	348.0	303.4	280.9
600	483.2	397.6	375.9	346.1	301.5	281.0

6.3 Time Normalisation

All six degradational experiments, now introduced, have been shown to exhibit the same general patterns of transport rate decline, see sections 5.3, 5.4 and 6.2. Where as Chapter 5 dealt with the general trend in transport behaviour between different relative depths, this chapter examines the specific development of bed and bedload compositions. In this chapter it is therefore important to compare points in different experiments that are at equal stages of evolution. To this end a method of time normalisation was implemented.

In order to do this, a point in the transport rate development, common to all experiments, had to be identified. The time each experiment took to evolve to that developed state was then compared. An obvious point to choose was the evolution from phase 1 to phase 2, see sections 5.3 and 5.4. The transition is identified as the point at which the transport rate first fell to below 5% of the initial transport rate measurement. Each transport rate data point was therefore plotted as a percentage of the first data point. The decline with time was then compared to a horizontal line representing 5% of the initial transport rate for each experiment. Figure 5.6 shows this data for Experiment 4. The other five experiments produced similar results. Due to the complexity of the experiments the initial transport rate readings were at slightly different times into each experiment. Although this has an effect on the vertical position of the resulting curves, the effect at the later stages of the experiments, when the transport was low, is negligible. The approximated times at which the transport rates first fell to below 5% of the initial transport are presented in table 6.8 below.

Normalisation was applied by scaling the time axis of each experiment so that, the time of the first sample below 5% of the initial transport rate is normalised time 1. The period between the start of an experiment and normalised time 1 is phase 1, and the period beyond normalised time 1 is phase 2. The phase 1 transport rates are shown in figure 6.4.

Table 6.8 Elapsed times and trap cycle numbers of first samples less than 5% of initial transport.

Experiment	Elapsed Time of Initial Bedload Trap Sample (minutes)	Initial Recorded Transport Rate (x10-3 kg/m/s)	Elapsed Time of First Trap Sample Less 5% (minutes)	Normalised Time 1 Transport Rate (x10-3 kg/m/s)	Bedload Trap Cycle Number
5	3.5	61.65	330	2.21	10
3	18	61.37	446	1.61	8
6	9	7.84	569	0.35	12
7	14	16.38	790.5	0.25	14
4	31.5	13.00	869	0.25	11
2	19.75	17.82	922	0.23	15

Table 6.9 below summarises the individual experiment durations and the number of trap cycles collected during each one. The durations of the six experiments, in normalised time are also compared.

Table 6.9 Normalised experiment durations

Experiment	Experiment Normalised Time Duration	Experiment Elapsed Time Duration (minutes)	Number of Collected Cycles
5	15.56	5134	48
3	8.49	3788	26
6	8.44	4800	39
7	6.08	4810	36
4	6.39	5555	30
2	4.51	4162	28

6.4 Review of Experiment Transporting Potential Ranking Order

The normalised time scales allow for a re-evaluation of the transporting potential of the experiments. Capacity can be evaluated in terms of the recorded transport rates, regression function transport rates and the total weight of material transported during the phase 1.

In figure 6.4 it can be seen that Experiments 5 and 3 produce the largest observed transport rates, but cross each other several times during phase 1. The transport rates from the other four experiments all fall closer together, with Experiments 2 and 4 producing slightly higher transport rates than 7 and 6.

Regression functions were fitted to the recorded transport data and normalised times. This was done to identify the general transport rate declines without the superimposed fluctuations discussed in sections 5.3 and 5.4. The same technique was used as is described in section 5.7. It should be noted that the transport data from the full experiment durations were used in the regression analysis, rather than just data from phase 1. The resulting regression functions, and estimates of transport rates throughout the phase 1 decline, are presented in table 6.10 below.

Table 6.10 Transport rates predicted by regressions using normalised time

Exp. No.	5	4	2	3	6	7
R^2 Value	0.875	0.818	0.705	0.814	0.793	0.849
Regr. Equation	$y=2.37x^{-1.01}$	$y=0.75x^{-1.02}$	$y=1.09x^{-0.79}$	$y=3.42x^{-0.82}$	$y=0.58x^{-0.73}$	$y=0.69x^{-0.83}$
Normal. Time	Unit Transport Rate ($x10^{-3}$ kg/m/s)					
0.25	9.61	3.09	3.25	10.69	1.59	2.17
0.5	4.77	1.52	1.88	6.05	0.96	1.22
1.0	2.36	0.75	1.09	3.42	0.58	0.69

Again the results illustrate that Experiments 3 and 5 produce transport rates higher than Experiments 2 and 4, which in turn produce transport rates higher than 7 and 6.

The third way of determining the transporting potential of the five experiments is by comparing the weight of material transported during phase 1. Again, the techniques are the same as described in sections 5.9, but this time using the normalised time scales, rather than experimental elapsed time. The results are contained in table 6.11.

Table 6.11 Weights of material transported during phase 1, from integration of transport rate decline curve.

Experiment Number	Weight of Transported Material (kg)
5	235.5
4	129.5
2	170.4
3	240.1
6	42.5
7	95.0

The same pattern of transport potential is shown. The steepest initial slope experiment and the deepest relative depth experiment. Experiments 5 and 3, transport the most sediment. While the middle initial slope experiments. Experiments 4 and 2, transport more material than the shallowest initial slope experiments, Experiments 6 and 7.

In table 6.12 the orders for unit stream power, regression transport rate and weight of material transported were decided purely on numerical magnitude. The order from the recorded transport rate curves was decided from visual inspection of the phase 1 duration (figure 6.4).

Table 6.12 Experiment ranking order of transporting potential

Data Type	Unit Stream Power	Recorded Transport Rate Decline Curves	Estimated Transport Rates From Regressions	Weights of Material Transported
Experiment Ranking Order. Decreasing Top to Bottom	3	5	3	3
	2	3	5	5
	5	2	2	2
	7	4	4	4
	4	7	7	7
	6	6	6	6

Although the different sets of data show slight differences in the overall order of the experiments there are clear trends. Firstly, transport potential increases with initial bed slope. For the bankfull case, Experiment 5 (0.0029) has the highest predicted transporting potential, followed by Experiment 4 (0.0026) and then Experiment 6 (0.0024). For the shallow overbank case, Experiment 2 (0.0026) has the higher transport potential and Experiment 7 (0.0024) the lower. The potential to transport sediment also appears to increase with increasing relative depth. At the shallowest initial slope, Experiment 7 (20mm overbank) shows greater transporting potential than Experiment 6 (bankfull). At the middle initial slope, Experiment 3 (65mm overbank) shows the greatest potential, followed by Experiment 2 (20mm overbank) and then Experiment 4 (bankfull).

The demonstrated agreement of order, within various groupings of the six experiments, is useful for examining the effect of varying transporting potential on the evolution of bed and bedload compositions.

The order of transporting potential predicted by the transport rates from regression analysis and from the weight of material transported during phase 1 is the same. The order predicted from visual inspection of the recorded transport rates during phase 1 (figure 6.4) is very similar. Indeed, other than Experiments 5 and 3 swapping positions the ranking order is the same. The slight difference in order between the methods could be explained by an over estimation of transport rates for Experiment 3 from the regression, or an over estimation of the weight of transported material. It is not clear which order the two experiments should be in. However, it is suggested that, for these two experiments, the less complex flow of the steeper bankfull experiment has greater transporting potential than the more complex flow structures of the shallower slope, deep overbank experiment. Further to this, it is speculated that the more complex flow structures of overbank flow have a retarding effect on the potential of the flow to transport. However, it is speculated that this retardation is not as great as retardation of sediment transport potential suggested by the effect of overbank flow on the predicted boundary shear stress. If this speculation is correct it would also explain the different overall order predicted from unit stream power. The use of unit stream power would therefore be over predicting the transport potential of the overbank flows. It is possible then, that the retarded potentials of the overbank experiments would mean the true overall order of transporting potential is 5, 3, 2, 4, 7, 6. This is the order suggested by the recorded transport rate data plotted against normalised time (figure 6.4).

6.5 Initial Bed Composition

One of the objectives of the work was to investigate the development of bed composition under different hydraulic conditions. It was therefore intended that the initial bed for each experiment should be similar. Similarity was tested through sampling and statistical analysis of the as laid beds. The statistical technique

employed was designed for problems involving groups of observations and is called One-Way Analysis of Variance. This technique is described in Swan and Sandilands (1995) and Davies (1973).

Each initial bed is assumed to be a sample in its own right. Each sample collected from that bed is then assumed to be a replicate of the bed sample. Analysis of variance then separates the total variance, amongst all the replicates of all the samples, into variance among samples and variance within each set of replicates. If the variation between replicates, due to variations in the as laid bed, is greater than the variation between samples, then the samples can be said to be statistically similar.

In order to identify if this is the case two hypotheses are formulated.

H_0 : the means of all the samples are the same

H_1 : at least one of the sample means is significantly different

The application of one-way analysis of variance assumes that: each set of replicates represents random samples from the different parent populations; that each parent populations variation is normally distributed; and that each parent population has the same variance.

A procedure for the analysis has been developed and formalised, and is contained within the ANOVA (ANalysis Of VAriance) table. The standard table lists: the sources of variation, a column of corrected sums of squares resulting from the various sources, the degrees of freedom associated with each source of variation, a column of mean squares (effectively a sample-based estimate of variance) and the F value. Significance is assessed using an F-test where F is the ratio of the mean squares of variation amongst samples to the mean squares of variation within each set of replicates.

The chosen hypothesis is then accepted or rejected, depending upon the relationship between the calculated F value and F-critical. F-critical is gained from published

statistical tables given a chosen level of significance. say 5%. and the degrees of freedom of the sources of variance used to calculate the F value. If the F value is significantly less than the F-critical value, the variation between samples is insignificant compared to the variations between replicates of the same sample.

Analysis of variance may be easier to understand if the extreme case. where all replicates are identical, is considered. This would result in the mean values of the replicates being the same as the individual replicates themselves. The variance calculated by considering all the observations would then be the same as that calculated by considering only the mean values. There would therefore be no unaccounted for variance due to differences within sets of replicates. Therefore the result would indicate, with 100% certainty. that the original samples were indeed identical. as each set of replicates had been drawn from separate parent populations having zero variances.

The ANOVA tables for the individual bed composition parameters of d_{16}, d_{50}, d_{84} and σ_g are presented below.

Table 6.13 ANOVA table for initial bed compositional parameter d_{16}

Source of Variance	Sum of Squares SS	Degrees of Freedom df	Mean Squares MS	F	F-critical	P-value
Between Beds	1.27	8	0.16	0.37	2.32	0.93
Within Bed	11.07	26	0.43			
Total	12.34	34				

Table 6.14 ANOVA table for initial bed compositional parameter d_{50}

Source of Variance	Sum of Squares SS	Degrees of Freedom df	Mean Squares MS	F	F-critical	P-value
Between Beds	0.69	8	0.09	0.70	2.32	0.69
Within Bed	3.21	25	0.12			
Total	3.90	34				

Table 6.15 ANOVA table for initial bed compositional parameter d_{84}

Source of Variance	Sum of Squares SS	Degrees of Freedom df	Mean Squares MS	F	F-critical	P-value
Between Beds	8.32	8	1.04	1.04	2.32	0.43
Within Bed	26.05	26	1.00			
Total	34.37	34				

Table 6.16 ANOVA table for initial bed compositional parameter σ_g

Source of Variance	Sum of Squares SS	Degrees of Freedom df	Mean Squares MS	F	F-critical	P-value
Between Beds	1.25	8	0.16	0.36	2.32	0.93
Within Bed	11.38	26	0.44			
Total	12.63	34				

For each set of results a level of significance of 5% was used in the selection of the F-critical values. In all cases F is well below F-critical and the P-values are high, i.e. much greater than 0.05. Therefore the differences between beds are no greater than the differences between replicates for the same beds. The initial beds can therefore be taken as being statistically similar.

In the light of this result it was decided to average all the samples of the initial beds to form a result which would then be taken as the initial bed composition for all the further analysis. The two sets of initial bed samples, those from volumetric and those from wax sampling, were treated differently in this respect. The volumetric samples were averaged using a weighted average technique, while the average of the wax samples was based purely on the number of samples. The resulting initial bed compositions are compared to the designed composition in figure 6.5. It can be seen that there is a good correlation between all three compositions. However, there is a lack of 2 mm and 8 mm material in the as laid beds compared with that in the designed mix. This is due to slight differences between the samples used to design the mix and the material that was actually used in the experiments.

During the following work the average initial bed obtained from the volumetric samples is used when comparing to other volumetric samples, such as bedload. The composition from the wax samples is used when comparing to other compositions gained by wax sampling, such as the final bed composition. This was done to try to eliminate any discrepancies in the results caused by the sampling techniques.

6.6 Effect of Initial Slope on the Evolution of the Bed Surface and Bedload Compositions.

In this section the effect of different initial bed slopes on bed surface and bedload composition will be examined. Firstly, for bankfull flows: Experiment 6 (slope 0.0024), Experiment 4 (slope 0.0026) and Experiment 5 (slope 0.0029). Then secondly, for a depth corresponding to the shallow overbank case: Experiment 7 (slope 0.0024) and Experiment 2 (slope 0.0026).

6.6.1 Initial and Final Beds

As bed degradation progressed a general coarsening of the bed was anticipated. It was expected that the wax samples of the final bed would contain a greater percentage of the coarse material. Initially the full range of the half-phi sieve data was examined for evidence of these changes. This proved difficult to analyse, and so the compositions were simplified into three ranges of size fractions; less than 2 mm, 2 mm to 5.66 mm and greater than 5.66 mm. The sub-division into three ranges was based on the observations of bedload samples. It was found that relative to the initial bed composition bedload samples were often lacking in material less than 2 mm and material greater than 5.66 mm. Implicit in the use of these ranges of size fractions is the assumption that material in each range will exhibit similar behaviour.

The changes between the initial and final beds in figure 6.6a shows a similar trend for all the bankfull experiments. The final bed has a smaller percentage of material in the less than 2 mm and the 2 mm to 5.66 mm sizes, and a larger percentage in the greater than 5.66 mm range than the initial bed. For all slopes the final bed is therefore coarser than the initial bed. A similar result was obtained for the shallow overbank experiments, figure 6.6b.

The shallowest slope experiment (0.0024), at both relative depths (Experiments 6 and 7), showed the least change in bed composition from the initial to the final bed.

For the next steepest slope (0.0026, Experiments 4 and 2) the percentage of fines (less than 2 mm) and coarse material (greater than 5.66 mm) in the final bed increased. While for the same experiments the percentage in the mid-range (2 mm to 5.66 mm) decreased between the initial and final bed. For the steepest slope in the bankfull case (0.0029, Experiment 5) a further increase in the percentage of the composition in the coarse fraction is observed. This is complemented by a reduction in the percentage of fine and no change in the percentage of mid-range when compared to the middle slope.

The subtlety of the bed compositional changes are surprising given the dramatic change in bedload transport rate. This suggests that bed rearrangement or restructuring does play a significant role in the development of a static armour, as suggested by authors such as Tait and Willetts (1991).

6.6.2 Initial and Final Fraction Mobility

Several papers have been published examining the mobility of size fractions within the bedload relative to the bed surface composition (Wilcock and Southard 1989; Wilcock 1992; Wilcock and McArdell 1993; Wilcock et al 1996; Wilcock and McArdell 1997; Wilcock 1997). Comparisons are made using graphs of the type shown in figure 6.7. In this figure size fraction diameter is plotted against $((p_i/f_i)*q_b)$ on log-log axes, where p_i is the percentage composition in the bedload, f_i is the percentage composition in the bed and q_b is the unit transport rate.

It was decided to investigate size fraction mobility in Experiments 6, 4, 5, 7 and 2 using this technique but with two modifications. A natural scale was used for the vertical axis as this makes it easier to compare changes in mobility. It was also decided not to multiply the ratio p_i/f_i by the unit sediment transport rate as only two or three mobility curves are to be compared in one figure using this technique. No information was available on bed surface composition during the experiments. Consequently, only initial and final size fraction mobility could be investigated in this way as only initial and final values of f_i were available.

The fraction mobility plots are presented in figures 6.8a to 6.8c for the bankfull experiments and figures 6.9a and 6.9b for the shallow overbank experiments.

In all the figures the horizontal broken line represents equal mobility. If a data point lies on this line then that fraction is present in the same proportions in both the bed and the bedload. If the data point lies above the line then the fraction is over represented in the bedload relative to its percentage in the bed. If it is below the line, the fraction is under represented relative to its percentage in the bed. The higher the value of a fraction's p_i/f_i ratio the more mobile it is. The vertical broken lines are placed at 2 mm and 5.66 mm and sub-divide the diagram into the ranges discussed in section 6.6.1 above.

Dealing first with the bankfull experiments (figures 6.8a to 6.8c), the following observations can be made:

(i) The mid-range fractions are generally the most mobile at both the start and end of all the experiments.

(ii) The shallowest slope experiment (Experiment 6) shows greater mobility of the coarse size fractions at the start than at the end. The mid-range shows little difference between the two periods and the fine fractions are more mobile at the end.

(iii) The steepest slope experiment (Experiment 5), shows almost the opposite trend. Initially the coarse material is less mobile than it is finally, with the fine material being greatly more mobile initially than finally.

(iv) Experiment 4, the middle slope experiment, shows a trend that falls between those observed for Experiments 5 and 6.

It is suggested that this is an indication that, in these bankfull flows, the composition of the bedload depends upon the initial bed slope. For the shallowest

slope. the initial transport contains a large proportion of mid-range material. common to all three bankfull experiments, but also some fine and coarse material. By the end of the experiment though, the bedload is weighted more towards the fine fractions. This may be due to the lower transporting power of the shallow slope experiment. Initially all the particles are mobile, to some extent, but when the bed is stable, at the end of the experiment, the flow only contains enough power to move the fines and mid-range material. For the steepest slope experiment, initially the bedload composition approaches that which would be associated with equal mobility, due to the higher transporting potential. By the end of the experiment most of the fine material has been removed to the trap, or moved to a stable position within the bed, and the potential to transport is applied to the mid-range and coarse material.

Turning to the shallow overbank experiments (figures 6.9a and 6.9b) the following observations can be made:

(i) The most mobile fractions are finer than for the bankfull experiments.

(ii) Both experiments demonstrate a similar trend to the flattest slope bankfull experiment. That is, most material is mobile to some degree initially and selective mobility of mainly fine material occurs at the end of the experiment.

(iii) Although both show the same general trend, the steeper of the two (Experiment 2) does show higher initial mobility of the larger fractions.

Again this trend is thought to be due to the transporting potential of the experiments and the same explanation as for Experiment 6 can be applied. The difference in behaviour between the two shallow overbank experiments is likely to be due to the slightly higher transporting potential of Experiment 2. However, the higher potential is not high enough to change the overall trend.

The use of the modified Wilcock fraction mobility analysis suggests that, there are differences in the evolution of the bed composition during these experiments.

However, as no direct measurements of bed composition were made during the experiments the technique cannot be applied to any intermediate points. Only the first and last bedload measurements can be related to the initial and final bed surface compositions. Other techniques are therefore required to further examine the evolution of the bedload composition throughout the experiments.

6.6.3 Cumulative Bedload Composition

If the sampling technique is consistent between experiments, the cumulative collected bedload can be used to examine differences between bedload compositions.

In order to determine if the sampling was consistent between experiments, mass curves for the percentage of cumulative collected bedload during phase 1 are presented in figure 6.10. The shape of the cumulative mass curve reflects the distribution of samples as a percentage of total mass collected during phase 1. If relatively less material was collected at the start of the phase, for one experiment from the set, the initial gradient of that curve would be significantly shallower. Then, towards the end, the gradient would be much steeper than the others as relatively more of the 100% of the collected sample weights were collected towards the end of phase 1.

Although there is some scatter between the full set of experiments the curves are generally similar. It was therefore assumed that the composition of the collected bedload would reflect the different evolutions of bedload composition, over phase 1 of the different experiments. The statistics of the sampling during phase 1 are presented in table 6.17 below.

Looking at figures 6.11a and 6.11b, the compositions of the phase 1 bedload for each experiment are compared to the initial bed composition. For all experiments the bedload has less fine and coarse material, but significantly more mid-range material, than the initial bed. This supports the observed changes in the initial and final bed compositions discussed in section 6.6.1.

Table 6.17 Phase 1 bedload sampling statistics

Experiment Number	Weight of Collected Bedload (kg)	Percentage of Transport Collected (%)	Percentage of Total Time Spent Sampling Bedload (%)
2	70.7	41.5	54.9
3	49.9	20.8	32.5
4	48.4	37.4	43.7
5	81.7	34.7	48.9
6	29.1	68.5	77.7
7	54.7	63.4	57.6

Experiment 6, the shallowest slope of the bankfull experiments (figure 6.11a), shows the least difference between the composition of the bedload and the initial bed. Experiment 4's bedload (middle slope experiment) shows a higher percentage of mid-range material and a lower percentage of fine and coarse material than Experiment 6. In Experiment 5 (steep slope experiment) the bedload composition reflects the greater transporting potential of the experiment when the weights of material transported is taken into account.

The percentage composition of coarse material is less than for the shallowest slope experiment, however, the steep slope experiment transports considerably more material. Experiment 6 transports 42.5 kg during phase 1, while Experiment 5 transports 235.5 kg. The larger percentage composition of coarse material, in the shallowest slope experiment, is due to the initial transport from the as laid screeded bed, and the low transport potential. The distribution of collected bedload from Experiment 5 (steepest slope) is similar to that from Experiment 6 (shallowest slope). This is due to Experiment 5's extra potential to transport a wider range of material.

Comparing the steepest initial bed experiment to the middle initial bed slope experiment (Experiment 5 to 4), the distribution of the collected bedload is greater. This also agrees with the changes in bed composition discussed in section 6.6.1.

Turning to the shallow overbank experiments (figure 6.11b), the same general trend between the bedload composition of the shallowest and the steeper initial bed slope experiments can be seen.

The different grading parameters for the cumulative collected bedload are presented for the two sets of experiments in table 6.18 below. The over all experiment order, in terms of unit stream power, is slightly different to the proposed order of transporting potential (see section 6.4). However, the orders within the presented sub-sections are the same using either method of ranking.

Table 6.18 Grading parameters for the cumulative collected bedload from phase 1, variable slope

Experiment Number	Initial Bed Slope	Unit Stream Power ($x10^{-3}$kg/m/s)	D5 (mm)	D16 (mm)	D50 (mm)	D84 (mm)	D95 (mm)	σ_g value
Bankfull								
6	0.0024	281.5	0.40	1.49	4.00	6.48	8.80	2.08
4	0.0026	302.0	0.59	2.21	4.06	5.85	7.67	1.63
5	0.0029	374.5	0.48	2.15	4.06	6.12	7.86	1.69
Shallow Overbank								
7	0.0024	343.2	0.39	1.78	4.30	6.54	8.02	1.92
2	0.0026	399.3	1.00	2.49	4.17	5.76	7.83	1.52

The d_{50} size grading parameter of the collected bedload remains constant, comparing the shallowest slope to the middle slope of the three bankfull experiments. While the d_{84} and d_{95} sizes decrease comparing the shallowest to the middle slope, and then increase again slightly comparing the middle slope to the steepest slope. The opposite is true for the d_{16} and d_5 sizes. There is a wider grading distribution of sizes in the composition of the collected bedload for the shallowest slope experiment. The grading then narrows for the middle slope experiment, before widening again slightly for the steepest slope experiment. This is reflected by the trend in σ_g values between the experiments.

The same increase in d_5 and d_{16} sizes and decrease in d_{84}, d_{95} and σ_g values is true for the shallow overbank experiments when comparing the shallowest to the steeper initial bed slope.

6.6.4 Progressive Composition of Cumulative Bedload (Phase 1)

One way to examine the evolution of the bedload composition is to monitor the changes in cumulative bedload composition throughout phase 1. Data relating to the evolution is presented in figures 6.12a to 6.12c and figures 6.13a to 6.13b, for the bankfull and shallow overbank experiments respectively. Once again the ranges of size fractions corresponding to sand, mid-range and coarse material have been used. Each size fraction is presented as a percentage of its final percentage within the composition of bedload collected during phase 1. Hence, at normalised time 1 each size fraction has a value of 100%.

In figure 6.12a it can be seen that the composition of the initial bedload of Experiment 6 lacks fines, while it has slightly more mid-range and coarse fractions compared to the composition of the total phase 1 bedload. The composition appears to stabilise at a normalised time of approximately 0.45. This is due to the bedload being mainly fine material, after the initial transport, which balances the weight of mid-range and coarse material transported initially. After time 0.45 the transport rate is low, and even though it is mostly fines it does not make a significant difference to the overall composition.

Experiment 4 (figure 6.12b) shows a similar trend, but with the initial composition of collected bedload having a higher percentage of coarse material. The experiment takes longer to stabilise, achieving stability around a normalised time of about 0.75. This is due to the fact that the bedload in the first few samples is somewhat coarser than that of Experiment 6.

The experiment with the steepest of the initial bed slopes (Experiment 5, figure 6.12c), shows a different pattern to the other two bankfull experiments. The initial collected bedload is finer, in composition, than the total collected over phase 1. The cumulative bedload also reaches something close to the final composition very quickly, at a normalised time of approximately 0.1. It then continues to fluctuate throughout phase 1. It is suggested that, this is due to the greater range of particle

sizes being transported by the experiment. All the size fractions are present from the start and only minor changes in cumulative composition occur through time.

Figure 6.13a shows the change in cumulative collected bedload composition with time, for the shallow initial slope experiment at the shallow overbank flow depth, Experiment 7. The pattern is different, from the bankfull experiments, although there are similarities. The initial composition has more fines, and less mid-range and coarse material, than the total collected bedload. This agrees with the results in section 6.6.2, when comparing the initial bankfull compositions to the initial shallow overbank compositions. As time progresses, the proportion of coarse material increases beyond that in the total bedload and then drops again. At the same time the proportion of fines drops from the initial high to below the final proportion. This demonstrates that, although the very first bedload composition was relatively fine, subsequent bedload compositions were coarser. This occurs while the bed stabilised and before the bedload became finer once more.

Looking at the changes in collected bedload composition for Experiment 2 (figure 6.13b), the pattern it most closely resembles is that of Experiment 7, the higher proportion of coarse material being accounted for by the greater transporting potential generated by the steeper initial bed slope.

6.6.5 Phase 1 Fraction Mobility

Figures 6.14a to 6.14c, 6.15a and 6.15b compare bedload compositions from phase 1, to the cumulative collected bedload composition from phase 1, and the initial bed composition for each of the experiments.

Looking first at figure 6.14a, for Experiment 6, the bedload becomes progressively finer with increasing normalised time (NT), agreeing with the observations made in sections 6.6.2 and 6.6.4. The same is true for Experiment 4 (figure 6.14b), but with a greater proportion of coarse material in the initial bedload compared to the cumulative bedload composition. The data from Experiment 5, the steepest of the

bankfull experiments, illustrated in figure 6.14c, clearly shows the opposite trend to Experiments 6 and 4, as described in previous sections. The bedload compositions at early normalised times have a lower proportion of coarse and mid-range material than the cumulative bedload. The bedload composition becomes coarser as time progresses and, it is suggested, as fines become less abundant.

Turning to figure 6.15a, for Experiment 7, the data agrees with that of the progressive changes in cumulative bedload shown in section 6.6.4. The initial bedload composition is finer than that of the cumulative bedload, but it then becomes coarser with time. The results from Experiment 2 (figure 6.15b), show the same trend but with slightly coarser material present in the early bedload composition, compared to the cumulative collected bedload composition.

Fraction mobility can be examined in more detail across the full range of fraction sizes using the modified Wilcock technique, employed in section 6.6.2 (figures 6.16a to 6.16c and figures 6.17a and 6.17b). This time the percentage by mass of a fraction in the bedload is not divided by its percentage by mass in the bed. Instead, the percentage in the bedload is divided by the percentage of that size fraction in the cumulative bedload at the end of phase 1. This means that fraction mobility is being compared irrespective of the availability of the fraction size within the bed at the time the sample was collected. It does however, mean that the evolution of the bedload composition can be examined, relative to the cumulative collected bedload composition.

The same trends are visible in figures 6.16 and 6.17 as those already described in figures 6.14 and 6.15. However, these figures illustrate that, although the three ranges of size fractions describe the general behaviour of the material, interpretation from the individual half-phi size fractions is considerably more complex. For example, there are several cases within the five figures where the bedload mobility line crosses the horizontal equal mobility line within one of the three ranges of size fractions. Using the three ranges of fraction size this resolution is lost and it is the average behaviour, of the fractions within the three ranges, that is viewed.

6.6.6 Phase 1 and Total Cumulative Bedload Composition

The relative importance of understanding the evolution processes occurring, during phase 1 of the transport decline, is apparent when figures 6.18a to 6.18c and 6.19a to 6.19b are studied. The figures show that there is little difference between the composition of the bedload collected during phase 1 and the composition of the bedload collected during the whole of the experiment. This is true for all of the experiments. It therefore appears that it is phase 1 of the experiment that has most impact in terms of the evolution of bed and bedload composition. This is despite the fact that a significant amount of bedload is collected after phase 1 is complete (table 6.19 below).

Table 6.19 Full experiment bedload sampling statistics

Experiment	Weight of Collected Bedload (kg)	Percentage of Bedload Collected After Phase 1 (%)	Percentage of Transport Collected (%)	Percentage of Time Spent Sampling Bedload (%)
2	95.6	26.0	38.0	34.9
3	119.1	58.1	23.4	27.9
4	74.1	34.7	36.4	37.9
5	150.6	45.8	43.9	51.1
6	61.7	52.8	63.4	53.5
7	86.2	36.5	52.4	48.8

In figure 6.18a (Experiment 6) it can be seen that the 52.8% of the total bedload collected after phase 1 has made the total cumulative bedload composition very slightly finer. This suggests that, the cumulative bedload collected after phase 1 is very similar in composition to that collected during phase 1, but contained a slightly higher proportion of fines relative to mid-range material. The 34.7% of the total bedload collected after phase 1 was complete in Experiment 4 (figure 6.18b), was again very similar in composition to that collected during phase 1. In this case the phase 2 material had a higher proportion of mid-range material, relative to fine material, compared to the phase 1 cumulative collected bedload. For Experiment 5, the 48.5% of the bedload collected after phase 1 contained a higher proportion of

mid-range and coarse material, relative to fine material. than the phase 1 bedload (figure 6.18c).

The equivalent results are shown in figure 6.19a for the shallower of the initial slopes experiment at the shallow overbank flow depth (Experiment 7). The figure shows that there is practically no difference between the compositions of the cumulative bedloads collected during phase 1 and the whole experiment. Figure 6.19b (Experiment 2) shows the same pattern as figure 6.18a (Experiment 6). The bedload collected after phase 1 has a slightly higher proportion of fines, relative to mid-range material, than that collected during phase 1.

6.6.7 Cumulative Transported Mass

Plotting the cumulative transported mass curves, for the full experiments (figures 6.20a and 6.20b), allows examination of bedload transport evolution beyond phase 1. In both figures the transported mass has been plotted relative to the cumulative mass transported at the end of phase 1 (normalised time 1). A horizontal line representing 100% and a vertical line representing normalised time 1 have been included in both figures, for ease of reference.

A degradational experiment with a mixed grain bed will eventually reach a condition of static equilibrium (see section 5.3). In this condition the bed is stable with negligible material entrained as bedload. This will occur as the result of a combination of bed coarsening and restructuring. In practise this will not be achieved due to sporadic bursts of turbulence occasionally disturbing the bed structure and releasing sediment. If the transport resulting from such disturbances is averaged out over time by the sampling process then a shallow linear increase in cumulative mass transported can be taken as a first approximation of stability. The gradient of such an increase is dependent on the experimental conditions. For a higher transport capacity experiment the static equilibrium bed is likely to be more stable than for a lower capacity experiment. The higher capacity experiment is also likely to have transported more material on its way to stability. The amount of material released

thereafter by sporadic bursts of turbulence will therefore be relatively smaller for the higher capacity experiment. Thus the linear gradient suggesting stability on a mass curve will be shallower.

Looking then at figure 6.20a for the bankfull experiments. Experiment 5 appears to reach practical stability around a normalised time of 5. after which time the percentage of mass transported increases linearly with time. Experiment 6 demonstrates a linear increase in the percentage of mass transported beginning sometime after a normalised time of 4. The lack of resolution of the curve around this time makes it difficult to identify the start of the linear increase. The gradient is significantly greater than for Experiment 5. The lack of resolution in the cumulative mass curve for Experiment 4 makes it difficult to identify any stability.

In figure 6.20b, the two shallow overbank experiments show very similar cumulative mass curves. Experiment 7 appears to demonstrate a spell of linear increase between normalised times of 3 and 5. However, after time 5 the gradient changes and a period of shallower increase is observed. Experiment 2 wasn't run as long as Experiment 5 in terms of normalised time. Towards the end of the experiment, at around a normalised time of 3 the cumulative mass curve appears to approach linearity. Again, the lack of data points on the curves prevents any firm conclusions being drawn. It may be that with better resolution of transport data, and using a normalised time scale, all the experiments would reach practical stability at around the same time.

6.6.8 Progressive Composition of Cumulative Bedload (Full Experiment)

A comparison between the phase 1 bedload composition and the total bedload composition has already been made for each experiment in section 6.6.6. However, figures 6.21a to 6.21c and 6.22a to 6.22b plot the progressive compositions of cumulative bedload throughout the full experiments, as a percentage of the

compositions at normalised time 1. This makes it possible to examine if the cumulative bedload composition stabilises before the experiments were stopped.

For Experiment 6 (figure 6.21a) visual inspection suggests that the cumulative composition stabilises at about 4.5 on the normalised scale. It is suggested that Experiment 4 (figure 6.21b) stabilises somewhere between normalised times of 2 and 4. While for Experiment 5 (figure 6.21c) stability does not seem to occur until 8 on the normalised time scale.

The cumulative bedload composition for Experiment 7 (figure 6.22a) appears to stabilise earlier than the bankfull equivalent (Experiment 6), at a normalised time of slightly less than 3. The steeper slope shallow overbank experiment (Experiment 2, figure 6.22b) appears to stabilise earlier still at 2.5, but has very few data points beyond this time to confirm stability.

Neglecting Experiment 5 there appears to be a trend in that, the cumulative collected bedload composition stabilises at earlier normalised times for steeper initial bed slopes.

6.7 Effect of Relative Depth Ratio on the Evolution of the Bed Surface and Bedload Compositions

The work in this section complements that of section 6.6. It evaluates the effect of relative depth on the evolution of the bed and bedload composition. Many of the figures from 6.6 are re-presented in this section in their new groupings of varying relative depth, purely for ease of reference.

Two sets of experiments are examined covering different relative depths at two different initial bed slopes. The shallower set, with an initial bed slope of 0.0024, contains a bankfull (Experiment 6) and a shallow overbank flow depth (Experiment 7). While the steeper of the two initial bed slopes, at 0.0026, contains the wider range

of flow depths of bankfull (Experiment 4). shallow overbank (Experiment 2) and deep overbank (Experiment 3).

6.7.1 Initial and Final Beds

Once again the same general trend is shown in each experiment. The final bed contains a higher proportion of coarse material, but a lesser proportion of mid-range material, and generally less fines, than the initial bed (figures 6.23a and 6.23b).

For the shallower of the two slopes, figure 6.23a, with increasing relative depth the final bed becomes coarser. The final bed of Experiment 7 contains a higher proportion of coarse material, a lower proportion of mid-range material, and practically the same proportion of fine material, as the final bed of Experiment 6. Experiment 7 is the shallow overbank experiment and Experiment 6 the bankfull experiment.

The same trend of coarsening final bed with increased relative depth ratio from bankfull (Experiment 4), to shallow overbank (Experiment 2), can be seen in figure 6.23b. The deeper overbank experiment shows an even smaller proportion of fines present in the final bed than the shallow overbank experiment. It also shows an equivalent proportion of mid-range material to Experiment 4, and a proportion of coarse material between the bankfull and shallow overbank experiments.

At the lower transporting potential, bankfull experiments, mid-range and fine material is removed in preference to coarse material. This makes the final beds coarser than the initial beds. With the increased transporting potential of the shallow overbank experiments, even more fine and mid-range material is removed relative to the coarse material. For the steeper of the two slopes, where a further increase in relative depth is examined, a further increase in transport potential results in more fine material being removed relative to the other two size fractions. However, the increased potential also allows a larger proportion of coarse material to be removed

than for the other relative depths. This demonstrates the ability to transport a wider size distribution of material.

6.7.2 Initial and Final Fraction Mobility

The modified Wilcock technique (see section 6.6.2) is again used to examine the fraction mobility within the bedload, figures 6.24a and 6.24b plus figures 6.25a to 6.25c. The same horizontal and vertical broken lines are superimposed on the figures to help identification of relative mobility and the three size fraction ranges.

As described in section 6.6.2, Experiment 6 and Experiment 7 (figures 6.24a and 6.24b), show the same general trends and the following observations can be made.

(i) Higher mobility of coarser fractions is demonstrated at the start of the experiments, relative to the initial beds, than at the end of the experiments, relative to the final beds.

(ii) Both experiments also show little difference in mid-range material mobility between the initial and final phases of the experiments. However, there is generally greater mobility of fines at the end of the experiments than at the start.

(iii) The fractions showing consistently the greatest mobility in Experiment 6 (bankfull), are larger than those consistently most mobile in Experiment 7 (shallow overbank).

The following observations were seen in figures 6.25a to 6.25c:

(i) Figure 6.25a illustrates the initial and final fraction mobilities of Experiment 4, the bankfull experiment at the steeper to the two slopes in this section. The most mobile fraction at both times falls towards the coarse boundary of the simplified mid-range. There is not much difference between initial and final mobility of the coarse fraction sizes while, at the end of the experiment, the mid-range sizes are more

mobile than initially. Initially the fine fractions are slightly more mobile than they are at the end.

(ii) Experiment 2, the shallow overbank case (figure 6.25b), shows the most mobile fraction is again finer than for the equivalent bankfull experiment, at least initially. The trend in initial and final mobilities is very similar to the equivalent relative depth at the shallower initial bed slope (Experiment 7), but shows larger size fractions being more mobile.

(iii) The most mobile size fraction initially, in Experiment 3 (deep overbank, figure 6.25c), is coarser than the most mobile fractions at both the other relative depths. The coarse fractions are more mobile initially than finally. There is not much difference between the initial and final mobilities of the mid-range material. At the end of the experiment the fine material is considerably more mobile than at the start.

At the shallower of the two slopes evolution of bedload composition follows the pattern described in section 6.6.2. That is, initially the bed is unstable, due to its screeded arrangement, and so material of all sizes appears in the initial bedload. However, because there is an abundance of fines in the initial bed, the relative mobility of them is lower than that of the coarse material. Later in the experiment the bed is in a more stable water-worked arrangement. The low transporting potential of the experiments can only entrain the finer material so its significance in the bedload increases. The interesting relationship here however, is that the most mobile fractions in the shallow overbank case are finer than in the bankfull case. It is suggested that, although the transporting potential of the shallow overbank experiment is greater (as discussed in section 6.4), it is not sufficiently greater to be able to entrain larger particles than its bankfull equivalent. The extra transporting potential is therefore concentrated on entraining larger quantities of finer material.

The same reasoning is proposed as an explanation for the pattern shown between the bankfull and shallow overbank experiments at the steeper slope. It is suggested in section 6.4 that Experiment 4 has a greater transporting potential than both the

experiments at the shallower slope. If this was true it would explain why, at the end of the experiment, the mobility of the mid-range material was higher, at the expense of the mobility of the fine material. The experiment, having just that little bit more potential, is able to entrain the larger, mid-range particles from the more stable, water-worked bed. The deep overbank experiment however has more transporting potential again, and is able to move substantial amounts of coarse material at the start, from the unstable screeded bed. This in turn makes the later bed considerably more stable than the other experiments at the same initial bed slope. Therefore at the end of the experiment, even with the extra potential, the remaining coarse material is stable. The potential is therefore applied to the finer fractions, explaining the increased fraction mobility.

6.7.3 Cumulative Bedload Composition

The composition of the cumulative bedload, during phase 1 of the sediment transport rate decline, is again used as a basis for examining bedload evolution. The validity of this has already been discussed in the introduction to section 6.6.3, with the aid of figure 6.10 and table 6.17.

The compositions of the cumulative collected bedloads for the experiments of different relative depth, at the two slopes are presented in figures 6.26a and 6.26b. The same general relationship can be seen with the initial bed composition. For each of the five experiments examined, the bedload composition has a lower proportion of fine and coarse material, and a higher proportion of mid-range material than the initial bed.

For the shallower slope experiments, Experiments 6 and 7, figure 6.26a, there is not much difference between the compositions of the collected bedload. The slightly higher transporting potential of the shallow overbank experiment has produced a composition with a slightly higher proportion of fine and mid-range material and less coarse material than the bankfull case. This agrees with the results in section 6.7.1.

Figure 6.26b, for the different relative depths at the steeper slope, shows practically the same trend between the bankfull and shallow overbank cases. However, the steeper initial bed slope has a slight effect. The shallow overbank experiment is able to entrain more mid-range and coarse material, relative to fine material, than the bankfull case, compared to the relationship at the shallower slope. Experiment 3, again shows that a further increase in transporting potential allows for a wider range of material to be transported. Experiment 3 has more fine and coarse material and less mid-range material than Experiment 2.

Examining the various cumulative bedload parameters, of the two sets of experiments, the results for the steeper slope follow the trend described in section 6.6.3. That is, for an increase in transporting potential from low to medium to high, the width of grading of the sediment decreases and then increases again. This illustrated by the decrease in σ_g value from Experiment 4 to 2 and then the increase from Experiment 2 to 3 in table 6.20 below.

The same trend in σ_g values is show between the bankfull and shallow overbank experiment at the shallower slope.

Table 6.20 Grading parameters for the cumulative collected bedload from phase 1, variable stage

Experiment Number	Stage Level	Unit Stream Power ($x10^{-3}$kg/m/s)	D5 (mm)	D16 (mm)	D50 (mm)	D84 (mm)	D95 (mm)	σ_g value
Initial Bed Slope 0.0024								
6	Bankfull	281.5	0.40	1.49	4.00	6.48	8.80	2.08
7	Shallow Overbank	343.2	0.39	1.78	4.30	6.54	8.02	1.92
Initial Bed Slope 0.0026								
4	Bankfull	302.0	0.59	2.21	4.06	5.85	7.67	1.63
2	Shallow Overbank	399.3	1.0	2.49	4.17	5.76	7.83	1.52
3	Deep Overbank	483.9	0.61	2.16	4.11	6.88	10.00	1.78

6.7.4 Progressive Composition of Cumulative Bedload (Phase 1)

Figures 6.27a to 6.27b and 6.28a to 6.28c describe the progressive composition of the cumulative bedloads for the two sets of experiments examined here. All the figures follow the same format described at the start of section 6.6.4. Most of the figures presented here have already been described and this section will therefore concentrate on the relationship between experiments of different relative depths.

Figures 6.27a and 6.27b present the progressive compositions of the cumulative bedloads for the bankfull and the shallow overbank experiments at the shallower of the two slopes. They show that, initially the greater transporting potential of the overbank experiment makes the collected bedload composition finer than that of the bankfull experiment. Looking at the successive compositions the overbank experiment shows a big increase in the proportion of coarse material collected due to the higher transporting potential. The compositions of both experiments appear to stabilise at around the same time.

At the steeper slope, the bankfull experiment (figure 6.28a) shows the same pattern of composition modification with time as the bankfull experiment at the shallower slope (figure 6.27a). However, Experiment 4 has a higher initial proportion of coarse material. The same trend between the bankfull and shallow overbank experiments is clear in figures 6.28a and 6.28b. This time the higher transporting potential causes the initial composition, of the shallow overbank collected bedload, to be coarser than the final composition. With a further increase in relative depth, to the deep overbank case (Experiment 3), there is less of a variation in composition proportions through time, figure 6.28c. The initial composition of the bedload is slightly coarser, with a higher proportion of coarse and mid-range material than the final cumulative collected bedload composition.

6.7.5 Phase 1 Fraction Mobility

Some of the figures presented in section 6.6.5 are presented here as figures 6.29a and 6.29b plus 6.30a to 6.30c, again to allow ease of reference for the reader. The evolution of the bedload composition through phase 1, compared to the cumulative collected bedload composition, can therefore be examined for the different relative depths.

Turning first of all to the shallower slope (figures 6.29a and 6.29b), the bankfull and shallow overbank experiments exhibit opposite trends. For the bankfull case (Experiment 6), the initial bedload is coarser, than the cumulative collected bedload, with later bedload compositions being finer. While for the shallow overbank case, the initial bedload composition is finer and becomes coarser with time, than the cumulative bedload composition. This may appear, at first glance, to contradict the mobility results from the modified Wilcock technique, presented in section 6.7.2. However, those results were for mobility relative to the compositions of the initial and final beds. It is therefore entirely possible that the bedload composition at the end of the experiment may be coarser than that at the start. At the same time the coarse size fractions are less mobile and the fine fractions more mobile, relative to the final bed composition, than they were relative to the initial bed composition.

At the steeper initial bed slope (figures 6.30a to 6.30c), the same trend between the bankfull and the shallow overbank case is seen. Continuing on to the deep overbank case (Experiment 3), the bedload composition does not vary significantly from the composition of the cumulative bedload collected during phase 1. It does however, resemble the behaviour of the bankfull case in terms of bedload evolution, with its initially slightly coarser composition evolving to a finer composition later.

The bedload evolution suggests that there is the same trend in behaviour between, the bankfull and shallow overbank cases, as there is between the increasing initial bed slopes of section 6.6.5. When initially the bed is in its original screeded arrangement the low transporting potential of the lowest relative depth (bankfull)

experiment favours the most prominent grains. These are the mid-range and coarse particles. When the bed stabilises into a water-worked arrangement, there is not enough transporting potential to move any more larger grains. The energy is therefore used to entrain smaller material, resulting in a progressively finer bedload. The next largest relative depth (shallow overbank) has slight more transporting potential. This means that initially, as well as moving the prominent, unstable, larger material, there is also enough energy to entrain finer material. This makes the initial bedload composition finer than that of the bankfull case, despite transporting a larger weight of coarse material. As the bed stabilises the accessible fines are removed and the greater transporting potential of the shallow overbank experiments is focused on the, still largely available, mid-range material. Progressively the bedload becomes coarser. The further increase in transporting potential at the largest relative depth (deep overbank), seems to cause a reverse in behaviour. Again the bedload is slightly coarser at the start and gets progressively finer. However, the proportion of coarse material in the bedload initially approaches that in the initial bed, indicating that there is sufficient potential to move all size fractions at almost equal mobility, when the bed is unstable. The potential of the experiment then produces a significantly more stable bed, than that produced by the lower relative depth experiments. As the stable water-worked bed develops, even the greater transporting potential is unable to transport the larger material in the same proportions. The bedload therefore becomes progressively finer as the transport rate dramatically declines.

Again the full fraction range mobility figures are presented to illustrate the differing mobilities within the simplified fractions, figures 6.31a and 6.31b plus 6.32a to 6.32c. The same trends, shown by the bar charts described above, are visible and the figures are produced in the same manner as described in section 6.6.5.

6.7.6 Phase 1 and Total Cumulative Bedload Composition

The compositions of the cumulative bedload at the end of phase 1 and at the very end of the experiments being examined, are presented in figures 6.33a and 6.33b plus 6.34a to 6.34c. They illustrate that, for increasing relative depth, as well as increasing

initial bed slope (section 6.6.6), phase 1 is most significant in terms of controlling bed surface and bedload composition evolution.

Looking first at the shallower slope experiments (figures 6.33a and 6.33b), the phase 1 and total cumulative bedload compositions are very similar for both the bankfull and shallow overbank cases. The phase 2 bedload in Experiment 6 is slightly finer than the phase 1 bedload making the overall total cumulative composition finer. The phase 2 bedload for Experiment 7 is slightly coarser, having the opposite effect.

Figure 6.34a (bankfull at the steeper slope, Experiment 4), shows very similar compositions to those produced by Experiment 7 (shallow overbank at steeper slope, figure 6.33b). This agrees with the results from section 6.4, suggesting that the two experiments lie next to each other in the ranking order of transporting potential. Experiment 4 being the more powerful, shows compositions containing greater percentages of mid-range material, relative to the fine and coarse fractions, than Experiment 7. The compositions of cumulative bedload collected in Experiment 2 (figure 6.34b), show the same trends as Experiment 6 (figure 6.33a). Again though, the higher transporting potential of Experiment 2 produces compositions with proportionally more mid-range material. Figure 6.34c presents the compositions for the deep overbank experiment, Experiment 3. It shows that the phase 2 bedload, 58.1% of total collected (see table 6.19), was coarser than the phase 1 bedload.

6.7.7 Cumulative Transported Mass

Once again the experiments are grouped according to their initial bed slope, so as to compare different relative depths, figures 6.35a and 6.35b. The figures present the data in the same way as described in section 6.6.7, but for the assessment of initial slope effect. However, this time the results are less clear.

From figure 6.35a it could be argued again that both experiments are approaching stability at a normalised time of around 5.

Turning to figure 6.35b, for the steeper initial bed slopes, it is very difficult to say if either the bankfull (Experiment 4), or the shallow overbank (Experiment 2), have reached stability. The deep overbank case (Experiment 3), appears to have gone through a period of stability between the normalised times of 3 and 7 but then the transport rate drops off again to practically nothing.

It would be unwise to draw any conclusions from these figures in terms of order of stabilisation due to the lack of resolution in the curves.

6.7.8 Progressive Composition of Cumulative Bedload (Full Experiment)

Figures 6.36a to 6.36b and 6.37a to 6.37c, are presented to examine trends between the stabilisation of the cumulative bedload composition and increasing relative depth. The figures cover the full lengths of the experiments.

Reviewing the shallower initial bed slope experiments first (figures 6.36a and 6.36b), the bankfull experiment (Experiment 6), appears to have a stable composition after a normalised time of 4.5. For Experiment 7, the shallow overbank case, composition stability is approached at a normalised time of 3.

For the steeper slope, the bankfull experiment (Experiment 4, figure 6.37a), approaches composition stability between a normalised time of 2 and 4. The shallow overbank case (Experiment 2, figure 6.37b), approaches stability at 2.5 on the normalised time scale. Instead of stabilising earlier still, as the bankfull to shallow overbank relationships might suggest, the deep overbank case (Experiment 3, figure 6.37c), doesn't appear to stabilise until a normalised time of 4.

The task of identifying stability of composition would be made significantly easier with greater resolution of the progressive curves.

6.8 Conclusions

In this chapter six degradational experiments have been examined, five of them were first introduced in Chapter 5. The individual transport potentials of the six experiments have been compared and an order of transporting potential proposed. Arranging the experiments into groups, the effects of initial bed slope on the evolution of bed surface and bedload compositions was examined. Re-arranging the experiments into new groups, the effects of relative depth ratio was then examined.

From the work carried out and the results presented in this chapter the following conclusions have been drawn.

1. The unit stream power, the different recorded transport rates, the transport rates estimated from regression curves and the estimates of cumulative transported bedload were all assessed for the individual experiments. All these results conclude that, as initial bed slope increases or relative depth increases the transporting potential of the flow increases.

2. The results also suggest that overbank flow reduces the transporting potential of an experiment. The reduction is not as much as one might predict from a direct relationship with boundary shear stress. It does not reduce the transporting potential of a shallow overbank experiment to less than that of a bankfull experiment at the same initial bed slope. Rather, the potential is reduced somewhat, in relation to the relative potential predicted by a direct relationship with unit stream power.

3. The different transporting potentials of the experiments cause differing amounts of bed coarsening between the initial bed and final bed compositions. The extent of coarsening taking place between the initial and final beds increases for both increasing initial slope and increasing relative depth.

4. The size fractions removed from the bed during armouring vary with experimental transporting potential. For the lower potential experiments (i.e. bankfull or shallow initial slope), mostly fine material is removed from the bed along with some mid-range material and very little coarse material. For medium potential experiments, it is still mostly fine and mid-range material that is removed but also a higher proportion of mid-range material. For the high potential experiments (i.e. deep overbank or steep slope), it is mostly mid-range material that is removed but with both the fine and coarse material also being moved.

5. Fraction mobility at the start and end of the experiments suggest that as well as the bed surface composition changing, there is also a change in bedload composition during degradation. The relationship between transporting potential and mobility evolution has proved complex and is not necessarily a smooth one. Clear differences have been seen in bedload evolutions for increasing initial bed slope and increasing relative depth. The lowest transporting potential is only able to remove the most unstable material from the initial screeded bed. This includes the material protruding furthest into the flow, mid-range and coarse material, making the initial bedload coarser. As the bed becomes water-worked, and therefore less unstable, the potential is insufficient to move the larger material. Thereafter the bedload consists of fine material, and becomes finer with time. For the higher transporting potential experiments almost all size ranges are mobile from the unstable screeded bed. As the bed itself is relatively fine this makes the initial bedload proportionally finer than some of the lowest potential experiments. The high potential continues to transport larger material in the bedload, causing the arrangement of the bed to become very stable, or armoured, in order to avoid entrainment. As this occurs the largest, and then successively smaller material, disappears from the bedload and the bedload becomes finer as the transport rate drops sharply. In between these two extremes are several points where a slight difference in transporting potential between two experiments, may cause confusion. Sometimes, a slight increase in potential does not mean the experiment with a higher potential is able to transport larger material. Instead, the extra transporting potential is used to transport larger proportions of the finer material, which is more easily entrained, making the bedload composition finer.

It is therefore difficult to arrange the order of the experiments in terms of transporting potential solely on the results of the evolution of bedload fraction mobility. It is concluded that fraction mobility results should be viewed in conjunction with actual transport rates.

6. Almost all the significant changes in bedload composition occur in phase 1 of the experiments while the initial transport rate is declining rapidly to a marginal rate. However, the marginal transport rate phase allows the final adjustment to stable bed surface and bedload compositions.

7. From the data available it appears that stability of bedload transport rate, indicating a stable bed surface composition, does not coincide with stability of the bedload composition. This conclusion is tentative due to the less than comprehensive set of results covering these topics. It may be that, plotted on a normalised time scale, all the experiments approach bed surface stability at about the same time. This is suggested by the data when examining the effect of increasing slope, but is not clear when examining the effect of increasing relative depth. For increasing slope there is also a suggestion that the time taken to reach bedload composition stability is less than that to reach bed composition stability, and that this time decreases with increasing slope. The steepest slope does not follow the trend and there is also no clear result of this from examination of the effect of increased relative depth.

6.9 Further Work

To add to the analysis presented in this chapter more detail of the transport rate decline, throughout the whole experiments, is required. It would also be advisable to run any future experiments for considerably longer durations, despite their seeming stability. This would allow clearer identification of the final bed and bedload composition stability.

However, it is suggested, as in section 5.13, that the analysis may be furthered by using sediment recirculation experiments. Using this approach stability would be

more definitely defined and more easily recognised as a constant bedload transport rate with time (NB the same disturbance of the bed by bursts of turbulence would occur but the resulting transport would be less significant compared to the equilibrium transport rate). The constant bedload transport rate would have to be monitored to identify constant composition. Again the composition may fluctuate with disturbance of the bed but the composition of the equilibrium transport itself would be constant. When achieved this would reflect the end of the evolution of the interaction between the bed and transported material. This would therefore allow examination of trends between the durations taken to reach one or both of the stability criteria by different experimental conditions.

Further experiments using the same initial bed material, at a wider range of initial bed slopes and relative depths would also compliment the results presented here. A larger data set would allow identification of which of the two variables, initial bed slope and relative depth, have the greatest influence on the transporting potential of an experiment. It would also allow further examination of the influence of overbank flow, in terms of its retarding effect on transporting potential. A sufficiently large data set would allow a researcher to assess whether the effect is strongest for a particular range of relative depths.

The restriction of the period of research work to three years has only allowed a limited amount of the data to be examined in any detail. Further funding of work would allow examination of lateral variations in bedload composition. Further work on the collected bed topography data may allow examination of grain structure or the development of arrangement throughout the experiments. In addition the bed topography data may allow examination of the developing bed roughness with declining transport rate. Also, in addition to the various parameters that could be examined with further funding, several other experiments where conducted using the same apparatus, see Chapter 3. These involved the supply of sediment at a constant rate to the upstream end of the channel. Examination of the results from experiments similar to those presented here would be complementary to this volume of work.

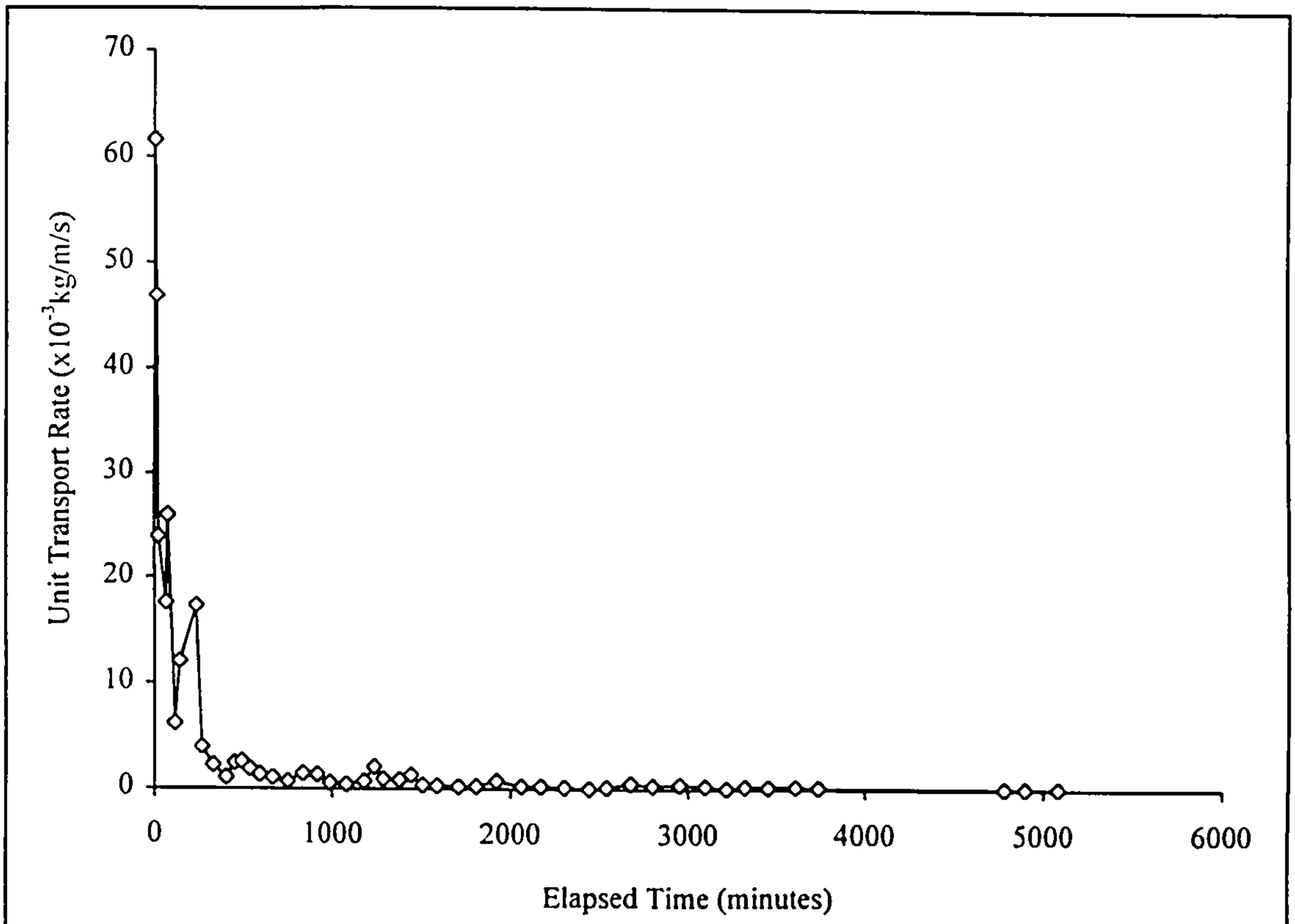

Figure 6.1 Unit Transport Rates for Experiment 5, Bankfull, Slope 0.0029

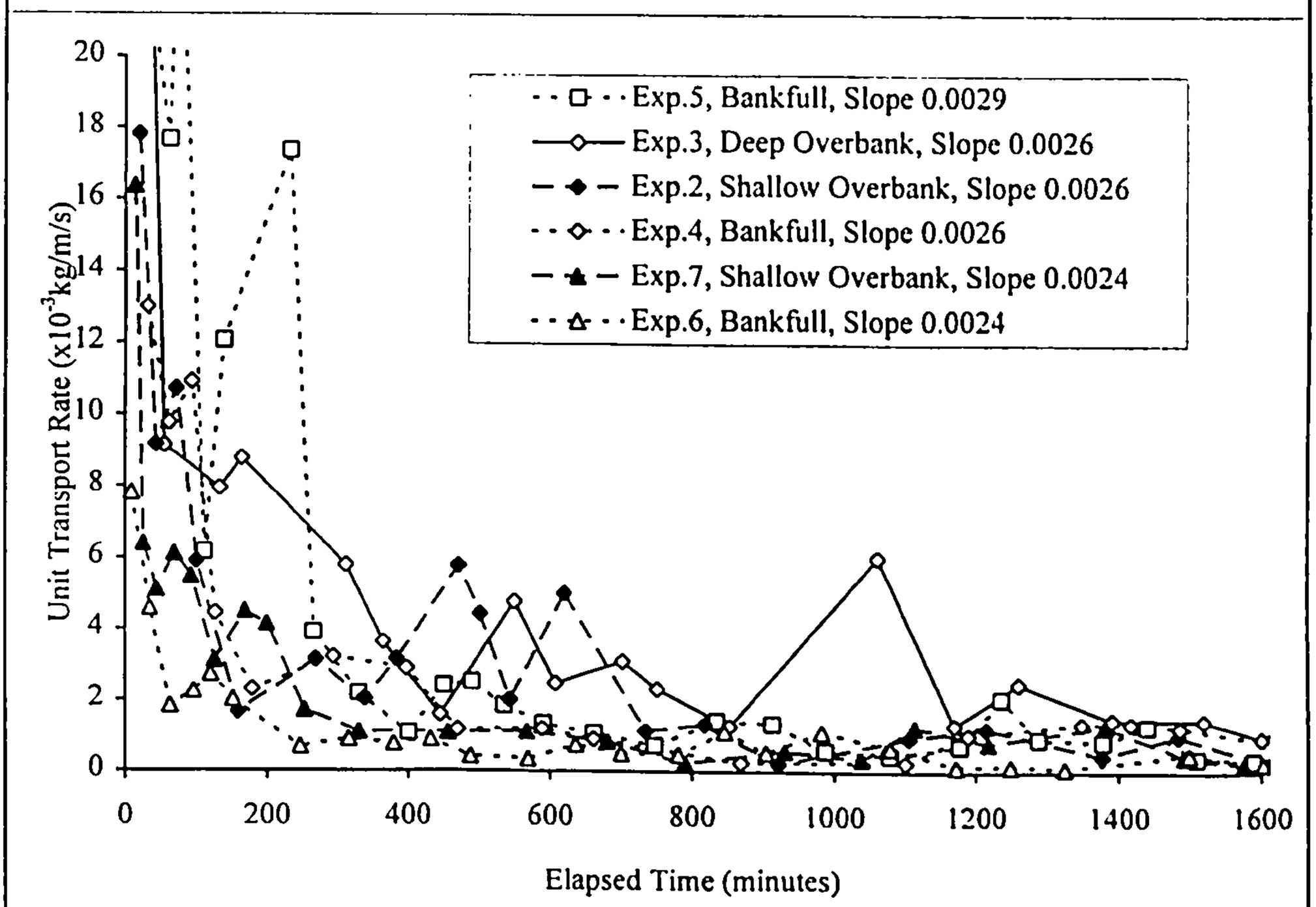

Figure 6.2 Unit Transport Rates on Shortened Axes, Experiments 2 to 7

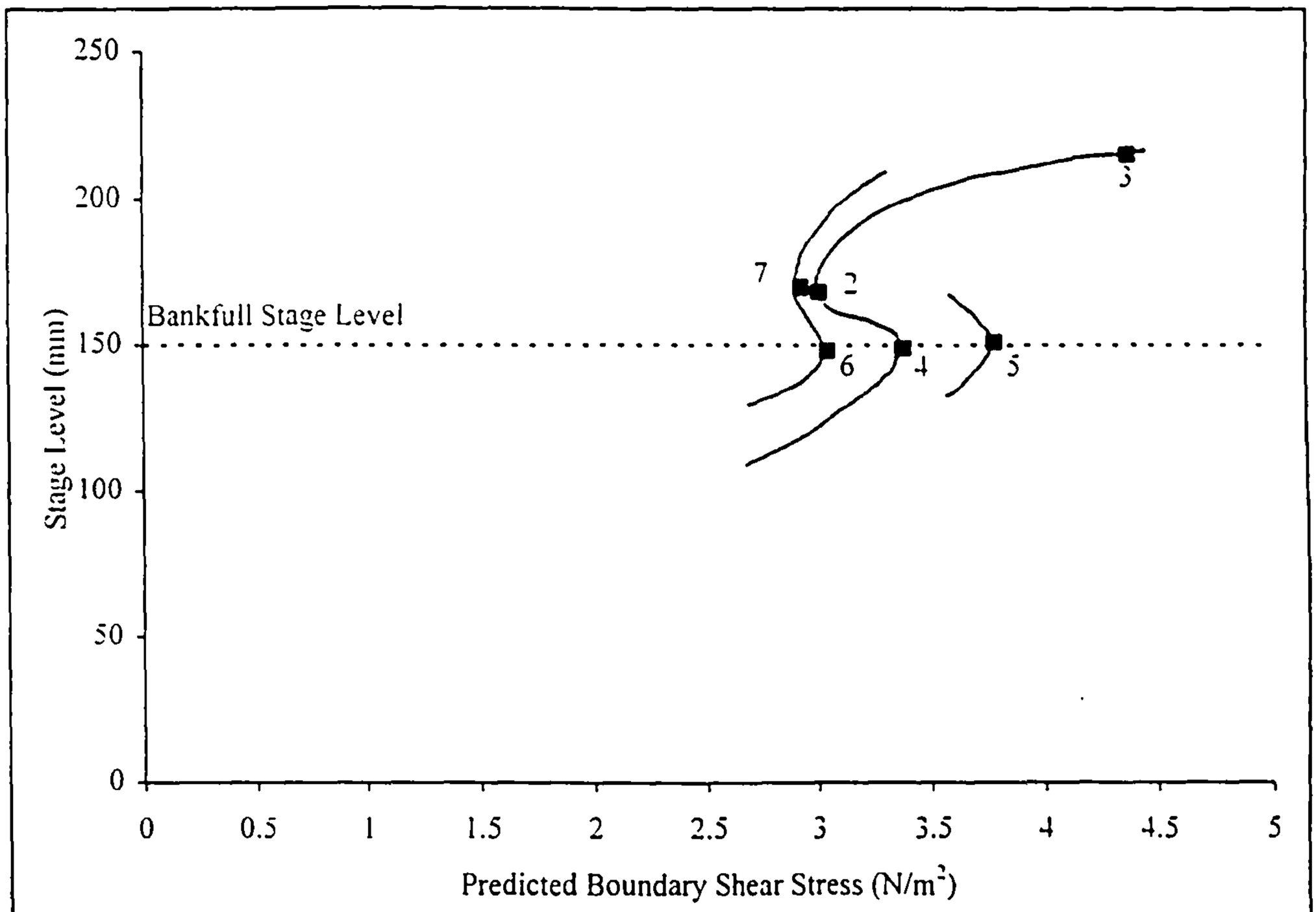

Figure 6.3a Stage Level Against Predicted Bed Shear Stress, Including Prediction of Idealised Variation, Time 0 Minutes

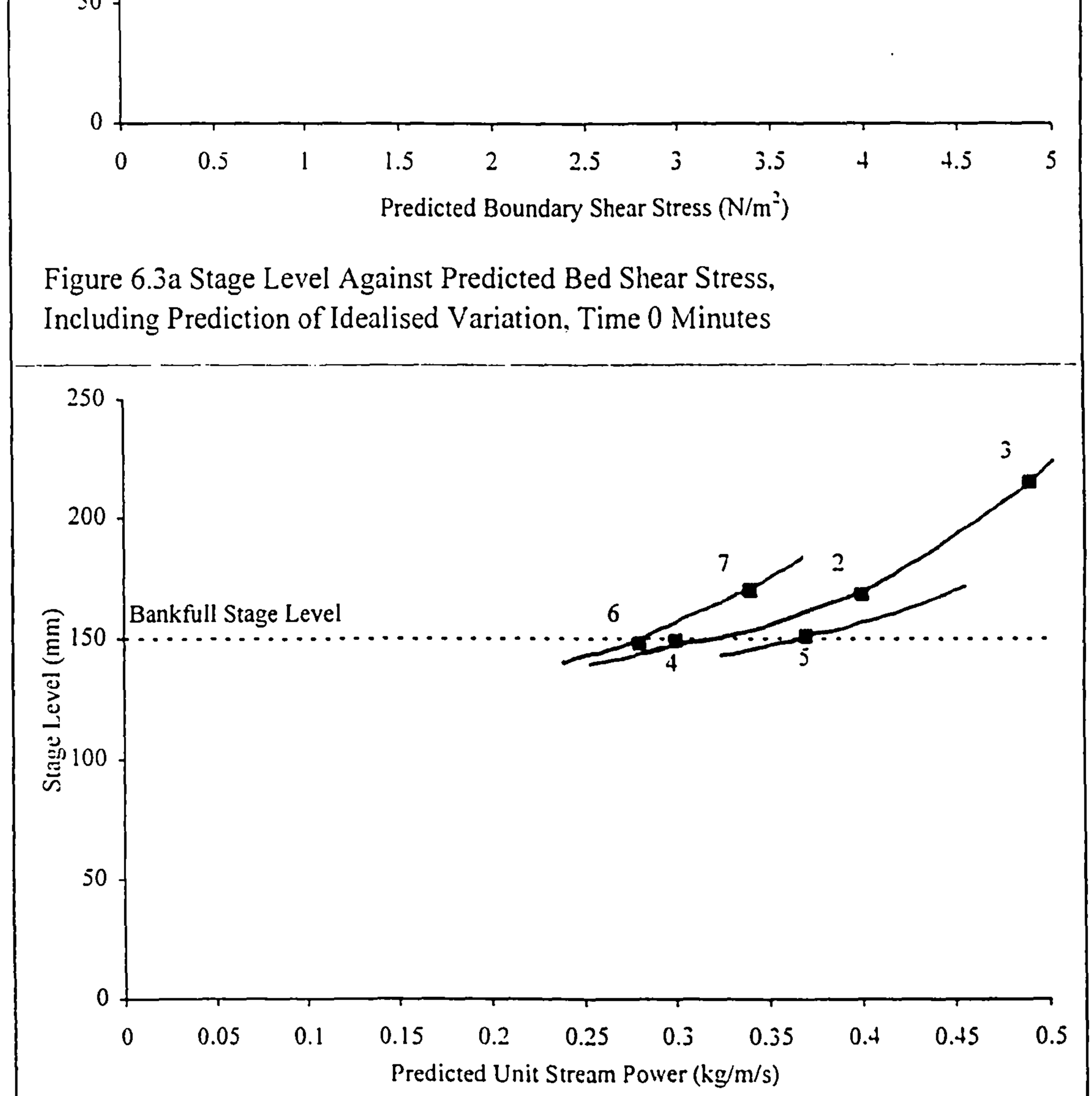

Figure 6.3b Stage Level Against Predicted Unit Stream Power, Including Prediction of Idealised Variation, Time 0 Minutes

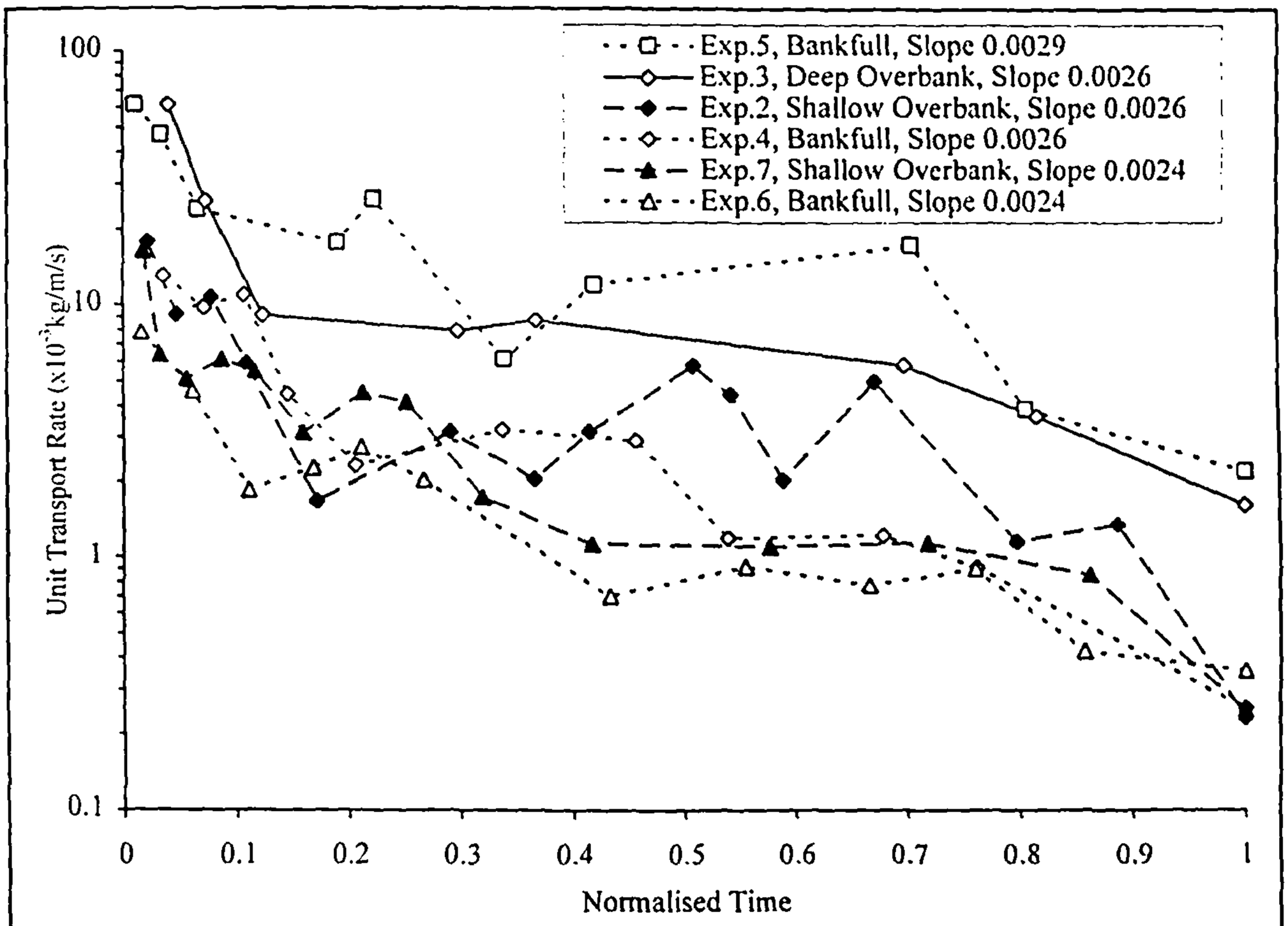

Figure 6.4 Unit Transport Rate Against Normalised Time, Phase 1 Only

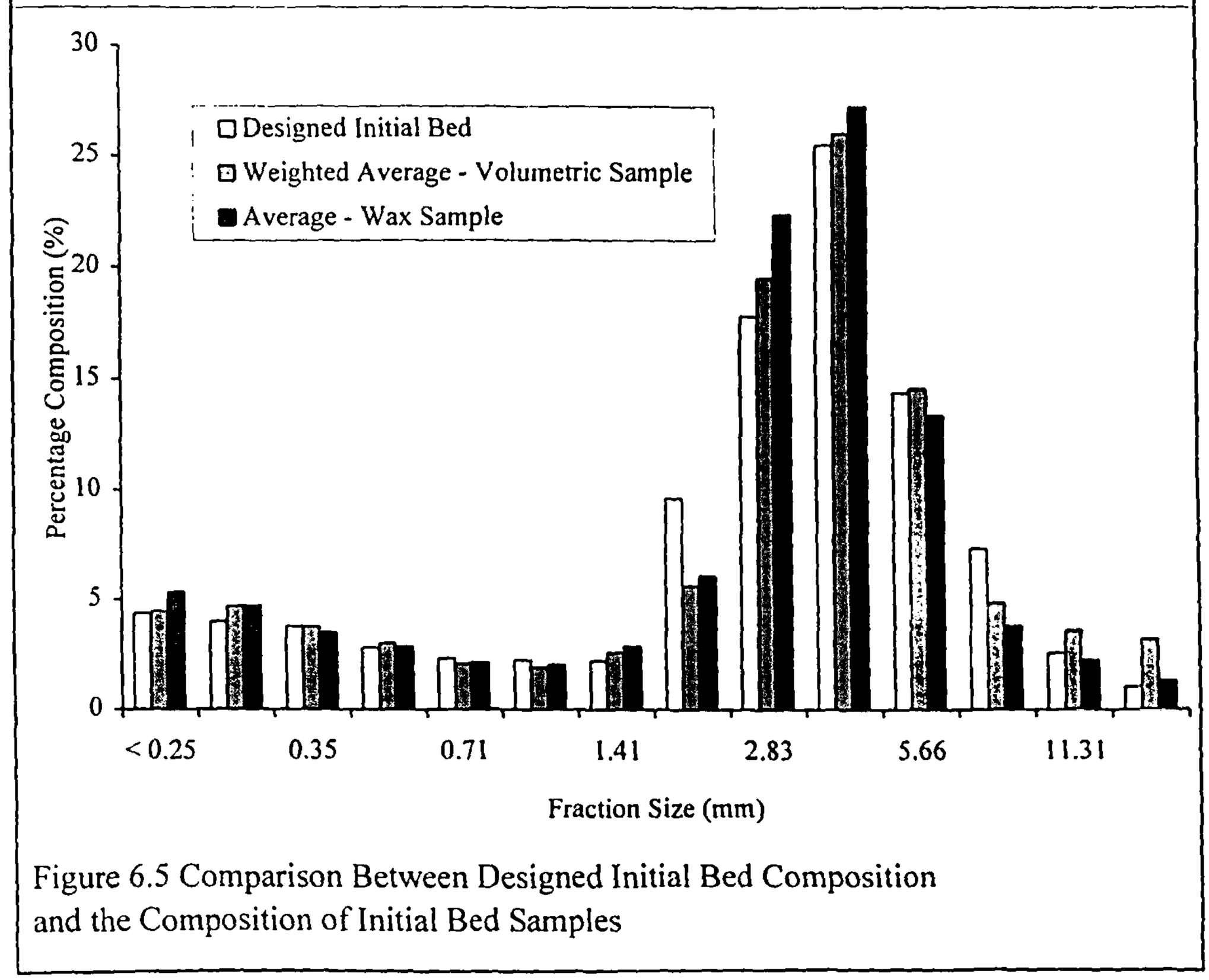

Figure 6.5 Comparison Between Designed Initial Bed Composition and the Composition of Initial Bed Samples

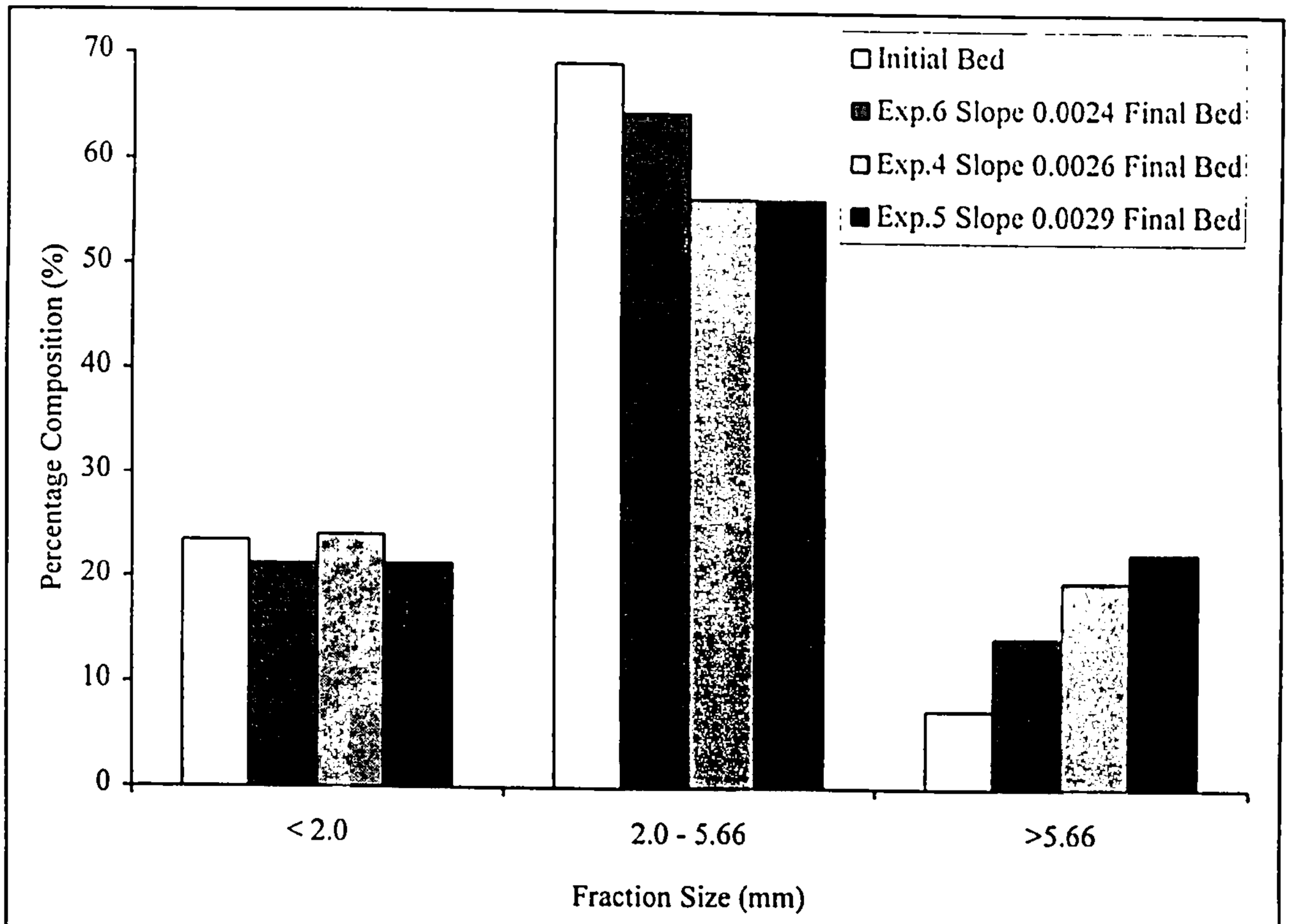

Figure 6.6a Initial and Final Bed Surface Compositions, Bankfull Experiments

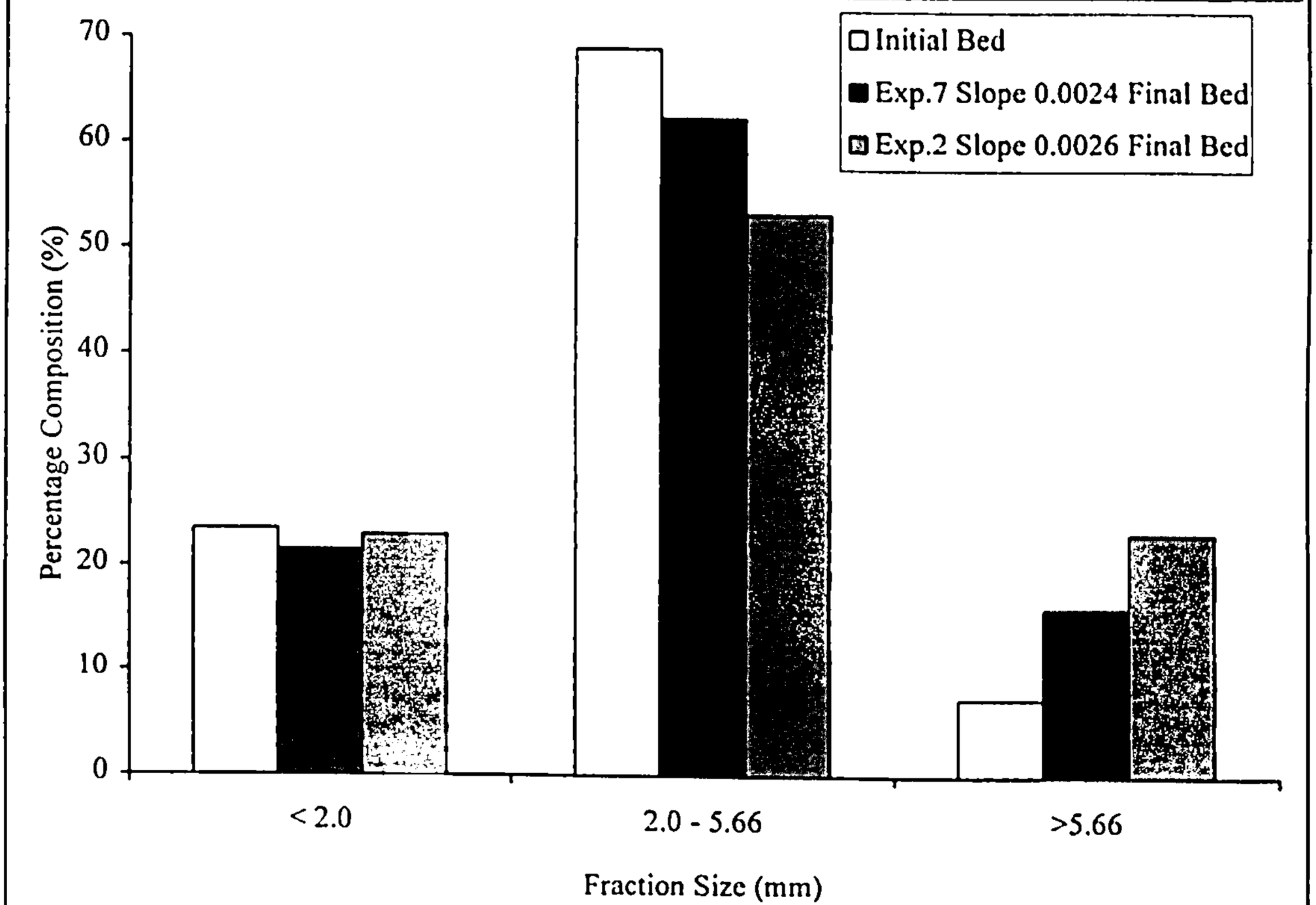

Figure 6.6b Initial and Final Bed Surface Compositions, Shallow Overbank Experiments

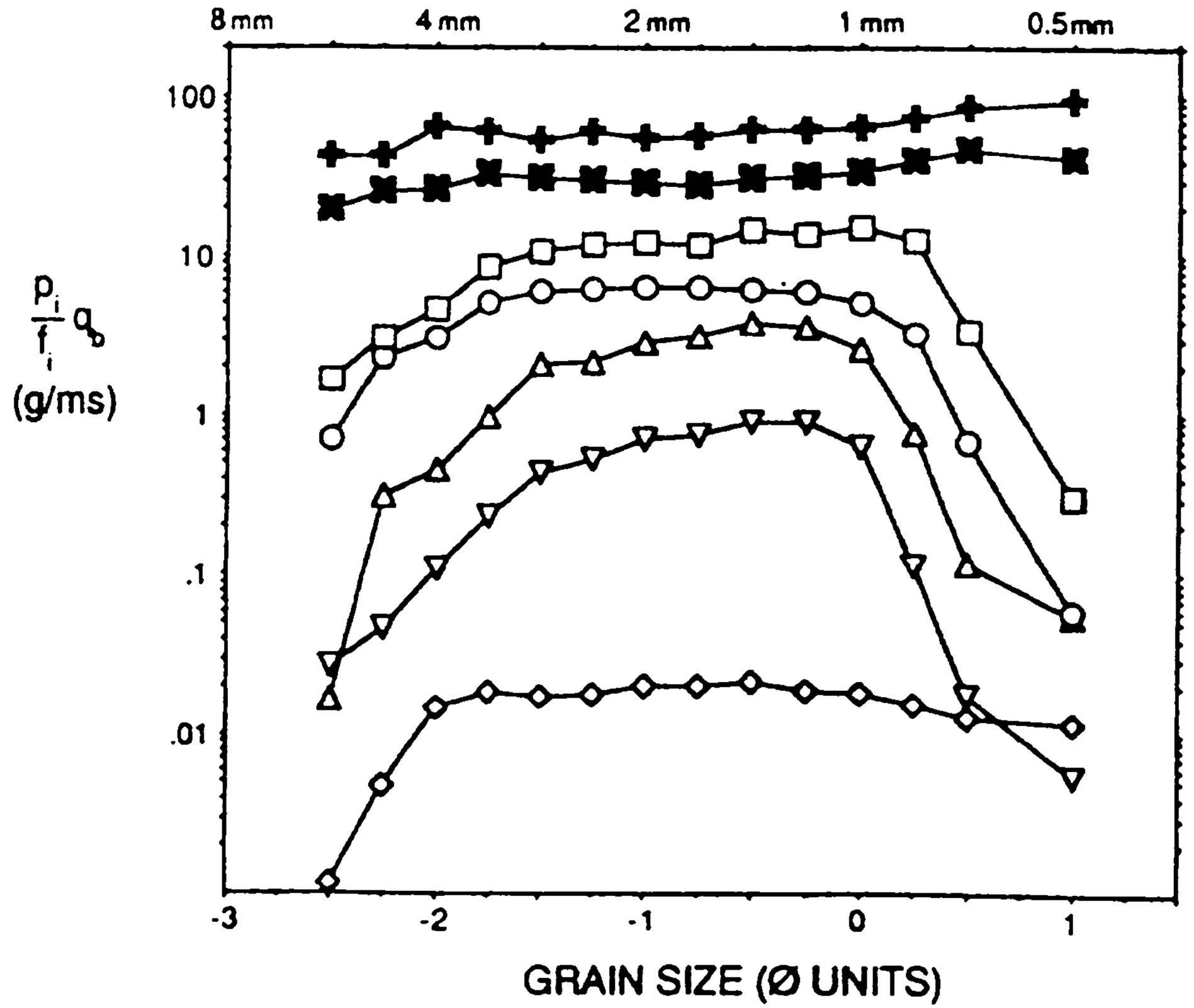

Figure 6.7 Wilcock Style Plot of Relative Fraction Mobility Against Grain Size [Wilcock and Southard (1989) - fig.4]

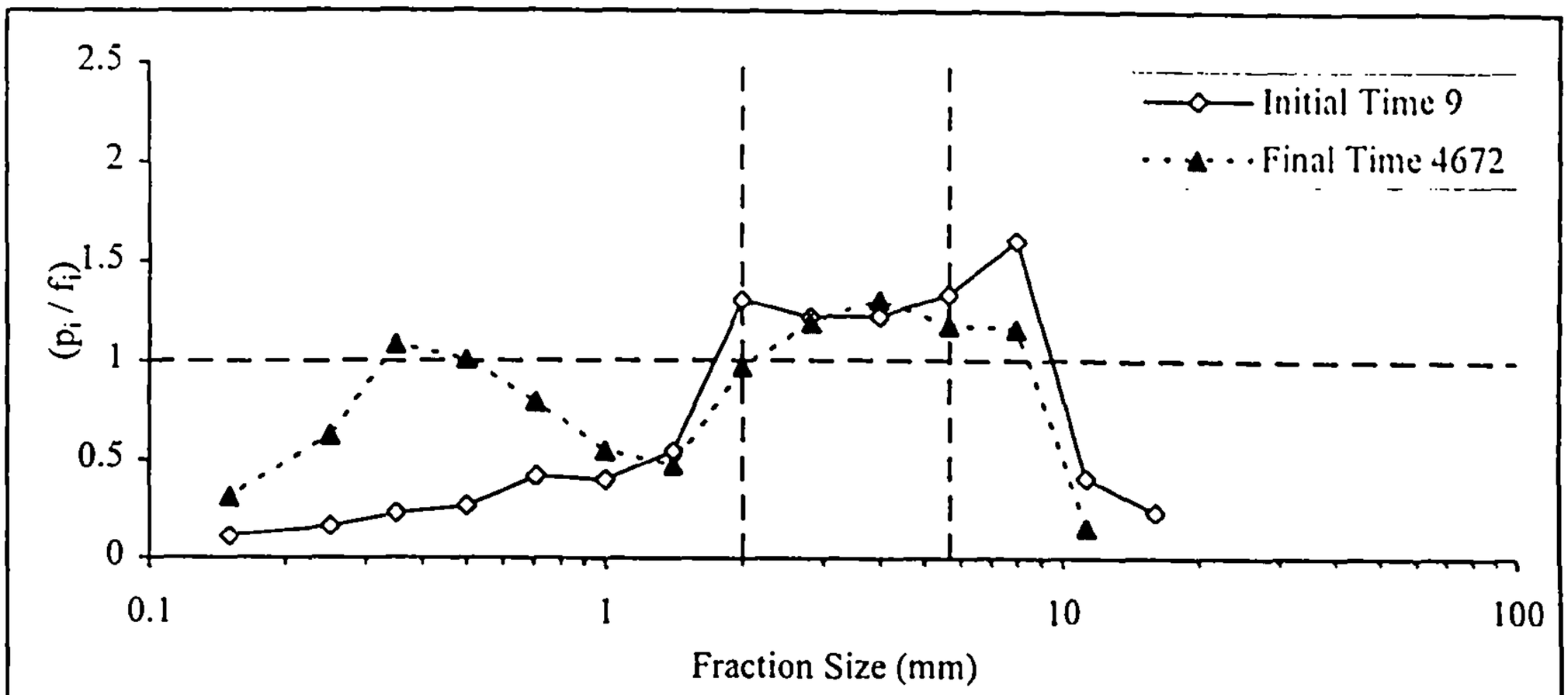

Figure 6.8a Initial and Final Fraction Mobility,
Experiment 6, Slope 0.0024, Bankfull

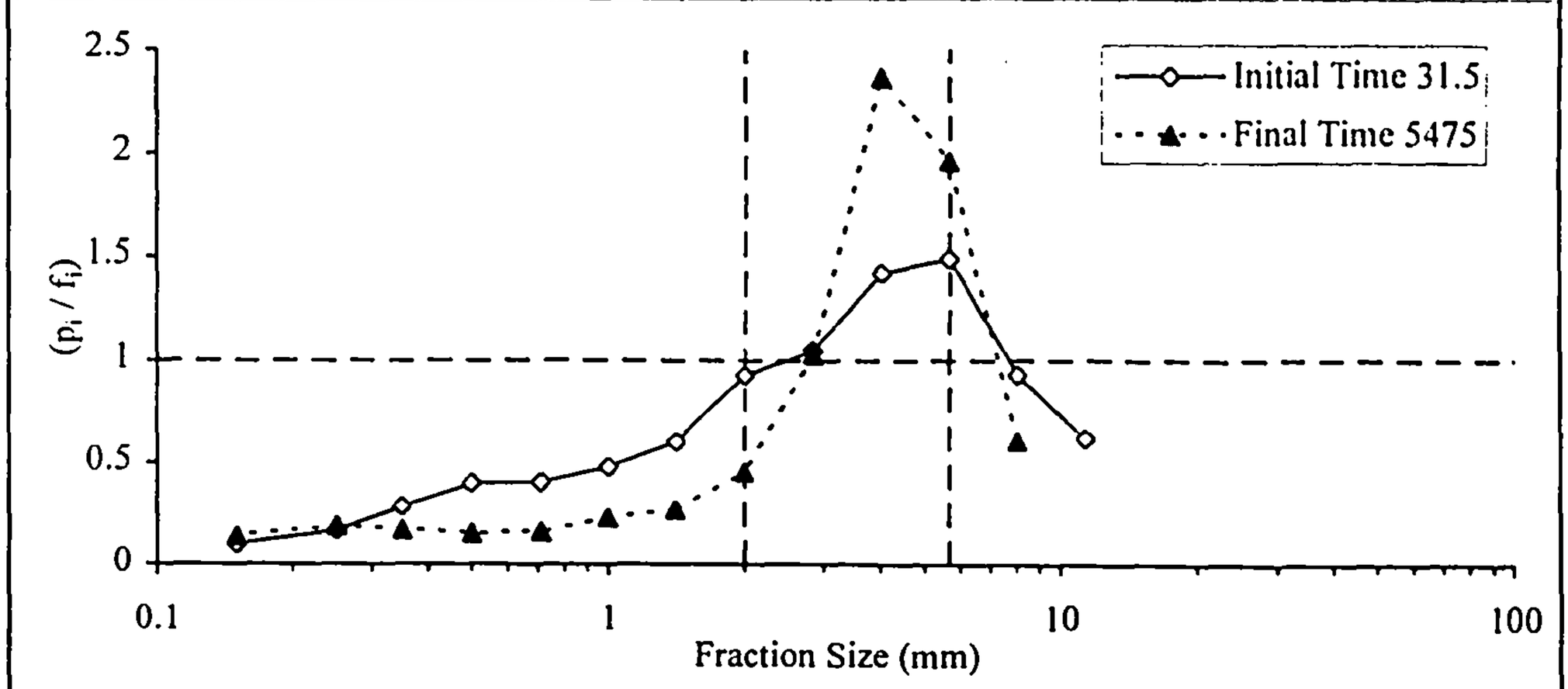

Figure 6.8b Initial and Final Fraction Mobility,
Experiment 4, Slope 0.0026, Bankfull

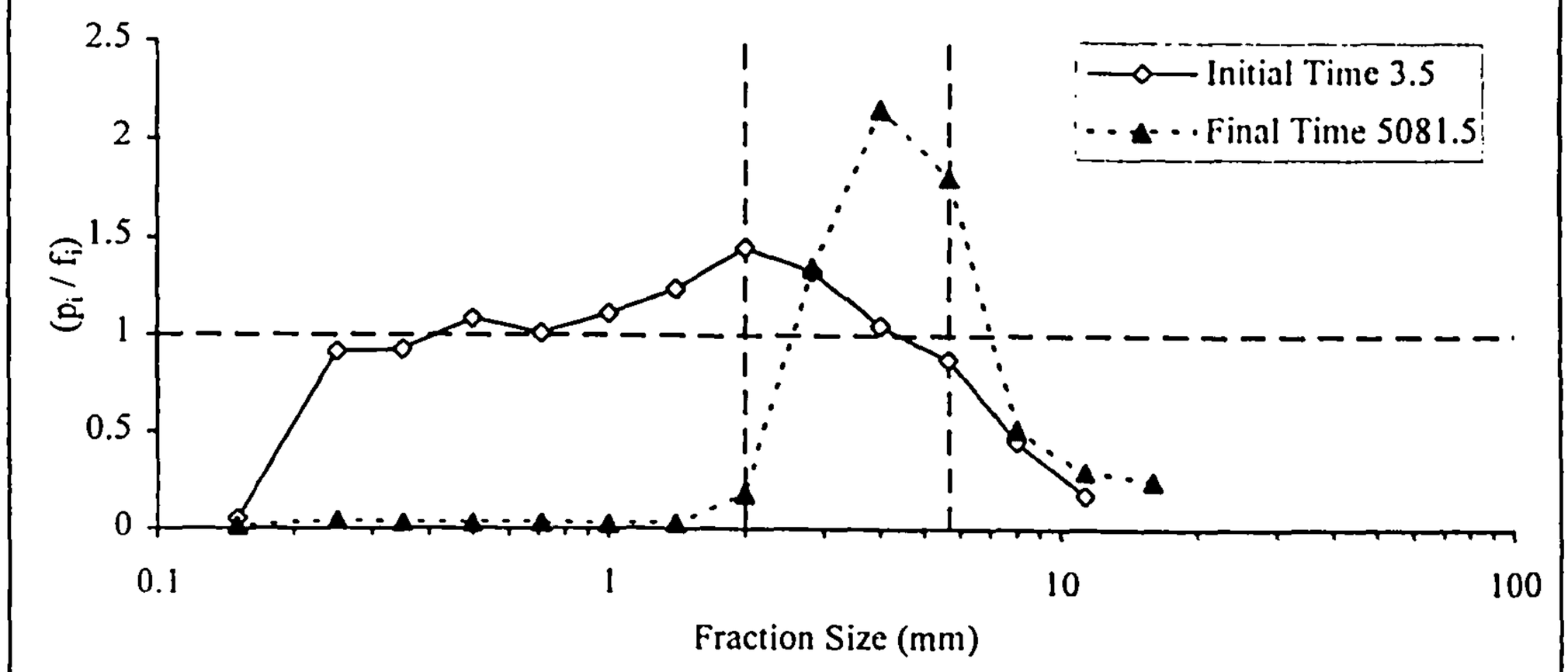

Figure 6.8c Initial and Final Fraction Mobility,
Experiment 5, Slope 0.0029, Bankfull

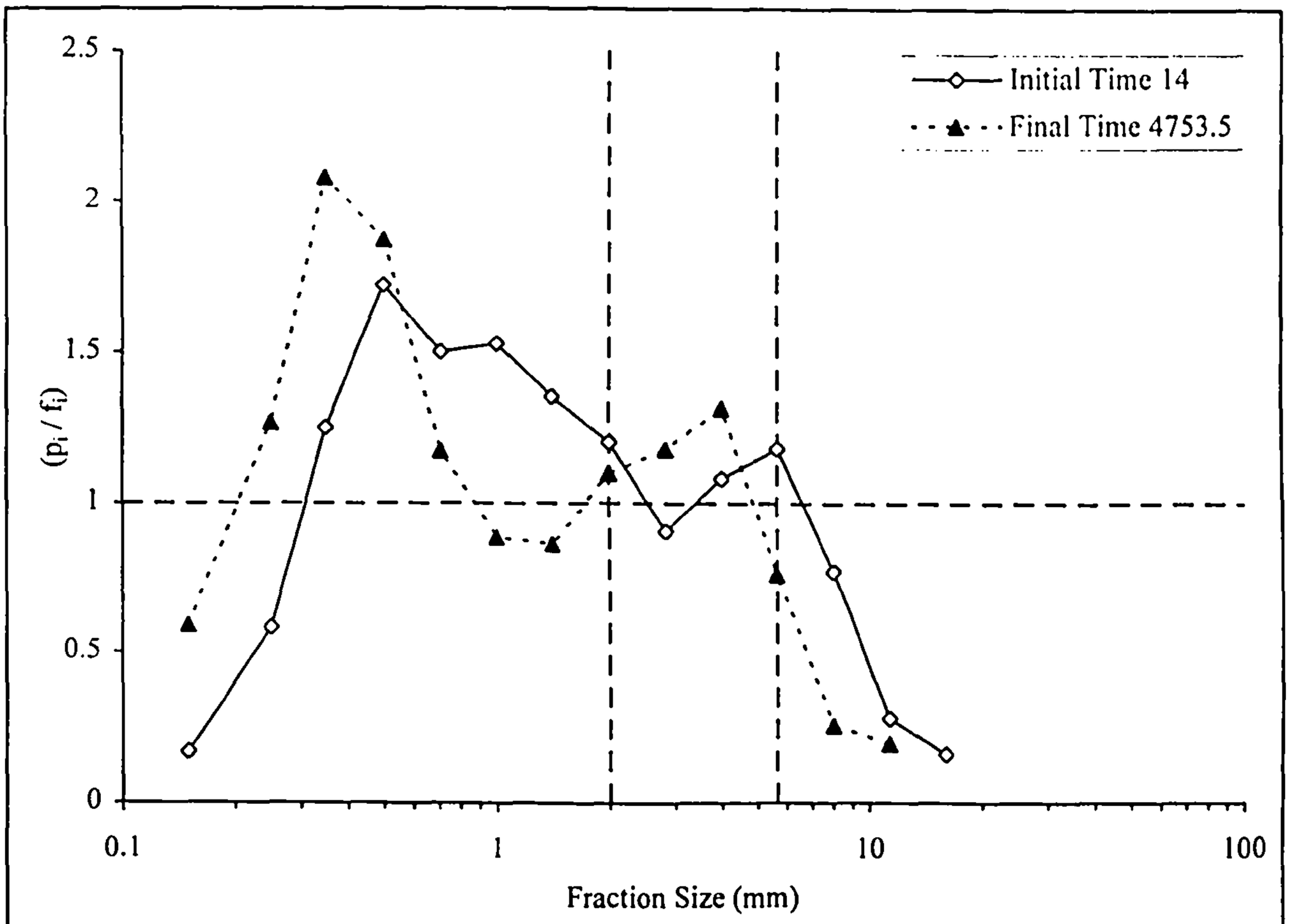

Figure 6.9a Initial and Final Fraction Mobility,
Experiment 7, Slope 0.0024, Shallow Overbank

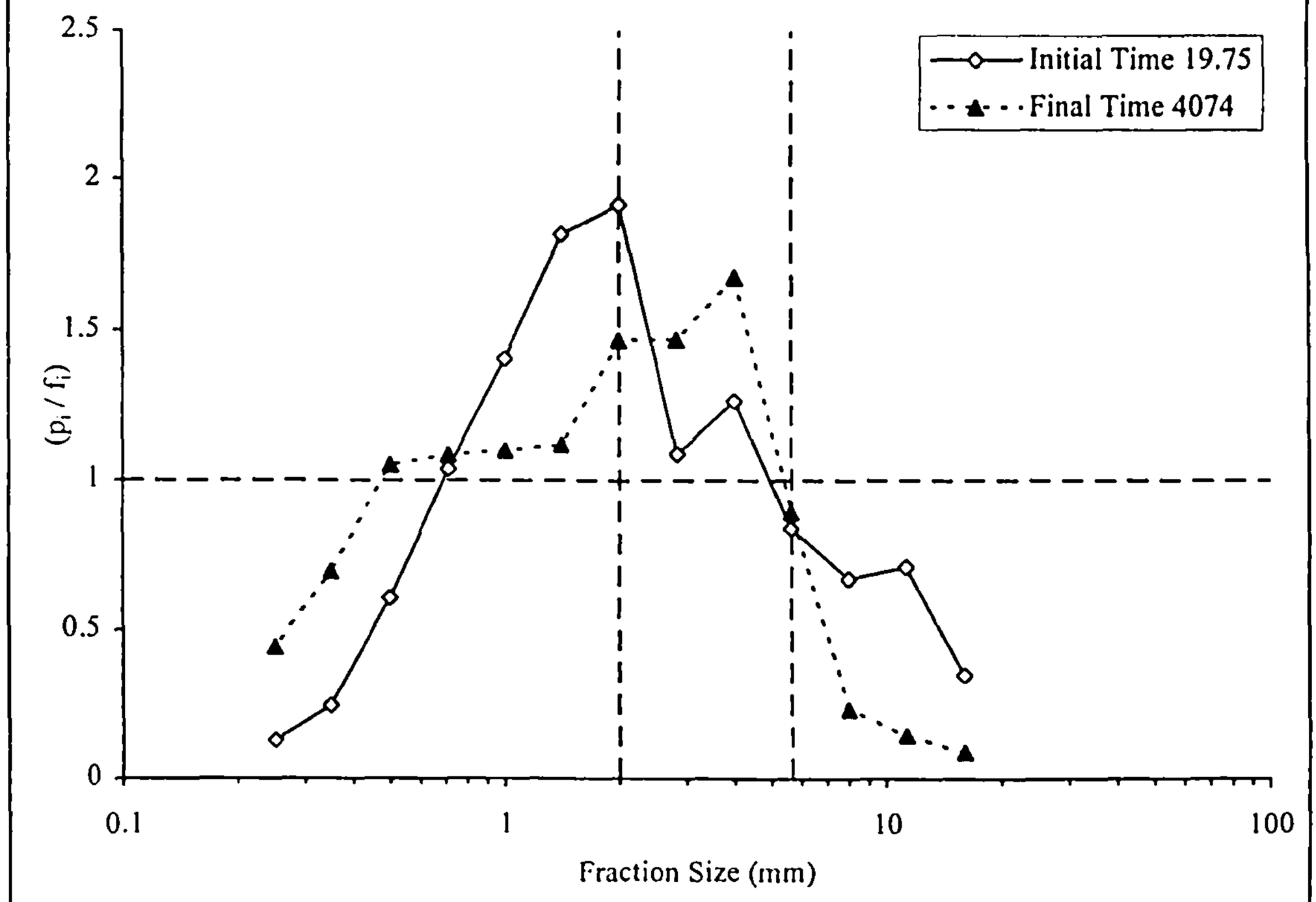

Figure 6.9b Initial and Final Fraction Mobility,
Experiment 2, Slope 0.0026, Shallow Overbank

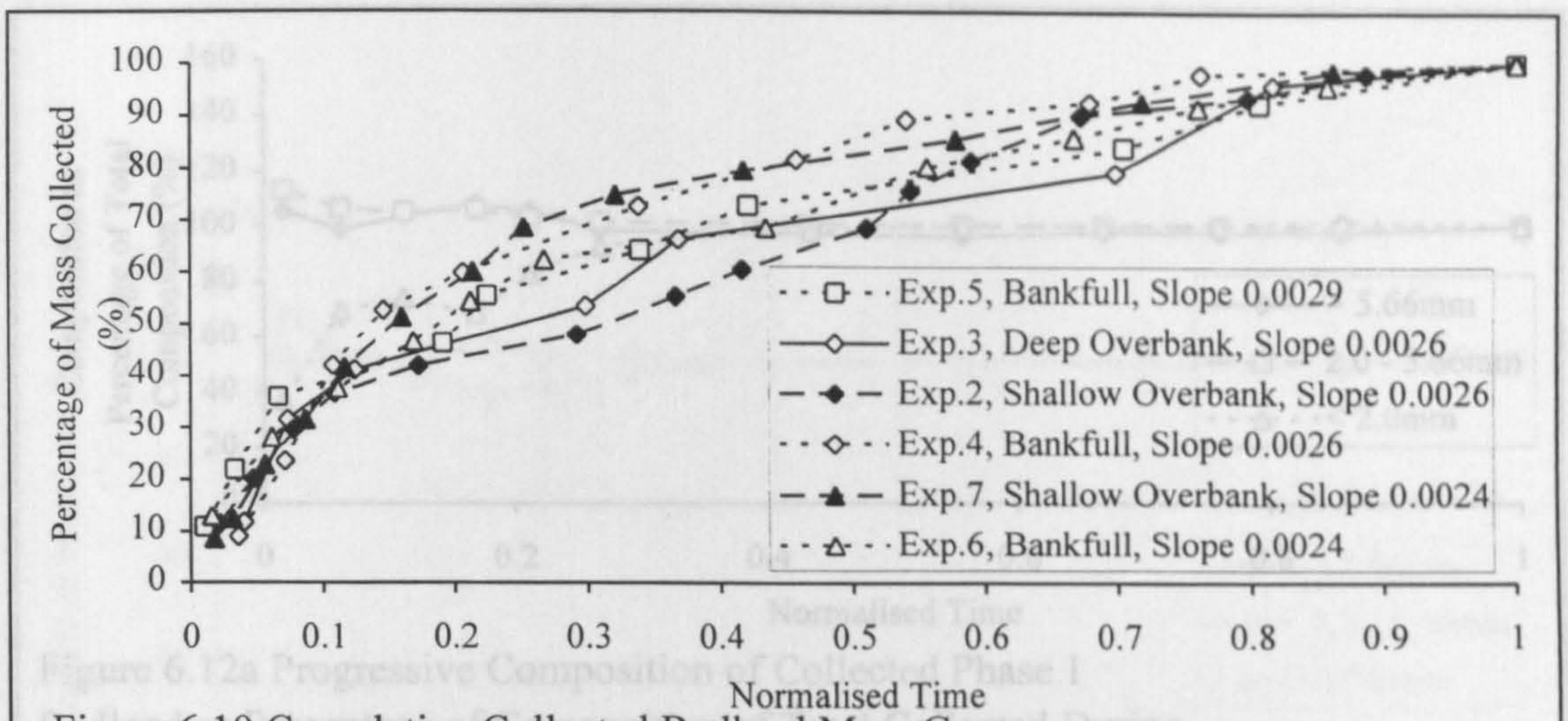

Figure 6.10 Cumulative Collected Bedload Mass Curves, Phase 1

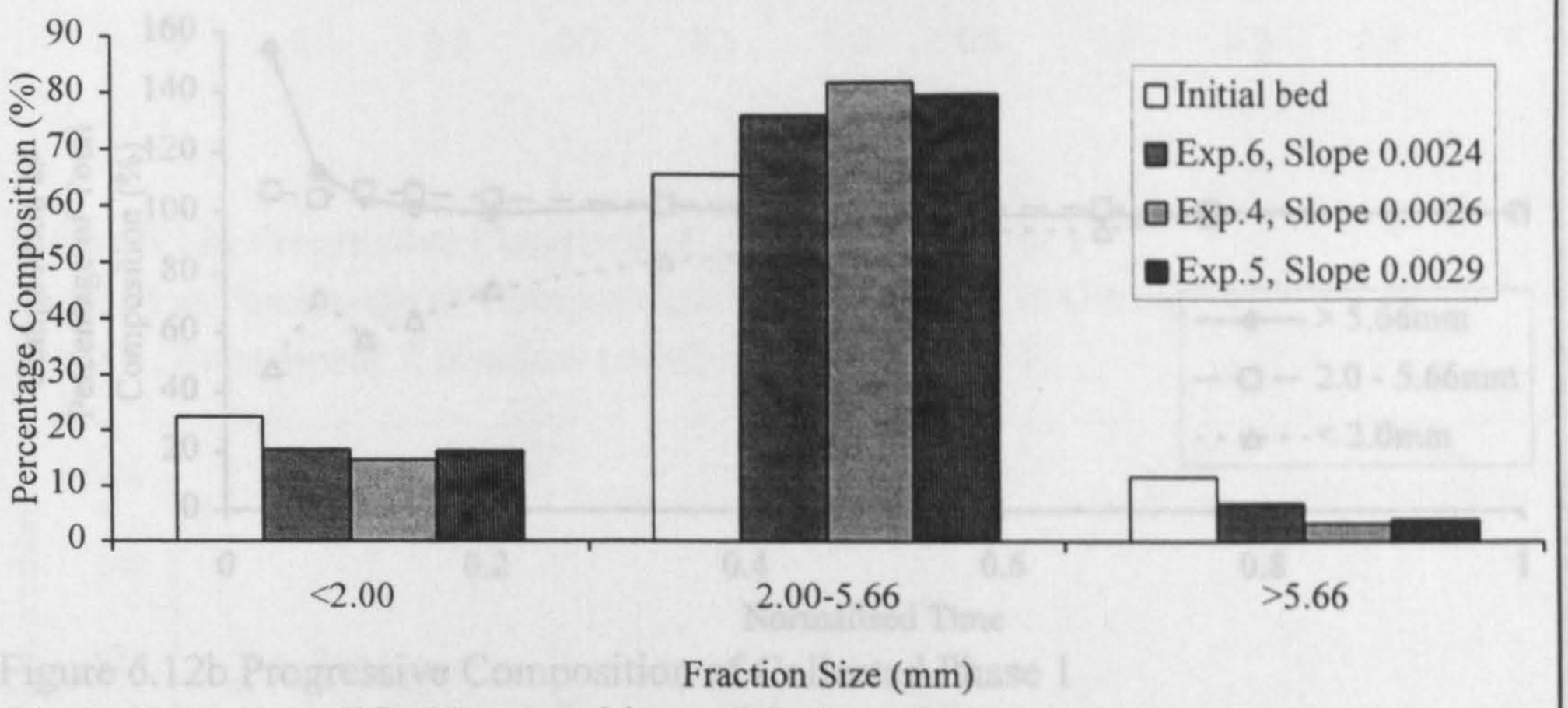

Figure 6.11a Simplified Compositions of Collected Phase 1 Bedload, Bankfull Experiments

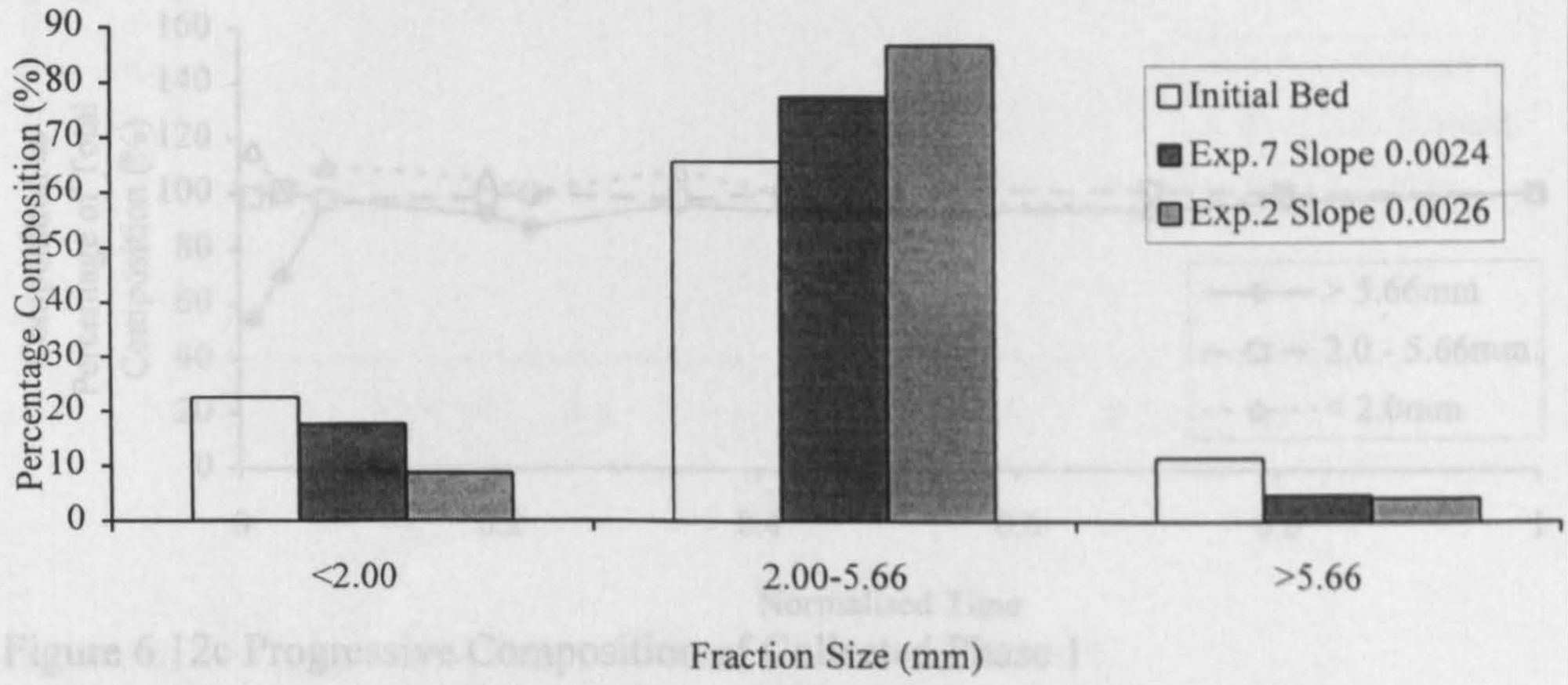

Figure 6.11b Simplified Compositions of Collected Phase 1 Bedload, Shallow Overbank Experiments

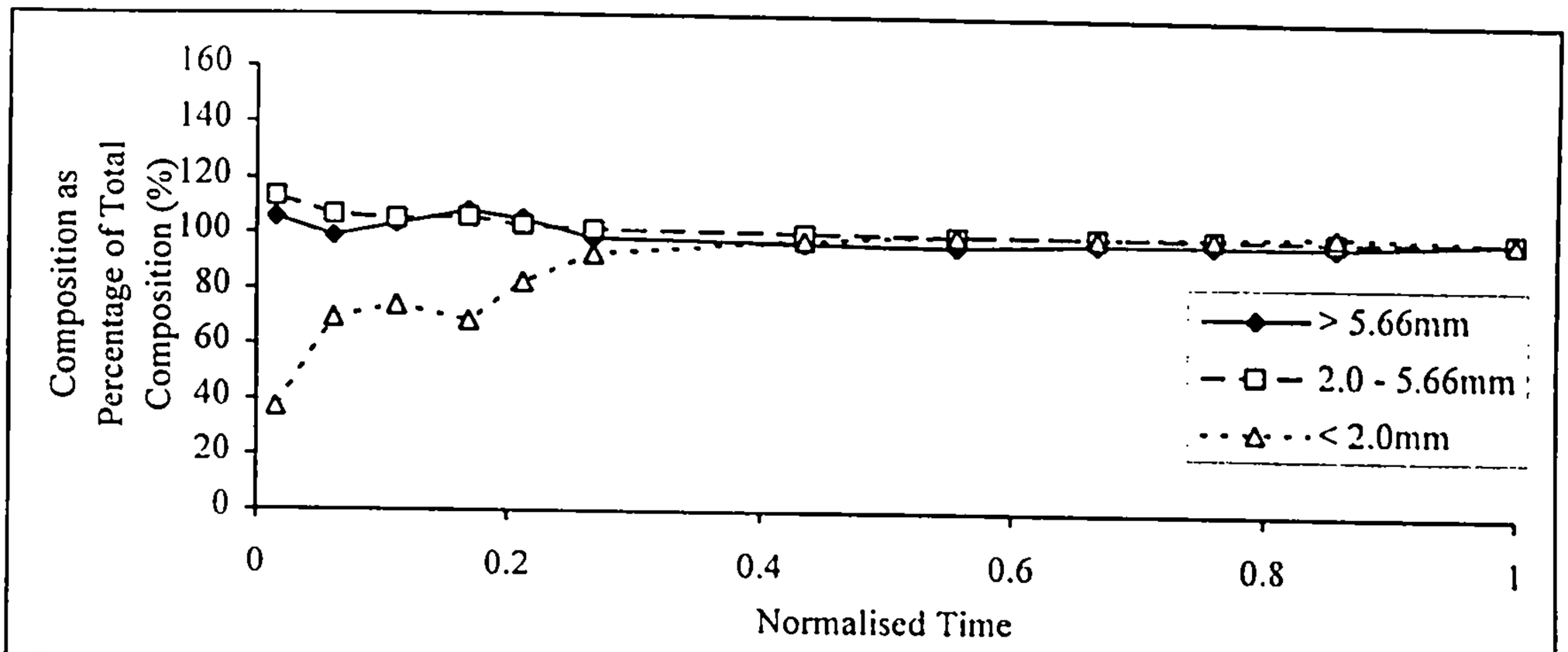

Figure 6.12a Progressive Composition of Collected Phase 1 Bedload as Percentage of Composition of Total Collected During Phase 1, Experiment 6, Bankfull, Slope 0.0024

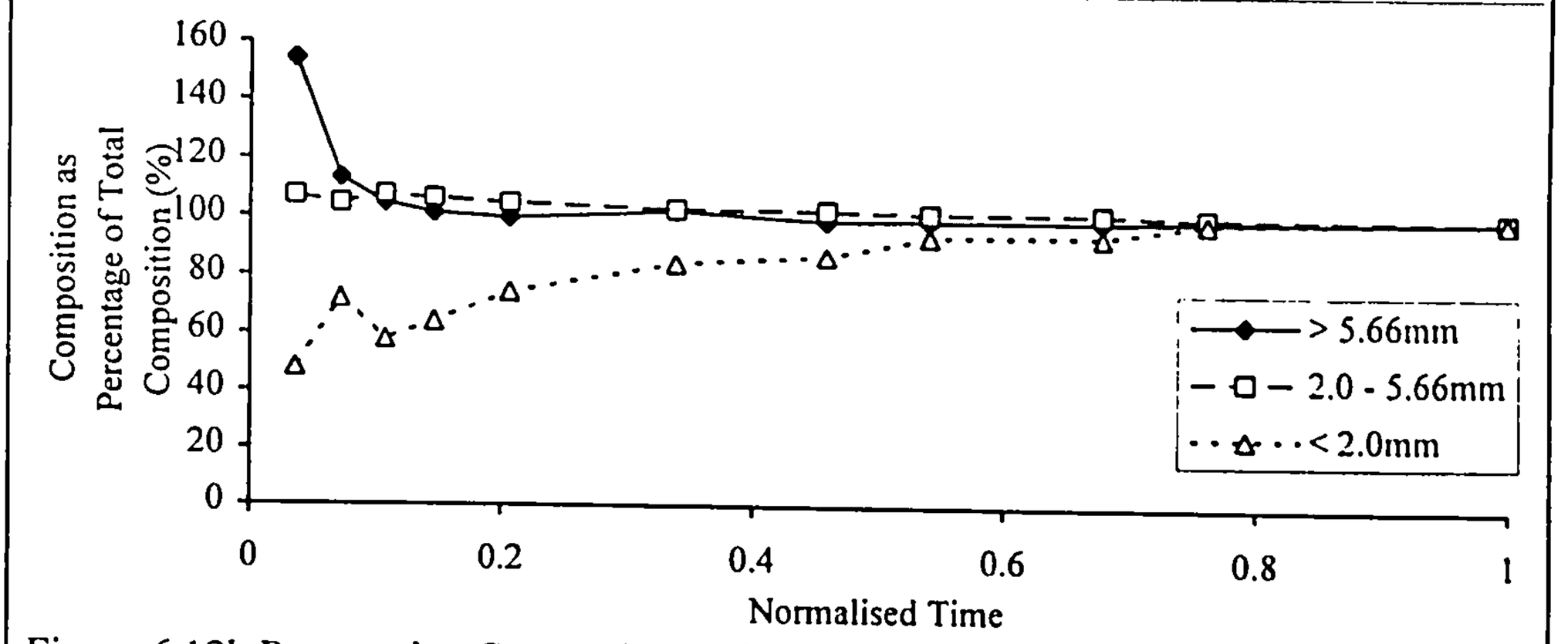

Figure 6.12b Progressive Composition of Collected Phase 1 Bedload as Percentage of Composition of Total Collected During Phase 1, Experiment 4, Bankfull, Slope 0.0026

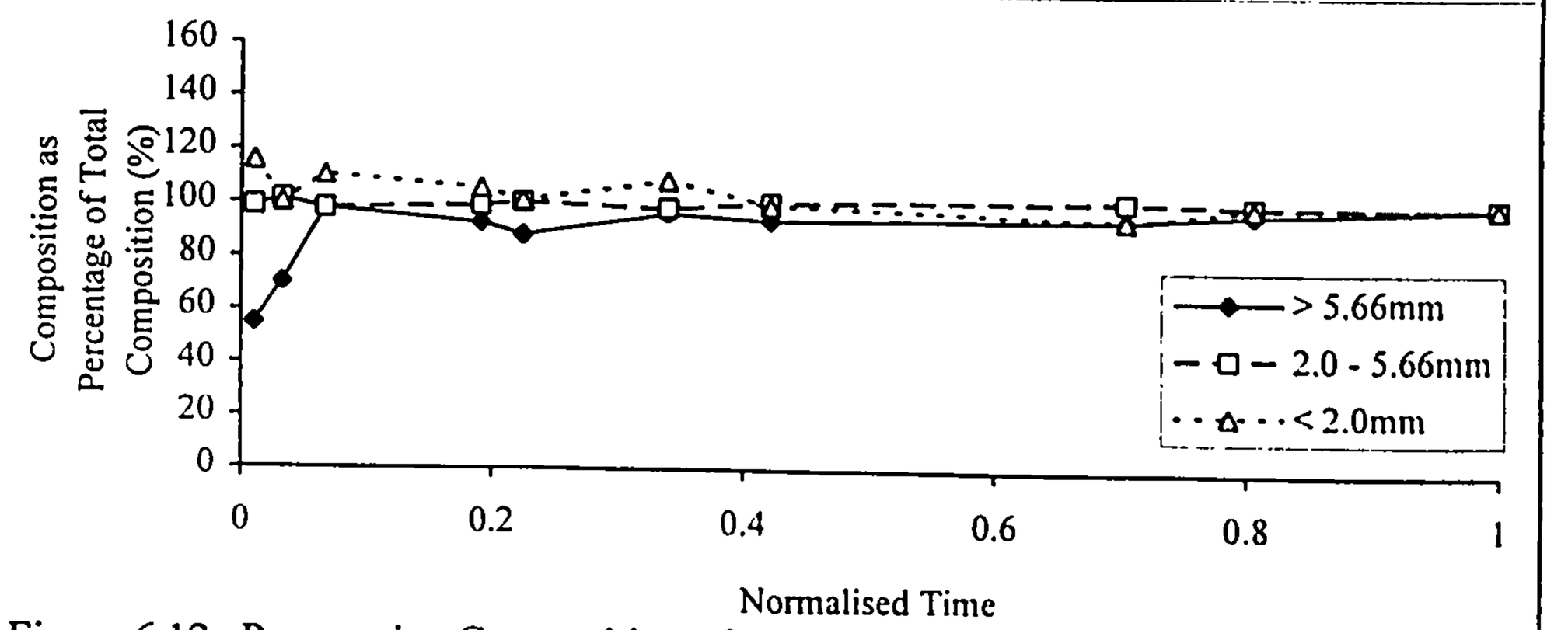

Figure 6.12c Progressive Composition of Collected Phase 1 Bedload as Percentage of Composition of Total Collected During Phase 1, Experiment 5, Bankfull, Slope 0.0029

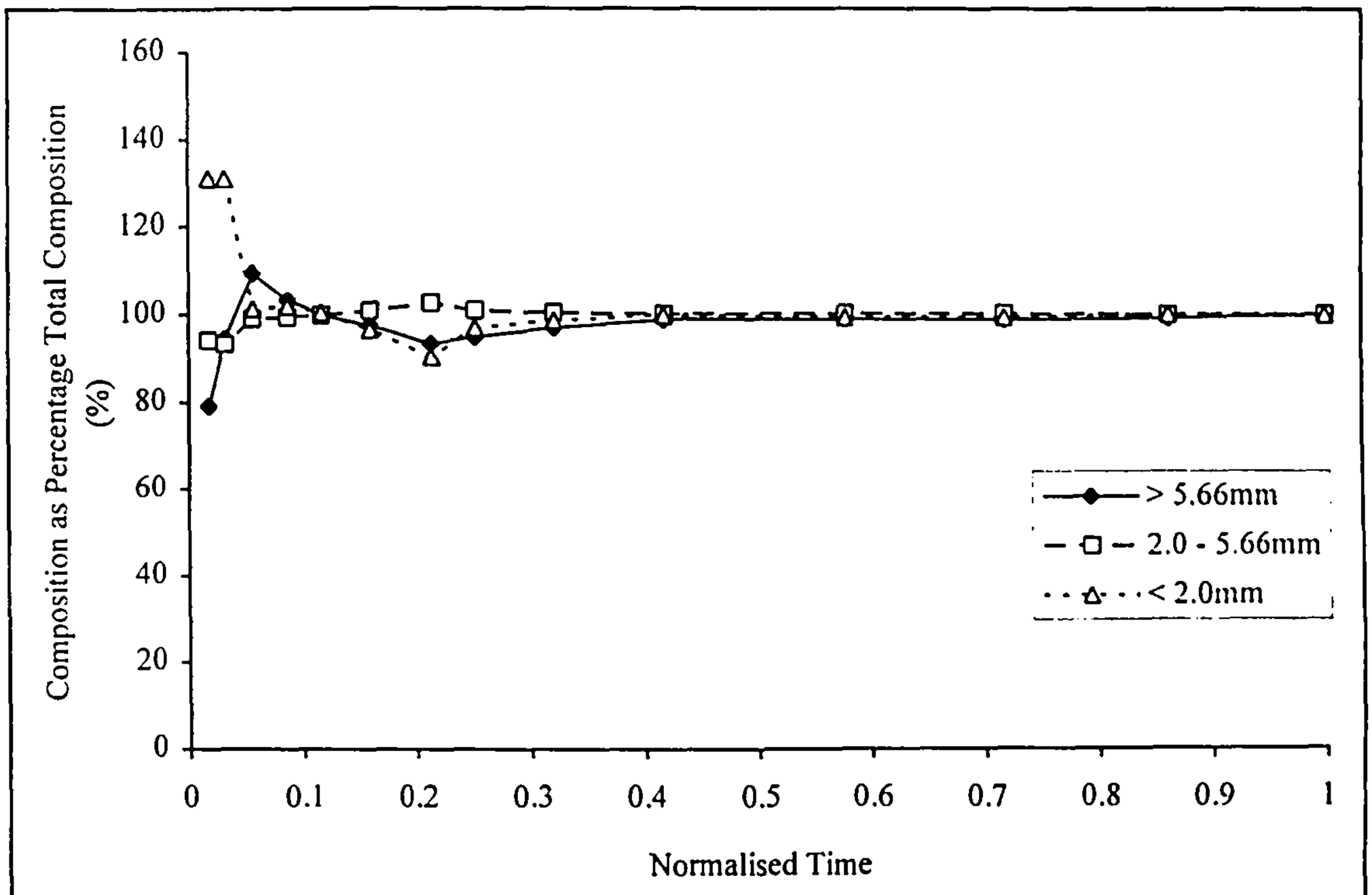

Figure 6.13a Progressive Composition of Collected Phase 1 Bedload as Percentage of Composition of Total Collected During Phase 1, Experiment 7, Shallow Overbank, Slope 0.0024

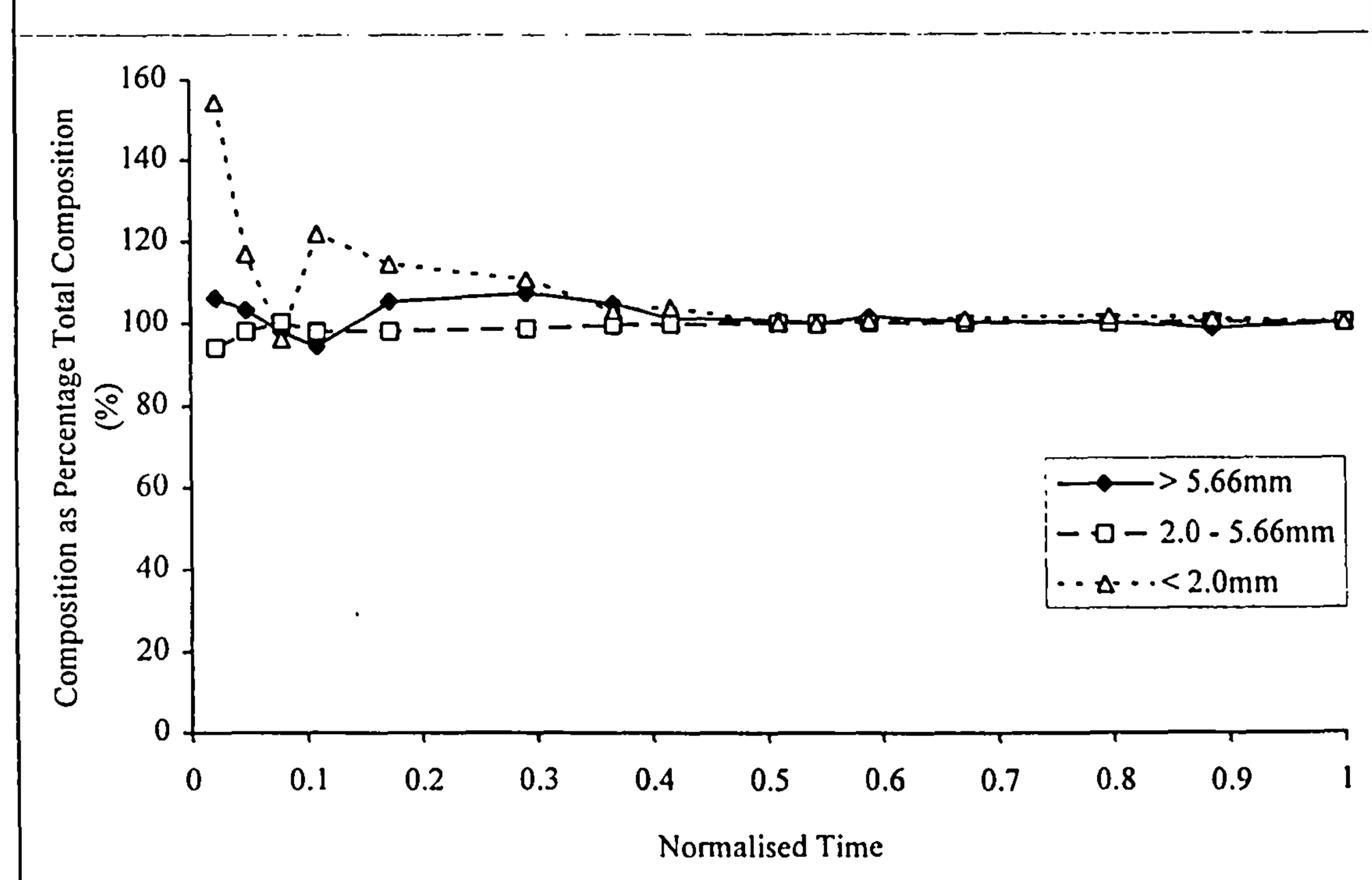

Figure 6.13b Progressive Composition of Collected Phase 1 Bedload as Percentage of Composition of Total Collected During Phase 1, Experiment 2, Shallow Overbank Slope 0.0026

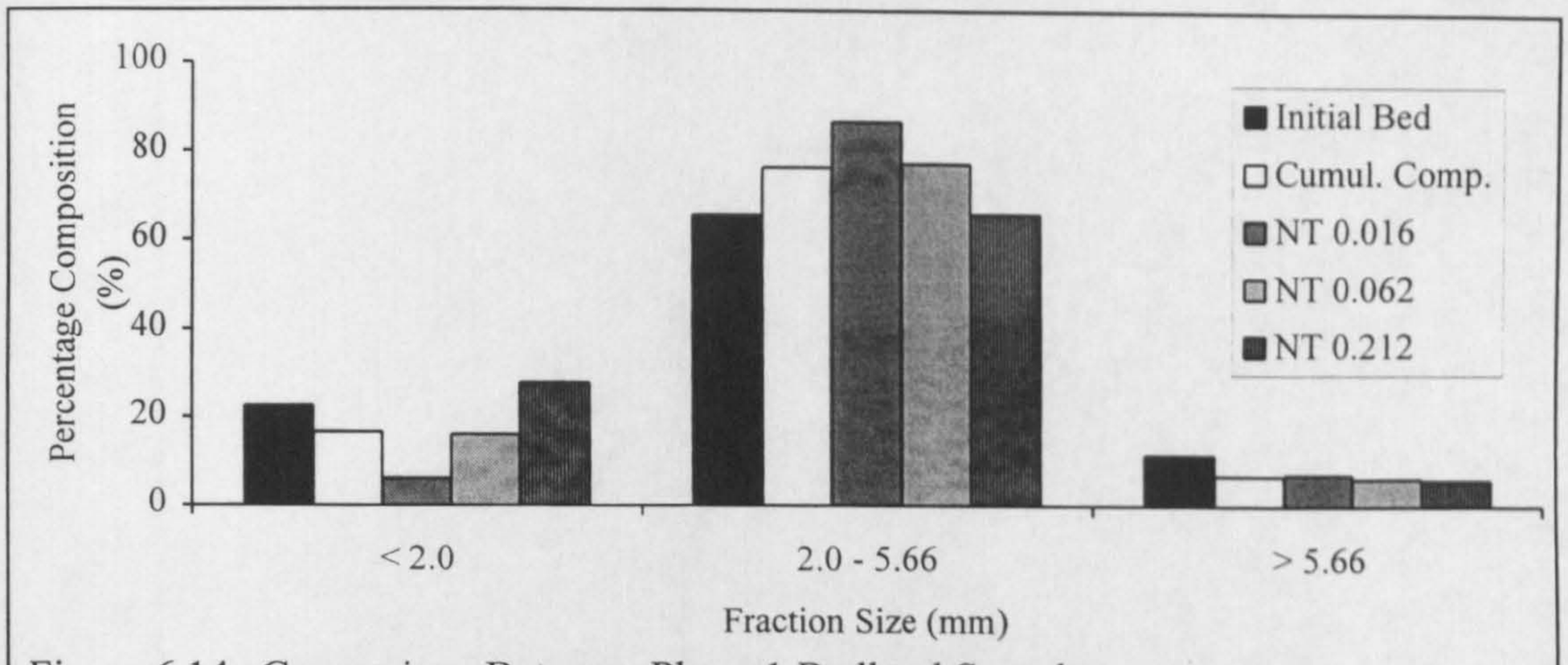

Figure 6.14a Comparison Between Phase 1 Bedload Samples, Cumulative and Initial Bed Simplified Compositions, Experiment 6, Bankfull, Slope 0.0024

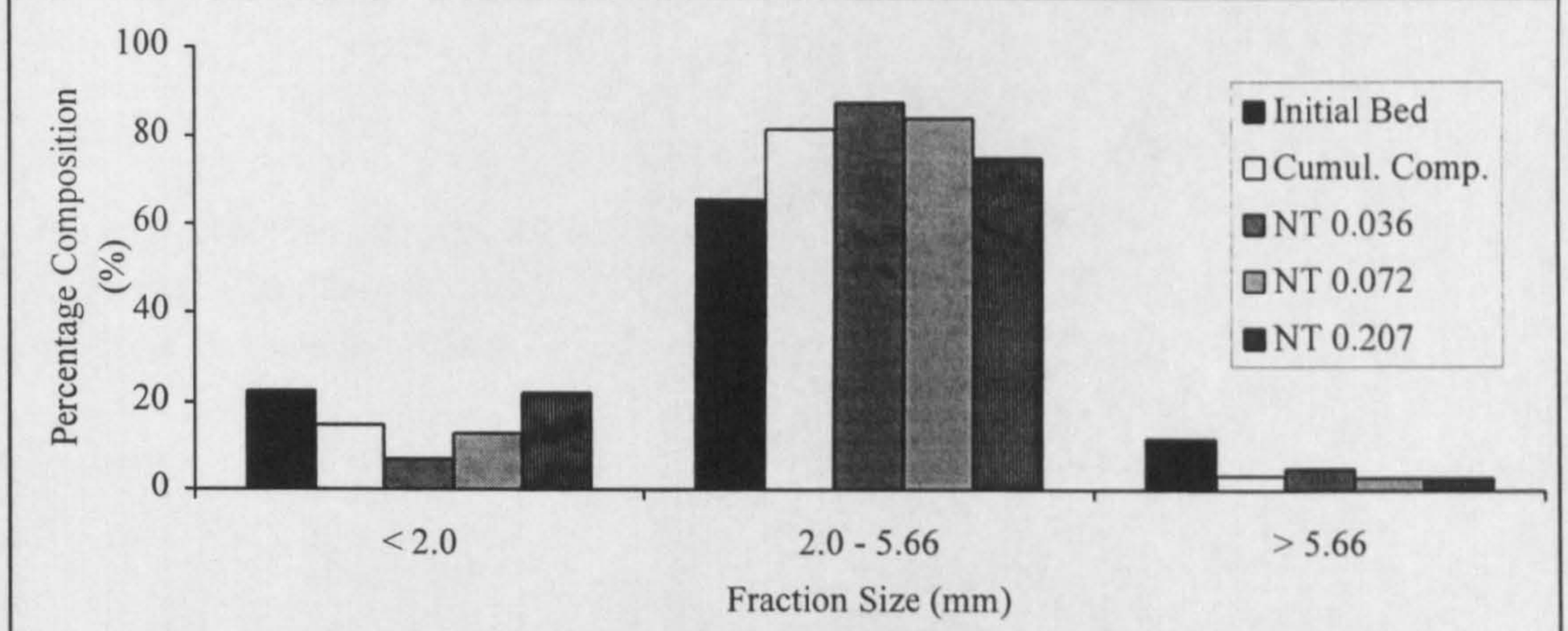

Figure 6.14b Comparison Between Phase 1 Bedload Samples, Cumulative and Initial Bed Simplified Compositions, Experiment 4, Bankfull, Slope 0.0026

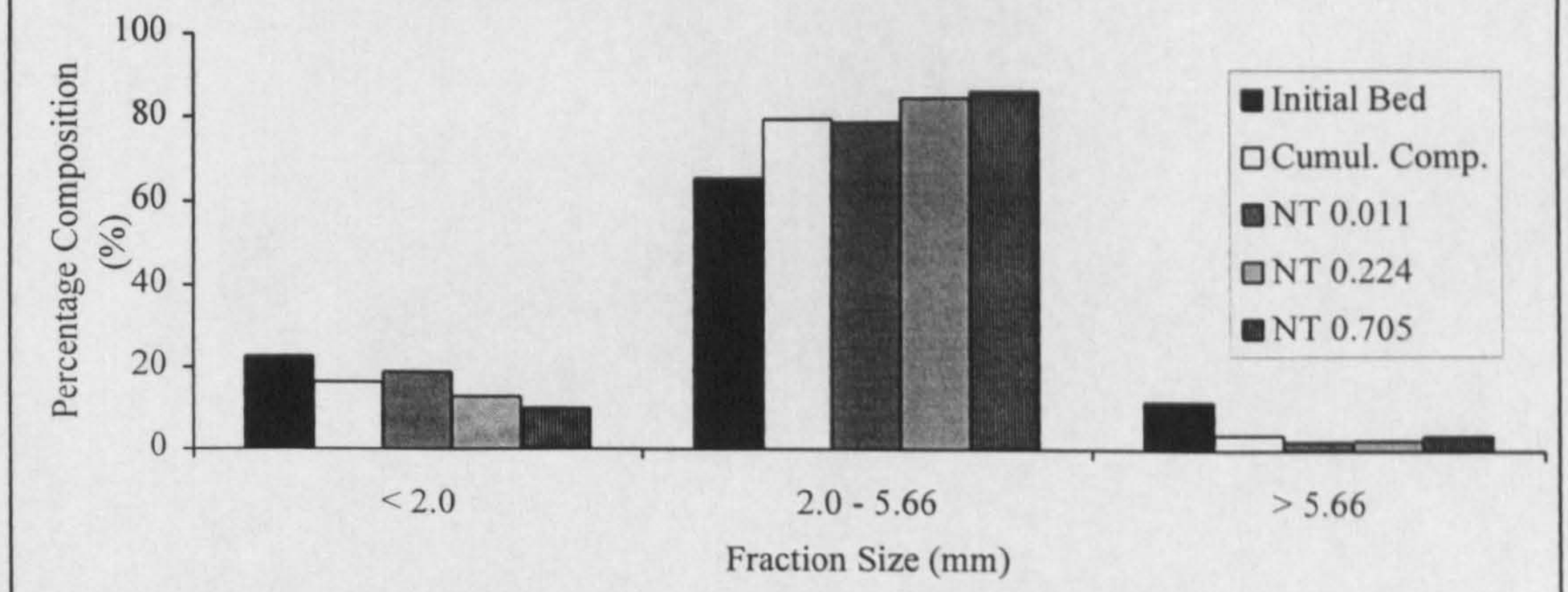

Figure 6.14c Comparison Between Phase 1 Bedload Samples, Cumulative and Initial Bed Simplified Compositions, Experiment 5, Bankfull, Slope 0.0029

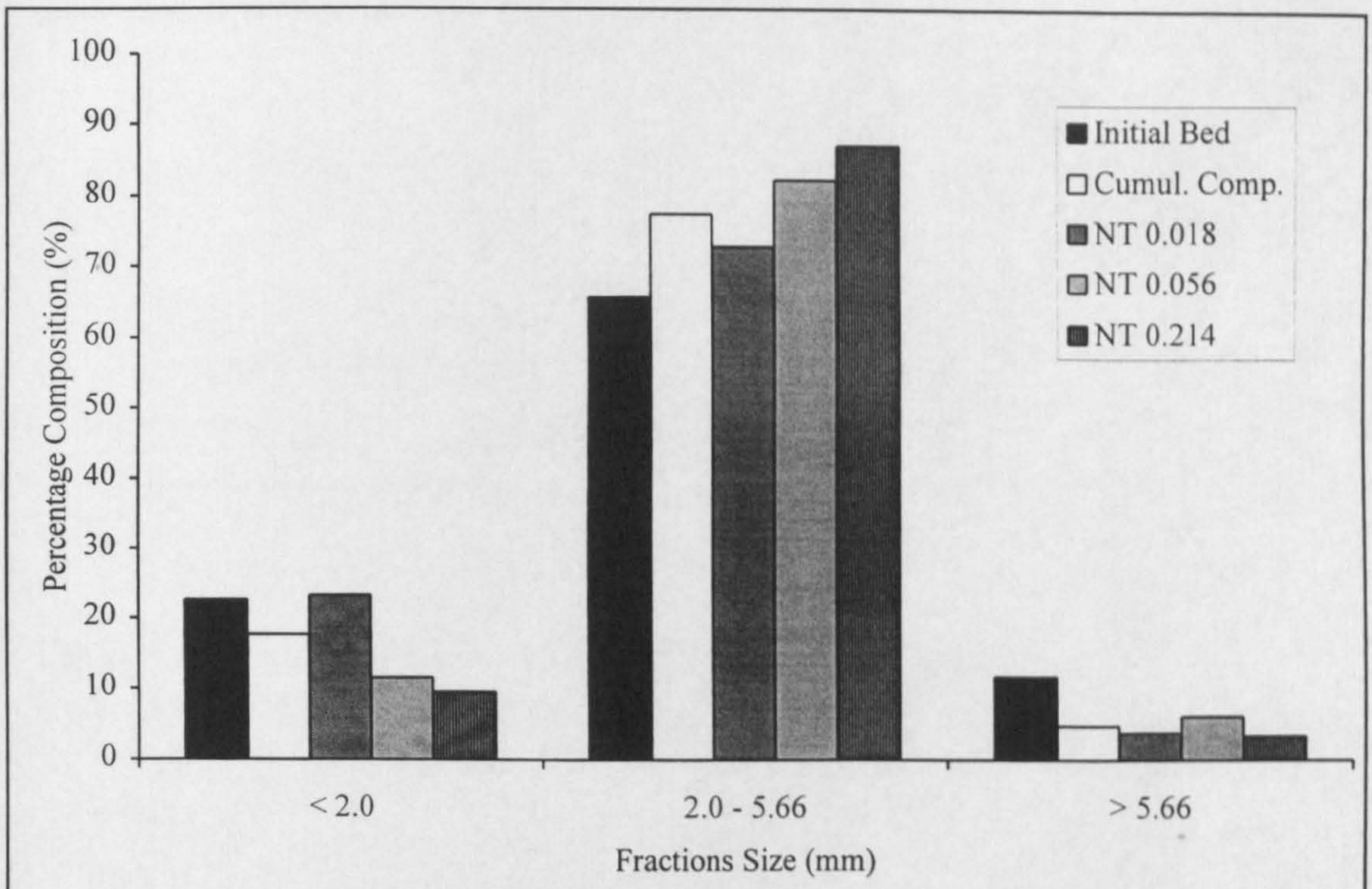

Figure 6.15a Comparison Between Phase 1 Bedload Samples, Cumulative and Initial Bed Simplified Compositions, Experiment 7, Shallow Overbank, Slope 0.0024

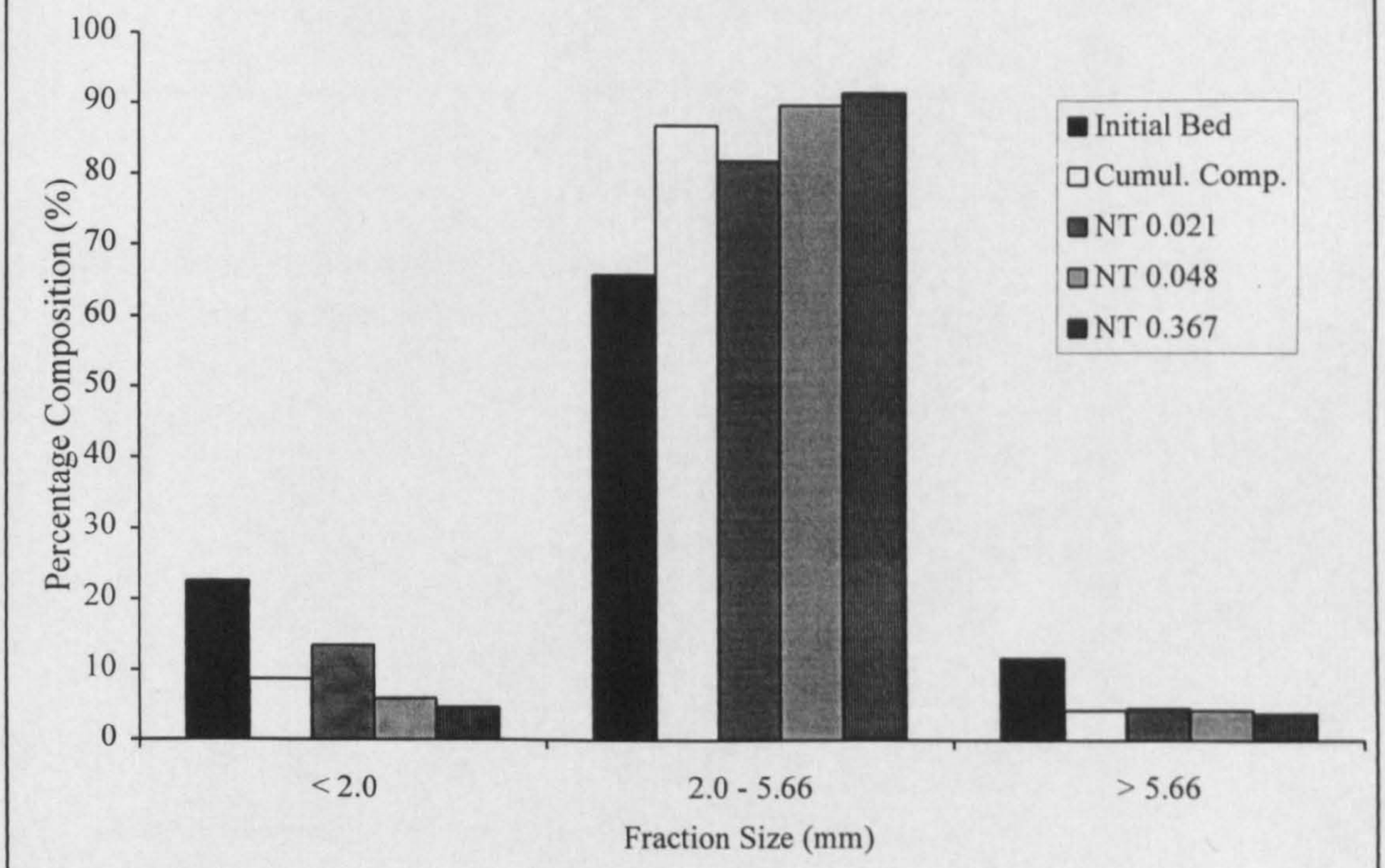

Figure 6.15b Comparison Between Phase 1 Bedload Samples, Cumulative and Initial Bed Simplified Compositions, Experiment 2, Shallow Overbank, Slope 0.0026

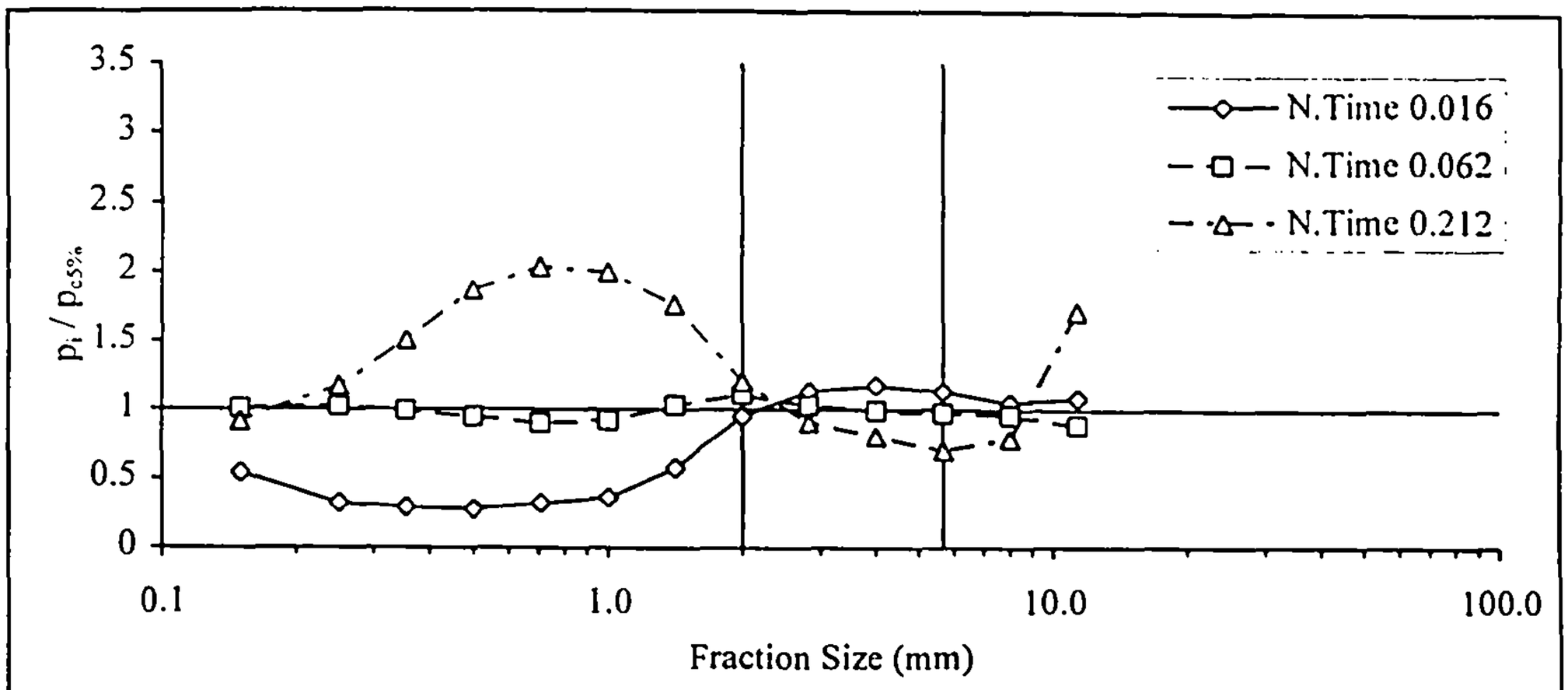

Figure 6.16a Fraction Mobility Relative to Total Collected Phase 1 Bedload Composition, Experiment 6, Bankfull, Slope 0.0024

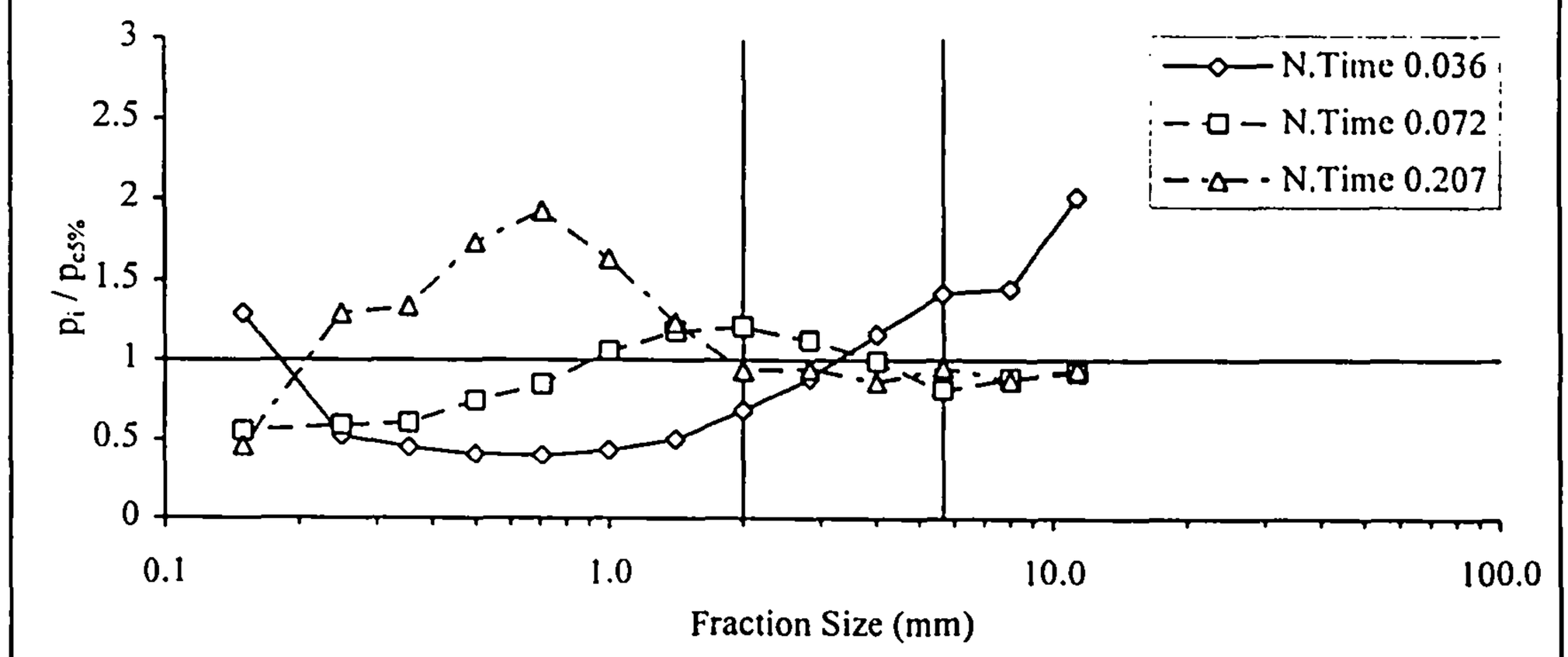

Figure 6.16b Fraction Mobility Relative to Total Collected Phase 1 Bedload Composition, Experiment 4, Bankfull, Slope 0.0026

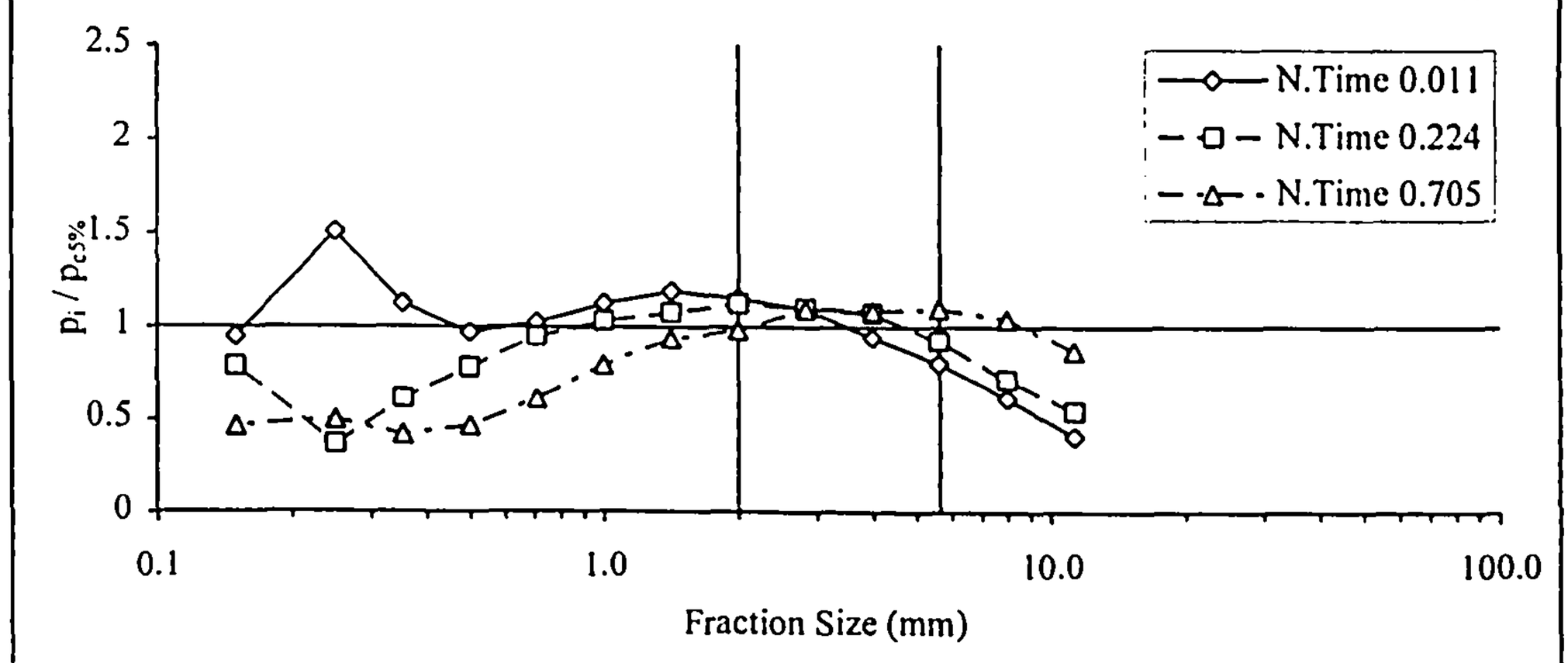

Figure 6.16c Fraction Mobility Relative to Total Collected Phase 1 Bedload Composition, Experiment 5, Bankfull, Slope 0.0029

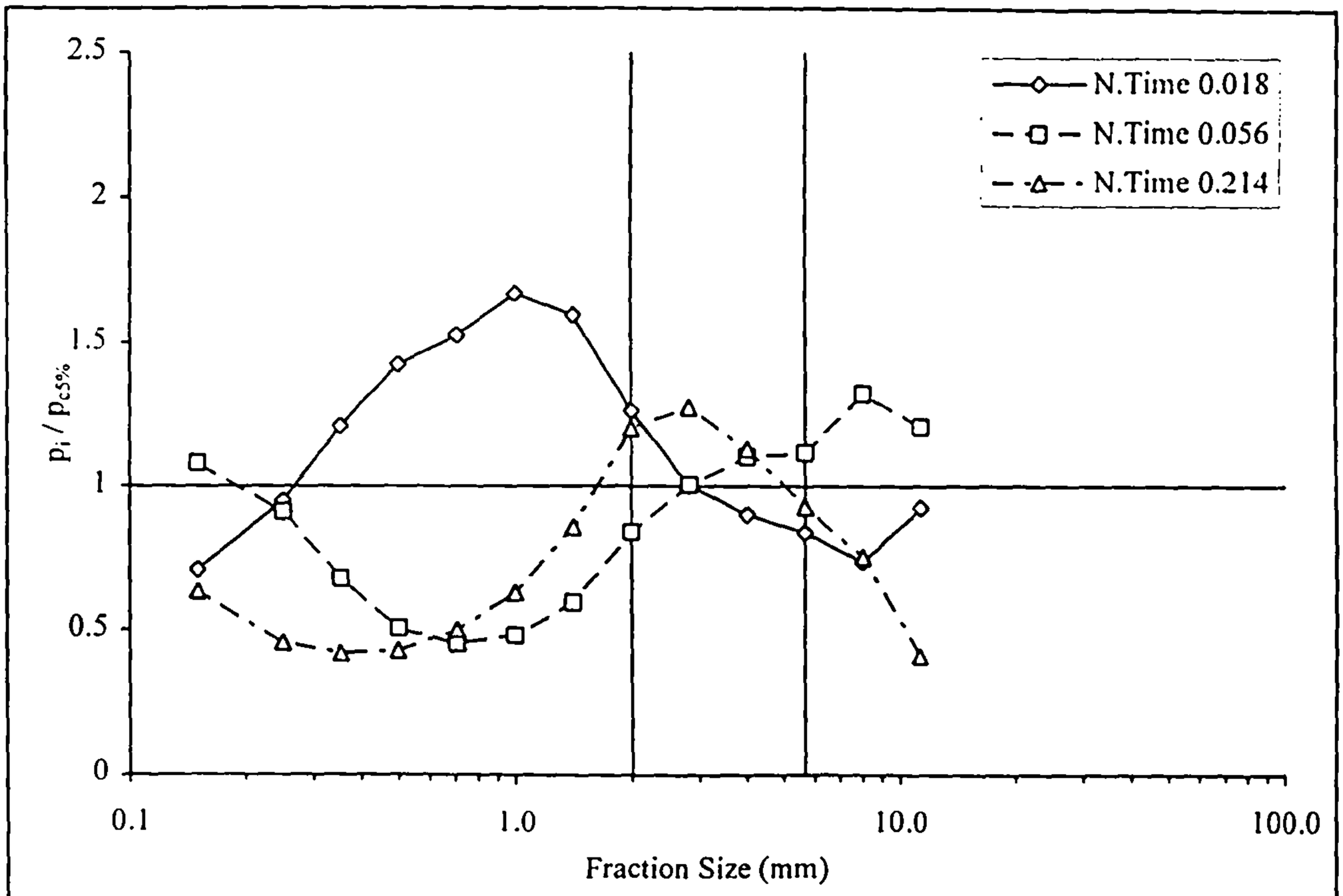

Figure 6.17a Fraction Mobility Relative to Total Collected Phase 1 Bedload Composition, Experiment 7, Shallow Overbank, Slope 0.0024

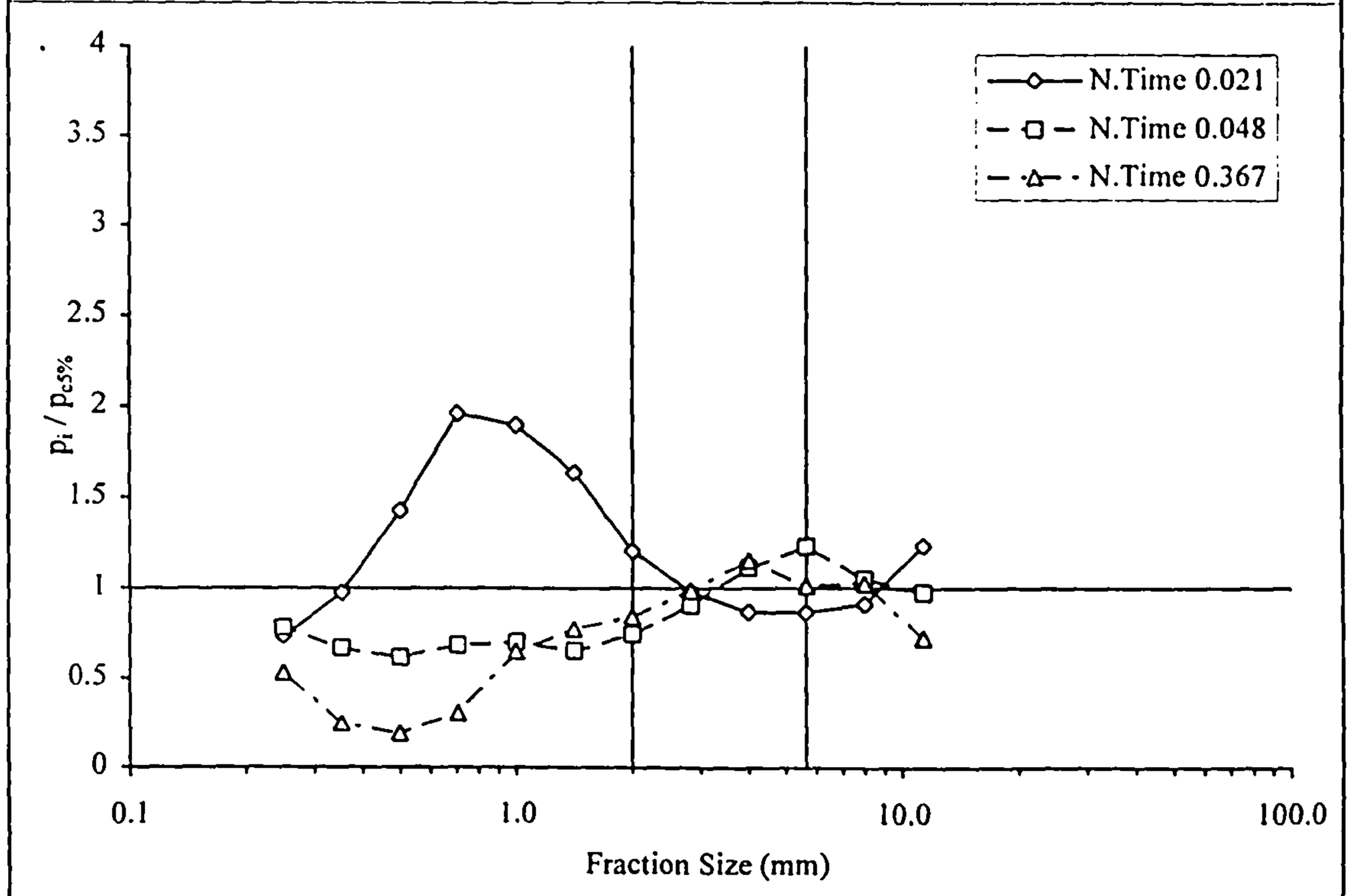

Figure 6.17b Fraction Mobility Relative to Total Collected Phase 1 Bedload Composition, Experiment 2, Shallow Overbank, Slope 0.0026

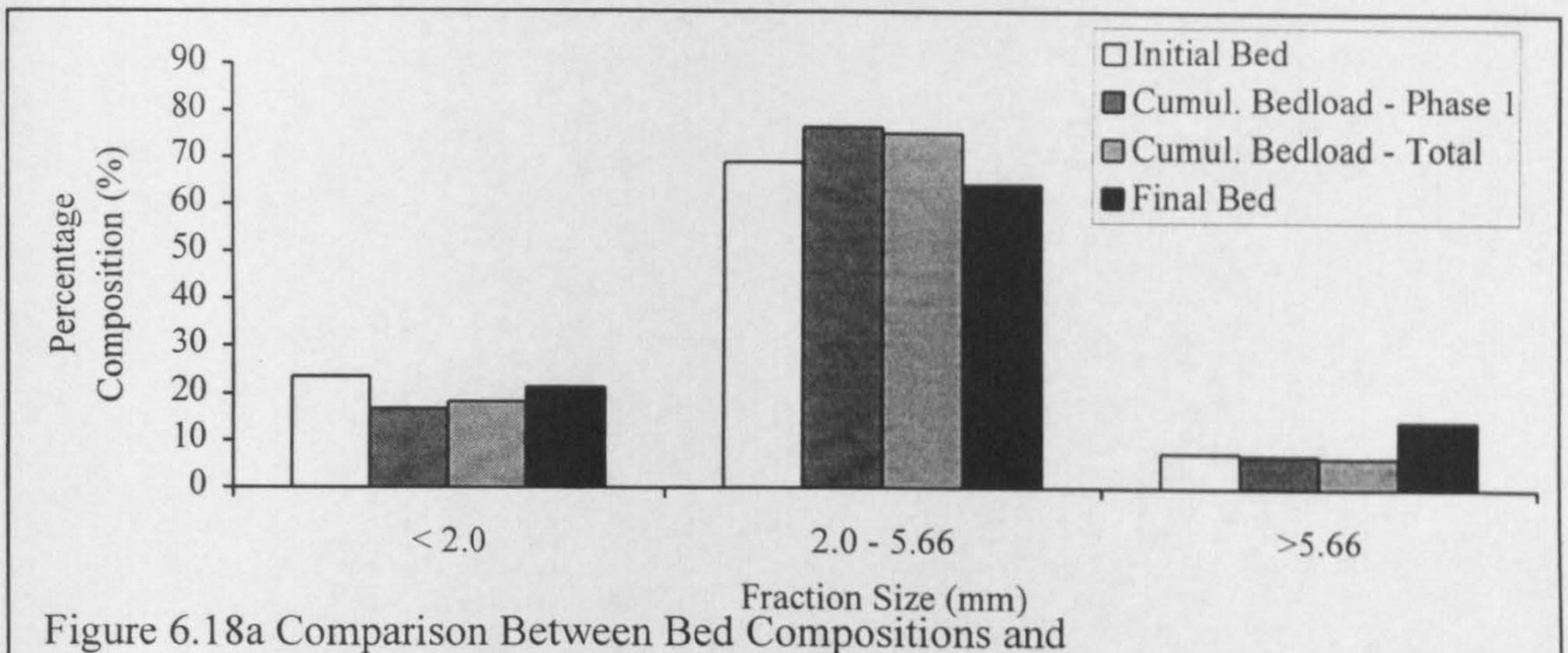

Figure 6.18a Comparison Between Bed Compositions and Cumulative Collected Bedload Compositions, Experiment 6, Bankfull, Slope 0.0024

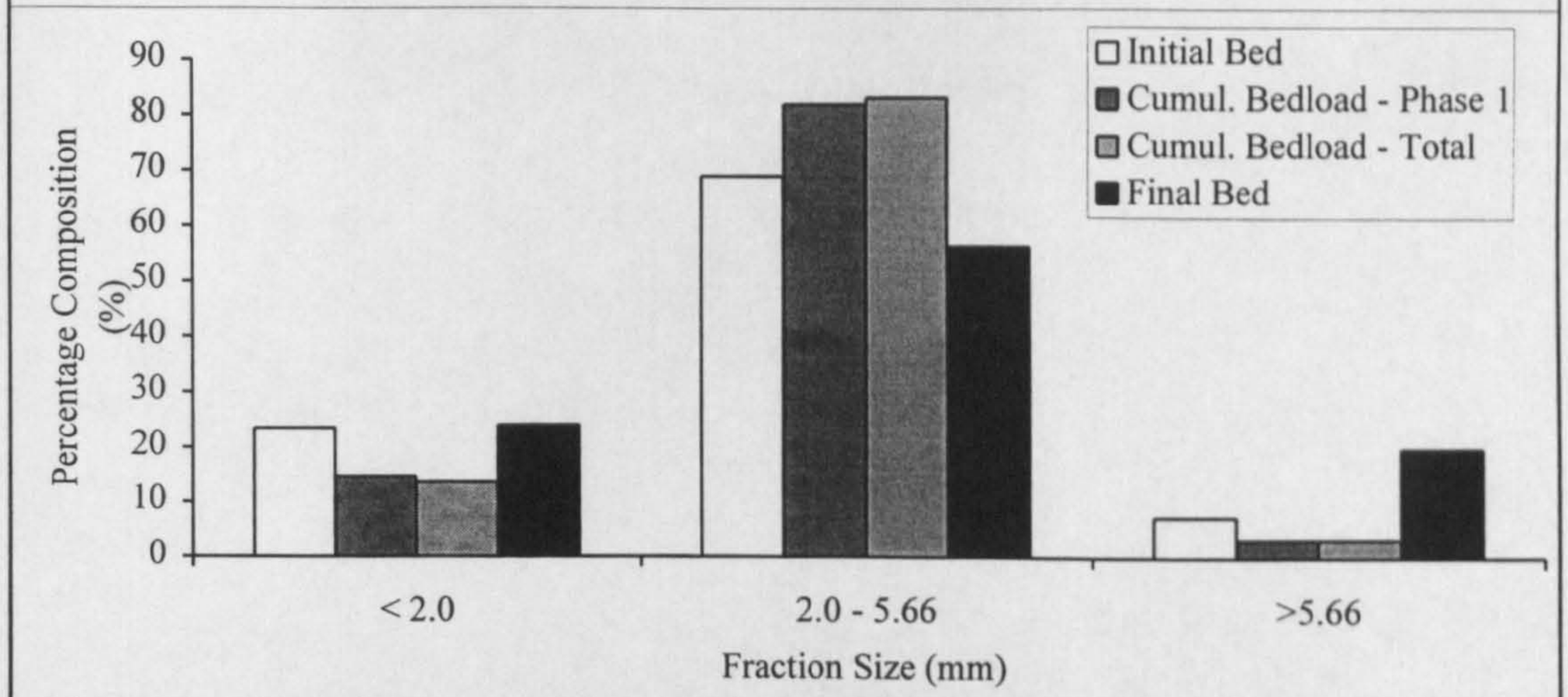

Figure 6.18b Comparison Between Bed Compositions and Cumulative Collected Bedload Compositions, Experiment 4, Bankfull, Slope 0.0026

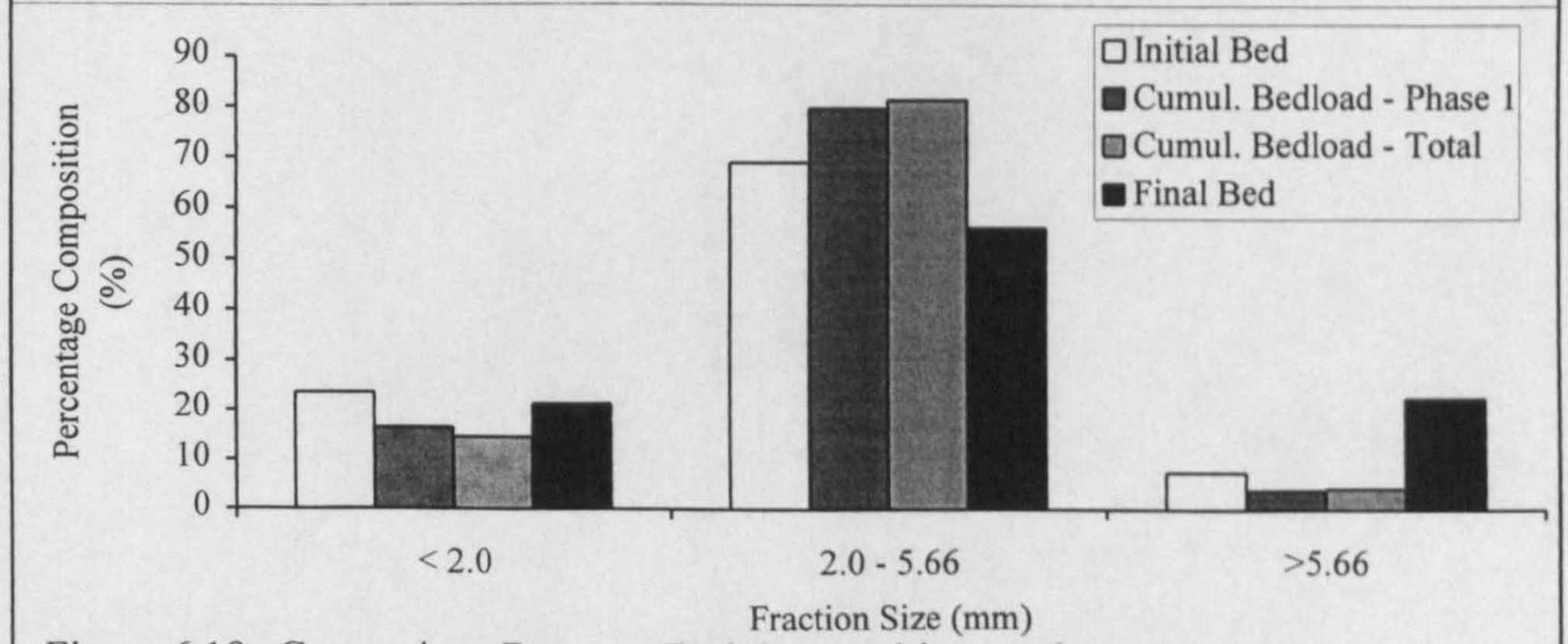

Figure 6.18c Comparison Between Bed Compositions and Cumulative Collective Bedload Compositions, Experiment 5, Bankfull, Slope 0.0029

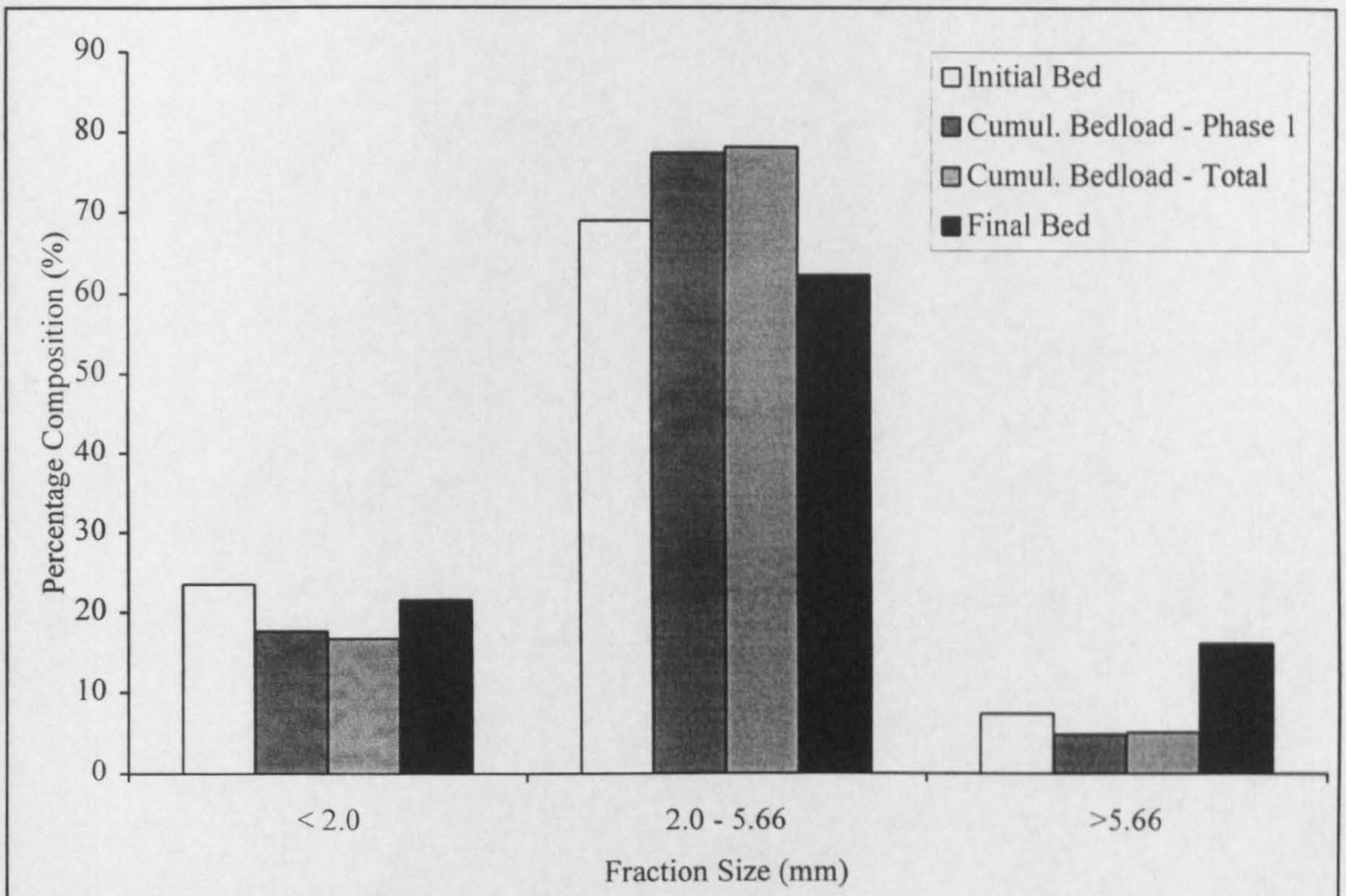

Figure 6.19a Comparison Between Bed Compositions and Cumulative Collected Bedload Compositions, Experiment 7, Shallow Overbank, Slope 0.0024

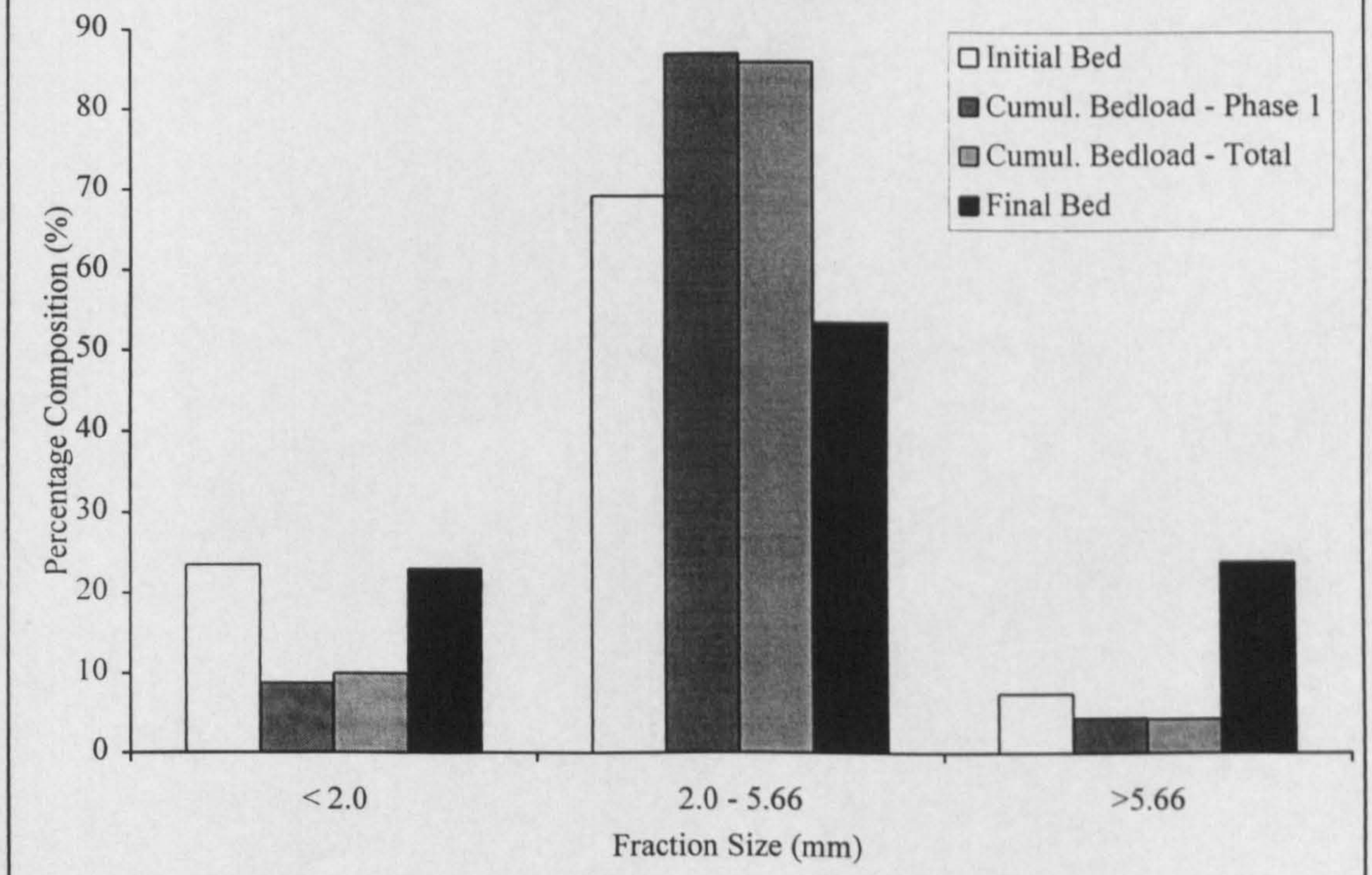

Figure 6.19b Comparison Between Bed Compositions and Cumulative Collected Bedload Compositions, Experiment 2, Shallow Overbank, Slope 0.0026

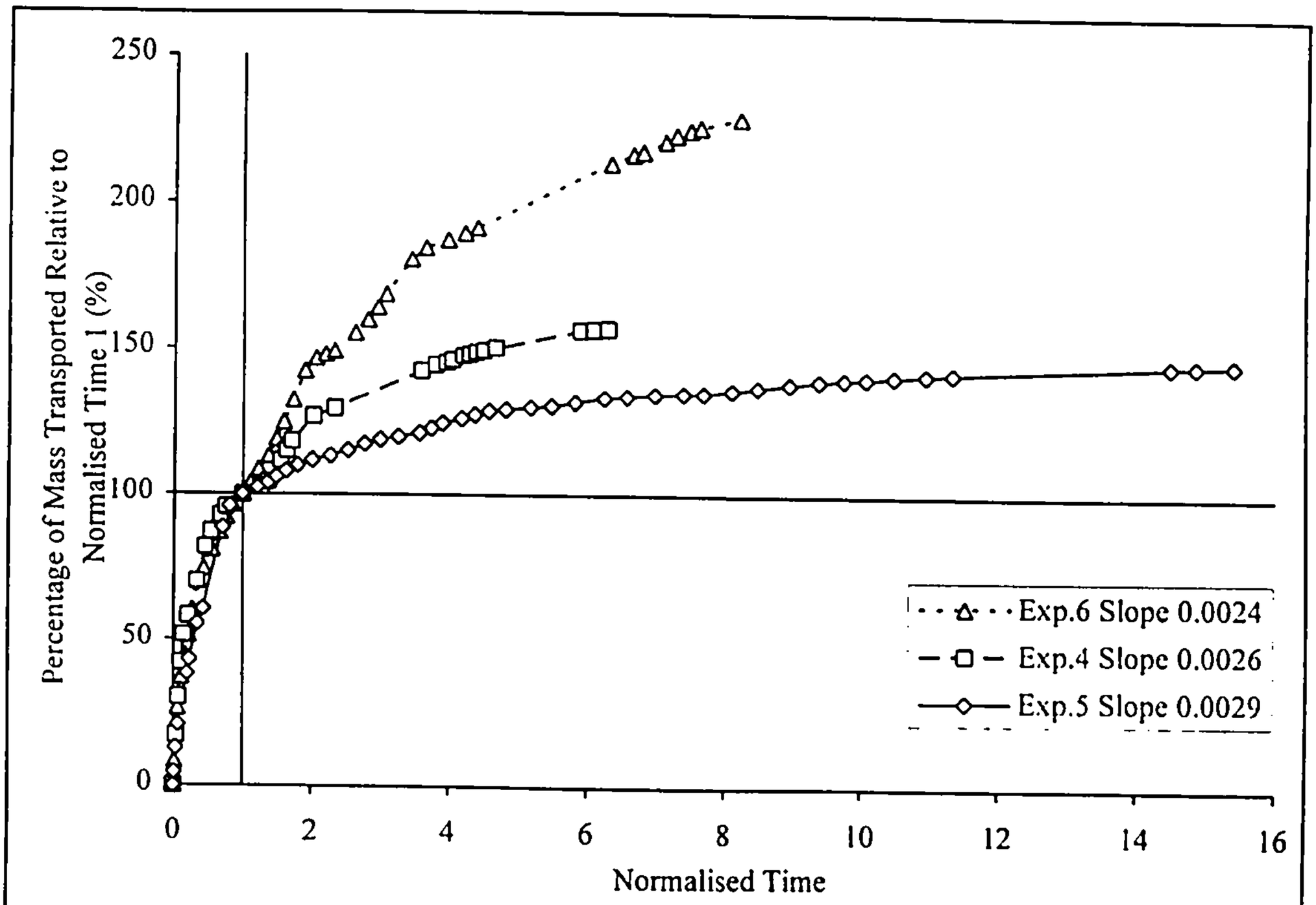

Figure 6.20a Cumulative Bedload Mass Curves for Full Experiments, Relative to Mass at Normalised Time 1, Bankfull

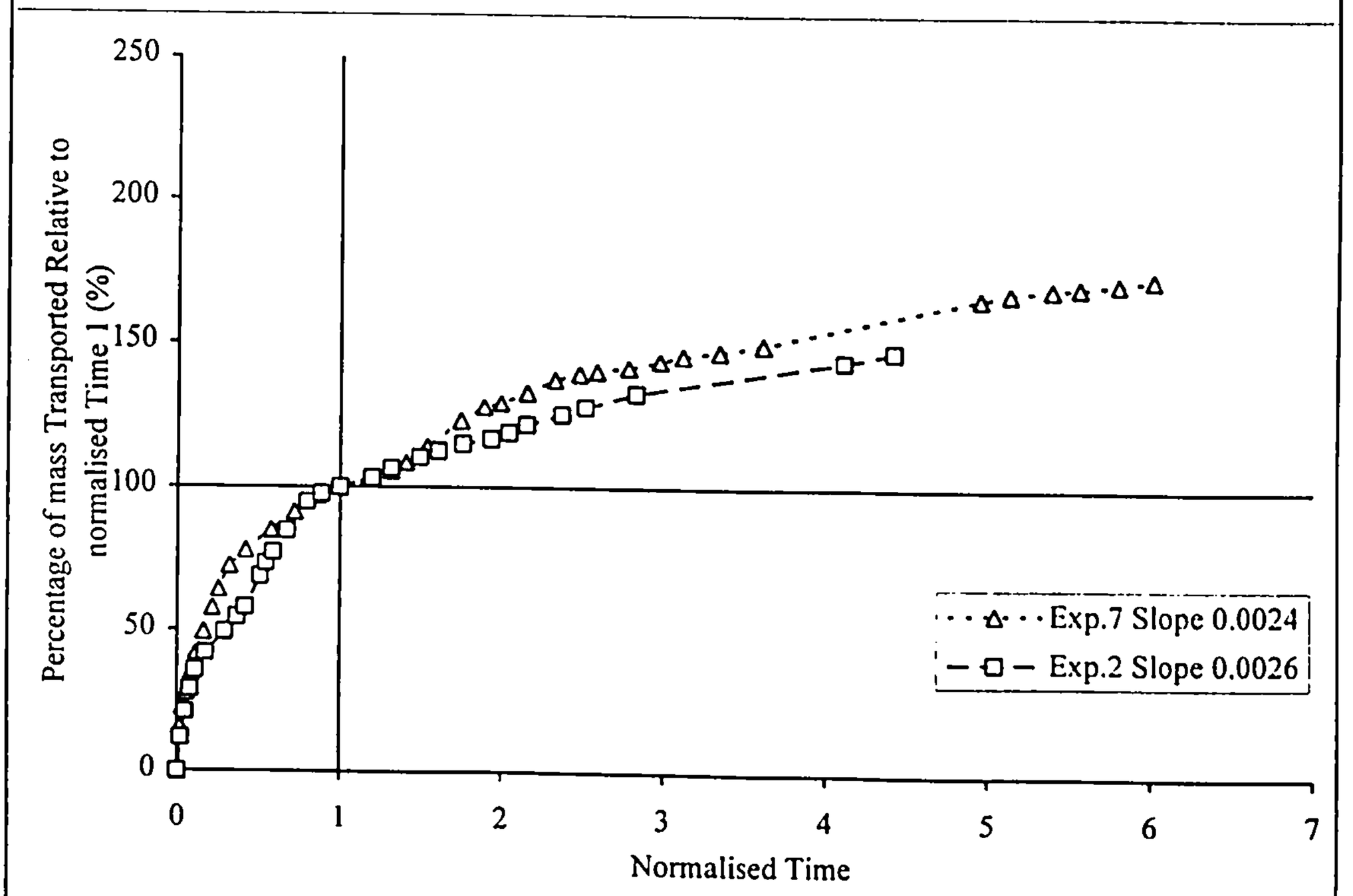

Figure 6.20b Cumulative Bedload Mass Curves for Full Experiments, Relative to Mass at Normalised Time 1, Shallow Overbank

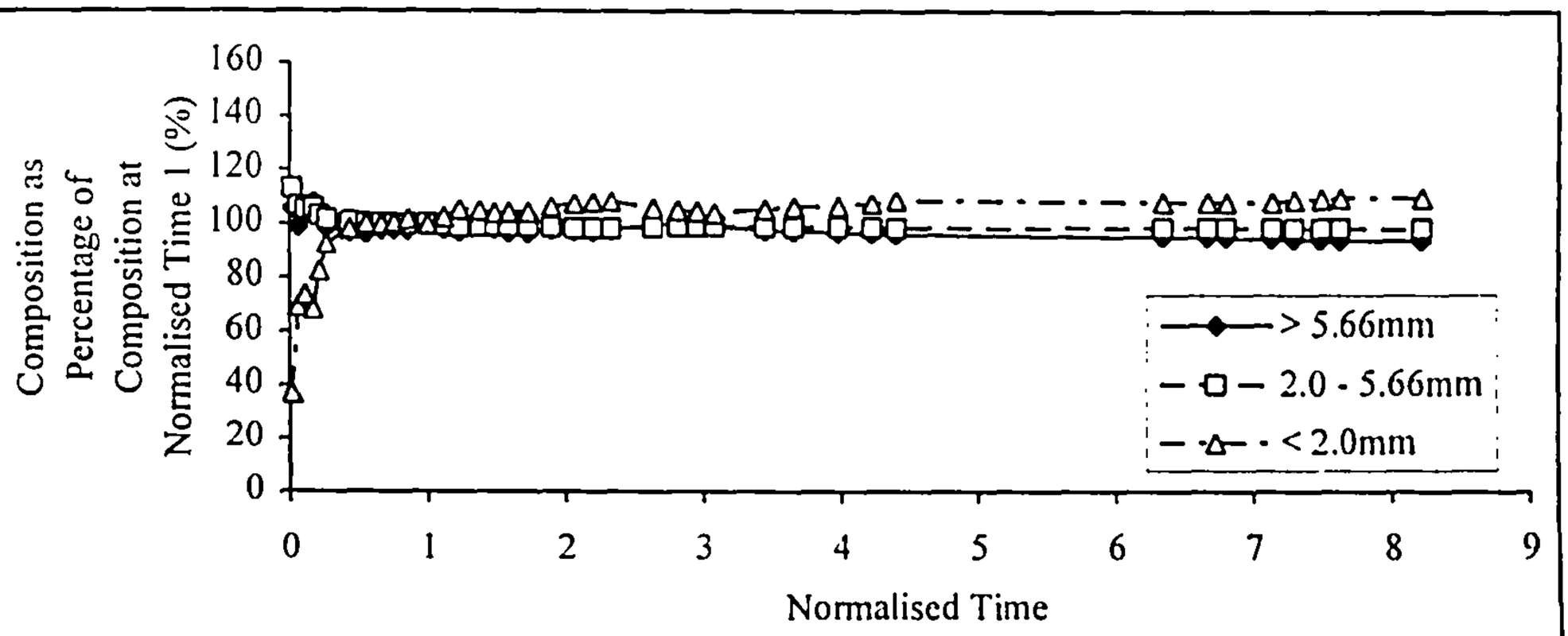

Figure 6.21a Progressive Composition of Cumulative Collected Bedload as Percentage of Composition at Normalised Time 1, Experiment 6, Bankfull, Slope 0.0024

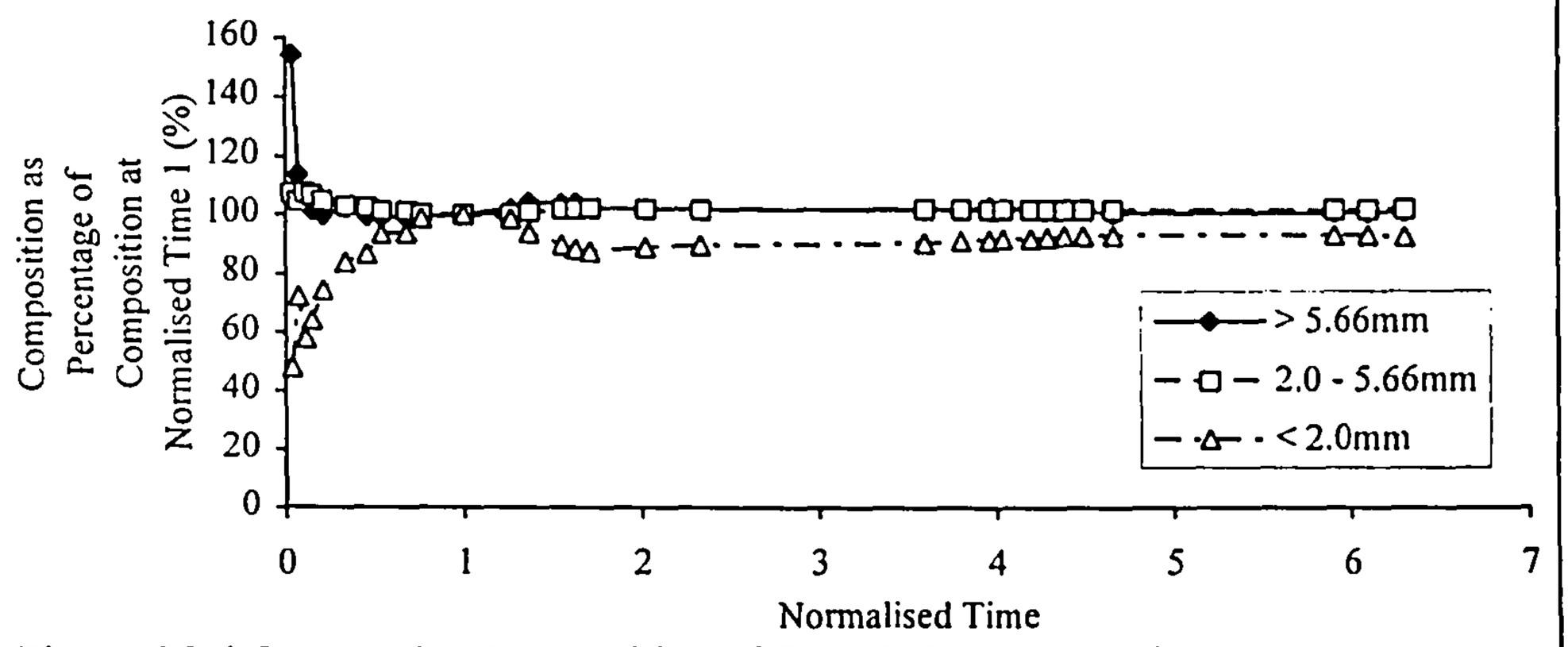

Figure 6.21b Progressive Composition of Cumulative Collected Bedload as Percentage of Composition at Normalised Time 1, Experiment 4, Bankfull, Slope 0.0026

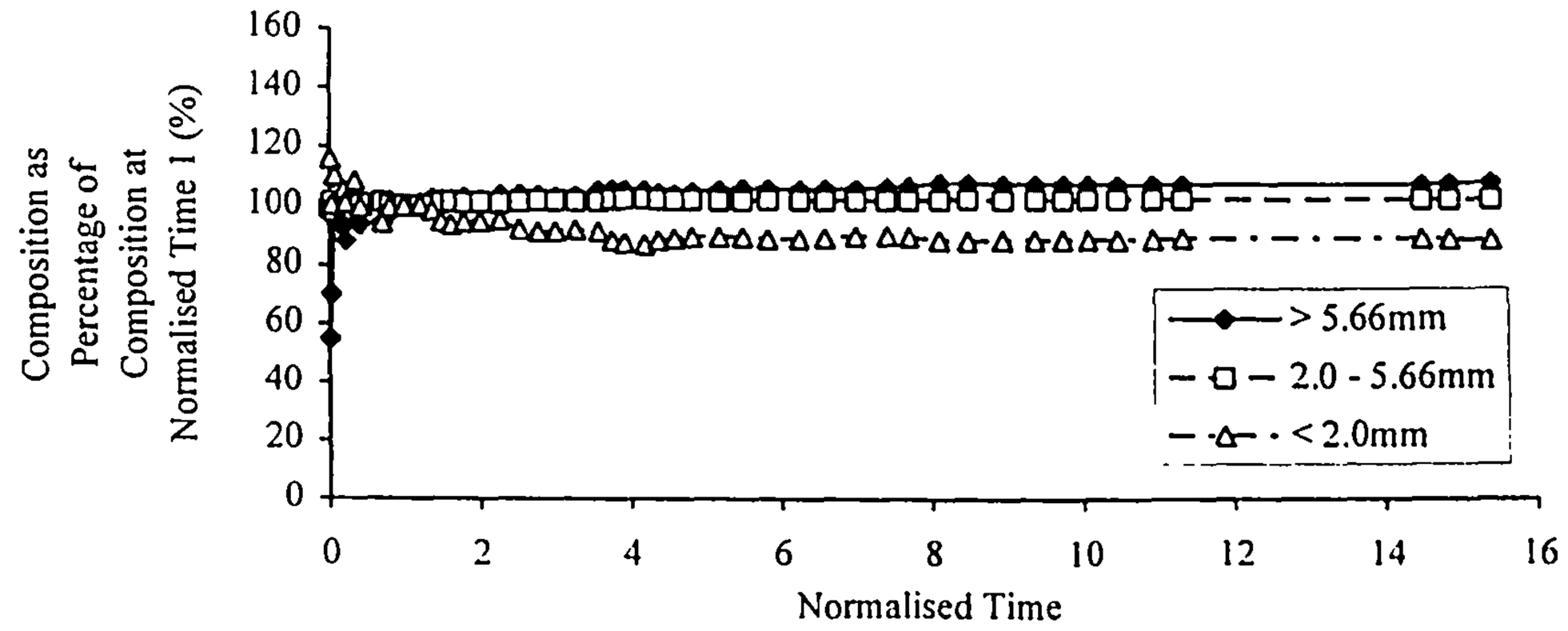

Figure 6.21c Progressive Composition of Cumulative Collected Bedload as Percentage of Composition at Normalised Time 1, Experiment 5, Bankfull, Slope 0.0029

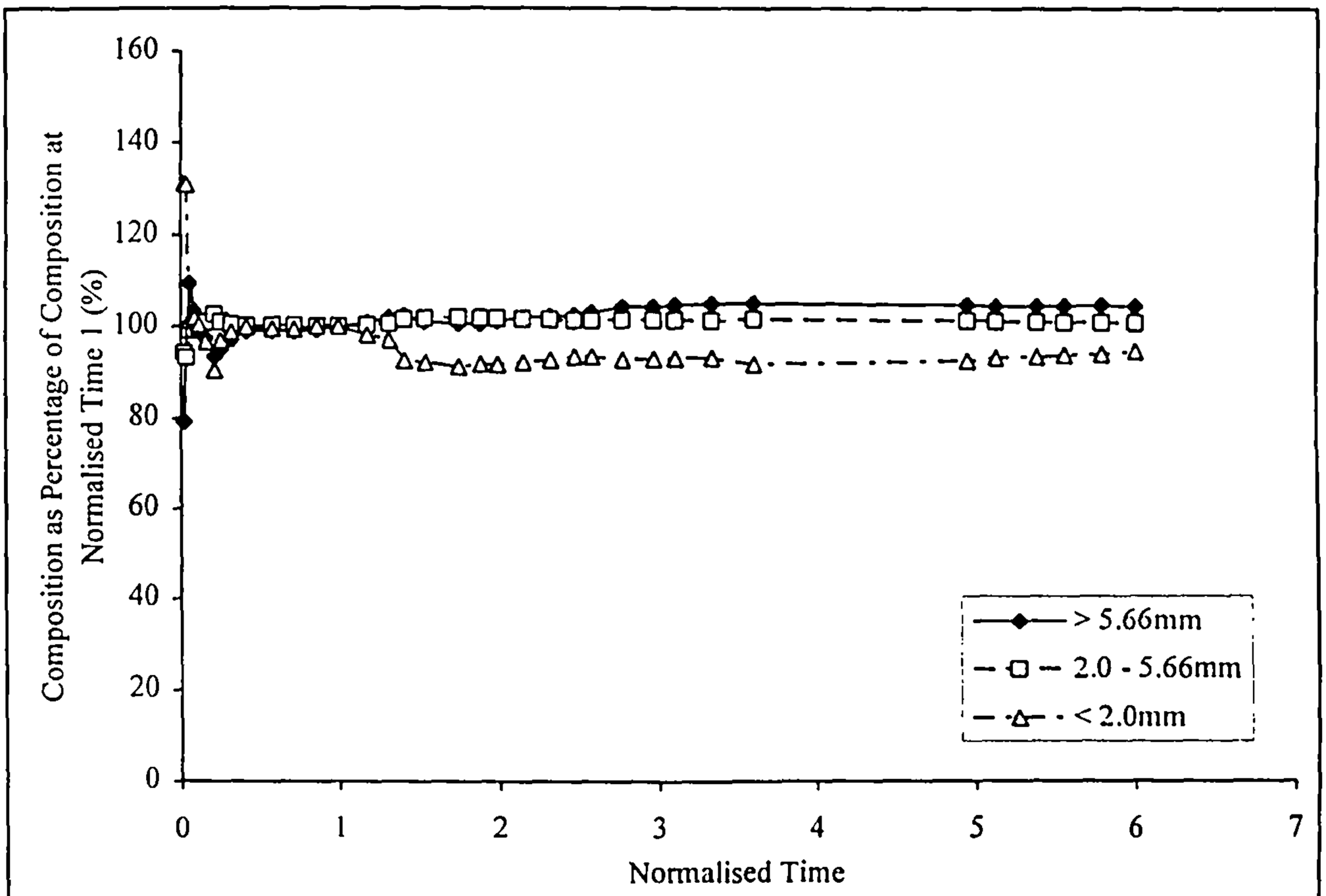

Figure 6.22a Progressive Composition of Cumulative Collected Bedload as Percentage of Composition at Normalised Time 1, Experiment 7, Shallow Overbank, Slope 0.0024

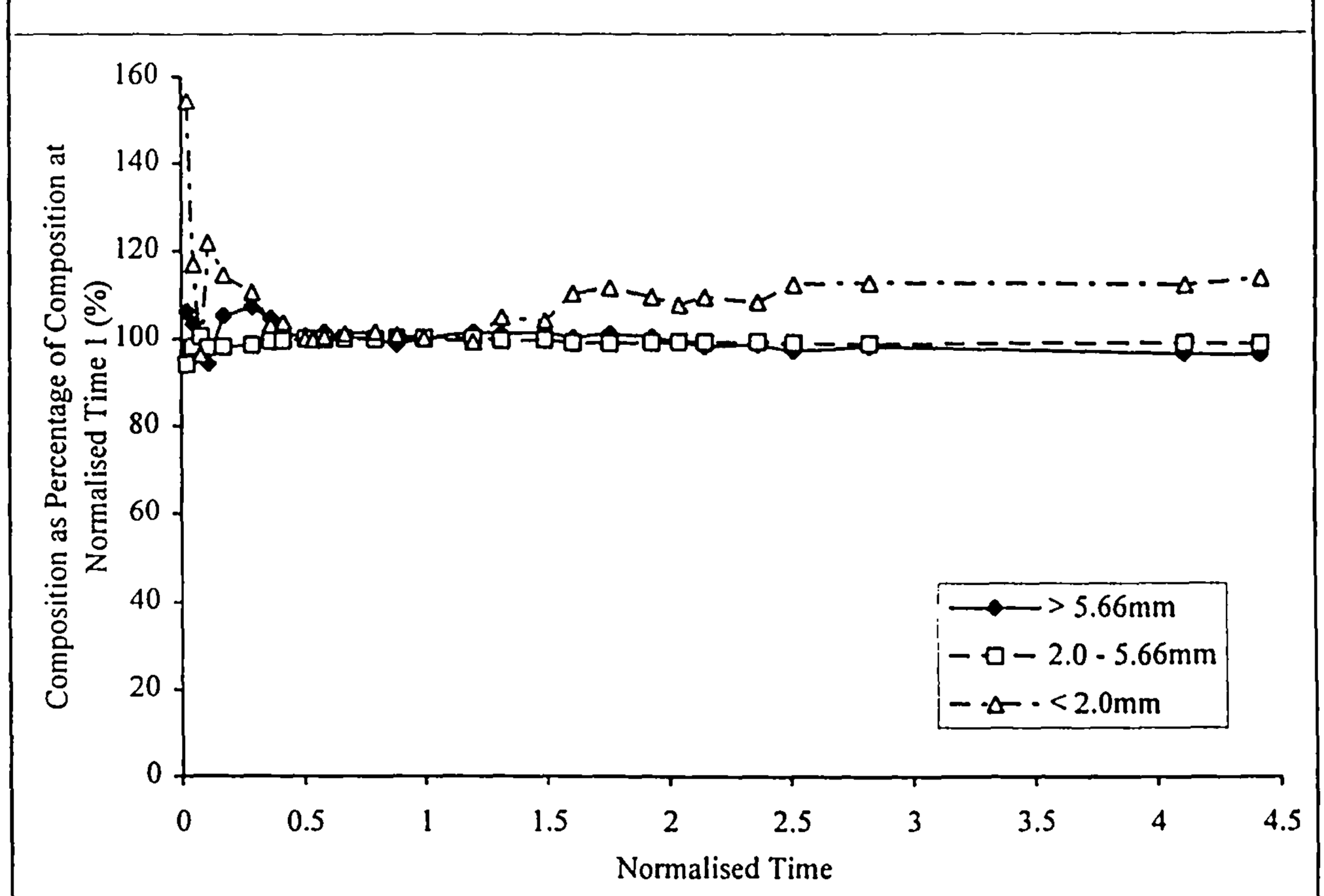

Figure 6.22b Progressive Composition of Cumulative Collected Bedload as Percentage of Composition at Normalised Time 1, Experiment 2, Shallow Overbank, Slope 0.0026

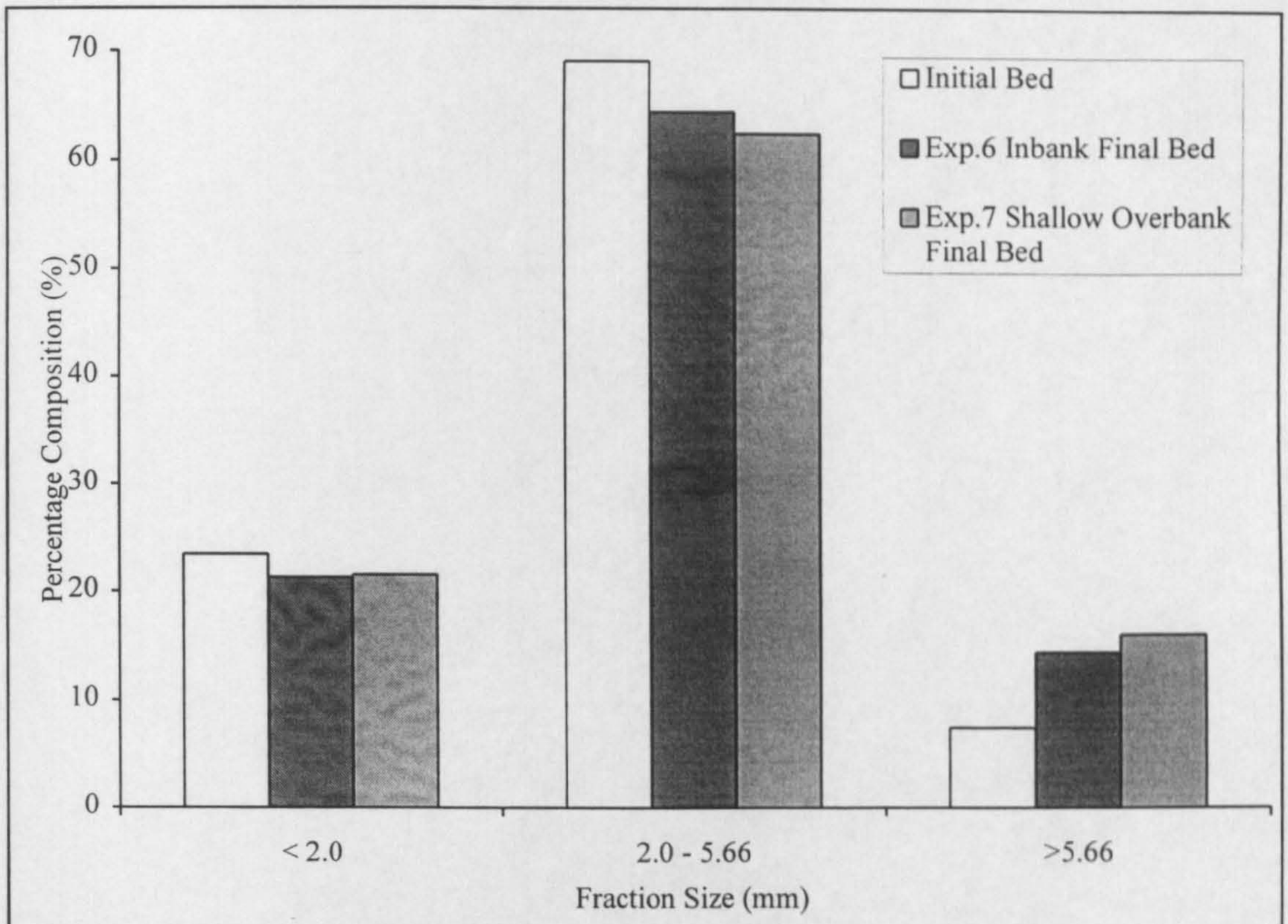

Figure 6.23a Initial and Final Bed Surface Compositions, Experiments with Initial Slopes of 0.0024

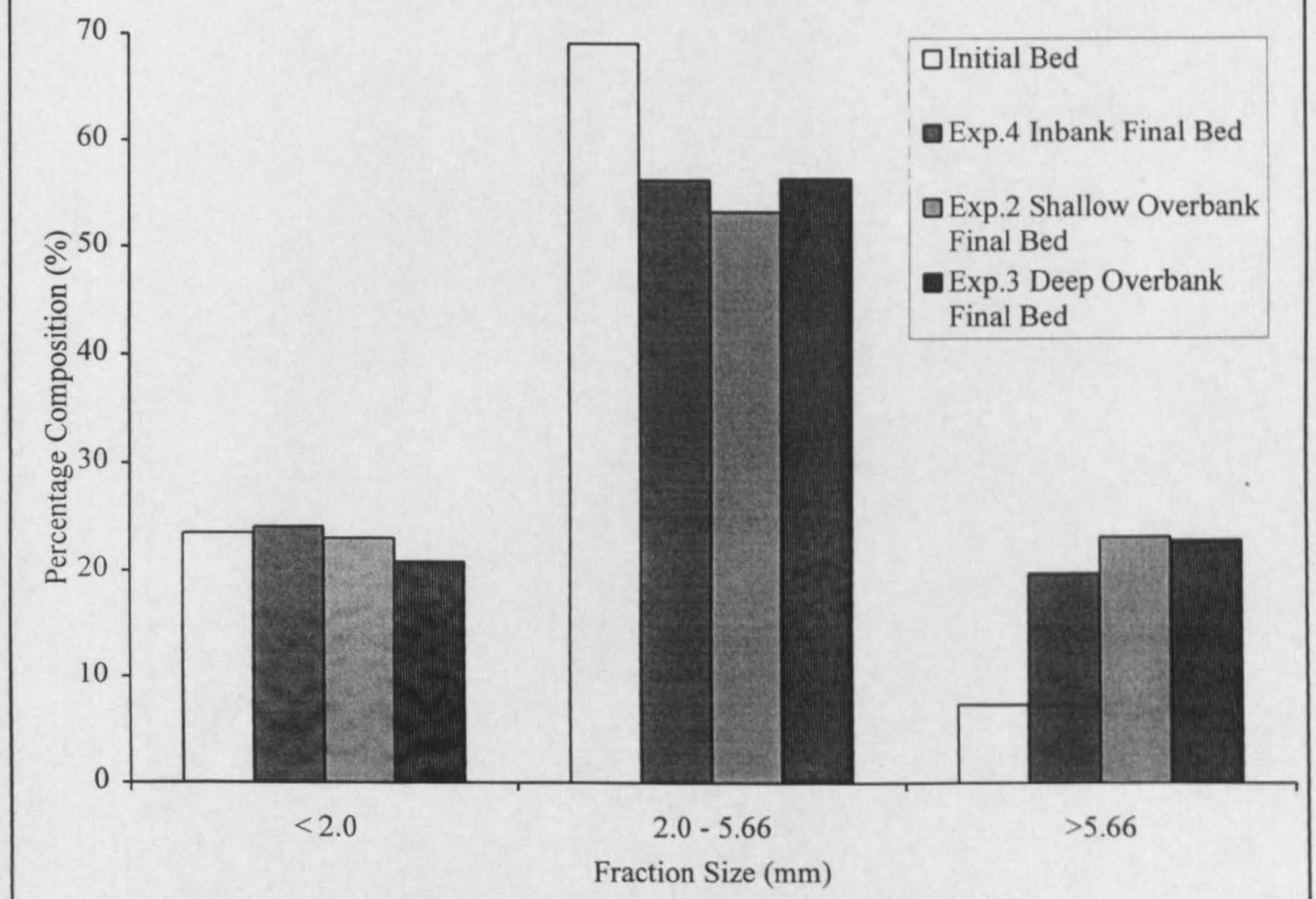

Figure 6.23b Initial and Final Bed Surface Compositions, Experiments with Initial Slopes of 0.0026

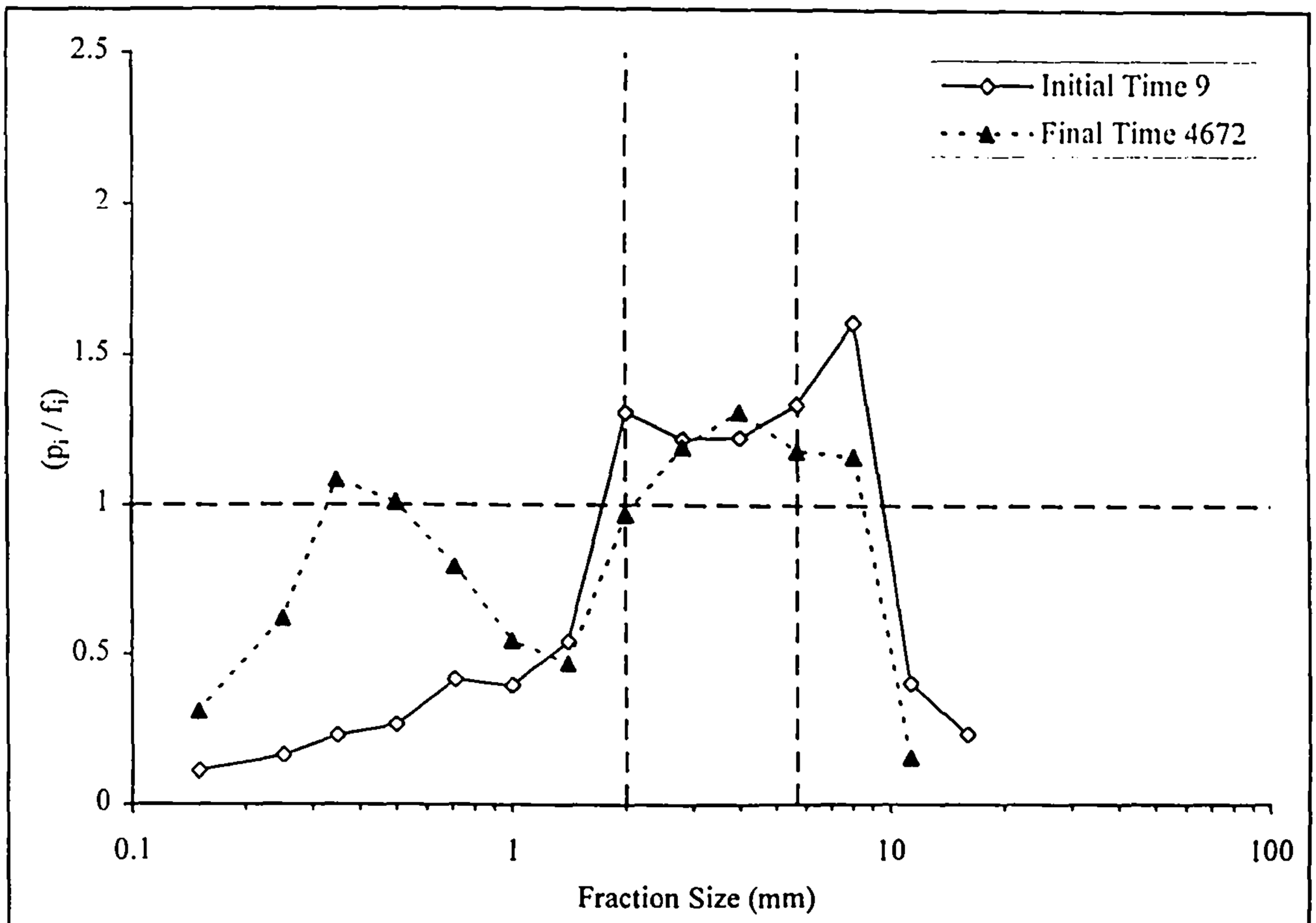

Figure 6.24a Initial and Final Fraction Mobility, Experiment 6, Slope 0.0024, Bankfull

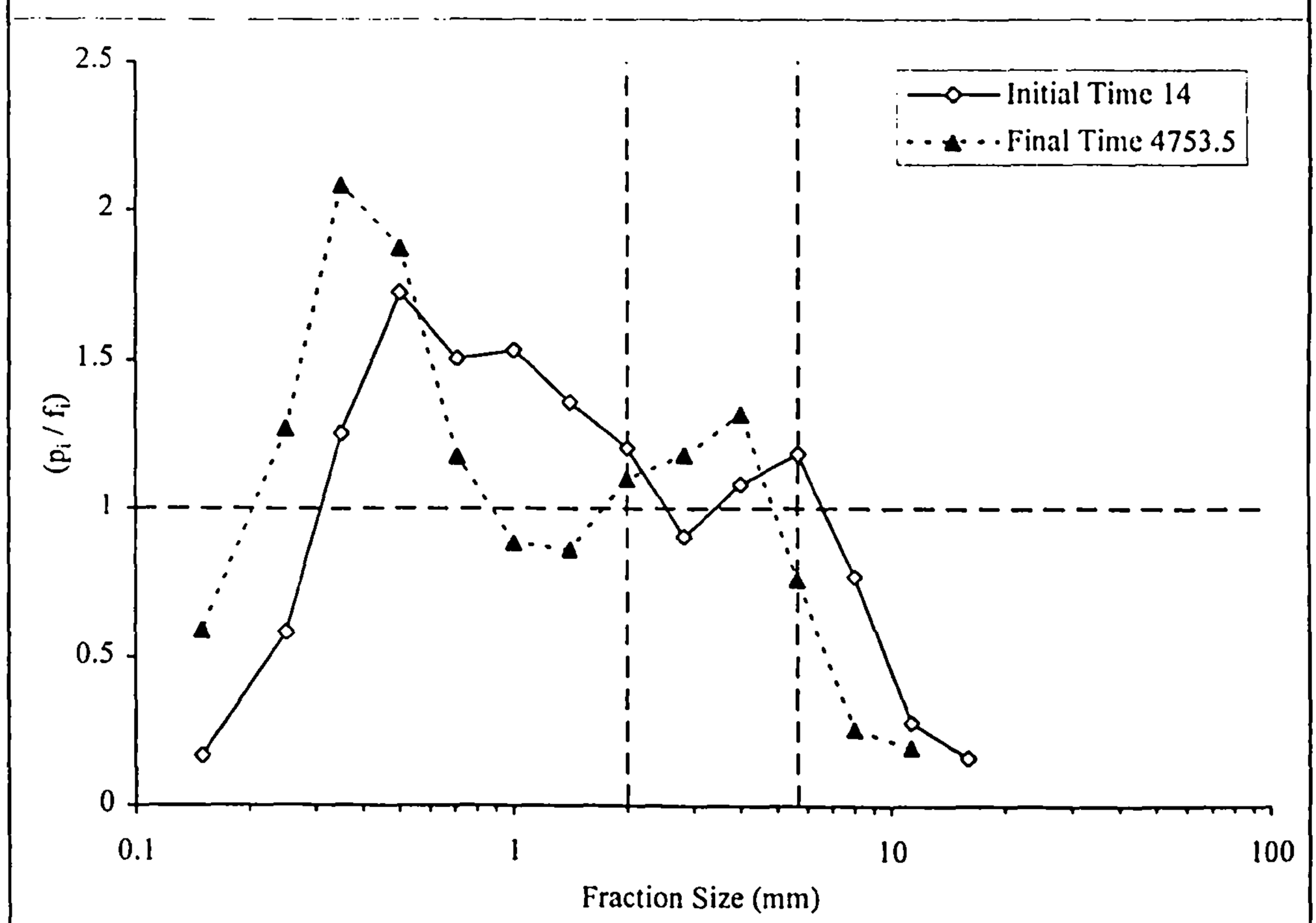

Figure 6.24b Initial and Final Fraction Mobility, Experiment 7, Slope 0.0024, Shallow Overbank

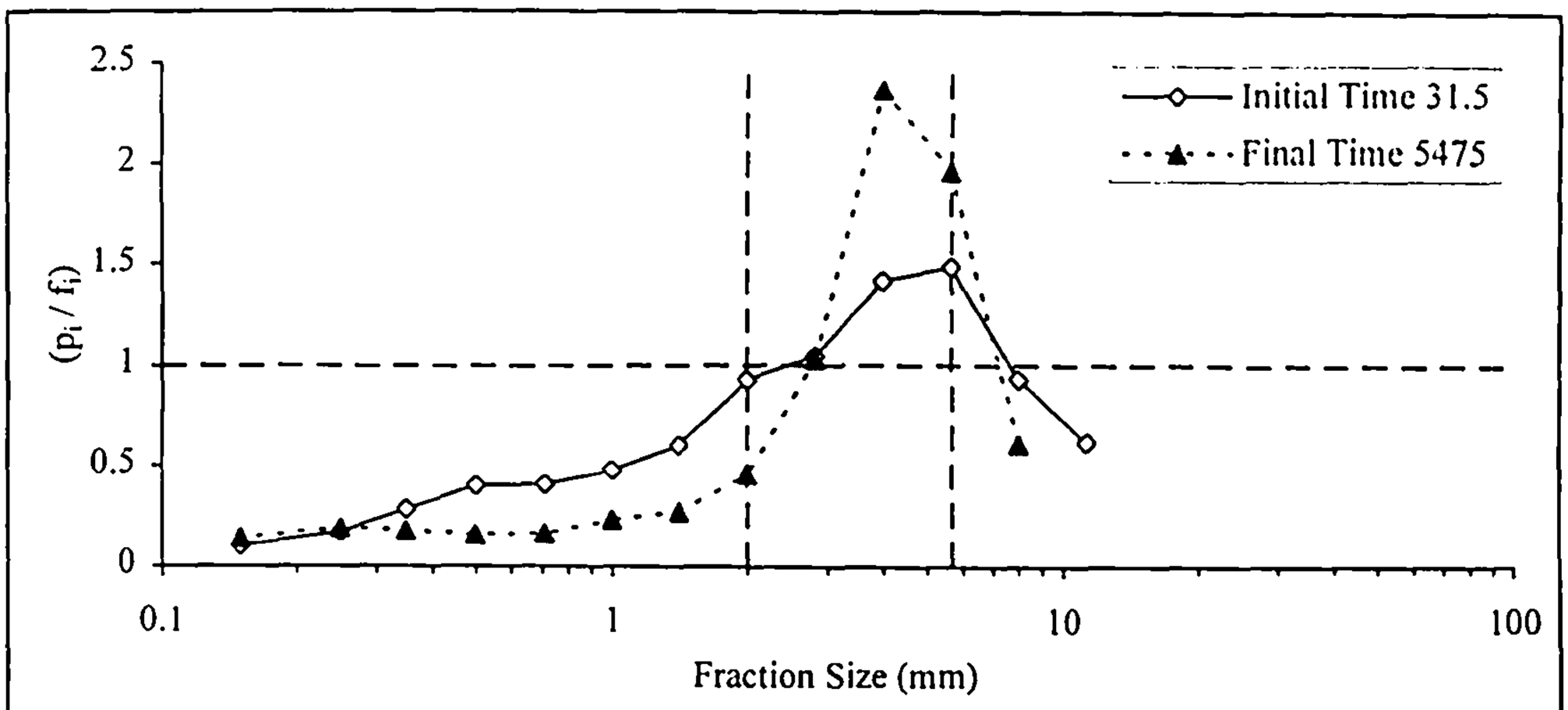

Figure 6.25a Initial and Final Fraction Mobility, Experiment 4, Slope 0.0026, Bankfull

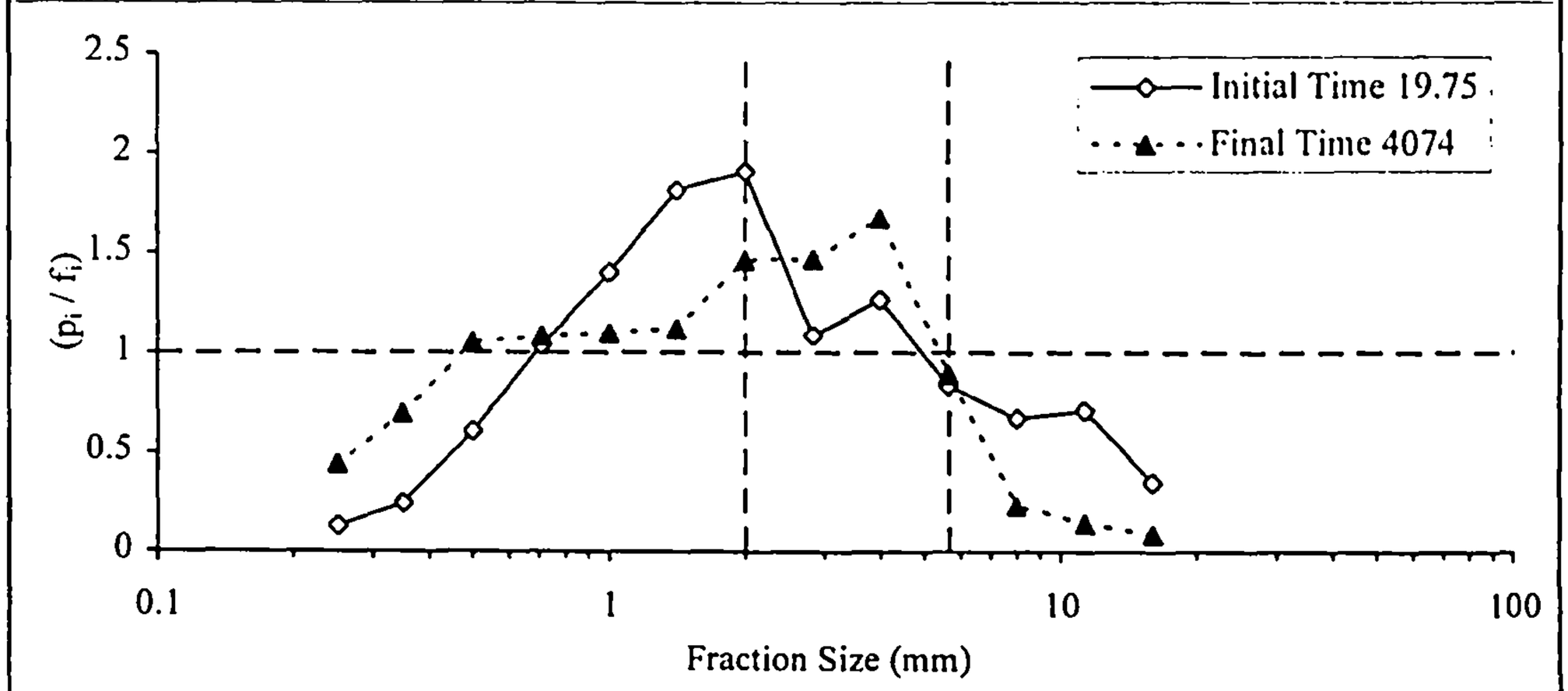

Figure 6.25b Initial and Final Fraction Mobility, Experiment 2, Slope 0.0026, Shallow Overbank

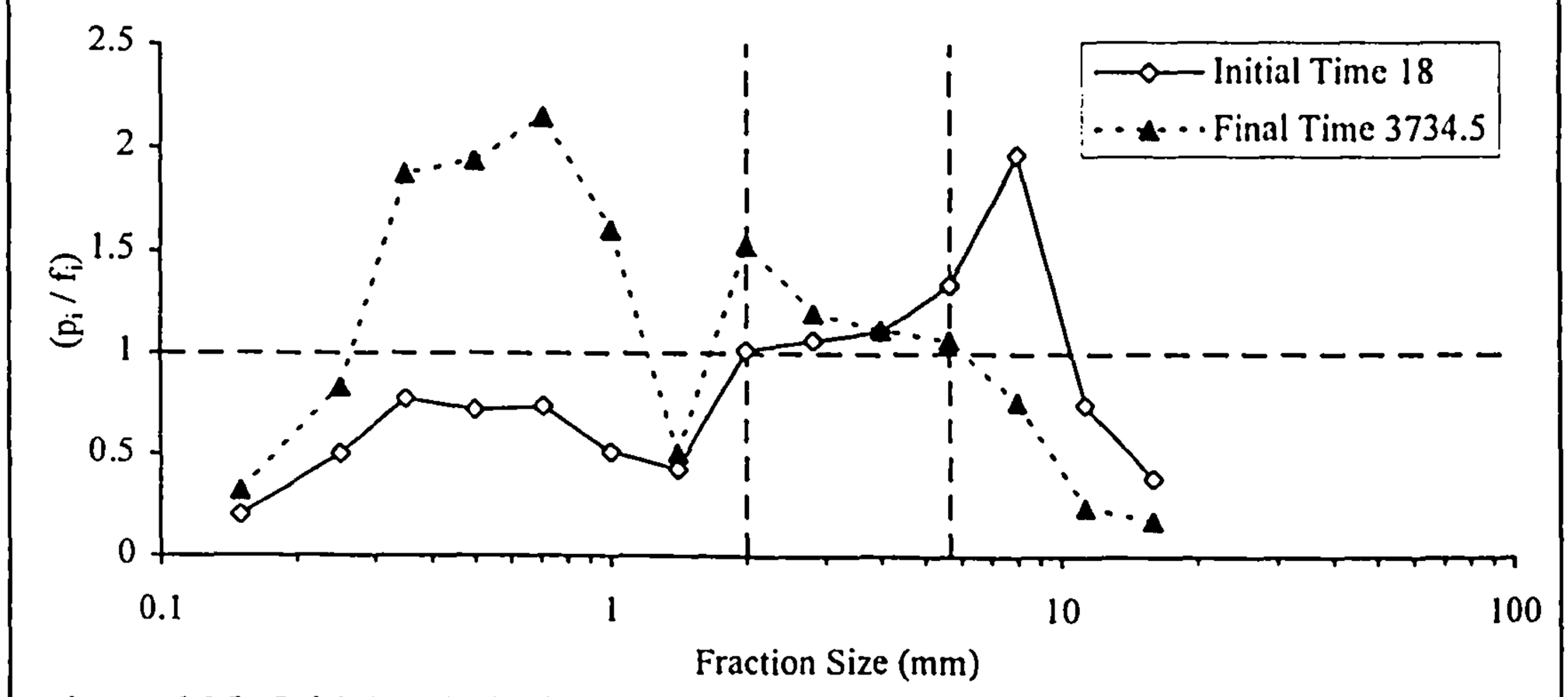

Figure 6.25c Initial and Final Fraction Mobility, Experiment 3, Slope 0.0026, Deep Overbank

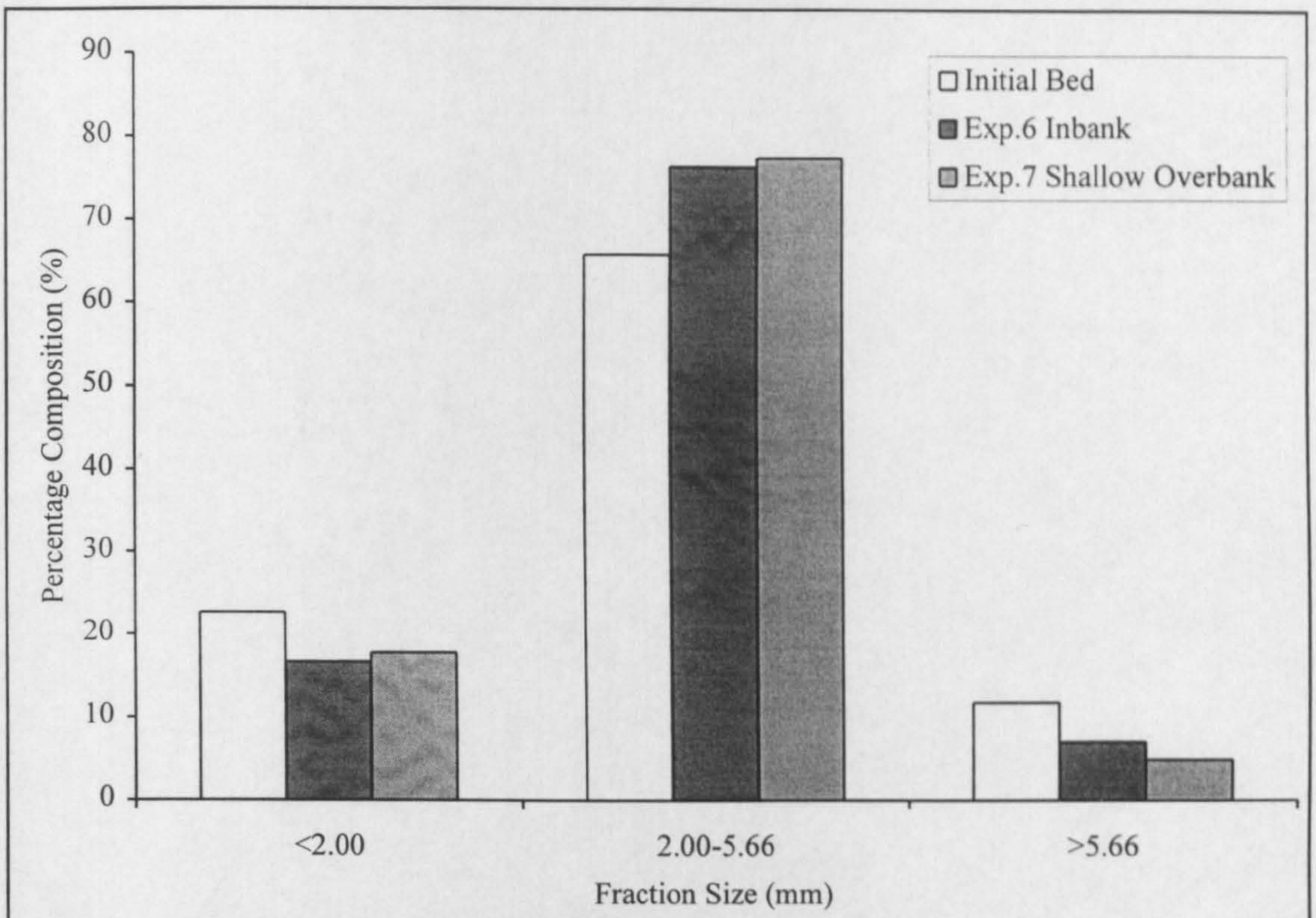

Figure 6.26a Simplified Compositions of Collected Phase 1 Bedload, Experiments with Initial Slopes of 0.0024

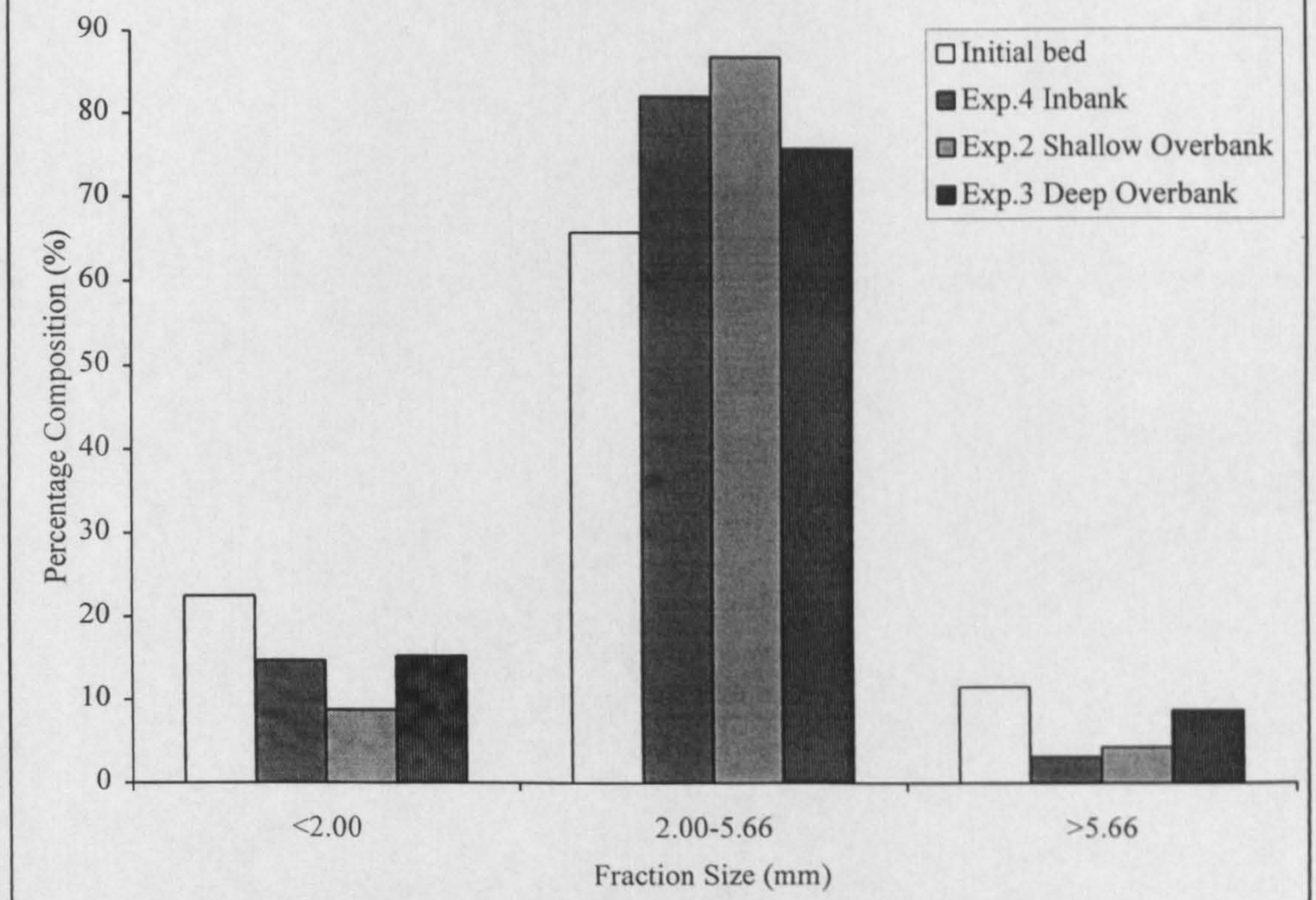

Figure 6.26b Simplified Compositions of Collected Phase 1 Bedload, Experiments with Initial Slopes 0.0026

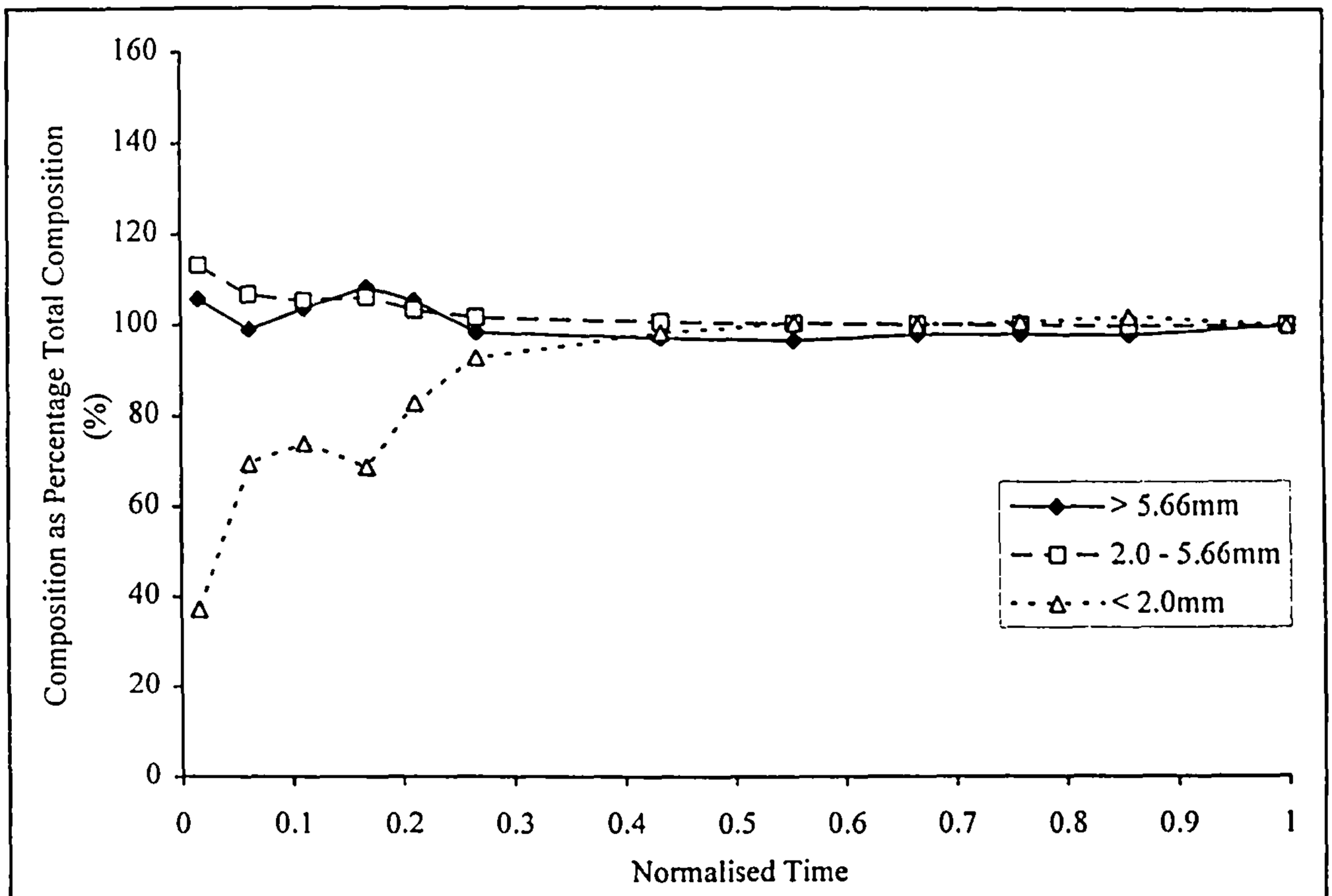

Figure 6.27a Progressive Composition of Collected Phase 1 Bedload as Percentage of Composition of Total Collected During Phase 1, Experiment 6, Bankfull, Slope 0.0024

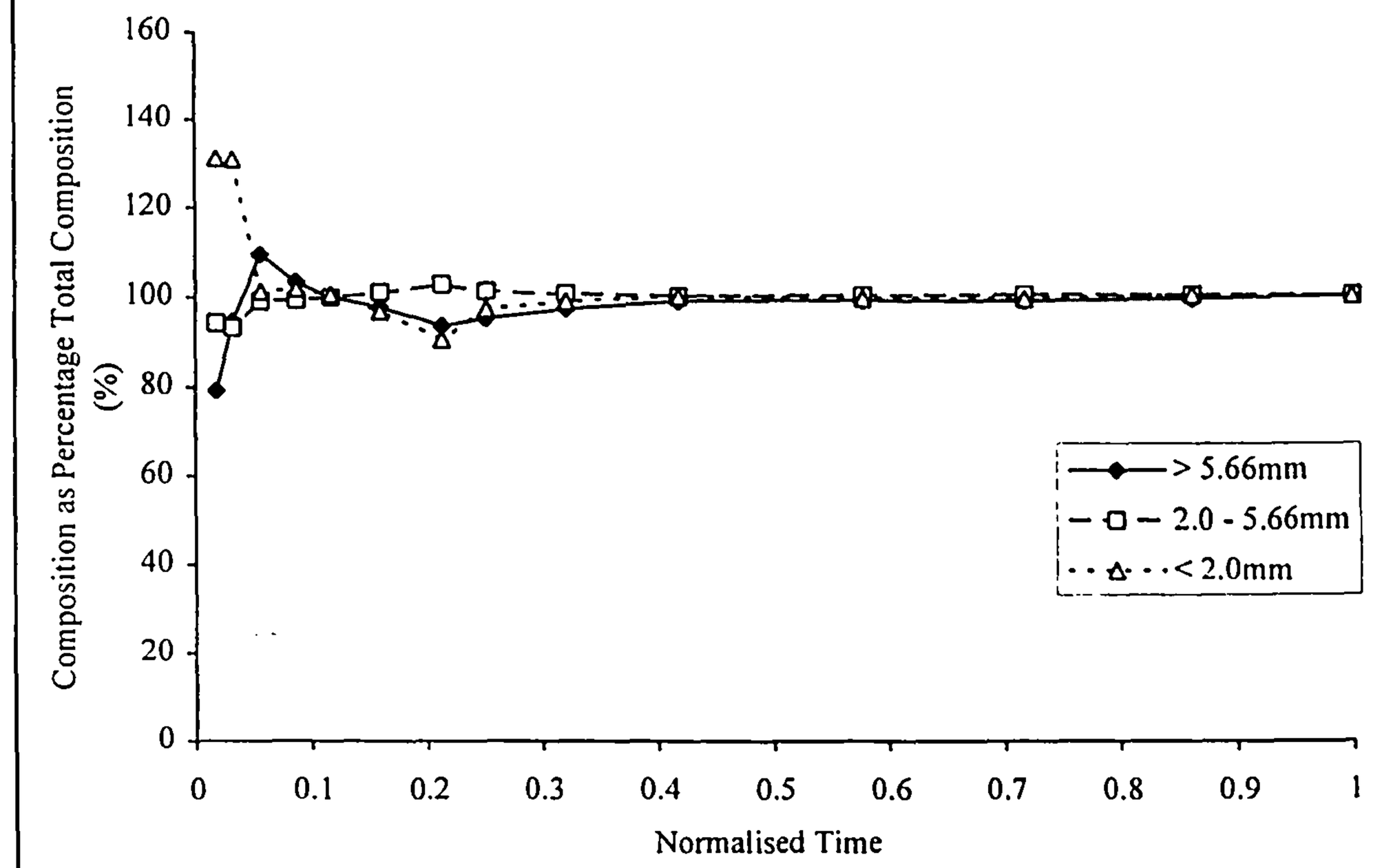

Figure 6.27b Progressive Composition of Collected Phase 1 Bedload as Percentage of Composition of Total Collected During Phase 1, Experiment 7, Shallow Overbank, Slope 0.0024

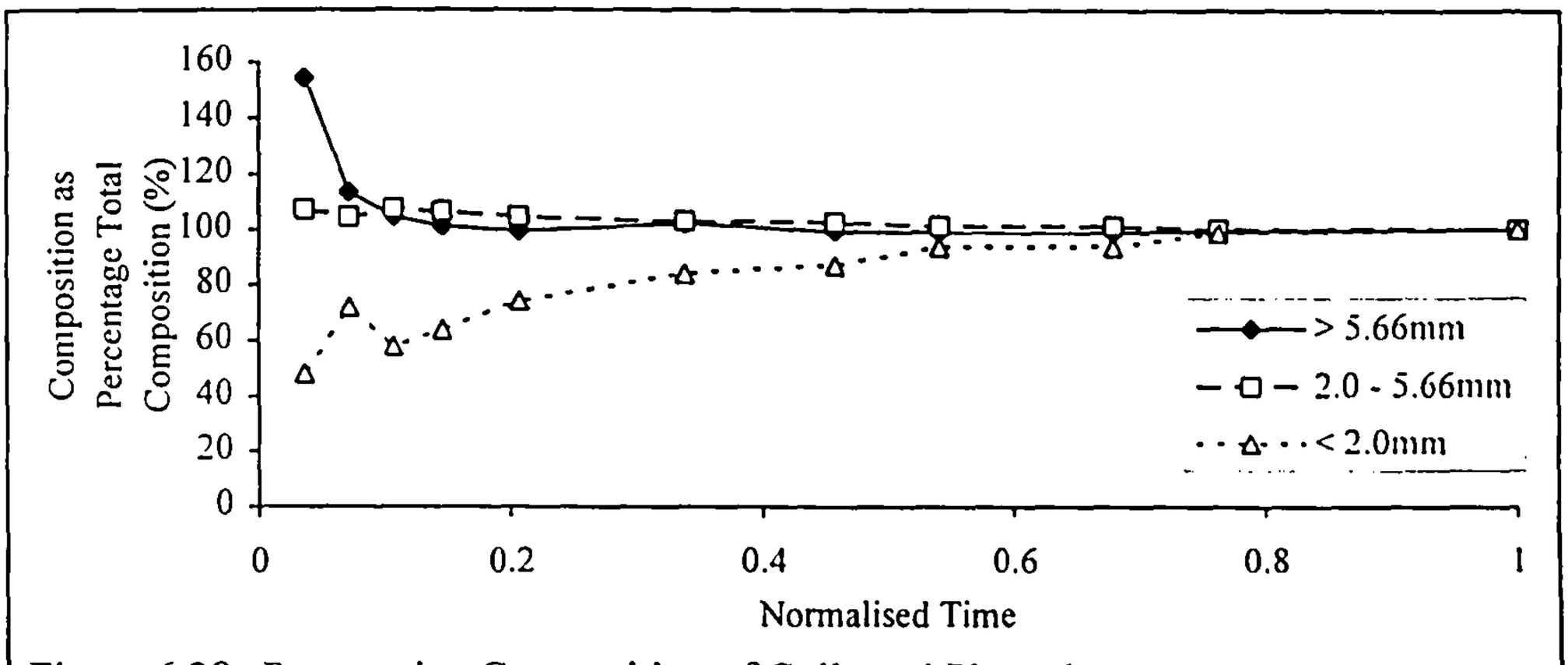

Figure 6.28a Progressive Composition of Collected Phase 1 Bedload as Percentage of Composition of Total Collected During Phase 1, Experiment 4, Bankfull, Slope 0.0026

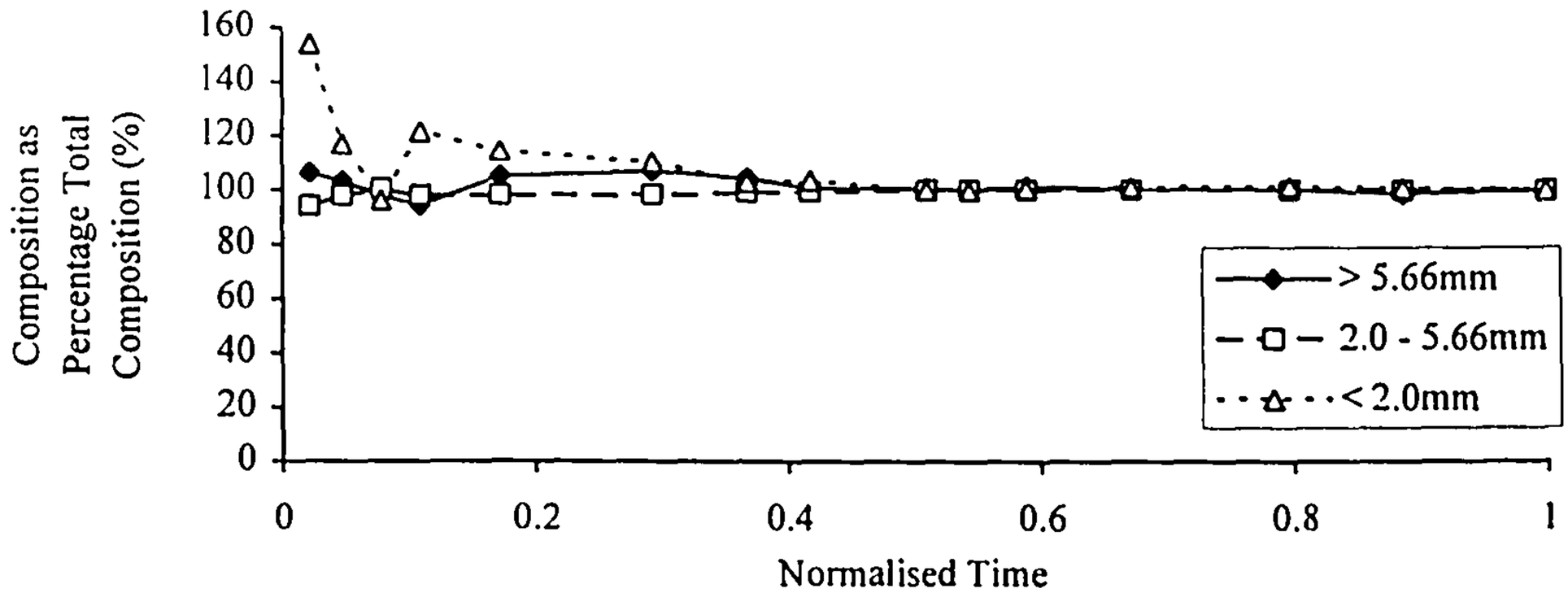

Figure 6.28b Progressive Composition of Collected Phase 1 Bedload as Percentage of Composition of Total Collected During Phase 1, Experiment 2, Shallow Overbank, Slope 0.0026

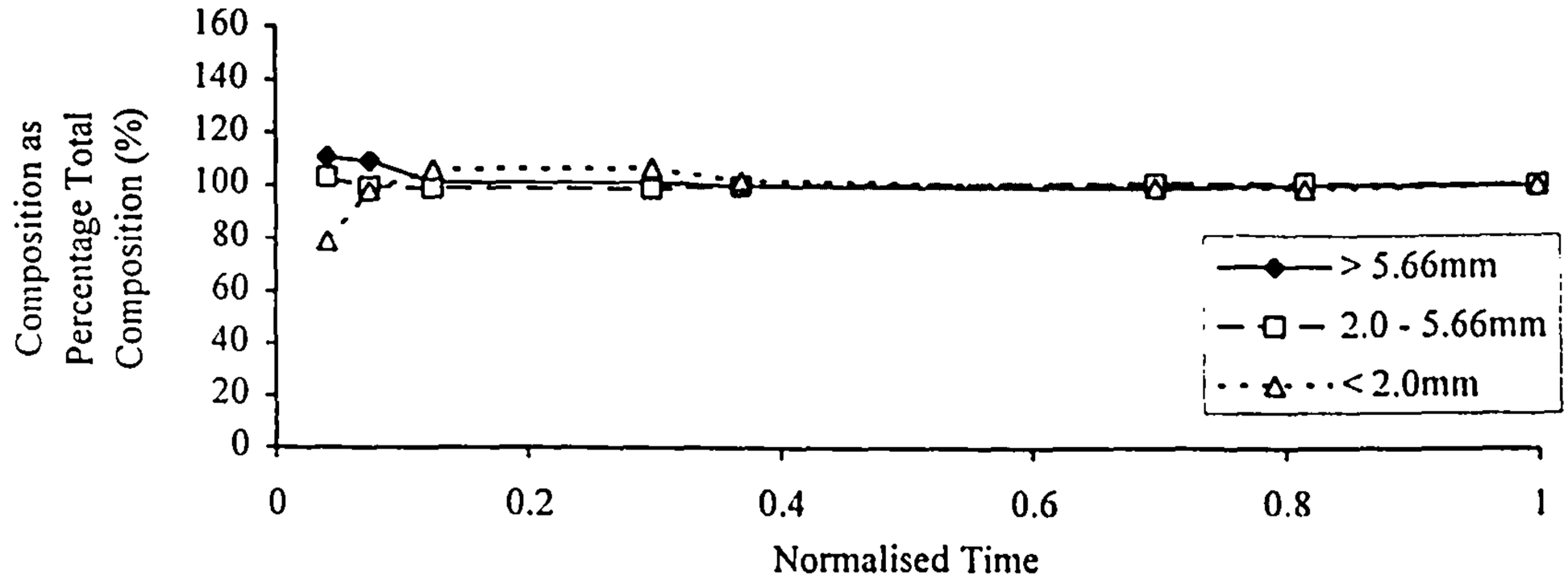

Figure 6.28c Progressive Composition of Collected Phase 1 Bedload as Percentage of Composition of Total Collected During Phase 1, Experiment 3, Deep Overbank, Slope 0.0026

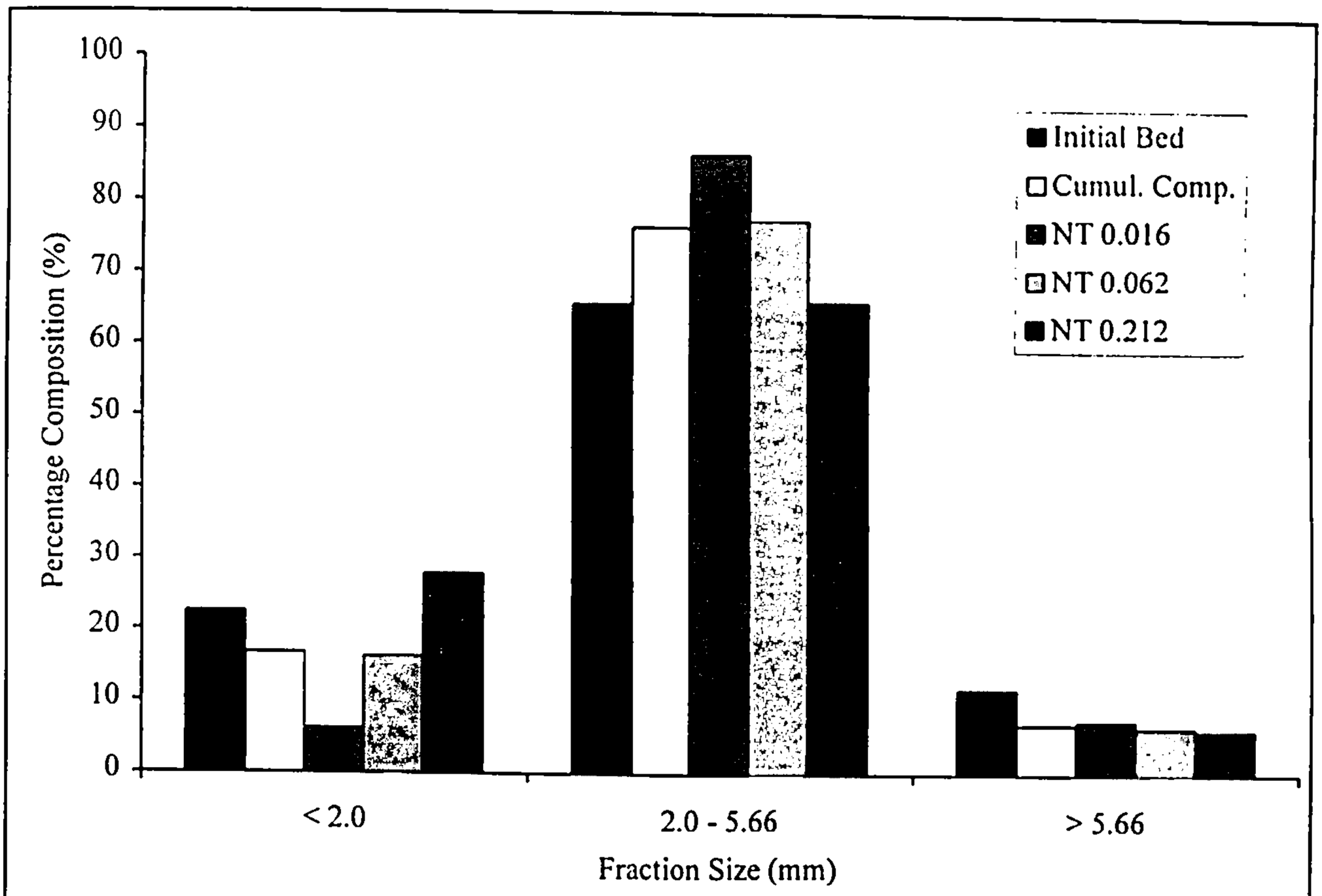

Figure 6.29a Comparison Between Phase 1 Bedload Samples, Cumulative and Initial Bed Simplified Compositions, Experiment 6, Bankfull, Slope 0.0024

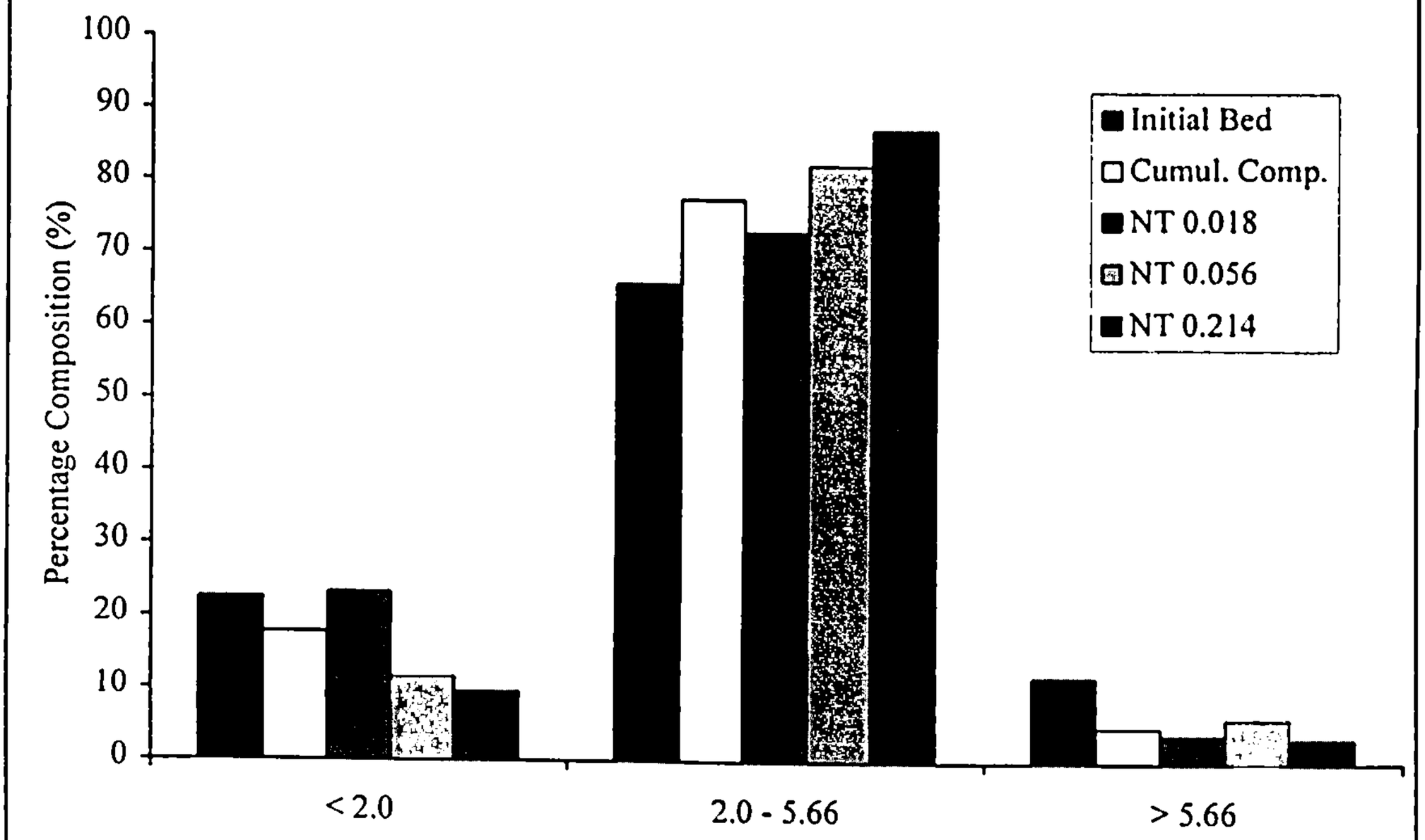

Figure 6.29b Comparison Between Phase 1 Bedload Samples, Cumulative and Initial Bed Simplified Compositions, Experiment 7, Shallow Overbank, Slope 0.0024

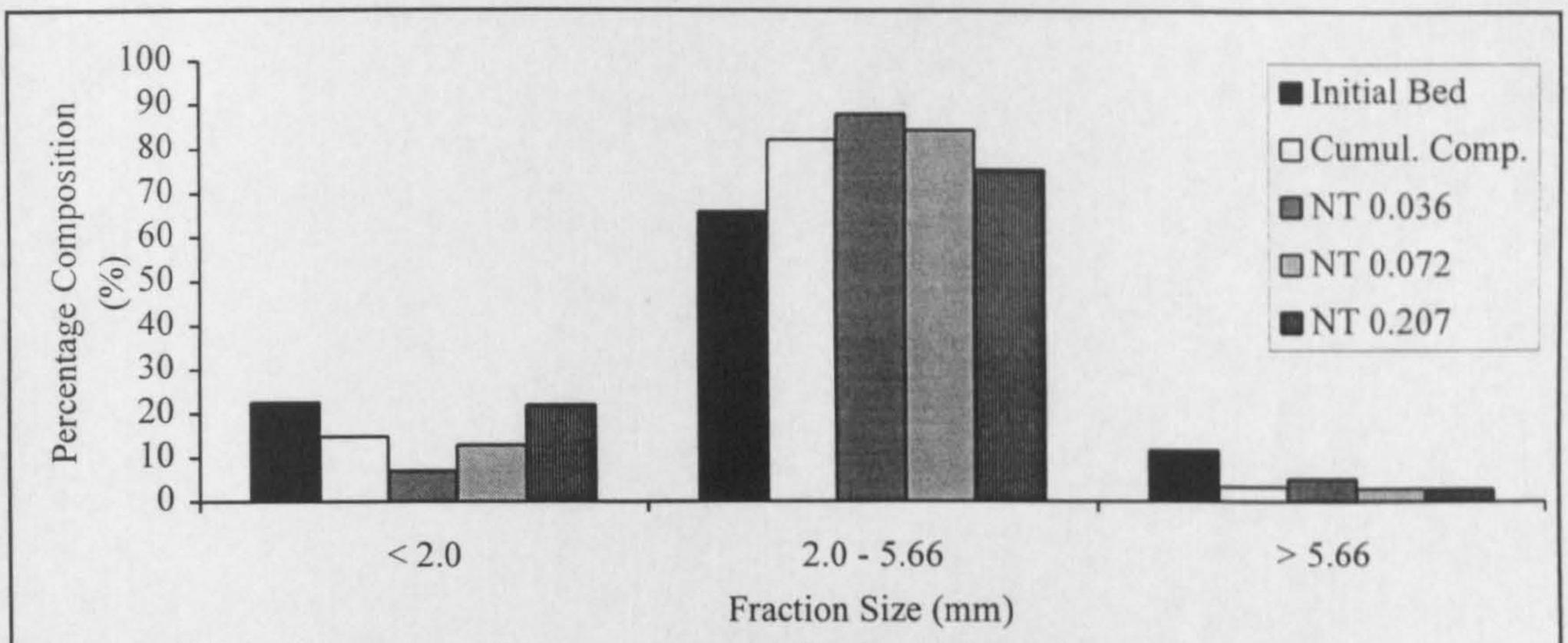

Figure 6.30a Comparison Between Phase 1 Bedload Samples, Cumulative and Initial Bed Simplified Compositions, Experiment 4, Bankfull, Slope 0.0026

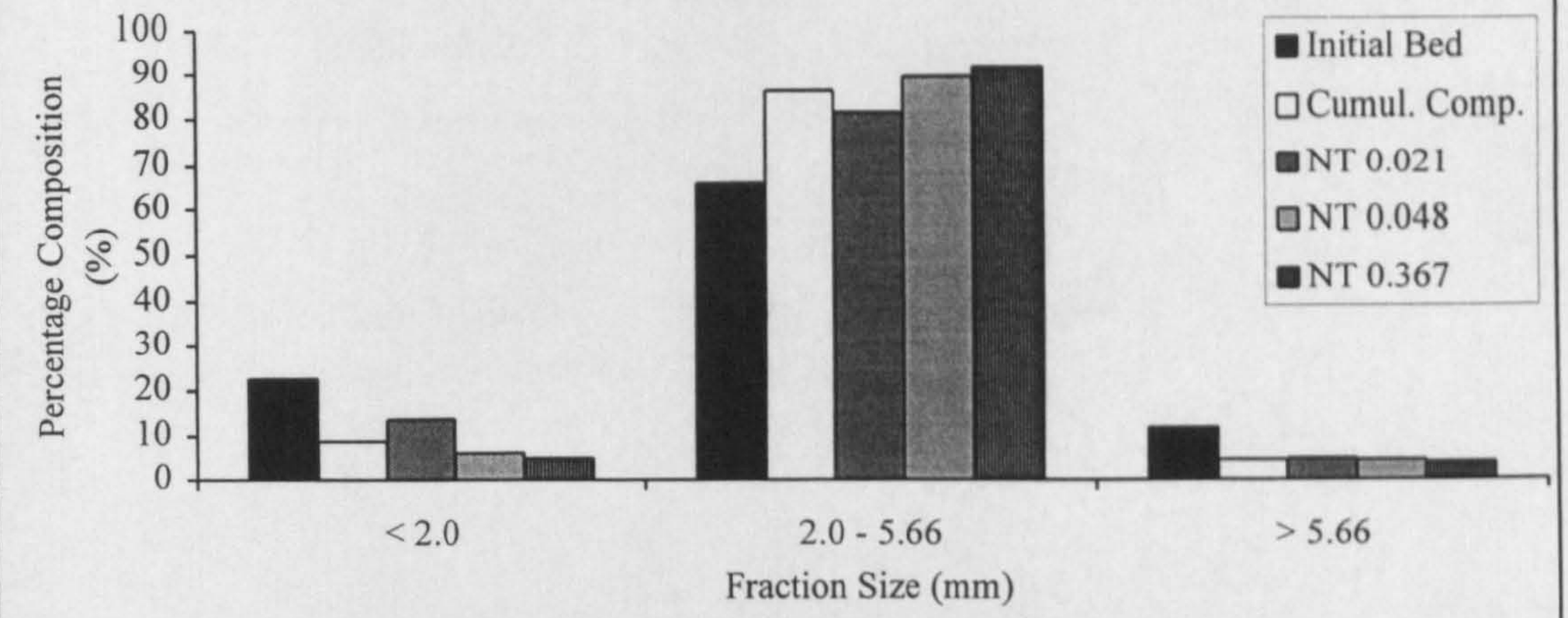

Figure 6.30b Comparison Between Phase 1 Bedload Samples, Cumulative and Initial Bed Simplified Compositions, Experiment 2, Shallow Overbank, Slope 0.0026

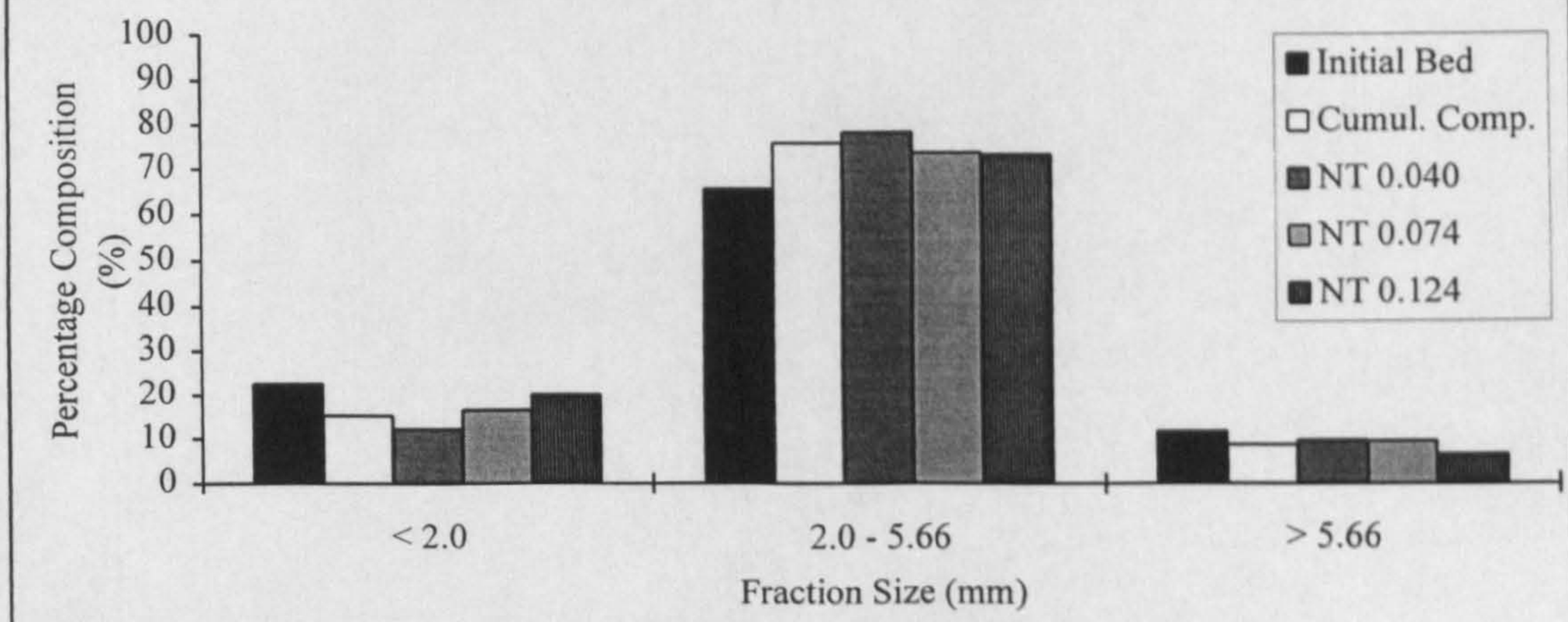

Figure 6.30c Comparison Between Phase 1 Bedload Samples, Cumulative and Initial Bed Simplified Compositions, Experiment 3, Deep Overbank Slope, 0.0026

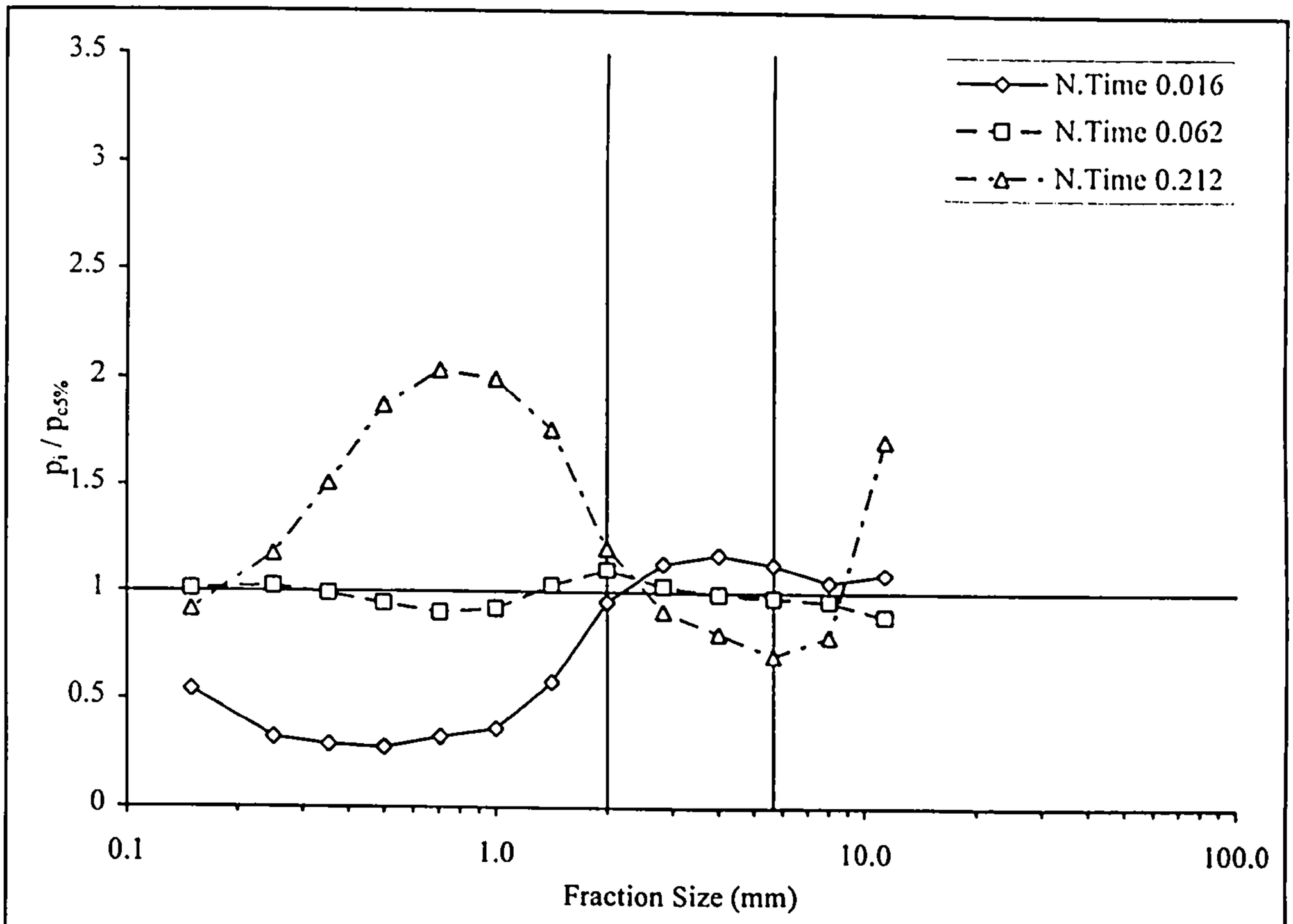

Figure 6.31a Fraction Mobility Relative to Total Collected Phase 1 Bedload Composition, Experiment 6, Bankfull, Slope 0.0024

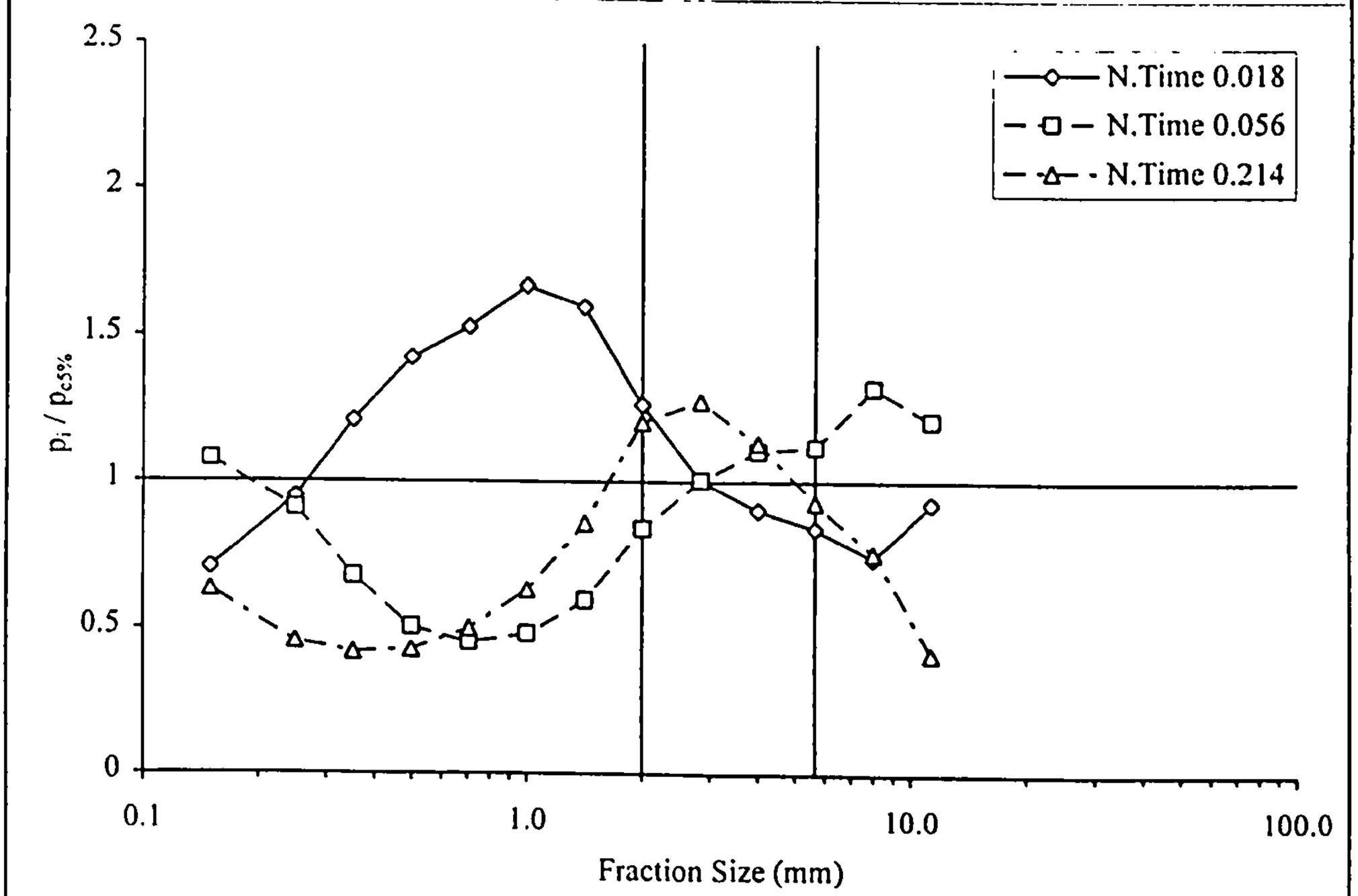

Figure 6.31b Fraction Mobility Relative to Total Collected Phase 1 Bedload Composition, Experiment 7, Shallow Overbank, Slope 0.0024

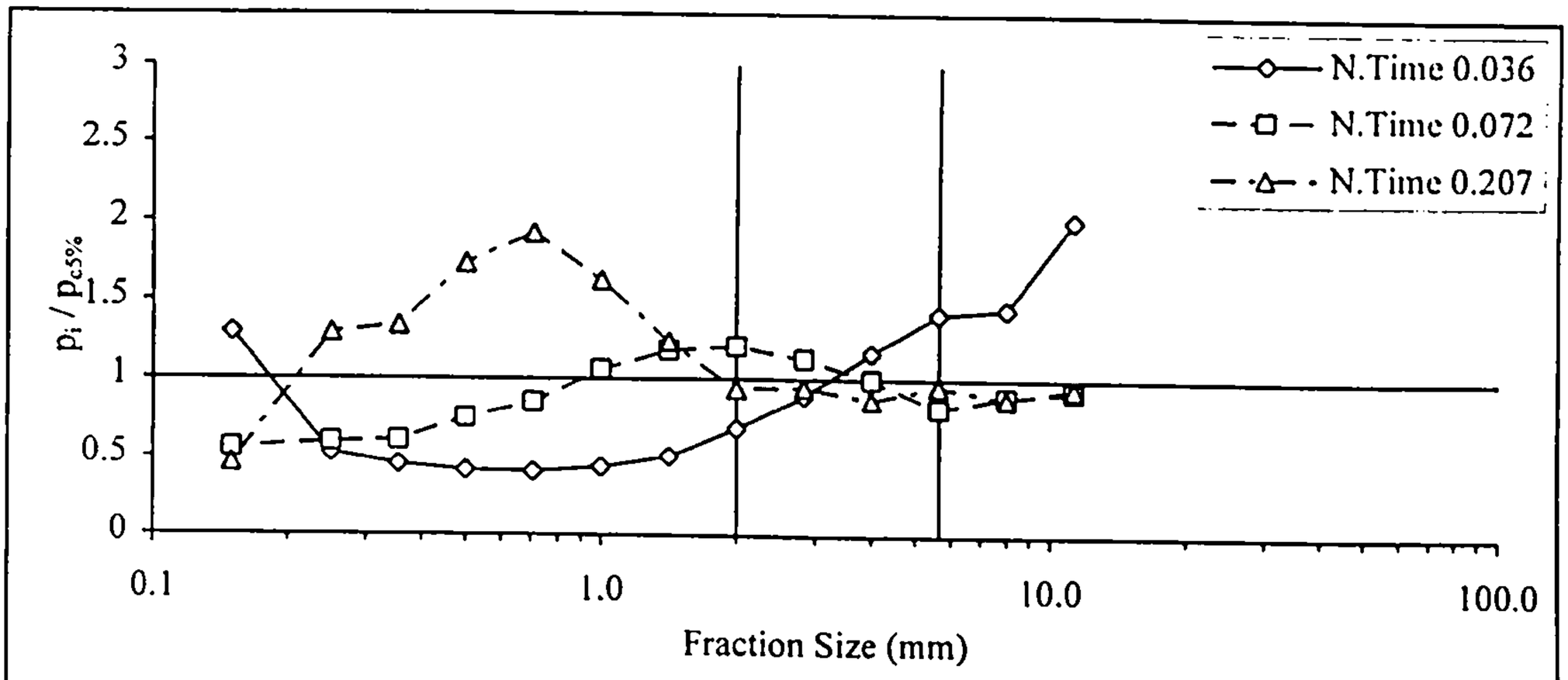

Figure 6.32a Fraction Mobility Relative to Total Collected Phase 1 Bedload Composition, Experiment 4, Bankfull, Slope 0.0026

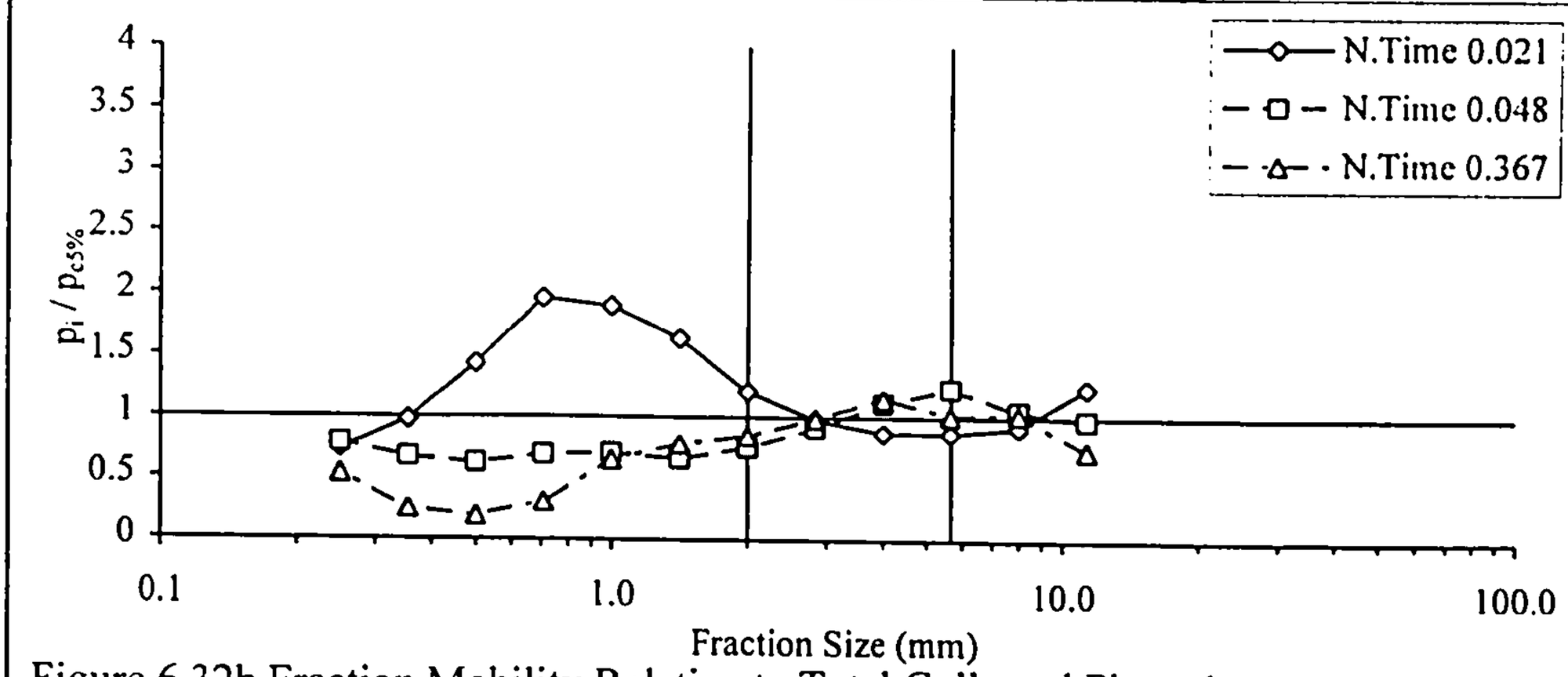

Figure 6.32b Fraction Mobility Relative to Total Collected Phase 1 Bedload Composition, Experiment 2, Shallow Overbank, Slope 0.0026

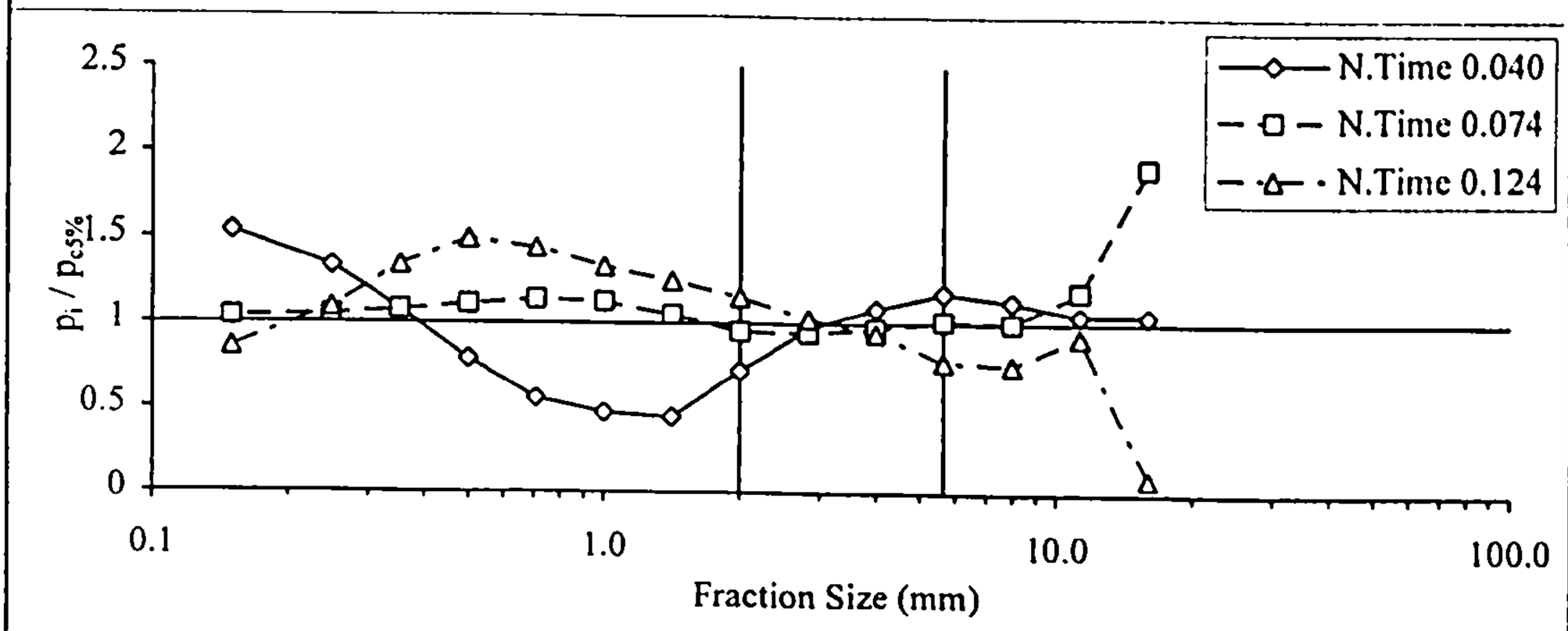

Figure 6.32c Fraction Mobility Relative to Total Collected Phase 1 Bedload Composition, Experiment 3, Deep Overbank, Slope 0.0026

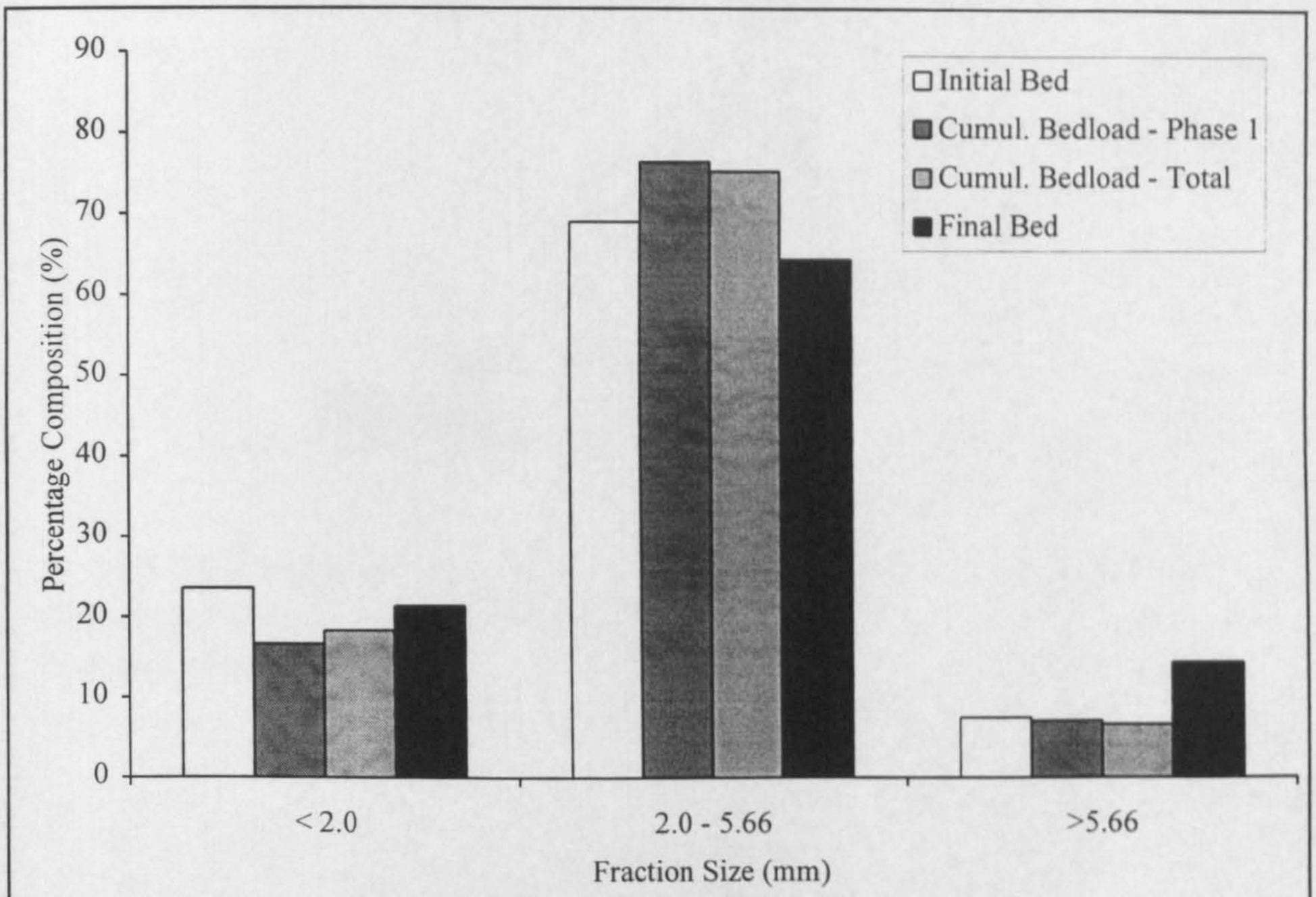

Figure 6.33a Comparison Between Bed Compositions and Cumulative Collected Bedload Compositions, Experiment 6, Bankfull, Slope 0.0024

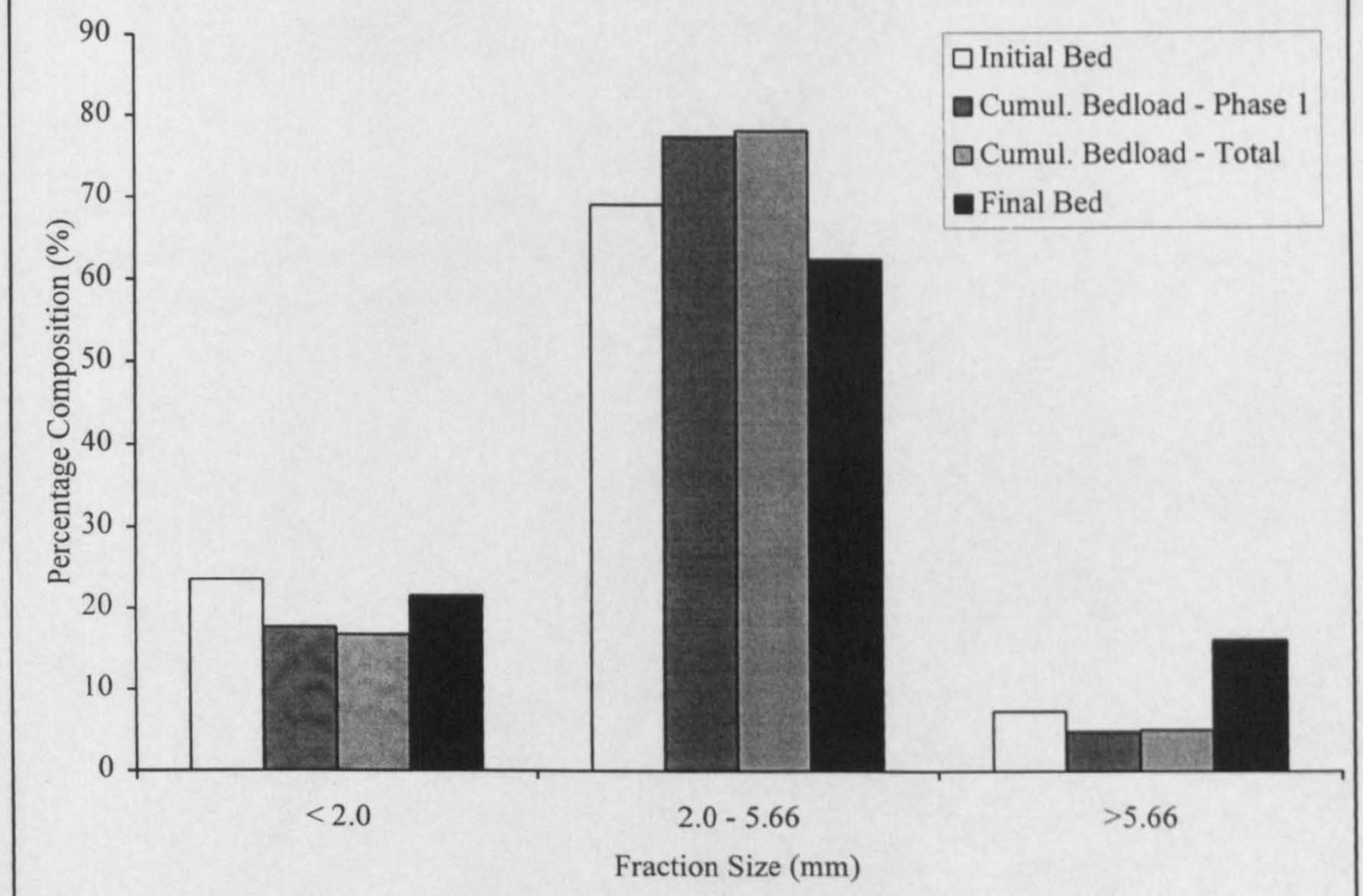

Figure 6.33b Comparison Between Bed Compositions and Cumulative Collected Bedload Compositions, Experiment 7, Shallow Overbank, Slope 0.0024

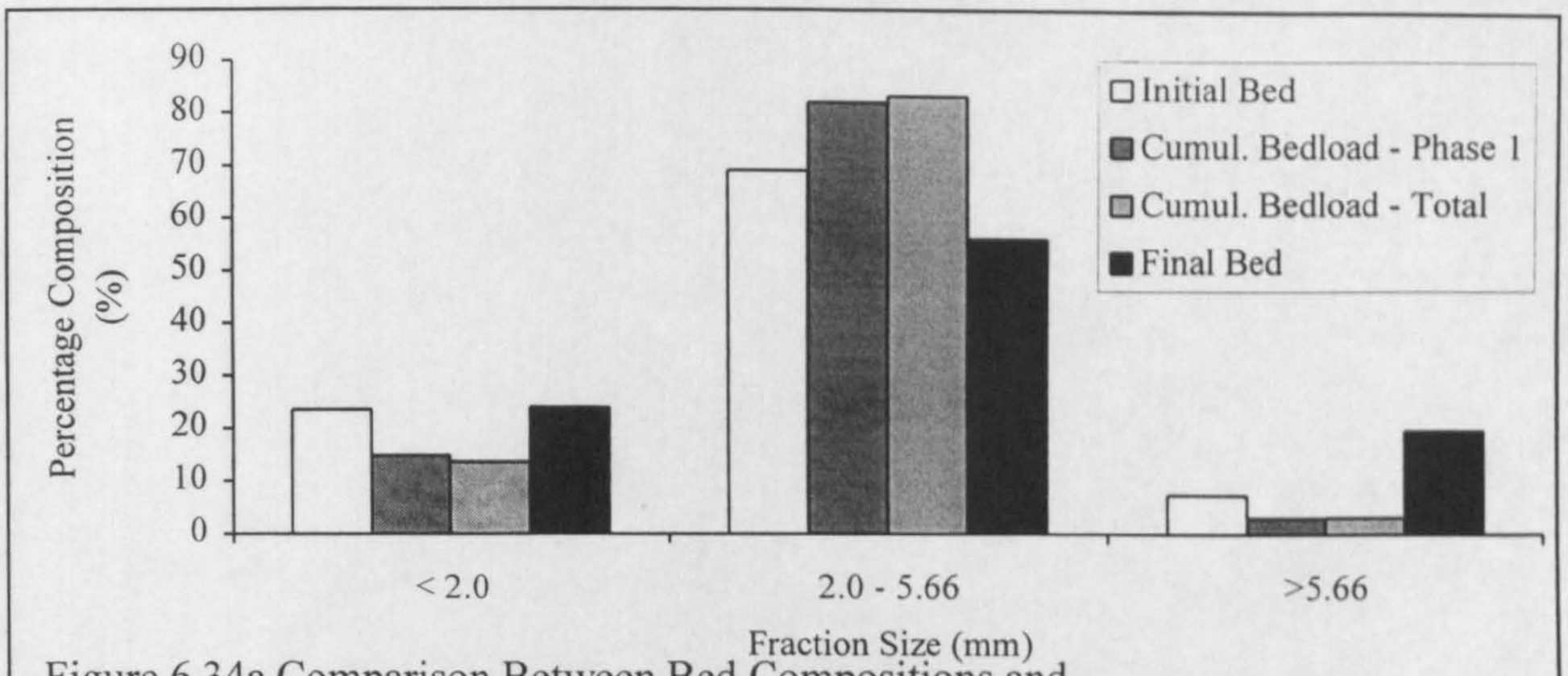

Figure 6.34a Comparison Between Bed Compositions and Cumulative Collected Bedload Compositions, Experiment 4, Bankfull, Slope 0.0026

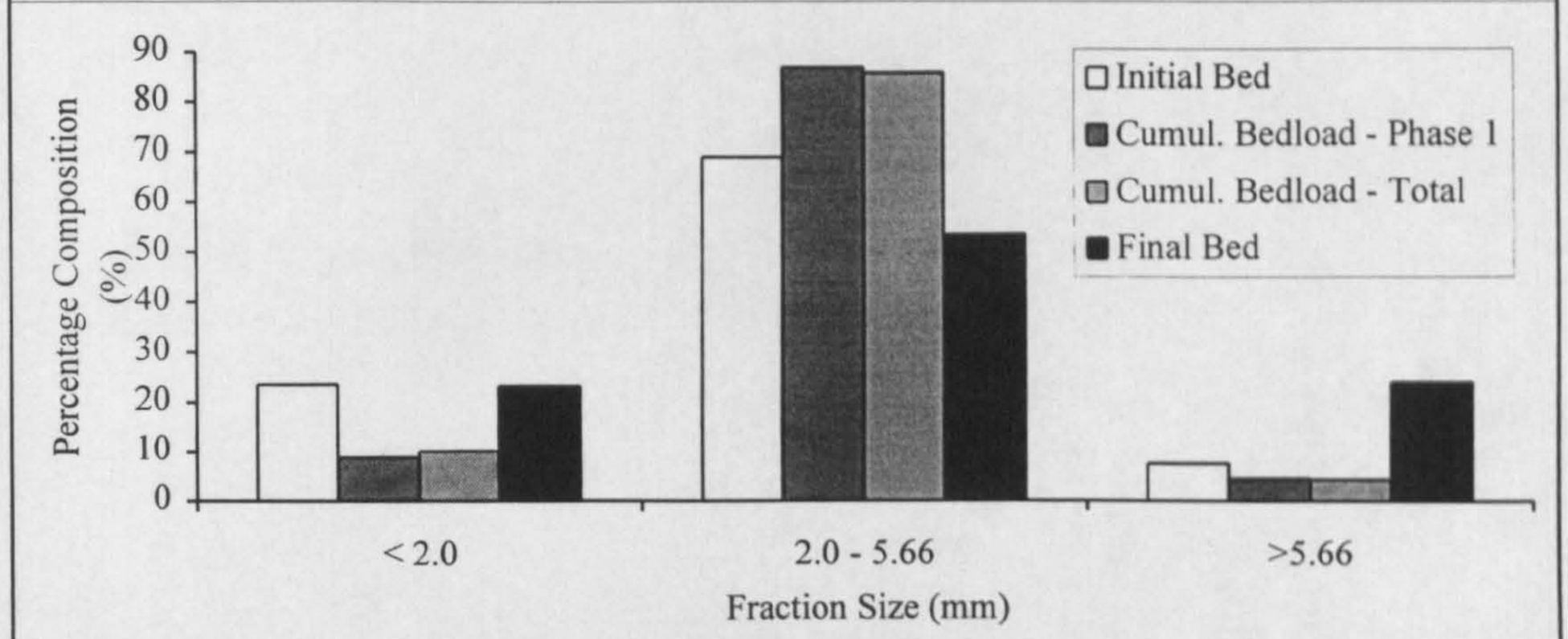

Figure 6.34b Comparison Between Bed Compositions and Cumulative Collected Bedload Compositions, Experiment 2, Shallow Overbank, Slope 0.0026

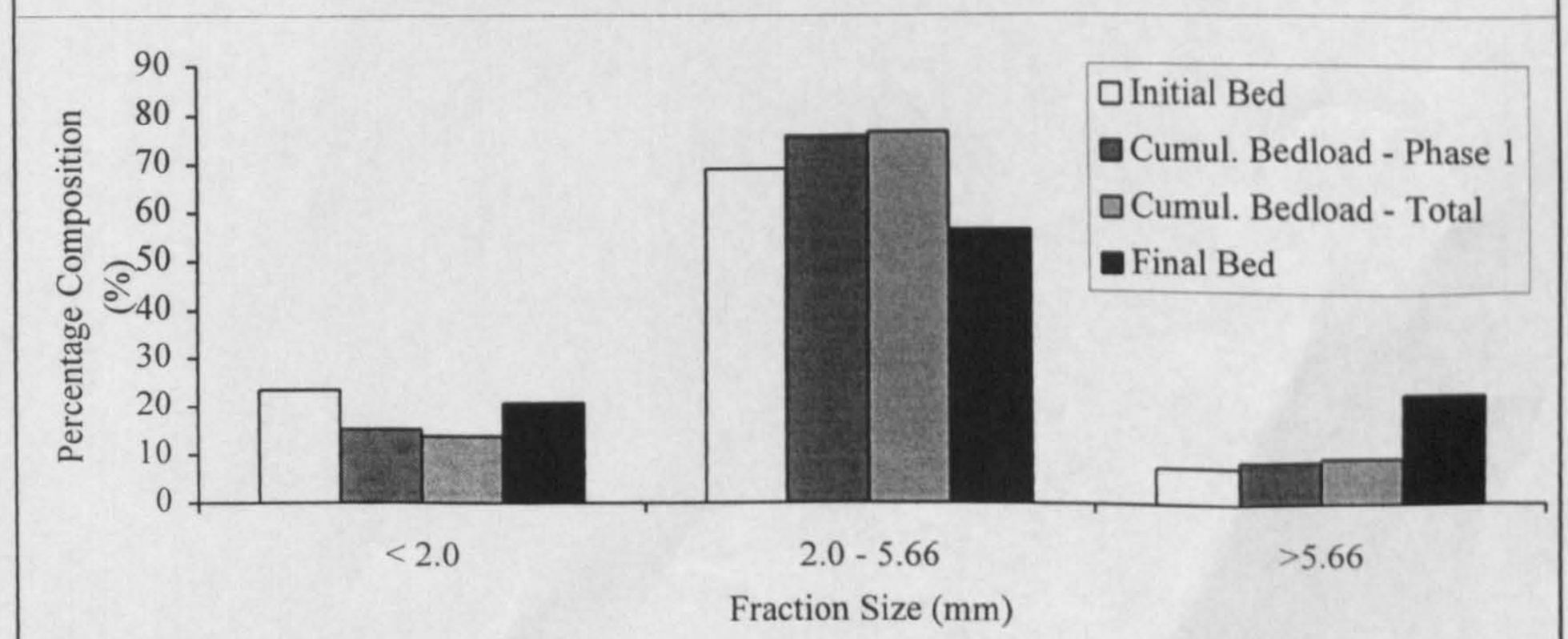

Figure 6.34c Comparison Between Bed Compositions and Cumulative Collected Bedload Compositions, Experiment 3, Deep Overbank, Slope 0.0026

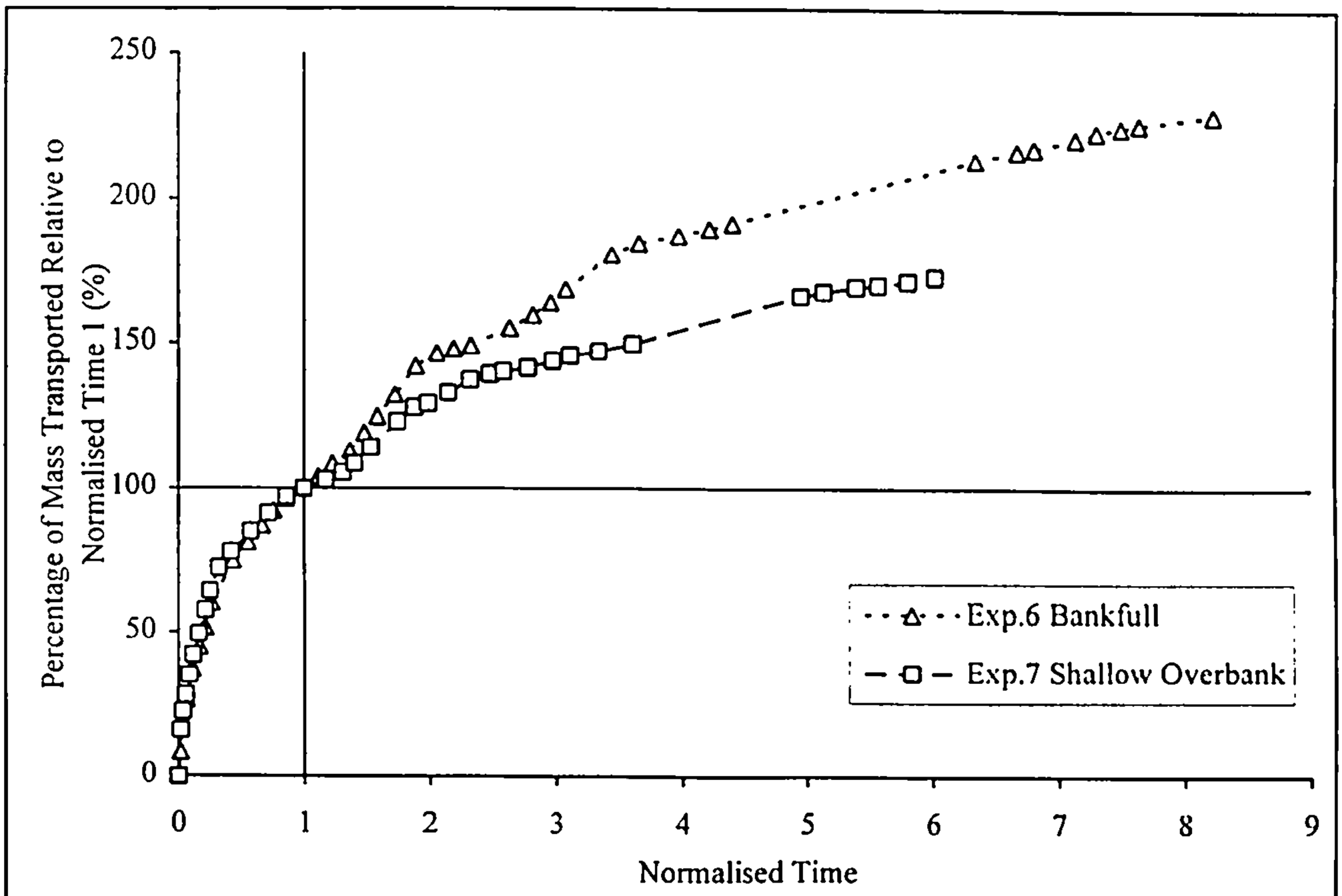

Figure 6.35a Cumulative Bedload Mass Curves for Full Experiments, Relative to Mass at Normalised Time 1, Slope 0.0024

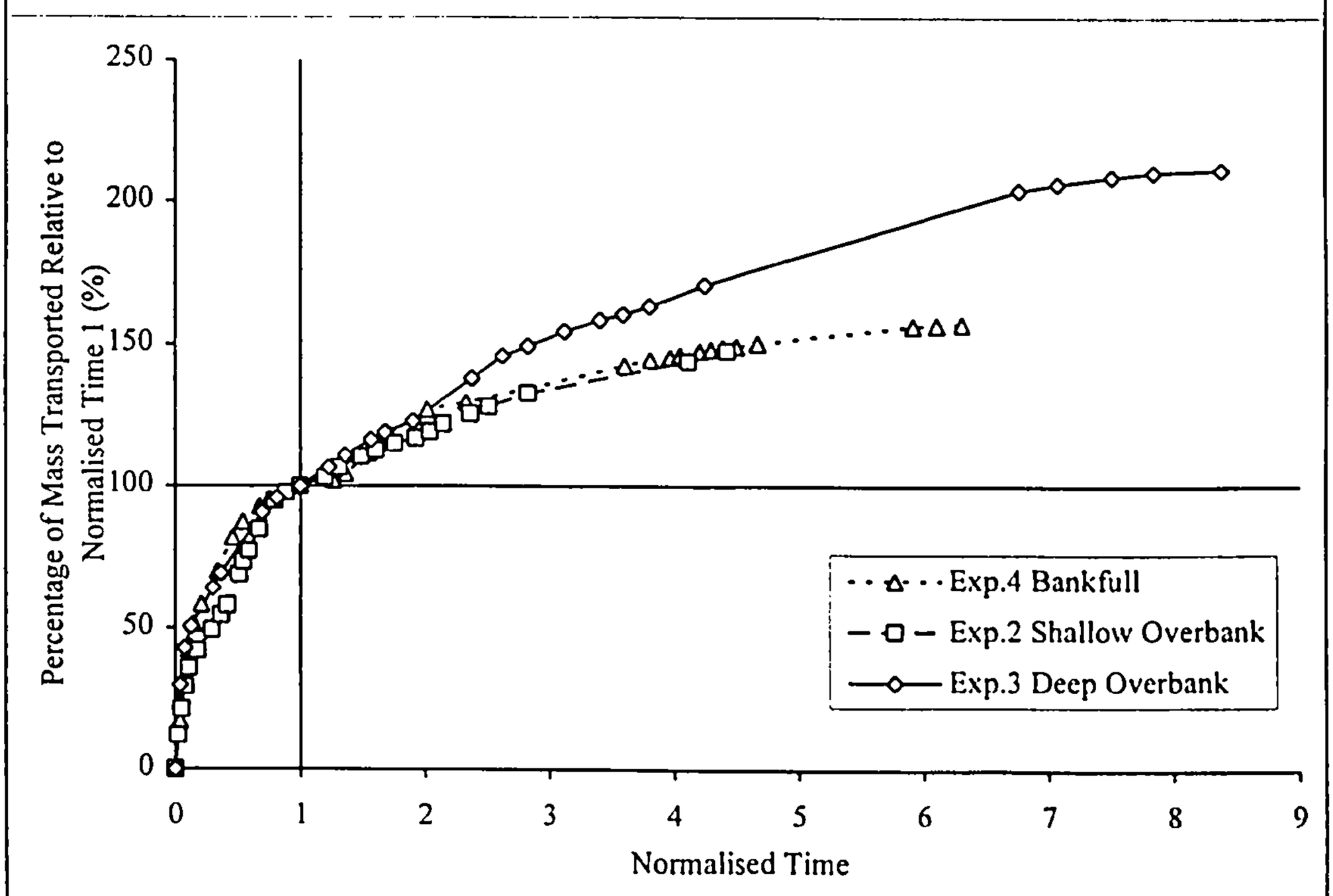

Figure 6.35b Cumulative Bedload Mass Curves for Full Experiments, Relative to Mass at Normalised Time 1, Slope 0.0026

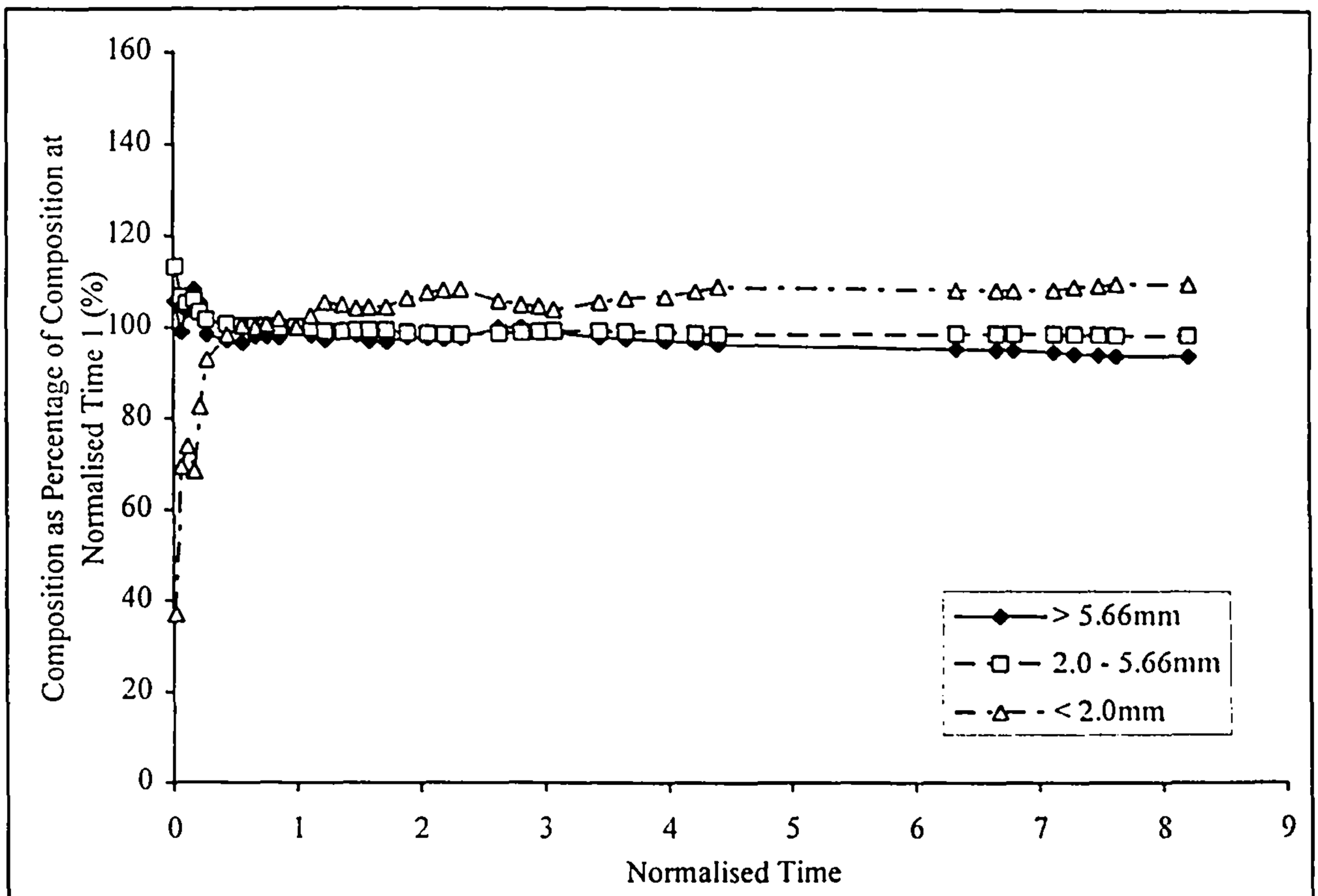

Figure 6.36a Progressive Composition of Cumulative Collected Bedload as Percentage of Composition at Normalised Time 1, Experiment 6, Bankfull, Slope 0.0024

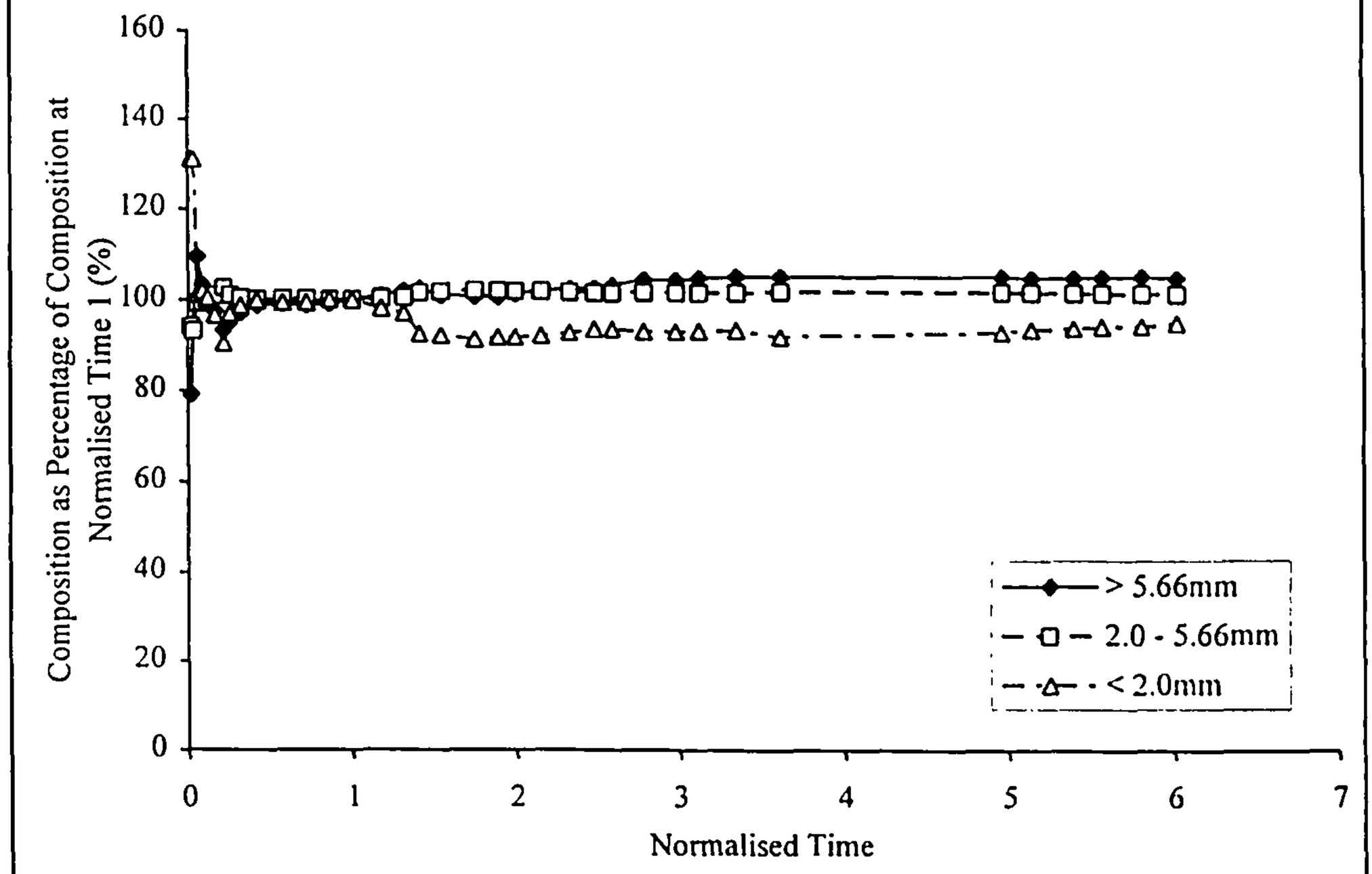

Figure 6.36b Progressive Composition of Cumulative Collected Bedload as Percentage of Composition at Normalised Time 1, Experiment 7, Shallow Overbank, Slope 0.0024

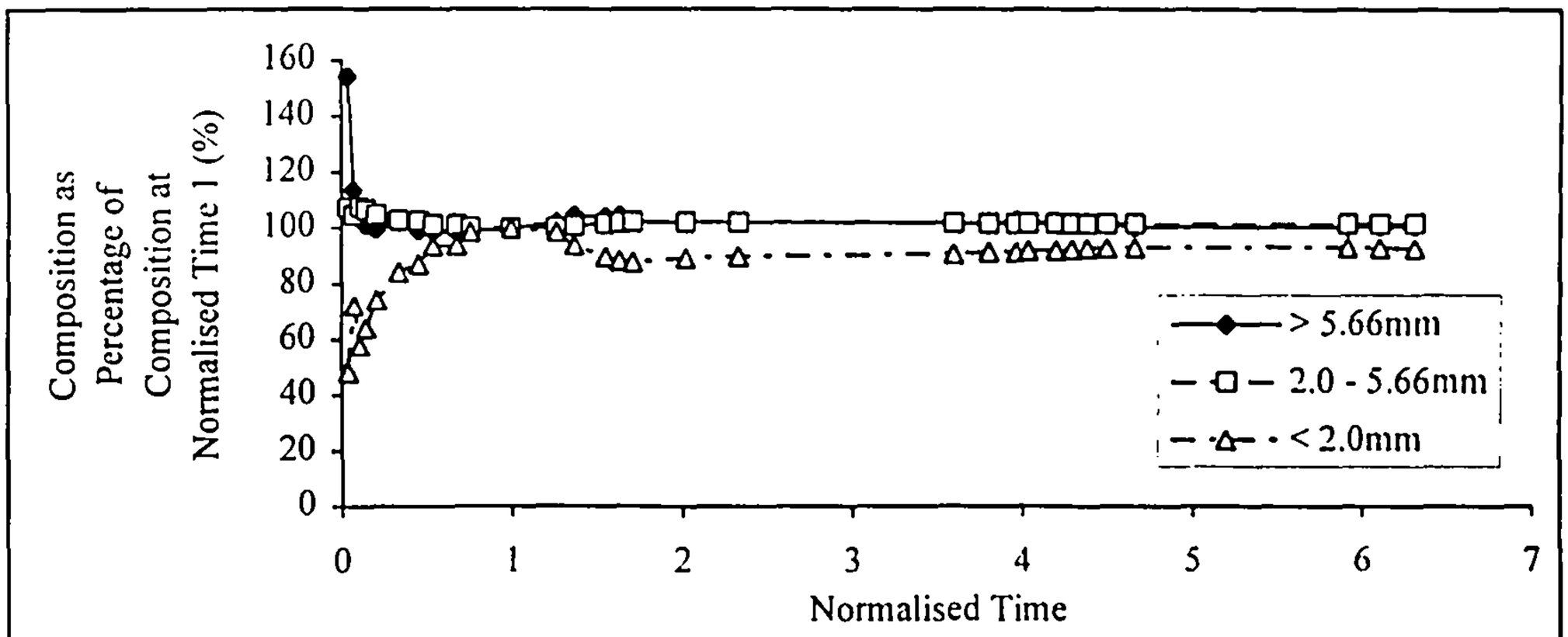

Figure 6.37a Progressive Composition of Cumulative Collected Bedload as Percentage of Composition at Normalised Time 1, Experiment 4, Bankfull, Slope 0.0026

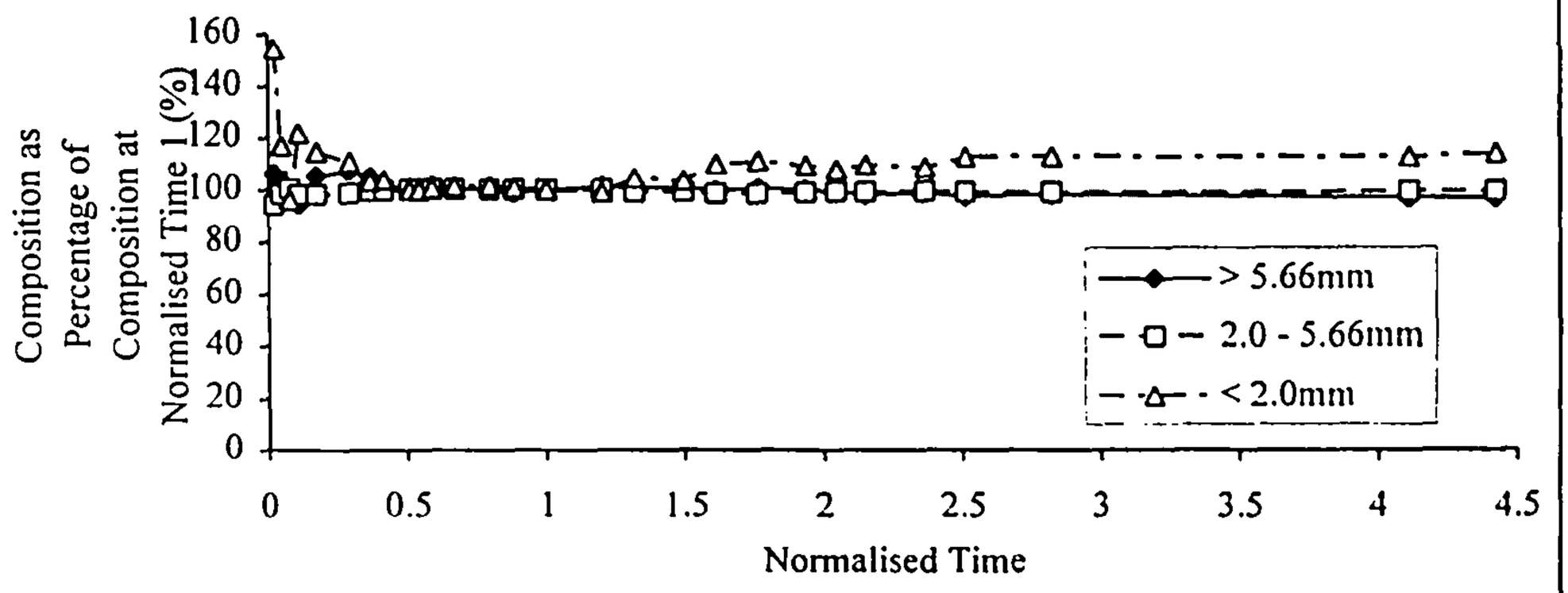

Figure 6.37b Progressive Composition of Cumulative Collected Bedload as Percentage of Composition at Normalised Time 1, Experiment 2, Shallow Overbank, Slope 0.0026

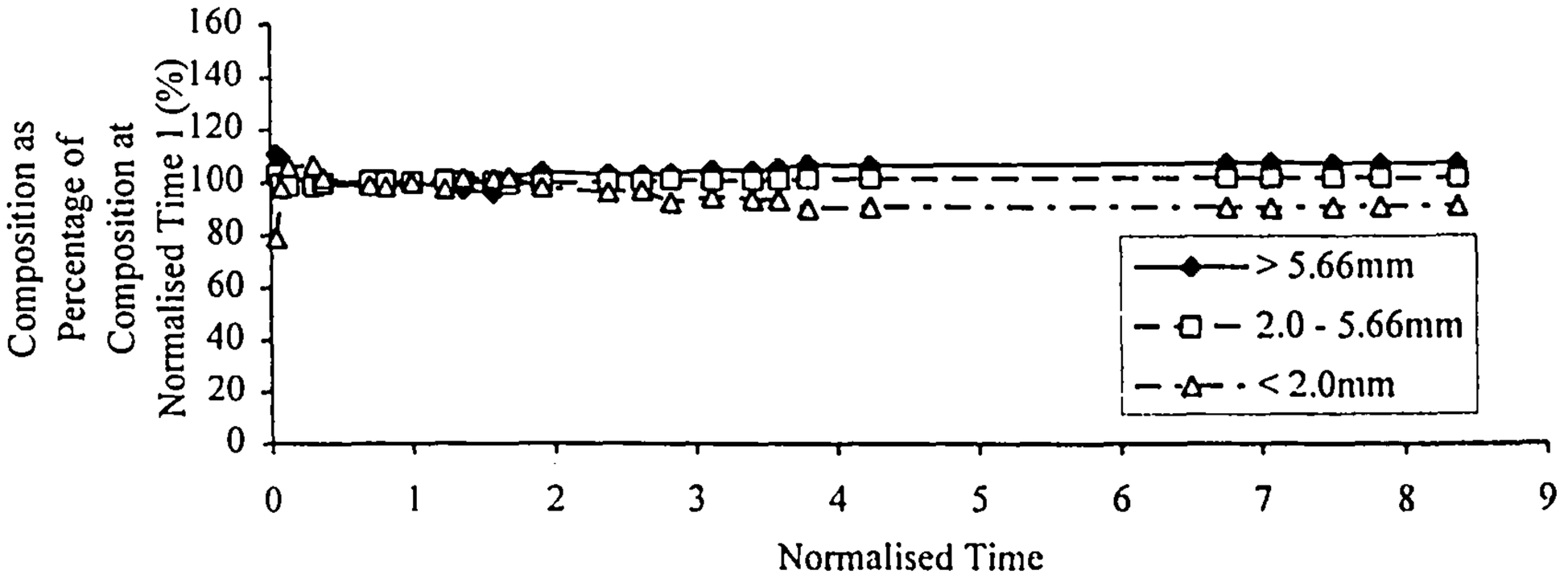

Figure 6.37c Progressive Composition of Cumulative Collected Bedload as Percentage of Composition at Normalised Time 1, Experiment 3, Deep Overbank, Slope 0.0026

Chapter 7

Summary of Conclusions and Suggested Further Work

7.1 Summary of Work

A project examining graded sediment transport in a straight compound channel has been reported. Fifteen experiments were completed during the three year period between October 1994 and October 1997. The experiments examined the response of two different bed mixes to three initial bed slopes, three stage levels, three upstream feed rates and two feed materials. The work was part of the larger Series C project carried out using the HR Wallingford Tilting Flume facility.

A review of literature relating to the topics of sediment transport and compound channel flow has been completed and presented in Chapter 2. Chapter 3 illustrates the full experimental programme completed and describes the experimental apparatus and procedures used. A review of the basic data processing carried out, to convert the raw collected data into a form usable for analytical purposes, is presented in Chapter 4.

From the full set of fifteen experiments, aspects of six were examined in detail. This allowed examination of the effects of initial bed slope and relative depth ratio on the behaviour of no feed degradational experiments. Detailed examinations have been made of the variation of transport rate, average boundary shear stress and unit stream power with relative depth ratio. The results of these are presented in Chapter 5. Examination of changes in bed and bedload compositions with time throughout the degradation process have also been completed and are described within Chapter 6.

7.2 Chapter 2 - Sediment Transport and Compound Channel Flow

The literature review covered topics closely related to the work presented within the rest of this thesis. An introduction was made to the ideas and principles of incipient motion and bedload transport. Uniform sediment transport prediction methods, commonly referred to in the literature, were also introduced. A brief section of the chapter was devoted to highlighting the additional complexities of graded sediment transport compared to those of uniform sediment transport. A selection of more common graded sediment transport prediction formulae and models were then introduced. The following section introduced the idea of hiding functions, employed to allow uniform transport prediction techniques to be applied to graded sediment transport. Within the chapter the need for better, more complete predictive techniques was discussed, suggesting small scale physical processes should be taken into account. The chapter also included a review of the extensive data sets currently available that would allow any such new approach to be tested. This was followed by a review of previous work carried out in examination of compound channel flow behaviour.

7.2.1 Conclusions

The following points are a summary of the conclusions drawn from, and presented in the chapter.

1. Graded sediment transport is a particularly complex process. It is therefore difficult to model.

2. Existing techniques for estimating sediment transport rates are based on macro parameters such as boundary shear stress, flow velocity and unit stream power. They have proven however, to be inaccurate for conditions significantly different than those from which they were derived. It is concluded that basing calculation techniques on global parameters may not be sufficient to produce accurate prediction models for graded sediment transport.

3. A new approach to the problem is required. It is suggested that for a prediction technique to be successful it will require to be holistic in its nature. It will therefore have to consider the smaller physical processes occurring within the overall transport process and their influences on it.

4. Existing transport prediction techniques are based on data collected from single channel flows. It is therefore questionable as to whether their limited prediction capabilities are applicable to overbank flow. Any new approach should seek to rectify this situation by being applicable to both conditions.

5. To develop an accurate prediction technique for graded sediment transport considerably more research is required. Firstly the understanding of the mechanics and the influence of small scale physical processes must be targeted. This will allow the basis of a new approach to be formed. Extensive detailed data sets must then be available to allow rigorous testing of any proposed technique across a wide range of imposed conditions.

7.3 Chapter 3 - Experimental Programme, Apparatus and Procedures

In Chapter 3 a detailed introduction is given to the experimental programme. A tabular description of all 15 experiments carried out within the three year period between October 1994 and October 1997 is given in table 3.1. The analytical groupings available within the first set of experiments (2 to 12) are discussed. These allow examination of the effect of different parameters on the experimental results. The three groupings presented, two of which are examined within this thesis, are variable initial slope, variable initial stage level and variable upstream feed rates.

A significant part of the chapter is dedicated to the description of the experimental apparatus. All the pieces of apparatus used in the collection of the data presented are described. A section is devoted to each of; the flume, the bed material, the sediment traps, the instrument carriage, the photography equipment, the bed composition

sampling equipment, the discharge measurement equipment and temperature gauge. Within the section on the instrument carriage the velocity profiling equipment was also discussed, along with the water surface profiling, the bed slope profiling and the bed surface texturing equipment.

The third and final section in Chapter 3 discussed the procedures adhered to during the recording of data with the equipment previously described. The section included descriptions of the procedures required during the setting up of each experiment followed by the procedures for the running and final shut down. The criteria for judging appropriate times to switch off the upstream sediment feed conditions and to stop the completed experiment were also described.

7.3.1 Conclusions

From the chapter the following conclusions can be drawn.

1. An extensive set of experiments have been completed examining the effects of initial bed slope, discharge stage level, upstream feed conditions and bed material composition on the resulting sediment transport.

2. A narrow range of initial bed slopes were covered in the experimental programme. These were appropriate to the bed material being used.

3. A more significant range of relative depth ratios were examined. These were limited by the flume discharge capacity and ultimately by the flume depth.

4. A range of upstream sediment feed conditions were imposed on the experiments. The rate of feed being related to the initial transport rate during phase 1 of Experiment 4.

5. For each experiment an extensive range of detailed measurements were taken making the resulting data sets attractive for further use in sediment transport research.

6. A consistent approach was taken towards the measurement and recording of the data. The implementation allows confidence to be placed in the resulting data sets.

7.3.2 Extended Programme and Further Measurements

It is unusual for any investigation to afford such an extensive range of experiments that no further experiments would be advantageous. The reasons for further experiments are discussed in Chapters 5 and 6 and in the summary of conclusions from those chapters later. If it was deemed appropriate to carry out further experiments in this series, and funding was available, then the extra work should cover a wider range of initial bed slopes. In addition to this, more experiments should be completed at the deep overbank flow depth and more relative depths, within the flume range, should be examined.

7.4 Chapter 4 - Data Processing

Chapter 4 reviewed the processing required to convert the raw collected data into a format that was easily usable in analysis.

7.4.1 Processing Required

The basic processing required is summarised briefly below.

1. The composition of samples collected using areal wax sampling required to be converted, to take account of the technique and to produce an equivalent volumetric composition.

2. All compositional data was converted to the half-Phi sieve scale unless the sample was originally sieved using a half-Phi set of sieves.

3. The rail survey levels were adjusted so that the regression resulting from them had a level of zero at the chainage of the concrete block datum, to which the other measurements were related.

4. The bedload data was processed to produce individual Excel workbooks for each experiment, within which, each sheet represented an individual cycle of readings. From the raw compositional data, grading parameters and unit transport rates were calculated for each of the left, centre and right traps along with the combined total bedload.

5. The recorded A/D readings from the longitudinal lasers and the wire potentiometer were initially processed to convert them to chainages and distances between the lasers and the bed. The data was then adjusted to the concrete block datum and adjusted to take account of the instrument rail slope. The resulting profiles for the left, centre and right lasers were then curtailed at 6 m and 16 m (the experimental length of the flume). Spurious readings were removed from each and the values across the width of the channel averaged to give the final bed profile.

6. The water surface profile data collected from the pointer gauges attached to the instrument carriage required basic processing. The collected profile was adjusted to take account of the slope of the instrument rails. Both the water surface profiles from the flume pointer gauges and those from the tapping point pointer gauges were then adjusted to relate the profiles to the concrete block datum.

7. Where it was appropriate some processing was carried out on the collected velocity profiles. The raw profiles included velocity measurements at levels through the flow depth related to the bankfull level of the channel. These velocity data were then related to either the bed level, from the longitudinal profile, or the water surface level, from the pointer gauge profiles. This was possible as all the levels of the

velocity, bed and water surface readings were able to be related to the concrete block datum.

8. The post-experimental processing of the bed surface texture data was carried out by Aberdeen University. The data within each texture file was checked for consistency, scanned for out of range readings and converted to X, Y and vertical level values in mm.

7.4.2 Availability of Processed Data

All the processed data from Experiments 2 to 12 (listed in section 3.1) is available from either the University of Aberdeen or the University of Glasgow. It is intended that the processed data from Experiments 13 to 16 will be available in the near future. Most of the data is available via the internet at the following address: http://www.civil.gla.ac.uk/research/GSRP. Texture data on CD and bed photographs can be obtained by contacting the departments of Civil Engineering at the above universities.

7.5 Chapter 5 - Comparison of Sediment Transport Rates: Bankfull and Overbank Flow

Chapter 5 was the first of the two main analysis chapters. Five degradational experiments were examined from the set described in Chapter 3. All five show the same characteristic transport rate decline, namely: an initially high transport rate followed by a steep decline and a period of marginal transport towards the end of the experiment. Two methods of estimating boundary shear stress from the data were examined; the Ackers 1-D method and the Wark Lateral Distribution Method (LDM). The predicted shear stresses were then compared to the relative depth ratios of the five experiments. Transport rate regressions were fitted to the measured data to allow estimates of transport at times not sampled. The fit of the applied regressions were found to be satisfactory by the author. The weights of material transported over

various periods during each experiment were estimated using the measured transport data. Both the results from the regression analysis of the transport rates and the estimated weights of material transported were compared to the predictions of boundary shear stress. Finally, estimates of unit stream power were calculated and these too compared to the relative depth ratios and transport capacities of the five experiments.

7.5.1 Conclusions

A summary of the conclusions presented at the end of Chapter 5 are outlined below.

1. The results show that transport rate is dependent on the applied hydraulic conditions. For the same bed material, higher transport rates occur for steeper initial bed slopes and higher stage levels.

2. Estimates of boundary shear stress in the main channel (obtained using a numerical model) showed this to vary with relative depth ratio for the same initial bed slope and the same initial bed material. The main channel boundary shear stress was found to be less for the shallow overbank flow than it was for the bankfull flow. While the shear stress experienced by the main channel during the deep overbank flow was greater than during both bankfull and shallow overbank cases.

3. The output from the flow model was also used to predict unit stream power. Unit stream power was found to vary monotonically with relative depth ratio. Experiments with a higher predicted unit stream power produced larger sediment transport rates.

4. When unit stream power and boundary shear stress are estimated as they have been here unit stream power based prediction methods may therefore form a better basis for the prediction of section averaged, sediment transport rates, in two-stage channels with gravel beds, than boundary shear stress based methods.

7.5.2 Further Work

Several ideas for further work arose during the completion of the analysis presented in Chapter 5. Some of the ideas involve analysis attempted during the work and some involve fresh research into areas highlighted by the results. What follows in this section is a summary of the ideas for further work presented at the end of Chapter 5.

1. It is suggested that one of the procedures used to estimate boundary shear stress and unit stream power may allow examination of developing gravel bed hydraulic roughness. Based on the estimate of the initially screeded gravel bed roughness the Wark LDM model could be used to estimate a suitable non-dimensional eddy viscosity. The non-dimensional eddy viscosity can be held constant throughout the experiment evolution. This allows the flow conditions predicted by the model to be matched to the conditions measured by iterative adjustment of the gravel bed roughness. The resulting evolution of bed roughness should then match the actual evolution as closely as the original estimate. The condition of keeping the initial estimate of non-dimensional eddy viscosity constant throughout the experiment requires further research.

2. The increase in unit stream power with increasing relative depth appears to diminish at larger relative depths. Further investigation of the relationship between the two would be advantageous in determining the relationship between unit stream power and sediment transport for overbank conditions.

3. Other methods of estimating the lateral distribution of parameters such as discharge, flow velocity, boundary shear stress and unit stream power should be investigated. This would allow a choice of model on which to base future work on a lateral distribution based, sediment transport, prediction model. More detailed data, on the lateral distribution of parameters in mobile boundary channels, need to be collected before work of this nature can be attempted. Additionally, further data sets regarding the lateral distribution of sediment transport should be collected.

4. If further experiments are to be conducted along the lines of those presented here, it is suggested they should be designed to fill in the gaps around areas of interest. The details of flow conditions and sediment transport behaviour should be studied at low relative depths initially, as these are the most common floods in reality. It is also suggested that re-circulation experiments, run to an equilibrium condition, are used. Such experiments allow a more direct comparison to be made between initial and final conditions, as the final conditions can be clearly defined.

7.6 Chapter 6 - Effects of Slope and Relative Depth on the Evolution of Bed Surface and Bedload Transport Compositions

In Chapter 6 the results from six degradational experiments were examined in detail. Five of these experiments had first been introduced in Chapter 5 and their characteristics determined. The sixth experiment was initially introduced and the same characteristics examined. Normalised time was examined and implemented to aid comparison of evolution processes. Measured values of sediment transport rates and weight of material transported, along with predicted values of boundary shear stress and unit stream power, were used to propose a ranking order of transporting potential. The proposed order was then used to help examine the evolution of the bed surface and bedload compositions with time.

7.6.1 Conclusions

The conclusions presented below are a summary of those drawn from, and included at the end of, Chapter 6.

1. In agreement with conclusion 1 in section 7.5.1, it was found that the transporting potential of an experiment was greater for a greater initial bed slope or greater relative depth.

2. All six degradational experiments produced final bed surfaces that were significantly coarser than the initial bed. Experiments with larger transporting potentials produced coarser final beds.

3. The size fractions removed from the bed were found to vary with transporting potential. During the low transport potential experiments more fine material, some mid-range material and little coarse material was removed from the bed surface. For the middle potential experiments it was still mostly fine and mid-range material that was removed but this time a higher proportion of mid-range sizes. During high potential experiments it was mostly mid-range material that was removed but also significant amounts of fine and coarse particles.

4. From the various methods used to assess the order of transport potential, the following suggestion is made. With reference to unit stream power transport potential is greater for overbank experiments than for bankfull experiments. Although, there is a slight reduction in the rate of increase in observed transport rate at the low overbank depth. The reduction in observed transport rate caused by overbank flow is less than that suggested by predicted variations in boundary shear stress.

5. All six experiments show changes in bedload composition during degradation. The relationship between transport potential and bedload composition evolution is complex however, and the data is difficult to interpret. The amounts and composition of material removed from the initial unstable screeded bed vary with transporting potential. This leads to water worked beds with varying degrees of stability and a range of bedload evolutions. The pattern of bedload evolution appears to be dependent on both the transporting potential of the experiment and the critical conditions of the bed material.

6. In all the experiments it appears that phase 1 (the initial steep decline to less than 5% of the initial transport rate) dominates in determining final bed composition and bedload evolution. However, the phase 2, marginal transport, period plays an important role in enhancing bed stability.

7.6.2 Further Work

The ideas for further work presented in this section are a summary of those in section 6.9.

1. More detail on the transport rate decline curves would lead to better resolution. When combined with longer running experiments this would allow for more accurate assessment of final stability.

2. The use of re-circulation experiments would also allow for a clearer definition of stability (Parker and Wilcock 1993). Transport rate stability can be taken as a constant bedload transport rate with time while bed surface stability can be said to have been achieved when the bedload composition stabilises.

3. In terms of carrying out further experiments to compliment the work presented here, the range of initial bed slopes examined should be extended. Further experiments should also aim to fill in the gaps in the range of relative depths examined. Extending the data set in such a way would allow assessment of which variables have the greatest effect on transporting potential. The extended data set would also allow further examination of the relative retardation effect of overbank flow on sediment transport.

References

Ackers, P., and White, W.R. (1973), "Sediment Transport: New Approach and Analysis", J. Hyd. Div.,ASCE, HY11,

Ackers, P., and White, W.R. (1990), "Sediment Transport: The Ackers and White Theory Revised", HR Wallingford Report No.SR237

Ackers, P. (1991), " The Hydraulic Design of Straight Compound Channels", Report SR281, HR Wallingford

Ackers, P. (1991b), "Discussion", J.Hyd. Res., 29(2), pp263-274

Ackers, P. (1992a), "Hydraulic Design of Two-Stage Channels", Proc. Instn. Civ. Engrs. Wat., Marit. And Energy, 96, pp 247-257

Ackers, P. (1992b), "Gerald Lacey Memorial Lecture: Canal and River Regime in Theory and Practise, 1929-1992", Proc. Instn. Civ. Engrs. Wat., Marit., and Energy, 96, Sept, pp167-178

Armanini, A., and Di Silvio, G. (1988), "A One-Dimensional Model for the Transport of a Sediment Mixture in Non-Equilibrium Conditions", J. Hyd. Res., IAHR, 26(3)

Armanini, A. (1995), "Non-Uniform Sediment Transport: Dynamics of the Active Layer", J. Hyd. Res., IAHR, 33(5)

Baird, J.I., and Ervine, D.A. (1982), "Rating Curves for Rivers with Overbank Flow", Proc. Instn. Civil Engrs., Part 2, 73, June, pp465-472

Baird, J.I., and Ervine, D.A. (1984), "Resistance to Flow in Channels with Overbank Flood-Plain Flow", Proc. 1st Int. Conf. Cannels and Channel Control Structures, Computational Mechanics Centre, Southampton, England and Springer Verlag, Heidelberg, Germany, pp4 137- 4 150

Bagnold, R.A. (1966), "An Approach to the Sediment Transport Problem from General Physics", US Geological Survey Professional Paper 422-J

Bagnold, R.A. (1973), "The Nature of Saltation and of Bedload Transport in Water", Proc. Royal Society of London, A332

Bagnold, R.A. (1980). "An Empirical Correlation of Bedload Transport Rates in Flumes and Natural Rivers", Proc. Royal Society of London. A 372, pp 453-473

Bagnold, R.A. (1986), "Transport of Solids by Natural Water Flow: Evidence for a Worldwide Correlation", Proc. Royal Society of London. A 405. pp 369-374

Bell, R.G., and Sutherland, A.J. (1983), "Nonequilibrium Bedload Transport by Steady Flows", J. Hyd. Eng., ASCE, Vol.109.

Bennett, S.J., and Bridge, J.S. (1995), "An Experimental Study of Flow, Bedload Transport and Bed Topography Under Conditions of Erosion and Deposition and Comparison with Theoretical Models", Sedimentology, 42, pp 117-146

Bettess, R. (1984), "Initiation of Sediment Transport in Gravel Streams", Proc. ICE. part 2, 77, pp79-88

Bettess, R. (1994), "Revised Scoping Study for Sediment Research in the Flood Channel Facility", HR Report No. SR365

Bettess, R. (1997), "Research on the Motion of Uniform and Non-uniform Sediments in Two-stage Channels", Proc. 27th IAHR Congress, California.

Bettess, R. (1997b), Personal Communication

Bishop, A.A., Simons, D.B., and Richardson, E.V. (1965), "Total Bed Material Transport", J.Hyd. Div., ASCE, Vol.91, No.HY2, pp175-191

Brown, A., and Willetts, B. (1997), "Sediment Flux, Grain Sorting and the Bed Condition", Proc. 27th IAHR Congress, California.

Brown, C.B. (1950), "Sediment Transportation", in Engineering Hydraulics, Ed. H. Rouse, John Wiley, New York

Cardoso, A.H., Graf, W.H., and Gust, G. (1989), "Uniform Flow in a Smooth Open Channel", J. Hyd. Res., IAHR, 27(5), pp603-616

Carling, P. (1984), "Deposition of Fine and Coarse Sand in an Open-Work Gravel Bed", Canadian Journal of Fisheries and Aquatic Science, 41, pp263-270

Chadwick, A.J., and Morfett, J.C. (1986), "Hydraulics in Civil Engineering", Published by Harper Collins Academic

Chow, V.T. (1959), "Open Channel Hydraulics", McGraw-Hill, London, International Student Edition

Clear Hill, H. (1994), "The Maidenhead, Windsor and Eton Flood Alleviation Scheme", Paper 45, 2nd Int. Conference on River Flood Hydraulics, York, England.

Cox, R.G. (1973), "Effective Hydraulic Roughness for Channels Having Bed Roughness Different from Bank Roughness", Misc. Paper H-73-2, US Army Engineers Waterways Experiment Station. Vicksburg, Mississippi

Crisp, D.T., and Carling, P. (1989), "Observations on Siting, Dimensions and Structure of Salmon Redds", J. Fish Biology, 34, pp119-134

Davies, B.E. (1974), "The Armouring of Alluvial Channel beds", M.S. Thesis, Univeristy of Canterbury, N.Z.

Davis, J.C. (1973), "Statistics and Data Analysis in Geology", Published by John Wiley and Sons

Day, T.J. (1980), "A Study of the Transport of Graded Sediments", HR Report No. IT190

Diplas, P. (1987), "Bedload Transport in Gravel Bed Streams", J. Hyd. Eng., 113, pp277-292

DuBoys, M.P. (1879), "Le Rhone et les Rivieres a Lit Affouillable", Annales de Ponts et Chausses, sec.5, Vol.18, pp141-195

Einstein, H.A. (1942), "Formulas for the Transportation of Bed Load", Transactions, ASCE, Paper No. 2140

Einstein, H.A. (1950), "The Bed-Load Function for Sediment Transport in Open Channels", Tech. Bull., 1026, US Dept. Of Agriculture

Einstein, H.A., and Banks, R.B. (1950), "Fluid Resistance of Composite Roughness", Transactions of American Geophysical Union. Vol.31, No.4, pp603-610

Elliott, S.C.A., and Sellin, R.H.J. (1990), "SERC Flood Channel Facility: Skewed Flow Experiments", J. Hyd. Res., IAHR, 28(2), pp197-214

Engelund, F., and Hansen, E. (1967), "A Monograph on Sediment Transport in Alluvial Streams", Teknisk Vorlag, Copenhagen

Ervine, D.A., Fuller, C., and Pender, G. (1997), "Sediment Transport in a Gravel Bed Channel during Overbank Flow", Proc. 27th IAHR Congress, California.

Fenton, J.D., and Abbott, J.E. (1977), "Initial Movement of Grains on a Stream Bed: the Effect of Relative Protrusion", Proc. Royal Society of London, 332A, pp523-537

Ferguson, R.I., and Ashworth, P.J. (1992), "Spatial Patterns of Bedload transport and Channel Change in Braided and Near-Braided Rivers", Dynamics of Gravel-Bed Rivers, Edited by Billi, Hey, Thorne and Tacconi. John Wiley & Sons

Ferguson, R.I. (1994), "Critical Discharge for Entrainment of Poorly Sorted Gravel", Earth Surface Processes and Landforms. Vol.19. pp179-186

Ferguson, R.I., Hoey, T.B., Wathen, S., and Werritty, A. (1996). "Field Evidence for Rapid Downstream Fining of River Gravels Through Selective Transport", Geology, Vol.24, No.2, pp179-182

Fortier, S., and Scobey, F.C. (1926), "Permissible Canal Velocities", Transactions of the ASCE, Vol.89

French, R.H. (1986), "Open-Channel Hydraulics", Published by McGraw Hill

Garcia, M., and Parker, G. (1991), "Entrainment of Bed Sediment into Suspension", J. Hyd. Eng., ASCE, 117(4), pp414-435

Gessler, J. (1965), "The Beginning of Bedload Movement of Mixtures Investigated as Natural Armoring in Channels", W. M. Keck Laboratory of hydraulics and Water Resources, California Institute of Technology, Pasadena

Gessler, J. (1970), "Self-Stabilizing Tendencies of Alluvial Channels", J. of Waterways and Harbors Division, ASCE, Vol.96, No.WW2, pp235-249

Gessler, J. (1990), "Friction Factor of Armoured River Beds", J. Hyd. Eng., ASCE, 116(4), pp531-543

Gibbs, C.J., and Neill, C.R. (1972), "Interim Report on Laboratory Study of Basket-Type Bedload Samplers", Research Council of Alberta, REH/72/2

Gibbs, C.J., and Neill, C.R. (1973) "Laboratory Testing of Model VUV Bedload Samplers", Research Council of Alberta, REH/73/2

Gleick, J. (1987), "Chaos, Making a New Science", Viking. Published by Penguin Group

Gomez, B. (1983), "Temporal Variations in Bedload Transport Rates: The Effect of Progressive Bed Armouring", Earth Surface Processes and Landforms. Vol.8, pp 41-54

Gomez, B. (1993), "Roughness of Stable, Armored Gravel Beds", Water Resources Research, 29(11), pp 3631-3642

Gomez, B. (1994), "Effects of Particle Shape and Mobility on Stable Armor Development", Water Resources Research, 30(?). pp 2229-2239

Grass, A.J. (1983), "The Influence of Boundary Layer Turbulence on the Mechanics of Sediment Transport", in Mechanics of Sediment Transport, Ed. B.M. Sumer and A. Muller, pp3-18, A.A Balkema, Rotterdam

Hardwick, R.I., and Willetts, B.B. (1991), "Changes with Time of the Transport Rate of Sediment Mixtures", J. Hyd. Res., IAHR, 29(1)

Henderson, F.M. (1966), "Open Channel Flow", Macmillian, New York

Hey, R.D. (1994), "Environmentally Sensitive River Engineering", The River Handbook II, Blackwell, Oxford

Hjulstrom, F. (1935), "The Morphological Activity of Rivers as Illustrated by River Fyris", Bulletin of the Geological Institute, Uppsala, Vol.25, Chapt.3

Hoey, T.B., and Sutherland, A.J. (1991), "Channel Morphology and Bedload Pulses in Braided Rivers: A Laboratory Study", Earth Surface Processes and Landforms, Vol.16, pp447-462

Hoey, T.B. (1992), Temporal Variations in Bedload Transport Rates and Sediment Storage in Gravel-Bed Rivers", Progress in Physical Geography, 16, 3, pp319-338

Hoey, T.B., and Ferguson, R. (1994), "Numerical Simulation of Downstream Fining by Selective Transport in Gravel Bed Rivers: Model Development and Illustration", Water Resources Research, 30(7), pp 2251-2260

Hoey, T.B., and Ferguson, R. (1997), "Controls of Strength and Rate of Downstream Fining Above a River Base Level", Water Resources Research, 33(11), pp 2601-2608

Hoey, T.B., Pender, G., and Fuller, C. (1997), "Bedload Grain-Size Distributions In Degradational Armouring Experiments", Proc. 27th IAHR Congress, California.

Holly Jr., F.M., and Rahuel, J.L. (1990), "New Numerical/Physical Framework for Mobile-Bed Modelling, Part 1: Numerical and Physical Principles", J. Hyd. Res., 28(4)

Horton, R.E. (1933), "Separate Roughness Coefficients for Channel Bottom and Sides", Eng. News Record, Vol.III, No.22, pp652-653

James and Brown (1977), "Geometric Parameters that Influence Floodplain Flow", Hydraulics Laboratory, US Army Engineer Waterways Experiment Station, Vicksburg, Mississippi

James, C.S. (1990), "Prediction of Entrainment Conditions for Nonuniform, Noncohesive Sediments", J. Hyd. Res., IAHR, 28(1)

James, C.S., and Wark, J.B. (1992), "Conveyance Estimation for Meandering Channels", Report SR329, HR Wallingford

James, C.S. (1993), "Entrainment of Spheres: an Experimental Study of Relative Size and Clustering Effects", Spec. Publs Int. Ass. Sediment, 17, pp 3-10

Kalinske, A.A. (1947), "Movement of Sediment as Bed-Load in Rivers", Transactions of the American Geophysical Union, Vol.28, No.4

Keller, R.J., and Rodi, W. (1988), "Prediction of Flow Characteristics in Main Channel / Flood Plain Flows", J. Hyd. Res., IAHR, 26(4)

Kirchner, J.W., Dietrich, W.E., Iseya, F., and Ikeda, H. (1990), "The Variability of Critical Shear Stress, Friction Angle and Grain Protrusion in Water Worked Sediments", Sedimentology, 37, pp647-672

Knight, D.W., Demetriou, J.D., and Hamed, M.E. (1983), "Hydraulic Analysis of Channels with Flood Plains", Int. Congress Hydr. Aspects of Floods and Flood Control

Knight, D.W., and Sellin, R.H.J. (1987), "The SERC Flood Channel Facility", J. Inst. Water and Environmental Management, Vol 1, No.2, pp198-204

Knight, D.W., and Shiono, K. (1990), "Turbulence Measurements in a Shear Layer Region of a Compound Channel", J. Hyd. Res., IAHR, 28(2)

Knight, D.W., and Abril C., J.B. (1996), "Refined Calibration of a Depth-Averaged Model for Turbulent Flow in a Compound Channel", Proc. Instn Civ. Engrs Wat., Marit., and Energy, 118, pp 151-159

Knight, D.W., and Shiono, K. (1996), "Chapter 5 : River Channel and Floodplain Hydraulics", Floodplain Processes, Edited by Anderson, Walling and Bates, John Wiley & Sons

Kuhnle, R.A. (1992), "Fractional Transport Rates of Bedload on Goodwin Creek", Dynamics of Gravel-Bed Rivers, Edited by Billi, Hey, Thorne and Taconi, John Wiley & Sons

Kuhnle, R.A. (1993), "Fluvial Transport of Sand and Gravel Mixtures with Bimodal Size Distributions", Sedimentary Geology, 85, pp17-24

Kuhnle, R.A., Bingner, R.L., Foster, G.R., and Grissinger, E.H. (1996), "Effect of Land Use Changes on Sediment Transport in Goodwin Creek", Water Resources Research, Vol.32, No.10, pp3189-3196

Li, Q. (1995), "Numerical Simulation of Non-Equilibrium Graded Sediment Transport", Ph.D Thesis, University of Glasgow

Little, W.C., and Mayer. P.G. (1976), "Stability of Channel Beds by Armouring", J. Hyd. Div., ASCE, Vol.102, HY11, pp1165-1180

Lorena, M. (1992), "Meandering Compound Flow", Ph.D Thesis, University of Glasgow

Mackie-Dawson, L.A., Walker. A.D., Atkinson. D., and Bibby. J.S. (1988), "Water Abstraction from the River Spey Area for Domestic and Agriculture Purposes and its Effect on Agriculture". Scottish Geographical Magazine. 104, 2, pp91-96

Marion, A. (1996), "Equilibrium Bed Material Composition for Well Graded Sediment Mixtures in a Compound Channel". HR Wallingford Ltd. Research Report, SR 474

Marion, A., McEwan, I., and Tait, S. (1997), "On the Competitive Effects of Particle Re-Arrangement and Vertical Sorting". Proc. 27th IAHR Congress. California, USA

Marion, A., and Fraccarollo, L., (1997), "A New Conversion Model for Areal Sampling of Fluvial Sediments", J. Hyd. Eng., ASCE, in press.

Mavis, F.T., and Laushey, L.M. (1948), "A Reappraisal of the Beginning of Bed-Movement, Competent Velocity", IAHR, 2nd Meeting Stockholm

Meyer-Peter, E., Favre, H., and Einstein, A. (1934), "Neuere Versuchsresultate uber den Geschiebetrieb", Schweiz Bauzeitung, Vol.103, No.13

Meyer-Peter, E., and Muller, R. (1948), "Formula for Bed-Load Transport", IAHR, 2nd Meeting, Stockholm

Myres, W.R.C., and Elsawy, E.M. (1975), "Boundary Shear in Channel with Flood Plain", J. Hyd. Div., ASCE, Vol.101, No.HY7

Myres, W.R.C. (1978), "Momentum Transfer in a Compound Channel", J. Hyd. Res., IAHR, 16(2)

Myres, W.R.C. (1987), "Velocity and Discharge in Compound Channels", J. Hyd. Eng., ASCE, Vol. 113, No.6, pp753-766

Myers, W.R.C., and Brennan, E.K. (1990), "Flow Resistance in Compound Channels", J. Hyd. Res., IAHR, 28(2)

Parker, G., Dhamotharan, S., and Stefan, H. (1982a), "Model Experiments on Mobile, Paved Gravel Bed Streams". Water Resources Research, 18(5), pp 1395-1408

Parker, G., Klingeman, P.C., and McLean, D.G. (1982b). "Bedload and Size Distribution in Paved Gravel-Bed Streams". J. Hyd. Div., ASCE, Vol.108, HY4

Parker, G., and Sutherland, A.J. (1990), "Fluvial Armor". J. Hyd. Res., IAHR, 28(5)

Parker, G. (1990), "Surface-Based Bedload Transport Relation for Gravel Rivers". J. Hyd. Res., IAHR, 28(4)

Parker, G. (1991), "Selective Sorting and Abrasion of River Channel. I : Theory", J. Hyd. Eng., ASCE, Vol.117, No.2

Parker, G., and Wilcock, P.R. (1993), "Sediment Feed and Recirculating Flumes: Fundamental Differences", J. Hyd. Eng., ASCE, Vol.119, No.11

Pender, G., Li, Q., and Ervine, D.A. (1993), "A Development of a Hiding Function for Van Rijn's Sediment Transport Formula", Advances in Hydro-Sciences and Engineering, Vol.1, pp 697-702

Pender, G., and Li, Q. (1995), "Comparison of Two Hiding Function Formulations for Non-Uniform Sediment Transport Calculations". Proc. ICE, 112, pp 127-135

Pender, G., and Li, Q. (1996), "Numerical Prediction of Graded Sediment Transport", Proc. Instn Civ. Engrs Wat., Marit. & Energy, 118, Dec., pp 237-245

Pender, G., Willetts, B.B., and Fuller, C. (1997), "A Comparison of Bedload Composition in Degradation Experiments with Man-made and Water Worked Beds", Proc. 3rd River Flood Hydraulics Conference, Stellenbosch, South Africa.

Phillips, B.C., and Sutherland, A.J. (1985), "Numerical Modelling of Spatial and Temporal Lag Effects in Bed Load Sediment Transport", 21st IAHR Congress, Melbourne, Australia.

Phillips, B.C., and Sutherland, A.J. (1990), "Temporal Lag Effect in Bed Load Sediment Transport", J. Hyd. Res., IAHR, 28(1)

Proffitt, G.T. (1980), "Selective Transport and Armouring of Non-Uniform Alluvial Sediments", Dept. Civil Eng., Univ. of Canterbury, N.Z., Res. Rept. 80/22

Proffitt, G.T., and Sutherland, A.J. (1983), "Transport of Non-Uniform Sediments", J. Hyd. Res., IAHR, 21(1)

Purseglove, J. (1989), "Taming the Flood. A History and Natural History of Rivers and Wetlands", Oxford University Press (with Channle 4 Television)

Rajaratnam, N., and Ahmadi, R.M. (1979), "Interaction Between Main Channel and Floodplain Flows", J. Hyd. Div., ASCE, Vol.105, No.HY5

Rajaratnam, N., and Ahmadi, R.M. (1981), "Hydraulics of Channels with Flood Plains", J. Hyd. Res., IAHR, 19(1)

Reeve, C.E., and Bettess, R. (1990), "Hydraulic Performance of Environmentally Acceptable Channels", Proc. Int. Conference on River Flood Hydraulics, Wallingford, UK, pp279-287, John Wiley and Sons

Reid, I., Frostick, L.E., and Layman, J.T. (1985), "The Incidence and Nature of Bedload Transport During Flood Flows in Coarse-Grained Alluvial Channels", Earth Surface Processes and Landforms, Vol.10, pp 33-44

Rouse, H. (1939), "An Analysis of Sediment Transportation in the Light of Fluid Turbulence", Soil Conservation Service Report No.SCS-TP-25, US Dept. Of Agriculture.

Samuels, P.G. (1985), "Modelling of river and Flood Plain Flow Using the Finite Element Method", Ph.D Thesis, Dept., of Mathematics, Univ., of Reading, Report No.SR61, HR Wallingford

Seed, D.J. (1996), "Lateral Variations of Sediment Transport in Rivers", HR Wallingford Report SR 454

Sellin, R.H.J. (1964), "A Laboratory Investigation into the Interaction Between the Flow in the Channel of a River and that Over its Flood Plain", La Houille Blanche, No.7

Sellin, R.H.J., Ervine, D.A., and Willetts, B.B. (1993), "Behaviour of Meandering Two-Stage Channels", Proc. Instn. Civ. Engrs. Wat., Marit., and Energy, Vol.101, June, pp99-111

Shields, A. (1936), "Application of Similarity Principles, and Turbulence Research to Bed-Load Movement", California Institute of Technology, Pasadena (translated from German)

Shiono, K., and Knight, D.W. (1989), "Transverse and Vertical Reynolds Stress Measurements in a Shear Layer Region of a Compound Channel", 7th Symp. Turbulent Shear Flows, Stanford

Shiono, K., and Knight, D.W. (1991), "Turbulent Open-Channel Flows with Variable Depth Across the Channel", J. Fluid. Mech., vol.222, pp617-646

Sutherland, A.J. (1987),"Static Armour Layers by Selective Erosion", in Sediment Transport in Gravel-Bed Rivers, C.R. Thorne et al. Wiley, Chichester, pp243-260

Sutherland, A.J. (1991). "Hiding Functions to Predict Self Armouring", Proc. International Grain Sorting Seminar, Ascona, Switzerland.

Swan, A.R.H., and Sandilands, M. (1995). "Introduction to Geological Data Analysis", Published by Blackwell Science

Tait, S.J., and Willetts, B.B. (1991). "Characterisation of Armoured Bed Surfaces", Proc. International Grain Sorting Seminar, Ascona, Switzerland.

Tait, S.J., Willetts, B.B., and Maizels, J.K. (1992). "Laboratory Observations of Bed Armouring and Changes in Bed Composition", In: Dynamics of Gravel-Bed Rivers, Edited by Billi, Hey, Thorne & Tacconi, Published by John Wiley & Sons Ltd.

Tait, S.J., and Willetts, B.B. (1992), "Physical and Numerical Experiments in Bed Armouring", Proc. 5th International Syn. on River Sedimentation

Tait, S.J. (1993), "The Physical Processes of Bed Armouring in Mixed Grain Sediment Transport", Ph.D Thesis, University of Aberdeen

Tait, S.J., and Willetts, B.B. (1995), "Turbulent Flow Adjustment Over a Stabilising Gravel Sediment Bed", 26th IAHR Congress, HYDRA 2000, London.

Tait, S.J., McEwan, I.K., and Marion, A. (1997). "Bed Re-Arrangement under Conditions of Variable Upstream Sediment Supply" ", Proc. 3rd River Flood Hydraulics Conference, Stellenbosch, South Africa.

Thorne, P.D., Williams, J.J., and Heathershaw, A.D. (1989). "In Situ Acoustic Measurements of Marine Gravel Threshold and Entrainment", Sedimentology, 36, pp61-74

US Bureau of Reclamation (1987), "Design of Small Dams", Denver, Colorado

USWES (1935), "Studies of River Bed Materials and Their Movement with Special Reference to the Lower Mississippi River", Paper 17

van Rijn, L.C. (1984a), "Sediment Transport, Part I: Bed Load Transport", J. Hyd. Eng., ASCE, Vol.110, No.10

van Rijn, L.C. (1984b), "Sediment Transport, Part II: Suspended Load Transport", J. Hyd. Eng., ASCE, Vol.110, No.11

Vanoni, V.A., ed. (1975), "Sedimentation Engineering", ASCE Task Committee for the Preparation of the Manual on Sedimentation of the Sedimentation Committee of the Hydraulics Division (Reprinted 1977)

Wark, J.B., Ramsbottom, D.M., and Slade, J.E. (1991). "Flood Discharge Assessment by the Lateral Distribution Method". Report SR277, HR Wallingford

Wark, J.B. (1993), "Discharge Assessment in Straight and Meandering Compound Channels", Ph.D Thesis, University of Glasgow

Wark, J.B., James, C.S., and Ackers, P. (1994), "Design of Straight and Meandering Compound Channels", R&D Report 13, National River Authority

Wark, J.B. (1997) Personal Communication

Wathen, S.J., Ferguson, R.I., Hoey, T.B., and Werritty, A. (1995). "Unequal Mobility of Gravel and Sand in Weakly Bimodal River Sediments", Water Resources Research, 30(8), pp 2087-2096

Wheeler, M.V.C., and Willetts, B.B. (1994), "The Behaviour, Interaction and Effect of Depositing Grains", Internal Paper, Dept. of Eng., University of Aberdeen.

White, C.M. (1940), "The Equilibrium of Grains on the Bed of an Alluvial Channel", Proc. Royal Society of London, Series A, Vol.174, pp332-338

White, W.R., Milli, H., and Crabbe, A.D. (1973a), "Sediment Transport: An Appraisal of Available Methods, Volume 1 - Summary of Existing Theories", HR Report No IT 119

White, W.R., Milli, H., and Crabbe, A.D. (1973b), "Sediment Transport: An Appraisal of Available Methods, Volume 2 - Performance of Theoretical Methods When Applied to Flume and Field Data", HR Report No IT 119

White, W.R., Milli, H., and Crabbe, A.D. (1975), "Sediment Transport Theories: A Review", Proc. ICE, Part 2, 59, June, pp265-292

White, W.R., and Day, T.J. (1980), "Sediment Transport in Gravel Bed Rivers", Management of Gravel Bed Rivers, Newtown, June 1980.

White, W.R., Paris, E., and Bettess, R. (1980), "The Frictional Characteristics of Alluvial Streams: A New Approach", Proc. ICE, Part 2, 69, pp 737-750

White, W.R., and Day, T.J. (1982), "Transport of Graded Gravel Bed Material", Paper 8 from Gravel-Bed Rivers, John Wiley and Sons

White, W.R. (1987), "Engineering Aspects of Fluvial Morphology", 22nd IAHR Congress, Lausanne.

Wilcock. P.R. (1988). "Methods for Estimating the Critical Shear Stress of Individual Fractions in Mixed-Size Sediment". Water Resources Research. 24(7), pp 1127-1135

Wilcock, P.R., and Southard, J.B. (1988), "Experimental Study of Incipient Motion in Mixed-Size Sediment", Water Resources Research. 24(7), pp 1137-1151

Wilcock, P.R., and Southard, J.B. (1989), "Bed Load Transport of Mixed Size Sediment: Fractional Transport Rates. bed Forms. and the Development of a Coarse Bed Surface Layer", Water Resources Research. 25(7), pp 1629-1641

Wilcock, P.R., (1992), "Experimental Investigation of the Effect of Mixture Properties on Transport Dynamics". In: Dynamics of Gravel-Bed Rivers. Edited by Billi, Hey, Thorne & Tacconi. Published by John Wiley & Sons Ltd.

Wilcock, P.R., and McArdell, B.W. (1993), "Surface-Based Fractional Transport Rates: Mobilization Thresholds and Partial Transport of a Sand-Gravel Sediment", Water Resources Research, 29(4), pp 1297-1312

Wilcock, P.R. (1996), "Estimating Local Bed Shear Stress From Velocity Observations", Water Resources Research, 32(11), pp 3361-3366

Wilcock, P.R., Barta, A.F., Shea, C.C., Kondolf, G.M., Matthews, W.V.G, and Pitlick, J. (1996), "Observations of Flow and Sediment Entrainment on a Large Gravel-Bed River", Water Resources Research, 32(9), pp 2897-2909

Wilcock, P.R., Kondolf, G.M., Matthews, W.V.G., and Barta, A.F. (1996b), "Specification of Sediment Maintenance Flows for a Large Gravel-Bed River", Water Resources Research, 32(9), pp 2911-2921

Wilcock, P.R. (1997), "The Components of Fractional Transport Rate", Water Resources Research, 33(1), pp 247-258

Wilcock, P.R., and McArdell, B.W. (1997), "Partial Transport of a Sand/Gravel Sediment", Water Resources Research, 33(1), pp 235-245

Willetts, B.B., Maizels, J.K., and Florence, J. (1987), "The Simulation of Stream Bed Armouring and its Consequences", Proc. ICE, Part 1, 82, pp 799-814

Willetts, B.B., McEwan. I.K., and Pender. G. (1997). "The Response of Graded Sediment Beds to High Stage Flows" ". Proc. 3rd River Flood Hydraulics Conference, Stellenbosch, South Africa.

Wormleaton, P.R., and Hadjipanos P. (1985), "Flow Distribution in Compound Channels", J. Hyd. Eng., ASCE, Vol.111, No.2, pp357-361

Wormleaton, P.R. (1988), "Determination of Discharge in Compound Channels Using the Dynamic Equation for Lateral Velocity Distribution". Int. Conference on Fluvial Hydraulics, Budapest

Wormleaton, P.R., and Merrit, D.J. (1990). "An Improved Calculation for Steady Uniform Flow in Prismatic Main Channel Flood Plain Sections". J. Hyd. Res., IAHR, 28(2), pp157-174

Yalin, M.S. (1977), "Mechanics of Sediment Transport", Published by Pergamon Press

Yang, C.T. (1972), "Unit Stream Power and Sediment Transport", J. Hyd. Div., ASCE, Vol.98, No.HY10, pp1805-1826

Yang, C.T. (1973). "Incipient Motion and Sediment Transport", J. Hyd. Div., ASCE, Vol.99, No.HY10, pp1679-1704

Yang, C.T. (1984), "Unit Stream Power Equation for Gravel", J. Hyd. Eng., ASCE, Vol.10, No.HY12, pp1783-1797

Yang, C.T. (1996), "Sediment Transport: Theory and Practice", Published by McGraw-Hill

Appendix A

Event Sheets

A.1 Experiment 2 - B/OB/0/1/400

Date (day.month.year)	Time (24 hour clock)	Elapsed Time (minutes)	Event
30.5.95	11.30		Trickle fill flume
	14.00		Bedding down flow established
31.5.95	09.56	0	Uniform flow established
			20mm overbank
	17.18	441	Shut-down
1.6.95	09.17	441	Re-start
	19.44	1067	Shut-down
2.6.95	09.11	1067	Re-start
		1547	Shut-down
5.6.95	08.51	1547	Re-start
	17.41	2077	Shut-down
6.6.95	14.45	2077	Re-start
	17.48	2261	Shut-down
7.6.95	09.34	2261	Re-start
	10.10	2297	Mini. prop frame failed. Possible scour at tapping point 3 as I-beam touching flow surface.
			OVERNIGHT RUN
8.6.95	17.15	4162	Final shut-down. End of Exp.2

A.2 Experiment 3 - B/OB2/0/1/400

Date (day.month.year)	Time (24 hour clock)	Elapsed Time (minutes)	Event
26.6.95	18.30		Trickle fill flume.
	19.30		Bedding down flow established
27.6.95	15.23	0	Uniform flow established 65mm overbank
	17.20	116	Shut-down
28.6.95	09.20	116	Placed larger rocks in bell mouth entry at bed level to prevent erosion
	11.11	116	Re-start
	16.24	426	Shut-down
29.6.95	11.45	426	Re-start
	17.00	727	Shut-down
30.6.95	09.45	727	Re-start
	16.35	1133	Shut-down
3.7.95	09.38	1133	Re-start
	16.45	1560	Shut-down
4.7.95	09.22	1560	Re-start
			OVERNIGHT RUN
5.7.95	16.40	3437	Shut-down
6.7.95	10.07	3437	Re-start
	16.00	3788	Final shut-down. End of Exp.3

A.3 Experiment 4 - B/IB/0/1/400

Date (day.month.year)	Time (24 hour clock)	Elapsed Time (minutes)	Event
25.7.95	12.30		Trickle fill flume.
	13.50		Bedding down flow established
26.7.95	08.56	0	Uniform flow established bankfull.
	18.02	545	Shut-down
27.7.95	08.40	545	Fitted floating pipe across upstream end of flume to calm water surface.
	08.45	545	Re-start
	09.42	602	Lowered tailgate by 2-4mm as water level higher than previous day.
	16.55	1026	Shut-down
28.7.95	09.12	1026	Re-start Lifted pipe (surface calming) to check if any effect on transport rate.
	09.30	1044	Re-set tapping point pointer datums. 2mm difference between old and new readings.
	20.10	1690	Shut-down
31.7.95	09.20	1690	Re-start
	09.45	1715	Tapping point 1 pointer not working. Replaced.
			OVERNIGHT RUN

Experiment 4 continued

Date (day.month.year)	Time (24 hour clock)	Elapsed Time (minutes)	Event
1.8.95	09.25		Replace Tapping point 3 pointer.
	17.26	3614	Shut-down
2.8.95	08.15	3614	Re-start
			OVERNIGHT RUN
3.8.95	16.38	5555	Final shut-down. End of Exp.4

A.4 Experiment 5 - B/IB/0/1/340

Date (day.month.year)	Time (24 hour clock)	Elapsed Time (minutes)	Event
9.8.95			Changed flume slope to 1/340
10.8.95			Trickle fill flume
			Bedding down flow established
11.8.95	09.43	0	Uniform flow established
			bankfull
	16.38	415	Shut-down
14.8.95	08.58	415	Re-start
	16.44	880	Shut-down
15.8.95	09.43	880	Re-start
	17.03	1320	Shut-down
16.8.95	10.01	1320	Re-start
	17.09	1749	Shut-down
17.8.95	09.07	1749	Re-start
	17.10	2229	Shut-down
18.8.95	08.45	2229	Re-start
	17.40	2760	Shut-down
21.8.95	09.00	2760	Re-start
	17.35	3275	Shut-down
22.8.95	08.44	3275	Re-start
			OVERNIGHT RUN
23.8.95			Tailgate slipped by 2mm
	15.43	5134	Final shut-down. End of Exp.5

A.5 Experiment 6 - B/IB/0/1/420

Date (day.month.year)	Time (24 hour clock)	Elapsed Time (minutes)	Event
1.9.95			Changed flume slope to 1/420
			Screeded bed not even.
			Re-screed
2.9.95	10.00		Trickle fill flume.
	13.30		Bedding down flow established
4.9.95	09.45	0	Uniform flow established
			bankfull
	16.35	409	Shut-down
		409	Lower texture laser z-axis by
			7mm
5.9.95	09.16	409	Re-start
	16.58	871	Shut-down
6.9.95	09.20	871	Re-start
	15.01	1211	Shut-down
7.9.95	09.31	1211	Re-start
	16.46	1645	Shut-down
8.9.95	09.23	1645	Re-start
	14.54	1976	Central mini. prop. jammed.
			Replaced
	15.37	2019	Shut-down
11.9.95	08.58	2019	Re-start
			OVERNIGHT RUN
12.9.95	15.06	3826	Shut-down
		3826	Changed location of texture
			area photos to cover full texture
			area.

Experiment 6 continued

Date (day.month.year)	Time (24 hour clock)	Elapsed Time (minutes)	Event
13.9.95	09.32	3826	Re-start
	12.40	4014	Battery failure in LHS Streamflo. Replace.
	17.25	4300	Shut-down
14.9.95	09.00	4300	Re-start
	17.19	4800	Final shut-down. End of Exp.6

A.6 Experiment 7 - B/OB/0/1/420

Date (day.month.year)	Time (24 hour clock)	Elapsed Time (minutes)	Event
25.9.95			Left longitudinal laser submerged in water within gaiter. Removed, opened, cleaned and dried.
27.9.95			Conveyor belt in place and operational
28.9.95			Trickle fill flume
			Bedding down flow established.
2.10.95	13.41	0	Uniform flow established
			20mm overbank.
			Tapping point 1 pointer and flood plain pointer both failed. Replaced
	16.45	154	Shut-down
		154	Lower texture laser z-axis by 8mm
3.10.95	09.03	154	Re-start
	17.06	637	Shut-down
		637	Lower texture laser z-axis by 0.5mm
4.10.95		637	Replaced tapping point 2 pointer gauge.
	09.15	637	Re-start
	16.38	1082	Shut-down
5.10.95	09.25	1082	Re-start

Experiment 7 continued

Date (day.month.year)	Time (24 hour clock)	Elapsed Time (minutes)	Event
	16.22	1499	Velocity profiling frame jammed. Datum re-set.
	17.06	1538	Shut-down
6.10.95	09.10	1538	Re-start
	16.42	1991	Shut-down
9.10.95		1991	Replace flood plain pointer.
	10.29	1991	Re-start
	17.19	2402	Shut-down
10.10.95	08.50	2402	Re-start
			OVERNIGHT RUN
11.10.95	17.10	4345	Shut-down
12.10.95	09.25	4345	Re-start
	17.10	4810	Final shut-down. End of Exp.7